Application of organic acid functionalized cellulose for batch and aqueous two-phase extraction of sulfonamides from different matrices

By

Shikweni Mbuyelo

17001697

A dissertation presented in fulfilment of the requirements for the

Degree Master of Science in Chemistry

Department of Chemistry

Faculty of Science, Engineering and Agriculture

February 2025

© University of Venda

Declaration

I, **Shikweni M (Student no: 17001697)**, declare that this research dissertation is my original work and has not been submitted for any degree at any other university or institution. The dissertation does not contain any other person's writing unless specifically acknowledged and referenced accordingly.

Signed (Student)…  … … ……. Date: … 25 February 2025

© University of Venda

Abstract

Antibiotics are among the most widely used drugs globally, with fluoroquinolones, macrolides and sulfonamides being commonly prescribed. Sulfonamides, which form the basis of several sulfa drugs, have significant applications in both medicinal and synthetic organic chemistry. While these substances are effective in their intended uses, their negative environmental impact raises serious concerns. Sulfonamides can have toxic effects on aquatic ecosystems, leading to the disruption of microbial communities, bioaccumulation in organisms and the development of antibiotic resistance. To mitigate these effects, cellulose and its functionalized derivatives were investigated for their ability to adsorb sulfonamides from real wastewater, milk and honey samples. To improve adsorption, cellulose was functionalized with oxalic and adipic acid. The resulting sorbents were then analyzed using FTIR, PXRD and SEM techniques. Based on FTIR analysis the optimal reaction time for cellulose functionalized with adipic acid and oxalic acid via hydrothermal treatment in an autoclave was 1 h at a temperature of 50°C. Furthermore, the FTIR data revealed the emergence of ester moieties from the esterification reaction of carboxyl groups in the organic acids and the hydroxyl groups on cellulose. Based on PXRD analysis for the adipic acid functionalized cellulose contained a hybrid of adipic acid and oxalic acid peaks, indicating functionalization of cellulose. Batch adsorption experiments were conducted using sulfonamide based analytical standards: sulfachloropyradazine and sulfabenzamide, to evaluate the adsorption capability of cellulose and its functionalized derivatives at varying temperature, time, and mass of sorbent. The multivariate based optimal conditions for the adsorption of sulfachloropyradazine and sulfabenzamide using cellulose was 25°C, 180 min and 5 mg and with extraction efficiency of 70 and 51%, respectively. The optimal conditions for adsorption of sulfachloropyradazine and sulfabenzamide using oxalic acid functionalized cellulose was 25°C, 30 min and 50 mg with extraction efficiency of 64 and 75%, respectively. Adsorption of sulfachloropyradazine and sulfabenzamide using adipic acid functionalized cellulose was 25°C, 30 min, and 5 mg with extraction efficiency of 70 and 51%, respectively. Although cellulose functionalized with adipic and oxalic acid showed some influence on the adsorption behavior of sulfachloropyridazine and sulfabenzamide, the adsorption of sulfachloropyridazine was slightly reduced from 70% with unmodified cellulose to 64% with the functionalized form. Functionalizing cellulose with adipic and oxalic acid adds carboxyl and hydroxyl groups, enhancing adsorption of sulfachloropyradazine and sulfabenzamide through stronger hydrogen bonding, electrostatic

© University of Venda

interactions, and possibly π-π stacking, compared to cellulose. Overall, the functionalization of cellulose with these acids is a promising approach for enhancing the adsorption of sulfonamides which could be applied in wastewater treatment.

Keywords: Sulfonamides, cellulose functionalization, oxalic acid, adipic acid, adsorption, wastewater treatment, sulfachloropyridazine, sulfabenzamide

© University of Venda

Dedication

I dedicate this dissertation to Almighty God, whose boundless wisdom, strength, and guidance have been my foundation throughout this academic journey. It is through His grace that I found the resilience to overcome challenges, the clarity to pursue knowledge, and the determination to bring this study to completion. To Him, I offer my deepest gratitude for making this achievement possible.

I also wholeheartedly dedicate this work to my beloved parents, Shikweni M.S and Shikweni S.T. Their unwavering love, moral support, and constant encouragement have been the pillars of my strength. Their sacrifices, prayers, and financial assistance have been invaluable throughout my pursuit of this master's degree. This accomplishment is as much theirs as it is mine, and I am forever grateful.

© University of Venda

Acknowledgements

- First and foremost, I would like to acknowledge the Almighty God for the gift of wisdom, knowledge, and strength, and for granting me the courage and perseverance to successfully complete this academic journey. His guidance has been my source of inspiration throughout the course of my studies.
- I extend my deepest gratitude to my supervisor, Dr T Mokgehle, for his exceptional guidance, patience, and continuous support throughout my master's research. His motivation, enthusiasm, and wealth of knowledge greatly enriched this study. His constructive feedback and insightful advice were invaluable during both the research and the writing of this dissertation. I could not have asked for a more dedicated and supportive supervisor.
- I am also profoundly grateful to my co-supervisors, Dr N.T. Tavengwa and Dr D.L. Ndou, for their constant availability, encouragement, and expert insights. Their valuable suggestions and feedback significantly contributed to the successful completion of this research.

© University of Venda

Table of contents

Declaration i

Abstract ii

Dedication iv

Acknowledgements v

Table of content vi

List of figures x

List of tables xv

Abbreviations xvii

Chapter 1: Introduction 1

1.1. Background of the research 2

1.2. Problem statement and motivation of study 5

1.3. Aim of the research 6

1.4. Objectives of the research 6

Chapter 2: Literature review 8

2.1. Introduction 9

2.2. Physico-chemical properties of sulfonamides and their application as antibiotics 9

2.2.1. Physico-chemical properties of sulfonamides 9

2.2.2. The application of sulfonamides as antibiotics 10

2.3. Sources and toxicological effects of sulfonamides 17

2.3.1. Sources of sulfonamides antibiotics in the environment 17

2.3.2. Toxicological effects of sulfonamides 17

2.4. Pollution pathways of sulfoamides in wastewater and food samples 19

2.4.1 Pollution pathways of sulfonamides in wastewater 19

© University of Venda

2.4.2 Pollution mechanisms of sulfonamides in food samples 21
2.4.3 Emergence of anti-resistant bacteria as a result of sulfonamide toxicity 21
2.5. Mechanisms of sulfonamide toxicity and emergence of antimicrobial resistant bacteria.. 22
2.5.1. Emergence of antimicrobial resistant bacteria 22
2.6. Extraction techniques for analysis of sulfonamides 23
2.7. Adsorption of sulfonamides using on batch and aqueous two-phase extraction 27
2.7.1. Batch adsorption 27
2.7.2. Aqueous two-phase extraction 28
2.8. Optimization 31
2.8.1. Univariate vs multivariate optimization 31
2.8.2. Importance of RSM and CCD 32
2.9. Theory of characterization techniques 33
2.9.1. Fourier Transform Infrared Spectroscopy (FTIR) 33
2.9.2. Brunauer-Emmett-Teller (BET) surface area analysis 33
2.9.3. X-ray diffraction (XRD) 33
2.9.4. Scanning electron microscopy (SEM) 33
Chapter 3: Materials and methods 35
3.1. Introduction 36
3.2. Chemicals and reagents 36
3.3. Equipment 36
3.4. Sample preparation 37
3.4.1. Functional group analysis 38
3.4.2. Crystallinity analysis 38
3.4.3. Surface morphological studies 39
3.4.4. Surface area analysis 39

© University of Venda

3.4.5. Computational methods 39
3.5. Multivariate optimization 40
3.6. Adsorption studies 40
3.6.1. Preparation and functionalization of cellulose 40
3.6.2. Sample preparation for aqueous two-phase extraction 44
3.7. Site description and sampling 48
3.7.1. Sample collection 49
3.7.2. Sample preparation and analysis 49
Chapter 4: Results and discussion 50
4.1. Introduction 51
4.2. Characterization of cellulose and its functionalization 51
4.2.1. Functional group analysis 51
4.2.2 Crystallinity analysis 55
4.2.3. Surface morphological analysis 59
4.2.4. BET surface area analysis 65
4.3. Density functional theory mechanism of adsorption 72
4.4. Batch adsorption 80
4.4.1. Response surface methodology for the extraction of sulfachloropyradazine and sulfabenzamide on cellulose 87
4.4.2. Response surface methodology for the extraction of sulfachloropyridazine and sulfabenzamide using oxalic acid functionalized cellulose 94
4.4.3. Response surface methodology for the extraction of sulfachloropyradazine and sulfabenzamide in adipic acid functionalized cellulose 103
4.5 Application studies for batch adsorption 112
4.5.1. Extraction of sulfonamides from milk, honey, and wastewater using a cellulose-based sorbent 112

© University of Venda

4.5.2. Extraction of sulfonamides from milk, honey, and wastewater using a cell@OA sorbent 115

4.5.3. Extraction of sulfonamides from milk, honey, and wastewater using a cell@AA sorbent 117

4.6. Aqueous two-phase extraction adsorption 121

4.6.1. Response surface methodology for the extraction of sulfachloropyradazine and sulfabenzamide from cellulose using aqueous two-phase extraction 135

4.6.2. RSM for the extraction of sulfachloropyradazine and sulfabenzamide from oxalic acid functionalized cellulose using aqueous two-phase extraction 142

4.6.3. Response surface methodology for the extraction of sulfachloropyradazine and sulfabenzamide using cell@AA in aqueous two-phase extraction 151

4.7. Application studies of aqueous two-phase extraction 162

4.7.1. Sulfonamide extraction from wastewater, honey, and milk using a cellulose-based sorbent 162

4.7.2. Extraction of sulfonamides from wastewater, honey, and milk using a cell@OA-based sorbent 165

4.7.3. Extraction of sulfonamide from wastewater, honey, and milk using a cell@AA-based sorbent 169

Chapter 5: Conclusion, challenges and future work 173

5.1. Conclusion 174

5.2. Challenges 175

5.3. Future work 175

Chapter 6: References 176

© University of Venda

List of figures

Figure 1.1: Structures of sulfonamide..... 2
Figure 1.2: Structure of adipic acid..... 4
Figure 2.1: General structure of sulfonamide antibiotics 10
Figure 2.2: Pollution pathways of sulfonamides 20
Figure 2.3: A schematic of the aqueous two-phase extraction 30
Figure 3.1: Simplified methodology for the functionalization of cellulose..... 38
Figure 3.2: Map of the WWTP location in Muledane, Thohoyandou..... 48
Figure 3.3: Basic processes in Thohoyandou WWTP 49
Figure 4.1: FTIR spectra of (a) cellulose, (b) oxalic acid, (c) cell@OA after 30 min autoclaving, and (d) cell@OA after 60 min autoclaving 53
Figure 4.2: FTIR spectra of cellulose, adipic acid and cell@AA and their derivatives treated under autoclave conditions (min) 54
Figure 4.3: PXRD patterns of cellulose, oxalic acid and cell@OA treated samples under different autoclaving durations (min)..... 56
Figure 4.4: PXRD patterns of cellulose, adipic acid and cell@AA treated samples under different autoclaving durations (min)..... 59
Figure 4.5: SEM micrographs of microcrystalline cellulose (MCC) at different magnifications (a) 1000x, (b) 450x, and (c) 510x at acceleration voltage of 15kV)..... 60
Figure 4.6: SEM micrographs of cell@OA after autoclaving for 60 min (a, b, c) and 30 min (d, e, f)..... 62
Figure 4.7: Surface morphology of cell@AA at different autoclaving times of 60 min (a, b, c) and 30 min (d, e, f) 64
Figure 4.8: BET analysis of cellulose: (a) pore volume and pore size distribution (b) adsorption-desorption isotherm 66
Figure 4.9: BET analysis of cell@OA: (a) pore volume and pore size distribution (b) adsorption-desorption isotherm 68
Figure 4.10: BET analysis of cell@AA: (a) pore volume and pore size distribution (b) adsorption-desorption isotherm 70
Figure 4.11: DFT optimization of sulfchloropyridazine adsorption on cellulose..... 76
Figure 4.12: DFT Modeling of adsorption behavior on a functionalized matrix 78

© University of Venda

Figure 4.13: Optimized interaction geometry between adsorbent and target molecule 79
Figure 4.14: Response surface plots for the extraction efficiency of sulfabenzamide with cellulose: (a) the effect of time (A) and temperature (B), (b) the effect of time (A) and cellulose mass (C) and (c) the effect of temperature (B) and cellulose mass (C)..... 89
Figure 4.15: Pareto chart for sulfachloroyridazine extraction in cellulose..... 90
Figure 4.16: Response surface plots for the extraction efficiency of sulfabenzamide with cellulose: (a) the effect of time (A) and temperature (B), (b) the effect of time (A) and cellulose mass (C) and (c) the effect of temperature (B) and cellulose mass (C)..... 93
Figure 4.17: Pareto chart for sulfabezamide extraction in cellulose..... 94
Figure 4.18: RSM plots for the extraction efficiency of sulfachloropyridazine with cell@OA: (a) the effect of time (A) and temperature (B), (b) the effect of time (A) and cell@OA mass (C) and (c) the effect of temperature (B) and cell@OA mass (C)..... 97
Figure 4.19: Pareto chart for sulfachloropyradazine extraction in cell@OA 98
Figure 4.20: RSM plots for the extraction efficiency of sulfabenzamide with cell@OA: (a) the effect of time(A) and temperature (B), (b) the effect of time (A) and cell@OA mass (C) and (c) the effect of temperature (B) and cell@OA mass (C)..... 101
Figure 4.21: Pareto chart indicating parameter significance in sulfabenzamide extraction in cell@OA 102
Figure 4.22: RSM plots for the extraction efficiency of sulfachloropyridazine with cell@AA: (a) the effect of time (A) and temperature (B), (b) the effect of time (A) and cell@OA mass (C), and (c) the effect of temperature (B) and cell@OA mass (C)..... 105
Figure 4.23: Pareto chart of sulfachloropyridazine extraction in cell@AA 106
Figure 4.24: RSM plots for the extraction efficiency of sulfabenzamide with adipic acid-functionalized cellulose: the effect of time (A) and temperature (B), (b) the effect of time (A) and cell@AA mass (C), and (c) the effect of temperature (B) and cell@AA mass (C)..... 109
Figure 4.25: Pareto chart of sulfabenzamide extraction in cell@AA..... 110
Figure 4.26: Chromatogram analysis of sulfonamides in different matrices..... 113
Figure 4.27: A chromatogram of sulfacholoropyridazine extracted from milk using a cellulose-based sorbent 115
Figure 4.28: A chromatogram of sulfachloropyradizine and sulfabenzamide extracted from milk using a cell@OA sorbent..... 117

© University of Venda

Figure 4.29: A chromatogram of sulfachloropyridazine and sulfabenzamide extracted from milk using a cell@AA sorbent 119
Figure 4.30: Optimal HPLC chromatogram of sulfachlopyridazine after extraction with cellulose in the presence of NaCl as a chaotrope 131
Figure 4.31: Optimal HPLC chromatogram of sulfabenzamide after extraction with cellulose in the presence of NaCl as a chaotrope 132
Figure 4.32: Chromatogram of sulfachloroptridazine after extraction with cell@OA in the 132
presence of NaCl as a chaotrope 132
Figure 4.33: Chromatogram of sulfabenzamide after extraction with cell@OA in the presence of Na_2CO_3 as a kosmotrope 133
Figure 4.34: Chromatogram of sulfachloroptridazine after extraction with cell@AA in the presence of NaCl as a chaotrope 134
Figure 4.35: Chromatogram of sulfabenzamide after extraction with cell@AA in the presence of Na_2CO_3 as a kosmotrope 134
Figure 4.36: Response surface plots for kosmotrope extraction efficiency of sulfachloropyradazine using cellulose, with (a) effect of ultrasonication time and mass of sorbent, (b) effect of ultrasonication time and % salt and (c) effect of mass of sorbent and % salt 137
Figure 4.37: Response surface plots for chaotrope extraction efficiency of sulfachloropyradazine using cellulose, with (d) effect of ultrasonication time and mass of sorbent, (e) effect of ultrasonication time and %salt, and (f) effect of mass of sorbent and %salt 138
Figure 4.38: Pareto chart of extraction for sulfachloropyradazine using cellulose 139
Figure 4.39: Response surface plots for kosmotrope extraction efficiency of sulfabenzamide using cellulose, with (a) effect of ultrasonication time and mass of sorbent, (b) effect of ultrasonication time and % salt and (c) effect of mass of sorbent and % salt 141
Figure 4.40: Pareto chart of extraction for sulfabenzamide using cellulose 142
Figure 4.41: Response surface plots for kosmotrope extraction efficiency of sulfachloropyradazine using cell@OA, with (a) effect of ultrasonication time and mass of sorbent, (b) effect of ultrasonication time and % salt and (c) effect of mass of sorbent and % salt 145

© University of Venda

Figure 4.42: Response surface plots for chaotrope extraction efficiency of sulfachloropyradazine using cell@OA with (a) effect of ultrasonication time and mass of sorbent, (b) effect of ultrasonication time and % salt and (c) effect of mass of sorbent and % salt 146

Figure 4.43: Pareto chart of extraction for sulfachloropyradazine using cell@OA 147

Figure 4.44: Response surface plots for kosmotrope extraction efficiency of sulfabenzamide using oxalic acid functionalized cellulose, with (a) effect of ultrasonication time and mass of sorbent, (b) effect of ultrasonication time and % salt and (c) effect of mass of sorbent and % salt..... 149

Figure 4.45: Response surface plots for chaotrope extraction efficiency of sulfabenzamide using Cel@OA, with (a) effect of ultrasonication time and mass of sorbent, (b) effect of ultrasonication time and % salt and (c) effect of mass of sorbent and % salt 150

Figure 4.46: Pareto chart of extraction for sulfabenzamide using cell@OA..... 151

Figure4.47: Response surface plots for kosmotrope extraction efficiency of sulfachloropyradazine using cell@AA, with (a) effect of ultrasonication time and mass of sorbent, (b) effect of ultrasonication time and salt concentration and (c) effect of mass of sorbent and salt concentration 154

Figure 4.48: Response surface plots for chaotrope extraction efficiency of sulfachloropyradazine using adipic acid functionalized cellulose, with (d) effect of ultrasonication time and mass of sorbent, (e) effect of ultrasonication time and salt concentration, and (f) effect of mass of sorbent and salt concentration 155

Figure 4.49: Pareto chart of extraction parameters for sulfachloropyradazine using adipic acid functionalized cellulose 156

Figure 4.50: Response surface plots for kosmotrope extraction efficiency of ssulfabenzamide using adipic acid functionalized cellulose, with (a) effect of ultrasonication time and mass of sorbent, (b) effect of ultrasonication time and salt concentration and (c) effect of mass of sorbent and salt concentration 159

Figure 4.51: Response surface plots for chaotrope extraction efficiency of sulfabenzamideusing adipic acid functionalized cellulose, with (d) effect of ultrasonication time and mass of sorbent, (e) effect of ultrasonication time and salt concentration, and (f) effect of mass of sorbent and salt concentration 160

Figure 4.52: Pareto chart of extraction parameters for sulfabenzamide using Cell@AA 161

© University of Venda

Figure4.53: Proposed mechanism of salting-out of (a) sulfabenzamide and (b) sulfachloropyridazine in the presence of NaCl and salting out (c) sulfabezanamide and (d) sulfachloropyridazine in the presence of Na_2CO_3 162

Figure 4.54: Chromatogram of sulfabenzamide extracted from milk using cellulose as the sorbent 164

Figure 4.55: Chromatogram of sulfabenzamide extracted from milk using cellulose as the sorbent 165

Figure 4.56: Chromatogram of sulfachloropyridazine extracted from milk using cell@OA as the sorbent 167

Figure 4.58: Chromatogram of sulfachloropyridazine extracted from milk using cell@AA as the sorbent 170

Figure 4.59: Chromatogram of sulfabenzamide extracted from milk using cell@AA as the sorbent 172

© University of Venda

List of tables

Table 2.1: Variety of sulfonamides and their medicinal applications 12
Table 2.2: Inlet and outlet concentrations of sulfonamides in wastewater treatment 20
Table 2.3: Extraction methods that have been applied to extract sulfonamides 26
Table 2.4: Adsorption of antibiotics and sulfonamides with different sorbents 28
Table 2.5: Summary of sulfonamide extraction using different sorbents 31
Table 3.1: Experimental parameters for batch adsorption sorbent performance analysis 42
Table 3.2: Experimental conditions and variables for the effects of salt type on sorbent performance for ATPE 45
Table 4.1: Surface area and pore volume analysis of cellulose and functionalized cellulose sorbents 71
Table 4.2: The relative energy (kcal/mol), enthalpies, and free energy for the interactions of cellulose, oxalic acid-functionalized (cell@OA) and adipic acid-functionalized cellulose (cell@AA) with DR1 and DR2 derivatives 74
Table 4.3: Sulfachloropyridazine and sulfabenzamide extraction efficiency using cellulose as the sorbent under various conditions 81
Table 4.4: Sulfachloropyridazine and sulfabenzamide extraction efficiency using cell@OA as the sorbent under various conditions 83
Table 4.5: Sulfachloropyridazine and sulfabenzamide extraction efficiency using cell@OA as the sorbent under various conditions 85
Table 4.6: Extraction efficiency of the cellulose-based sorbent for sulfonamide removal from different matrices 115
Table 4.7: Extraction efficiency of cell@OA sorbent for sulfonamide removal from different 117
Table 4.8: Extraction efficiency of cell@AA sorbent for sulfonamide removal from different matrices 118
Table 4.9: Extraction efficiency of sulfachloropyridazine and sulfabenzamide using cellulose as sorbent under varying conditions 122
Table 4.10: Extraction efficiency of sulfachloropyridazine and sulfabenzamide using cell@OA as sorbent under varying condition 125

© University of Venda

Table 4.11: Extraction efficiency of sulfachloropyridazine and sulfabenzamide using cell@AA as sorbent under varying condition 128
Table 4.12: Extraction efficiency of cellulose-based sorbent for sulfachloropyridazine extraction from different matrices 163
Table 4.13: Extraction efficiency of cellulose-based sorbent for sulfabenzamide extraction from different matrices 164
Table 4.14: Extraction efficiency of cell@OA-based sorbent for sulfachloropyridazine extraction from different matrices 166
Table 4.15: Extraction efficiency of cell@OA-based sorbent for sulfabenzamide extraction from different matrices 168
Table 4.16: Extraction efficiency of cell@AA-based sorbent for sulfachloropyridazine extraction from different matrices 169
Table 4.17: Extraction efficiency of cell@AA-based sorbent for sulfabenzamide extraction from different matrices 171

© University of Venda

Abbreviations

µg L^{-1}	Micrograms per liter
ATPE	Aqueous Two-Phase Extraction
BET	Brunauer–Emmett–Teller
CCD	Central Composite Design
DLLME	Dispersive Liquid-Liquid Micro Extraction
FTIR	Fourier Transform Infrared Spectroscopy
HIV	Human Immunodeficiency Virus
HPLC	High-performance liquid chromatography
LC	Liquid Chromatography
MSPD	Matrix Solid Phase Dispersion
pH	Potential Hydrogen
PLE	Pressurized Liquid Extraction
PXRD	Powder X-Ray Diffraction
QTOF-MS	Quadrupole Time of Flight Mass Spectrometry
QuEChERS	Quick, Easy, Cheap, Effective, Rugged and safe
RSM	Response Surface Methodology
SAs	Sulphonamides
SDZ	Sulfadiazine
SEM	Scanning Electron Microscope
SPE	Solid Phase Extraction
UAE	Ultrasonic Assisted Extraction

© University of Venda

Chapter 1: Introduction

© University of Venda

1.1. Background of the research

Antibiotics have been widely employed in a variety of disciplines, most notably human health care (Chen et al., 2019) and livestock husbandry (Shao et al., 2021). However, antibiotic contamination has become a global concern due to its negative impact on the environment (Bilal et al., 2020; Chaturvedi et al., 2021) and the ecological system (Mehmood et al., 2020; Shukla et al., 2021). Antibiotic misuse promotes the establishment and spreads of antibiotic-resistant bacteria (Mithuna et al., 2024), posing a risk to human health (Tharanyalakshmi et al., 2024). Some of the antibiotics that are responsible for these toxic effects include flouroquinolones (Yang et al., 2021), macrolides (Kovalakova et al., 2020), penicillins (Cizmas et al., 2020) and sulfonamides (McDonald et al., 2020).

This study was focused on sulfonamides, a synthetic (man-made) antibiotic that contains the sulfonamide chemical group. They are also known as sulfa medications (Scott & Njardarson, 2019). Sulfonamides are among the most extensively used antibiotics in the world (Li et al., 2021). This class of compounds is mostly used in primary care medicine to treat urinary tract (Lim et al., 2021) and upper respiratory tract infections (Wong et al., 2021). These medications have remained popular because they are well tolerated by patients with desirable action against common bacterial infections. The chemical structures of sulfachloropyridazine and sulfabenzamide, the sulfonamide antibiotics used in this study, are depicted in Fig. 1.1. Sulfachloropyridazine includes a chlorinated pyridazine ring, whereas sulfabenzamide has a benzamide functional group. Both compounds have a sulfonamide (-SO_2-NH-) component, which is essential for their antibacterial properties.

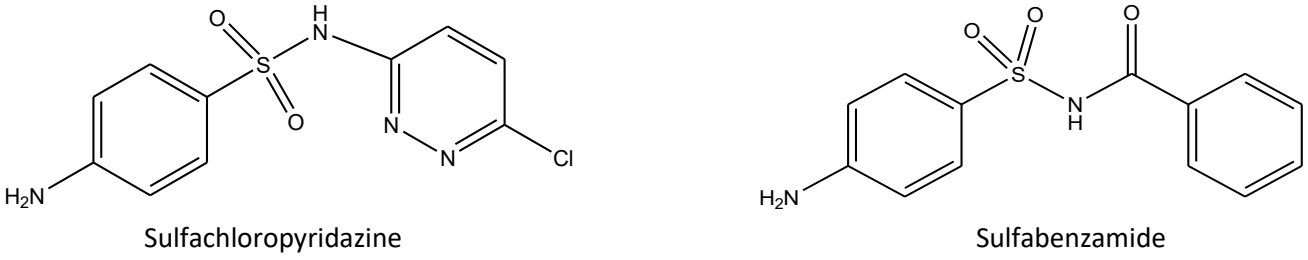


Figure 1.1: Structures of sulfonamide

Sulfonamides have been utilized as preventative agents in chemotherapy for a variety of illnesses (Ovung & Bhattacharyya, 2021). More than 30 medicines with sulfa drug as a functional group

© University of Venda

are in clinical use, with bioactivities which include antibacterial (Das Mahapatra et al., 2024), antifungal (Patra et al., 2024), antiprotozoal (Sepay et al., 2024), anti-inflammatory (Chattopadhyay et al., 2024) and translational initiation inhibitors (Sinha et al., 2024). Sulfonamides have recently been used as anticancer agents (Sadawarte et al., 2021), antiviral HIV agents (El-Gaby et al., 2020), and against Alzheimer's disease (Ammar et al., 2020). They are beneficial in the treatment of ulcerative colitis (Patil et al., 2021), urinary intestinal (Jagrut et al., 2021), and ophthalmic infections, as well as obesity (Rajput et al., 2021). Besides their crucial significance in human medicine, sulfonamides have shown potential in the fields of veterinary and agricultural sciences (Cheong et al., 2020)

As much as sulfonamides are desired for their antibiotic effects, these compounds suffer from poor biodegradability. This would mean that the compounds are not kept in the blood for a long time and are hence easily excreted as faeces and urine by patients. These compounds would subsequently find their way into the aquatic environment yielding antibiotic resistant bacteria (ARB) which is responsible for close to a million deaths per year (Nguyen et al., 2021; Singh et al., 2024). Antibiotics create selective pressure in aquatic habitats, allowing resistant microorganisms to live and multiply (Lajqi Berisha et al., 2024). Bacteria can exchange resistance genes via horizontal gene transfer, particularly in biofilms (Poceva Panovska et al., 2024). Additionally, persistent antibiotic residues contribute to resistance. These resistant bacteria can enter human populations via water, food, or recreational activities, causing serious health dangers (Hajrulai-Musliu et al., 2024). Furthermore, residual sulfonamides can harm aquatic life such as cyanobacteria (Zhou et al., 2022) and fish (Yun et al., 2022), damaging the whole ecosystem. Hence, a variety of remediation methods have been studied by scientists which include QuEChERS (Szarka et al., 2020), matrix solid phase dispersion (Chatzimitakos et al., 2019), pressurized liquid extraction (Moret et al.,2023), dispersive liquid-liquid microextraction (Rykowska et al., 2021), solid phase extraction (Khatibi et al., 2021), and ultrasonic assisted extraction (Mehta et al., 2022).

Several of the sample preparation techniques discussed above have demonstrated high extraction efficiencies under specific conditions. However, their performance can be inconsistent across different sample matrices, target analytes, and operational settings, which may limit their overall applicability for comprehensive antibiotic extraction. Some of the setbacks of these remediation

© University of Venda

methods include high costs (Barp et al., 2023), time-consuming multi-step processes (Khatibi et al., 2021), limited extraction efficiency (Mehta et al., 2022), introduction of analytical errors (Szarka et al., 2020), high power consumption (Patel et al., 2019), low percentage of oil recovery (Picot-Allain et al., 2021), and high dependence on moisture content (Perez-Vazquez et al., 2023). Therefore, there is a dire need for efficient cost-cutting extraction methods for reconcentration, through adsorption of sulfonamides from aquatic systems.

This study is closely aligned with various sustainable development goals (SDGs), particularly those pertaining to environmental sustainability, water quality, and public health. SDG 6: Clean Water and Sanitation is relevant. The extraction of sulfonamides from wastewater tackles water contamination, which is an increasing global concern (Kushwaha et al., 2023). Pharmaceutical pollutants, particularly sulfonamides, endanger human health and aquatic environments (Agarwal et al., 2023). Therefore, this study was directed at improving water quality and lowering pollution from harmful chemicals using biodegradable materials such as cellulose to remove pollutants. Furthermore, functionalizing cellulose with adipic and oxalic acids improves its adsorption properties, allowing for more efficient removal of pharmaceutical pollutants from wastewater (Liyanage et al., 2021). Adipic acid enhances the surface area for interaction, but oxalic acid introduces carboxyl groups that improve cellulose's ability to adsorb sulfonamides, making this strategy both environmentally friendly and very effective in combating water pollution (Bolla et al., 2022). Fig. 1.2 shows the structure of adipic acid

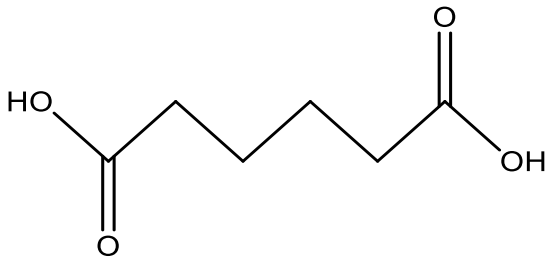


Figure 1.2: Structure of adipic acid

This study also connects to SDG 3: Good Health and Well-being, as pharmaceutical contaminants like sulfonamides in water have been linked to the development of antimicrobial resistance and

© University of Venda

other health risks (Riya, 2021). By developing an efficient method to remove these harmful substances from wastewater, it helps to reduce potential threats to public health which focuses on reducing deaths and illnesses caused by hazardous chemicals and pollution. This study also aligns with SDG 9: Industry, Innovation, and Infrastructure, which promotes sustainable industry and technological innovation. The use of organic acid-functionalized cellulose for wastewater treatment is a novel, ecologically friendly technique that may impact the design of more sustainable water treatment infrastructure positively (Ingrassia et al., 2024). The development of this environmentally benign process for extracting sulfonamides from wastewater adds to worldwide efforts to attain cleaner water, better health, and responsible chemical management, all of which are critical for accomplishing the SDGs.

1.2. Problem statement and motivation of study

Consumption of antibiotics has been on the rise, with usages involving the prevention of bacterial/fungal infections for both humans and animals, and sometimes even applied to promote animal growth (Azzano, 2023). As much as these antibiotics have been helpful, these compounds also exhibit toxic effects to the environment. One class of antibiotics that is notorious for this property are sulfoamides. Sulfonamides possess poor biodegradability and would hence pass through human/animal digestive systems and be excreted via urine and faeces, which subsequently find their way into the aquatic environment (Parashar et al., 2020). Once sulfonamides are in the water environment, they yield antibiotic resistant bacteria (ARB) carrying antibiotic resistance genes (ARGs) which alone is responsible for 700 000 deaths per year (Singh & Sillanpää, 2022; Perveen, 2023; Das et al., 2024). If no thorough action is taken to reduce this carnage, the death toll may reach 10 million per year by 2050 (Capuozzo et al., 2024).

To remediate this problem, extraction methods have been studied to limit the prevalence of toxic antibiotic residues in the environment. Extraction methods such as ultrasonic assisted extraction (UAE), pressurized solvent extraction (PSE), and solid phase extraction (SPE) have been studied. However, these techniques are time consuming and require many organic solvents which lack selectivity. Another form of remediation for dealing with antibiotics that researchers studied utilizes adsorption. These include column adsorption and reduced pressure adsorption. Column adsorption has been avoided by many researchers due to problems associated with clogging

© University of Venda

(Naboulsi et al., 2024). Studies have shown that the incorporation of sand can minimize clogging and improve flow of the analyte solution through adsorbent (Ordonez et al., 2022).

Inorganic, non-biodegradable materials were commonly used as adsorbents or in solid-phase extraction (SPE), but their environmental impact was becoming increasingly concerning. As a result, there has been an increased push to investigate more sustainable alternatives. Although cellulose-based materials have previously been functionalized and used to preconcentrate sulfonamides, this study took a novel approach by using organic acid-functionalized cellulose as a biodegradable and environmentally friendly sorbent for efficient sulfonamide extraction. This study involved comparing two functionalized cellulose materials with unfunctionalized cellulose for the adsorption of sulfonamides using both batch and aqueous two-phase extraction (ATPE) methods. While batch adsorption was applied to wastewater samples, ATPE was specifically employed for the extraction of sulfonamides from complex biological matrices such as milk and honey. Through the aid of chemometric computational methods designs such as central composite design (CCD), the optimal extraction conditions for each technique studied in the extraction of sulfonamides will be assessed.

1.3. Aim of the research

The aim of this study was to apply functionalized cellulose for batch and aqueous two-phase extraction for the adsorption of sulfonamides from wastewater, honey, milk and determined via HPLC-PDA.

1.4. Objectives of the research

- To functionalize cellulose through acid hydrolysis with adipic and oxalic acids and then characterize its physicochemical properties using techniques such as Fourier Transform Infrared Spectroscopy (FTIR), Scanning Electron Microscopy (SEM), X-ray Diffraction (XRD) and Brunauer-Emmett-Teller (BET).

- To investigate the effectiveness of organic acid-functionalized cellulose in extracting sulfonamides from wastewater, honey, and milk as well as its potential for environmental remediation and food safety monitoring.

© University of Venda

- To optimize the extraction parameters for sulfabenzamide and sulfachloropyridazine using Central Composite Design (CCD). For batch adsorption, the optimization focused on time, temperature, and sorbent mass. For aqueous two-phase extraction (ATPE), applied to milk and honey samples, the optimization included ultrasonication time, sorbent mass, salt concentration, and salt type.

- To investigate the extraction effeciency of sulfabenzamide and sulfachloropyridizine, using the optimized conditions and evaluate the nature of intermolecular interaction processes between cellulose and functionalized cellulose with sulfonamides in milk, honey and wastewater. Density Functional Theory (DFT) was used to gain molecular-level insight into the interaction mechanisms between the adsorbents and the target sulfonamides.

© University of Venda

Chapter 2: Literature review

© University of Venda

2.1. Introduction

This chapter examines the fundamental features and applications of sulfonamide antibiotics, as well as their existence in environmental systems, and the issues posed by their toxicological effects and contribution to antimicrobial resistance. Furthermore, it examines methods for their extraction and removal from environmental and food matrices, with an emphasis on adsorption techniques and optimization strategies for efficient removal.

2.2. Physico-chemical properties of sulfonamides and their application as antibiotics

Antibiotics are drugs that either kill or slow the growth of microorganisms (Hussein et al., 2023). They are prescribed by doctors to treat bacterial infections. Antibiotics accomplish this by destroying bacteria and blocking their reproduction (Abbas et al., 2023). They are potent medications that cure certain infections and, when taken correctly, can save lives (Jabbar et al., 2023). They either prevent germs from multiplying or kill them (Jawad et al., 2023).

Sulfonamides (SAs), or sulfa drugs, exhibit specific physico-chemical properties that support their role as effective antibacterial agents. They are weak acids and structurally like para-aminobenzoic acid (PABA), which allows them to inhibit the bacterial enzyme dihydropteroate synthase in folate synthesis, thereby halting bacterial DNA production (Ibrahim et al., 2022). Sulfonamides generally exhibit moderate lipophilicity which enhances their ability to permeate bacterial cells. They also bind to plasma proteins, impacting both their distribution in the body and their bioavailability. These properties contribute to their bacteriostatic action against a broad spectrum of Gram-positive and Gram-negative bacteria (Nguyen, 2020). In clinical applications, sulfonamides are used to treat a range of infections, such as urinary tract infections, respiratory infections, and certain gastrointestinal infections (Ovung & Bhattacharyya, 2021). However, due to increased bacterial resistance, sulfonamides are often used in combination with other agents such as penicillin, trimethoprim and quinolones to enhance their efficacy.

2.2.1. Physico-chemical properties of sulfonamides

Sulfonamides are ammonia benzene sulfonic group derivatives with a benzene ring, para-amino group, and sulfonaphthalamide group chemical structures (Zhou et al., 2022) as shown in Fig. 2.1. Sulfonamides have various characteristics and functions due to their different -R groups and their polarity changes with pH (Yun et al., 2022). Sulfaguanidine (SGM) and sulfasalazine (SSZ) are

© University of Venda

small-molecule sulfonamides that are water-soluble and have a low Henry constant, which can be modestly adsorbed by soil, making them easily dispersed in the environment (Wang et al., 2022). Sulfonamide medications, which are widely used in livestock farming and animal husbandry to treat and prevent illnesses in animals produced for food, milk, eggs, or other products, are soluble in polar solvents such as ethanol, acetone, acetonitrile, and chloroform but insoluble in nonpolar solvents (Noomen et al., 2021). This group has a wide variety of polarity with amphoteric properties (pK 4.6- 11.5) due to the basic character of the para-NH_2 group and due to N-H linkage adjacent to the sulfonyl group. Sulfonamides are invaluable in medical science due to their physicochemical features, such as solubility (Wang et al., 2021), stability (Bu et al., 2021), and reactivity (Yu et al., 2021). These features support their efficiency and extensive application as antibiotics, allowing them to suppress bacterial development and treat diverse diseases.

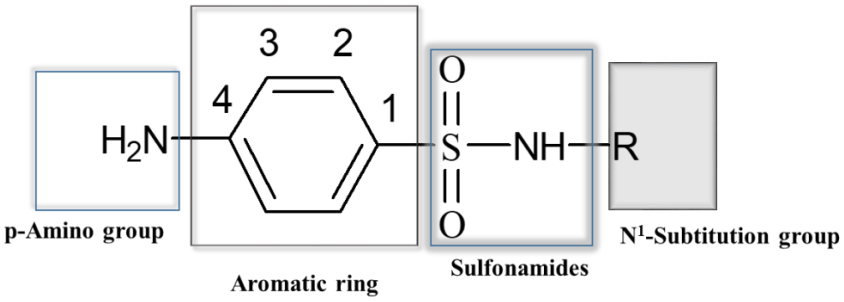


Figure 2.1: General structure of sulfonamide antibiotics

2.2.2. The application of sulfonamides as antibiotics

Sulfonamides are mostly used to treat bacterial infections and some fungal infections. They are especially efficient against urinary tract infections because they tend to concentrate in the urine (Rohilla & Sharma, 2023). Sulfonamides are utilized in the treatment of tonsillitis (Rohilla & Sharma, 2023), inflammatory bowel disease, malaria, skin, eye infections, burns, septicemia, meningococcal meningitis and bacillary dysentery (Ovung & Bhattacharyya, 2021). One example of sulfonamide, sulfaquinoxaline, is used in veterinary medicine to treat coccidiosis in cattle and sheep (Akinci & Albay, 2020).

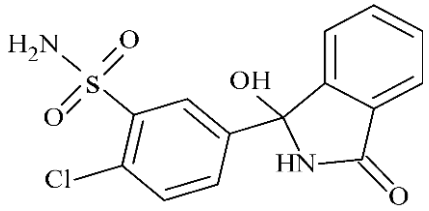
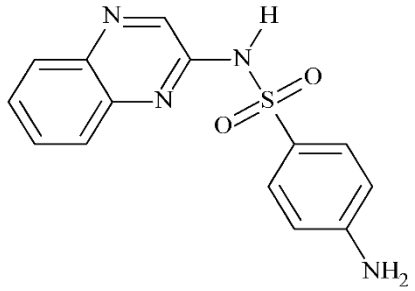
In veterinary practice, sulfonamides have been of benefit as antibiotic agents for several decades and are the fifth most widely used group in veterinary antibiotics in European Union countries, accounting to 2% of sales in 2020 (Lees et al., 2021). Sulfonamides show antimicrobial activity

© University of Venda

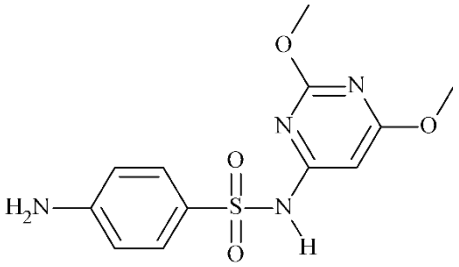
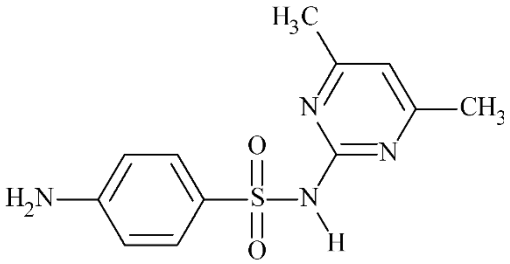
with tri-methoprim, that is why they are frequently co-administered with this compound (Davis, 2024). Among many sulfonamides that have been defined, only a few are approved for animals as veterinary medicine. The most frequently used sulfonamides are sulfadiazine, sulfadimidine, sulfamethoxazole, sulfadoxine and sulfadimethoxine. Sulfonamides and their therapeutic applications include drugs like sulfadimethoxine and sulfasalazine, as shown in Table 2.1 Sulfonamide antibiotics were widely recognized for their efficacy in treating bacterial infections. However, their use raised concerns about their origins and the toxicological effects they exhibited, which had serious consequences for both human health and the environment.

© University of Venda

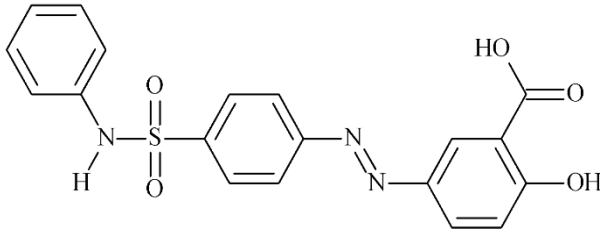
Table 2.1: Variety of sulfonamides and their medicinal applications

Sulfonamide	Function /target of sulfonamide	References
Chlorthalidone 	Improves blood pressure and swelling	Chung et al. (2023)
Sulfaquinoxaline 	Edible tissue	Noak et al. (2019)

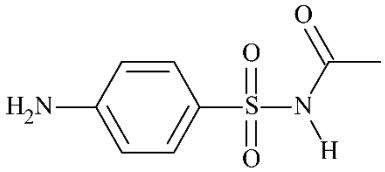
© University of Venda

Sulfadimethoxine	Inhibits bacterial synthesis of folic acid	Amp et al. (2019)
		
Sulfadimidine	Muscle, Liver	Selzer et al. (2019)
		
Sulfasalazine	Rheumatoid arthritis and ulcerative colitis	Choi & Fenando (2020)

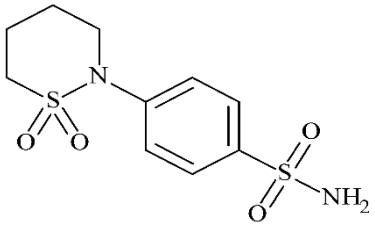
© University of Venda



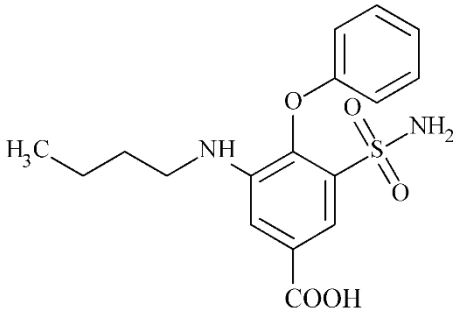
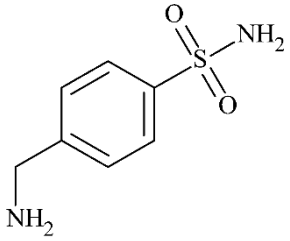
Sulfacetamide | Skin infections | Amp et al. (2019)



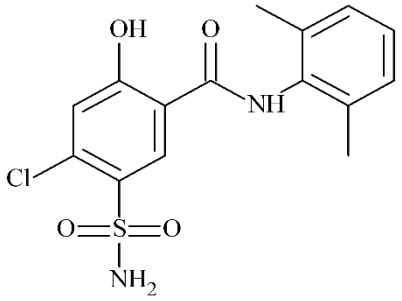
Sultiame | Epilepsy | Powell et al. (2019)



© University of Venda

Bumetanide	Kidney	Noack et al. (2019)
		
Mafenide	Fungus infections	Chung et al. (2023)
		

© University of Venda

Xipamide 	The peritubular capilallaries	Selzer et al. (2019)

© University of Venda

2.3. Sources and toxicological effects of sulfonamides

2.3.1. Sources of sulfonamides antibiotics in the environment

During and after use, a considerable amount of the medication or medicine is removed unmetabolized through urine or feces. However, the human body extensively metabolizes sulfonamides, resulting in the excretion of different metabolites into the environment. (Lean et al., 2020). Some of these metabolites are inert, yet some are still active against bacteria or can easily be converted back to the active sulfonamides compound through either wastewater treatment or microorganisms. Sulfonamides are often used as antibiotics in the treatment of bacterial illnesses in both animals and humans within the human digestive tract (Leal et al., 2020). Once present in the environment, these antibiotics and their metabolites can cause many issues such as antibiotic resistance (ABR) and disruptions in aquatic organisms endocrine and reproductive systems (Amaral et al., 2020; Chaturvedi et al., 2021; Mishra et al., 2023). These contaminants also lead to environmental pollution, which can disrupt the entire ecosystems (Ferreira et al., 2020).

Antibiotics, primarily sulfonamides (Zhou et al., 2022), have been detected in subsurface water, surface water (Yun et al., 2022), sewage treatment plants (Wang et al., 2022), drinking water (Zhou et al., 2022) and many other water settings. The high detection rate of sulfonamides (SAs) in water environments is due to their widespread use and strong their hydrophilicity nature, which indicates that sulfonamides can easily enter any water environment through drainage and rains (Wang et al., 2022). Residual sulfonamides are built in the aquatic environment due to both biodegradation and non-biodegradation mechanisms; their presence encourages the development of drug-resistant strains and has a deleterious influence on animal and plant growth. Sulfonamide antibiotics in the environment were largely found in pharmaceutical waste, agricultural runoff, and inappropriate disposal. These toxins cause toxicological concerns to ecosystems and human health.

2.3.2. Toxicological effects of sulfonamides

Antibiotics are efficient at treating bacterial infections, but they can also cause a variety of adverse effects. Nausea (Ahmed et al., 2020), vomiting (Fouda et al., 2020), diarrhea (Foudah et al., 2020) and abdominal pain (Fouda et al., 2020) are common, less severe symptoms. Antibiotics can also disturb the balance of gut bacteria, potentially leading to fungal diseases like candida or, in more severe circumstances, illnesses such as clostridium difficile infections (Ahmed et al., 2020). Sulfonamide medications can cause severe acute haemolytic anaemia (red cell destruction),

© University of Venda

agranulocytosis, and a decrease in blood platelets. As a result, antibiotics are not always the recommended option because the related toxicological side effects may put the patient in undue danger (Ovung & Bhattacharyya, 2021). Ovung & Bhattacharyya (2021) examined parameters that influence the toxicity of sulfonamides, and these include the drug's duration and dosage, the presence of the heterocyclic ring in N1 substituted sulfonamides, its solubility in blood and other biological fluids, the patient's kidney state, age, and nutritional status. According to a study conducted by El-Gaby et al. (2020), sulfonamides are hazardous to blood cells, with sulfanilamide derivatives being the most toxic among the sulfonamide group while sulfadiazine being the least detrimental. Sulfamethoxazole has the potential to be harmful to the environment, particularly when found near water. Animal toxicity studies have shown that sulfadiazine is less toxic than other sulfonamides, such as sulfadoxine, sulfamethoxazole, sulfapyridine, sulfadiazine, and sulfanilamide. Despite its lower toxicity, sulfadiazine remains highly effective against common pathogens and has been widely used to treat human bacterial infections (Rana et al., 2023).

Sulfonamides have a variety of toxicological consequences on humans, animals, and the environment. Sulfamethoxazole, which is frequently used with trimethoprim, can induce skin rashes (Zhou et al., 2022), anemia (Yun et al., 2022) and severe allergic responses such as Stevens-Johnson syndrome (Wang et al., 2022). Prolonged exposure may potentially cause kidney damage due to crystallization in the renal tubules. In the environment, SMX is extensively identified in water systems and has been demonstrated to disturb microbial communities, contributing to the spread of antibiotic resistance (Dai et al., 2023). Sulfadiazine, another frequent sulfonamide, can induce liver damage, jaundice, and fever in humans, as well as gastrointestinal and kidney damage in animals (Zhou et al., 2022). Environmental contamination, particularly agricultural runoff, has been found to affect soil microorganisms and water quality. In humans, sulfathiazole is linked to hepatotoxicity and renal damage (Song et al., 2023), whereas in animals, it can cause gastrointestinal distress (Yuan et al., 2023) and reproductive toxicity (Duan et al., 2023). Its persistence in water bodies is problematic because it damages aquatic life and leads to the development of antibiotic resistance (Wang et al., 2023).

Sulfamethazine, which is predominantly used in veterinary treatment, has been shown to accumulate in animal tissues, posing risk to human health through the ingestion of infected meat and milk. It also contributes to antibiotic resistance in aquatic habitats by leaching into water

© University of Venda

systems (Yun et al., 2022). Lastly, sulfapyridine, another veterinary sulfonamide, can induce gastrointestinal issues (Zhou et al., 2022), liver damage (Yun et al., 2022), and haematological alterations (Wang et al., 2022) in people. In animals, it has been associated with nephrotoxicity and reproductive problems. Environmental contamination from this sulfonamide also impacts microbial populations, leading to the developing problem of antibiotic resistance.

2.4. Pollution pathways of sulfoamides in wastewater and food samples

2.4.1 Pollution pathways of sulfonamides in wastewater

Antibiotics in wastewater produced in industrial and agricultural activities are eliminated by sewage treatment and are released into water, resulting in variable degrees of pollution of the surrounding aquatic environment (Wang et al., 2022). Antibiotics that have been present in an aquatic environment for a long period might cause genotoxicity and histopathological alterations in a variety of aquatic organisms (Zhou et al., 2022), as illustrated in Fig. 2.2. A significant portion of the medication remains unchanged and is eliminated through excretory mechanisms. These excretions are then released into the environment as manure or sewage (Ovung and Bhattacharyya, 2021). Such observations provide grounds for an investigation into sulfonamide drugs, covering their detection and distribution in the surrounding environment. Table 2.2 displays sulfonamide inlet and outlet concentrations in wastewater treatment.

© University of Venda

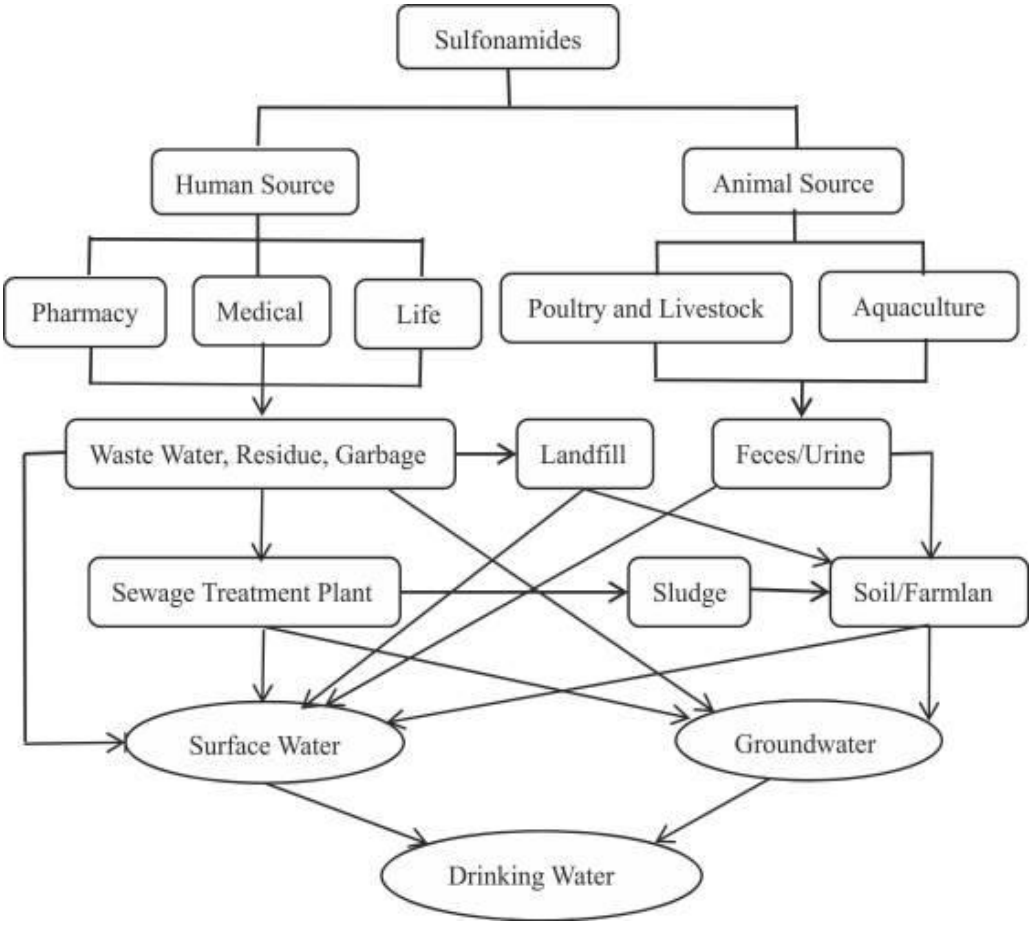


Figure 2.2: Pollution pathways of sulfonamides

Table 2.2: Inlet and outlet concentrations of sulfonamides in wastewater treatment

Sulfonamide	Inlet concentration (μg/L)	Outlet concentration (μg/L)	Removal efficiency (%)	Reference
Sulfapyridine	10	1.40	86.0	Qin et al. (2020)
Sulfamethoxazole	0.31	0.15	51.6	Chen et al. (2020)
Sulfadiazine	10	1.10	88.9	Li et al. (2020)
Sulfamethazine	10	3.20	68.2	Xue et al. (2020)

© University of Venda

2.4.2 Pollution mechanisms of sulfonamides in food samples

An inappropriate use of sulfonamides results in residues in animal-derived foods such as milk and honey. Because of the possible threats to human health, such as antibiotic resistance and allergic reactions, contamination processes and their implications are being actively researched. Sulfonamides enter milk predominantly because of their use to treat mastitis and other diseases in dairy animals (Gao et al., 2024). These antibiotics are given either directly to the udder or systemically. Residues can remain in milk if withdrawal intervals are not rigorously followed. The transfer of sulfonamides to milk is affected by factors such as dosage (Cui et al., 2024), administration route (Chen et al., 2024) and the animal's metabolism (Yang et al., 2024). Testing for residues often involves chromatographic methods like HPLC to ensure levels remain below regulatory limits, which vary globally but are stringent in many regions to protect consumers.

Sulfonamide contamination in honey is commonly caused by treating bee colonies for bacterial illnesses such as European foulbrood (Morariu et al., 2024). These antibiotics are sometimes used illegally or incorrectly, leaving residues in the final honey product. Environmental pH and storage circumstances can impact sulfonamide persistence in honey, making residue detection more difficult (Avasilcai et al., 2024). These residues are monitored and controlled using advanced analytical techniques, such as liquid chromatography with tandem mass spectrometry, in accordance with European and worldwide safety regulations.

2.4.3 Emergence of anti-resistant bacteria as a result of sulfonamide toxicity

The growth of antibiotic-resistant bacteria due to sulfonamide toxicity is a major issue because of the long-term presence in the environment (Bombaywala et al., 2021). Sulfonamides are frequently excreted unmetabolized, resulting in their buildup in agricultural produce via animal dung or wastewater (Aggarwal et al., 2022). These residues infiltrate ecosystems and contribute to the emergence of antibiotic resistance genes (ARGs) in microbial populations. Such genes, such as sul1, are frequently found in bacterial populations exposed to sulfonamide pollution, which raises the predominance of resistant strains over time (Verma et al., 2022).

For instance, studies indicate that even low concentrations of sulfonamides can alter bacterial community structures in biofilms and soil environments, facilitating the horizontal transfer of ARGs (Kergoat et al., 2021). Furthermore, sulfonamide residues in animal dung used as fertilizer might transmit these genes, making the resistance problem broad (Kumar et al., 2024). This is

© University of Venda

exacerbated by the persistence of sulfonamides in various environments due to their chemical stability and resistance to breakdown through commonly used waste treatment methods (Dileep et al., 2024).

2.5. Mechanisms of sulfonamide toxicity and emergence of antimicrobial resistant bacteria

Sulfonamides, as synthetic antibiotics, have been widely used in both human and veterinary medicine, making them ubiquitous in various environmental compartments (Felis et al., 2020). The primary mechanism of sulfonamide toxicity was the inhibition of dihydropteroate synthase, an enzyme essential for bacterial folate synthesis, which slowed bacterial growth (Capasso & Supuran, 2019). However, widespread environmental contamination acted as a selective pressure on bacterial populations, allowing antimicrobial-resistant strains to emerge (Capasso & Supuran, 2019). Bacteria acquired resistance by a variety of processes, including the acquisition of resistance genes generating drug-resistant dihydropteroate synthase variations, enhanced production of efflux pumps to expel the antibiotic and enzymatic alteration or destruction of the sulfonamide molecule (Jhalora & Bist, 2024). These resistance traits could be passed down horizontally among bacterial communities, accelerating the spread of resistance (Jhalora & Bist, 2024).

Furthermore, the persistence of sulfonamides in aquatic environment created ecotoxicological concern to nom-target animals like algae (Duan et al., 2022), crabs (Cui et al., 2022) and fish (Jia et al., 2022) which could destabilize marine ecosystem. Combining sulfonamides with other environmental contaminants, such as heavy metals, can have synergistic or antagonistic effects on aquatic organisms (Du et al., 2024). These findings highlight the need for comprehensive environmental risk assessments and strategies to prevent antibiotic resistance from environmental pollutants.

2.5.1. Emergence of antimicrobial resistant bacteria

Antimicrobial resistance is becoming an increasingly serious hazard to human, animal, and environmental health (Taneja & Sharma, 2019). Overuse of these antibiotics is a major cause of antimicrobial resistance. Another aspect is the absence of new drugs to combat the problem (Arshad et al., 2018). Bacteria can resist antibiotics in two ways: endogenous vertical evolution and exogenous horizontal evolution (Laws et al., 2019). Vertical evolution refers to the acquisition of resistance through spontaneous mutation within the bacterial genome, which is then passed on

© University of Venda

to progeny, whereas horizontal evolution refers to the transfer of resistance genes between unrelated bacteria (Rahman et al., 2019). Bacterial resistance to sulfonamides has been frequently reported with some of the reported resistance cases being due to (i) resistance bacterial genes to trimethoprim-sulfamethoxazole (used as prophylaxis for the treatment of severe respiratory tract infections) (*Pneumocystis carinii*) (Ovung & Bhattacharyya, 2021), (ii) resistance genes to sulfadiazine resulted in phenotypic conversion showing a lack of sensitivity to polymyxin B for *Serratia marcescen* (Huemer et al., 2020), (iii) resistance bacterial genes to sulfonamides spread and distributed in soils and were detected around poultry farms in China (Brugger et al., 2020), (iv) resistance bacterial genes to sulfonamides discovered in environment (Zinkernagel et al., 2020), and (v) trimethoprim-SN resistance spread among pathogenic bacteria (Mairpady Shambat et al., 2020). With antibiotic resistance to sulfonamide medications rising, significant effort must be put into developing new and effective antibiotics (Ovung & Bhattacharyya, 2021). Sulfonamides can be extracted using different extraction methods such as dispersive liquid-liquid microextraction (DLLME), matrix solid phase dispersion (MSPD), pressurized liquid extraction (PLE) and QuEChERS.

2.6. Extraction techniques for analysis of sulfonamides

Sulfonamide extraction methods are required for assessing a wide range of matrices, including food, water, and biological materials. These approaches allow for the isolation and concentration of sulfonamides from complicated mixtures, ensuring precise detection and quantification in environmental and pharmaceutical studies. Dispersive liquid-liquid extraction microextraction (DLLME), a miniature liquid-liquid extraction method, requires fewer organic solvents (Dmitrieva et al., 2020). For example, DLLME was successfully used by researchers to detect sulfonamide residues in milk samples (Dluhošová et al., 2024). However, it has drawbacks such as numerous extractions and long extraction times (Rykowska et al., 2021). QuEChERS, is a simple approach that involves initial partitioning and extract clean-up with dispersive solid-phase extraction (Morais et al., 2018). This method is commonly used for extracting sulfamethazine and sulfamethoxazole from fruits and vegetables (Yang et al., 2024). Despite its ease of use and popularity, QuEChERS has several shortcomings. It is less successful for non-polar chemicals, which had low extraction efficiency (Zhou et al., 2024). The approach also suffers from matrix effects, which frequently necessitate additional cleanup processes to increase accuracy and eliminate interference. In some complicated matrices (Yu et al., 2024), QuEChERS does not

© University of Venda

accomplish complete extraction, resulting in decreased recoveries for specific chemicals (Meng et al., 2024). While the technique was simple, it required physical manipulation, such as shaking and vortexing, which add variability to the findings.

Matrix solid phase dispersion (MSPD) is widely used to extract chemical elements from plants, as well as organic pollutants from food and environmental samples (Chatzimitakos et al., 2019). MSPD had its own set of limitations. The process is time-consuming, particularly during sample preparation and clean-up stages (Zgoła-Grześkowiak et al., 2024), and the solid-phase materials used is typically single-use, increasing operational costs (Grześkowiak et al., 2024). Sample losses frequently occurr during grinding and dispersion steps, which impact analytical accuracy (El-Deen, 2024). Furthermore, MSPD require specialized equipment and skilled personnel to ensure consistent results, and the extraction conditions often need rigorous optimization for different matrices, making the method labor-intensive and challenging to standardize. It was used to detect sulfadiazine and sulfathiazole in meat and fish products. Pressurized liquid extraction (PLE), also known as accelerated solvent extraction (ASE), used high temperatures (50-200°C) and pressures (500-3000 psi) to keep the solvent liquid for short period (5-10 min) (Barp et al., 2023). PLE was successful in extracting sulfonamides from soil and sediment matrices (da Silva et al., 2020). Although it is a green technology, its drawbacks were expensive equipment costs and the requirement for precise parameter adjustment, such as temperature and pressure (Moret et al., 2023).

Solid-phase extraction (SPE) is used to separate, enrich, and purify components from aqueous solutions depending on their physical and chemical characteristics (Patel et al., 2019, Badawy et al., 2022, Suseela et al., 2023). Researchers used SPE to identify sulfonamide residues in wastewater and river water samples (Cui et al., 2021). However, this approach is solvent and time-intensive, posing automation issues such as uneven flow and cartridge clogging (Panchal et al., 2021). Ultrasonic-assisted extraction (UAE) uses ultrasonic energy and solvents to extract target chemicals from plant matrices (Kumar et al., 2021). UAE was used to investigate sulfonamides in honey and milk (Ashraf et al., 2024), but it faced several problems, including costly costs, potential unwanted molecular alterations, and the necessity for optimization (Mehta et al., 2022). Table 2.3 highlights the numerous sulfonamide extraction methods used, including the disadvantages of each, the types of sulfonamides extracted, concentration ranges, and pertinent references. This

© University of Venda

comparison demonstrates the adaptability and limitations of several methods for isolating sulfonamides from various matrices.

© University of Venda

Table 2.3: Extraction methods that have been applied to extract sulfonamides

Extraction method	Disadvantages	Type of sulfonamides extracted	Concentration	Sample	Reference
Matrix solid phase dispersion (MSPD)	Additional purification is usually required	Sulfadiazine	50 µg/kg to 500 µg/kg	Meat	Chatzimitakos et al. (2019)
Pressurized solvent extraction (PSE)	High cost of the equipment	Sulfathiazole	50 µg/kg to 500 µg/kg	Animal tissue	Picot-Allain et al. (2021)
Solid phase extraction (SPE)	Time consuming Blocking the cartridges	Sulfapyridine	1 ng/L to 500 ng/L	Wastewater	Khatibi et al. (2021)
Pressurized liquid extraction (PLE)	Requires high pressure Expensive	Sulfadimethoxine	10 ng/g to 1 µg/g	Fish tissue	Moret et al. (2023)
Ultrasonic assisted extraction (UAE)	Require optimization Expensive	Sulfamethazine	10 ng/L to 1 µg/L	Milk	Mehta et al. (2022)
QuEchERS	Extraction efficiency is low	Sulfamethoxazole	10 µg/kg	Vegetables	Szarka et al. (2020)
Dispersive liquid-liquid Microextraction (DLLME)	An additional solvent is required	Sulfamethoxazole	5 µg/L	Wastewater	Rykowska et al. (2021)

© University of Venda

2.7. Adsorption of sulfonamides using on batch and aqueous two-phase extraction

2.7.1. Batch adsorption

Batch adsorption is the process of mixing a set amount of adsorbent with a solution containing the target solute, allowing the solute to accumulate to the adsorbent's surface over time (Sazali et al.,2020). The batch adsorption process has been widely used for separating and purifying biomolecules, contaminants and pollutants. Batch extraction has long been a popular and effective method for eliminating pollutants from both natural and synthetic wastewater (Morin-Crini et al., 2022). Solid adsorbents, such as activated carbon (Ajala et al., 2023), alumina (Akinnawo et al., 2023), or modified clays (Bamisaye et al., 2023), have long been employed to capture target molecules on their surfaces. As summarized in Table 2.4, different adsorbents have been utilized for the removal of various antibiotics and sulfonamides: activated carbon was used for tetracycline, alumina for sulfamethoxazole, modified clays for ciprofloxacin, and coconut-shell biochar for a range of sulfonamides including sulfadiazine, sulfamethazine, and sulfamethoxazole. Due to its high surface area and porosity, activated carbon was effectively employed to adsorb tetracycline from wastewater (Ajala et al., 2023). Alumina was used to remove sulfamethoxazole, indicating a significant affinity for sulfonamides under acidic conditions (Akinnawo et al., 2023). Organo-clays and other modified clays were used to adsorb ciprofloxacin, demonstrating their ability to bind antibiotics through hydrophobic and electrostatic interactions (Bamisaye et al., 2023). Coconut-shell biochar activated with KOH and magnetically modified with $FeCl_3$ showed strong adsorption capabilities for sulfonamide antibiotics, such as sulfadiazine (Sun et al., 2022), sulfamethazine (Zheng et al., 2022), and sulfamethoxazole (Xiao et al., 2022). Batch adsorption relied heavily on parameters such as pH, temperature, adsorbent dose, and starting adsorbate concentration (Raj & Krishnan, 2023). Scientists adopted the batch adsorption procedure to determine the viability of adsorbent-adsorbate systems because it was simple, easy, and cost-effective (Patel, 2022). Table 2.4 displays the adsorption capabilities of several sorbents for antibiotics and sulfonamides.

© University of Venda

Table 2.4: Adsorption of antibiotics and sulfonamides with different sorbents

Sorbent	Sulfonamides/antibiotics	Reference
Activated carbon	Tetracycline	Ajala et al. (2023)
Alumina	Sulfamethoxazole	Akinnawo et al. (2023)
Modified clays	Ciprofloxacin	Bamisaye et al. (2023)
Coconut-Shell Biochar	Sulfadiazine, Sulfamethazine, Sulfamethoxazole	Sun et al. (2022)

2.7.2. Aqueous two-phase extraction

ATPE is a straightforward separation process that combines equilibration, phase separation, and solute concentration all in one step (Chong et al., 2020). It was regarded as environmentally friendly since users could choose phase-forming components such as alcohols (Chong et al., 2020), polyethylene glycol (Stefanova et al., 2020), and salts (Zhang et al., 2020). For example, sulfamethoxazole was extracted with good selectivity and efficiency using polyethylene glycol (PEG) and phosphate salt. Similarly, PEG-citrate aqueous two-phase systems successfully recovered tetracycline, confirming the method's ability to separate antibiotics from trash. Magnetic nanoparticles were also used in ATPE systems to remove sulfonamides such as sulfadiazine, allowing for facile nanoparticle recovery by magnetic separation. Table 2.5 summarizes the use of different sorbents such as PEG-phosphate, PEG-citrate, and magnetic nanoparticles in ATPE systems for extracting sulfamethoxazole, tetracycline, and sulfadiazine, as reported by recent studies.

ATPE has several advantages, including high capacity (Singla & Sit, 2023), low interfacial tension (Chao and Shum, 2020), high yield (Singla & Sit, 2023), high selectivity (Albertsson et al., 2020), reduced processing time and energy requirements (Leong et al., 2021), and scalability (Yao et al., 2024). It also allowed continuous processing, and typical organic-aqueous phase extraction equipment and processes could be easily applied to ATPE (Singla & Sit, 2023). Extraction in ATPE environments was controlled by molecule size, hydrophobicity, and electrostatic

© University of Venda

interactions, making it perfect for separating proteins, enzymes, and tiny chemical compounds (Singla & Sit, 2023).

ATPE isolates and purifies biomolecules by using two immiscible aqueous phases. When a combination was poured into a separatory funnel, it spontaneously divided into two layers: an organic phase on top and an aqueous phase on the bottom. Biomolecules were divided into various phases based on their physicochemical features, including hydrophobicity, charge, and size. Molecules attracted to the organic phase tended to rise to the surface, whereas those attracted to the aqueous phase remained at the bottom. This separation enabled the selective isolation of certain biomolecules. Once the layers had developed, the phase containing the target analyte could be separated for further analysis or processing. The technique's efficiency stemmed from its capacity to gently separate biomolecules, keeping their structure and functionality while allowing for purification based on their unique interactions with the two phases. ATPE was an invaluable tool in a variety of biochemical and medicinal applications requiring selective separation (Liu et al., 2020).

In this study, organic acid-functionalized cellulose was incorporated into the ATPE system as a hybrid material with dual functionality. It served not only as a partition modifier, influencing the distribution of sulfonamides between the two phases, but also as a solid-phase sorbent within the extraction environment. The functionalized cellulose introduced active carboxyl and hydroxyl groups that interacted selectively with sulfonamide molecules through hydrogen bonding and electrostatic interactions. These interactions enhanced the partitioning of target sulfonamides (such as sulfabenzamide and sulfachloropyridazine) into the preferred phase, thereby improving extraction efficiency. This integration of cellulose into the ATPE system created a hybrid separation mechanism that combined the selectivity of adsorption with the tunability of phase separation, making the process more effective for antibiotic remediation from complex aqueous matrices. Fig. 2.3 depicts a schematic of the aqueous two-phase extraction (ATPE) method for biomolecule purification.

© University of Venda

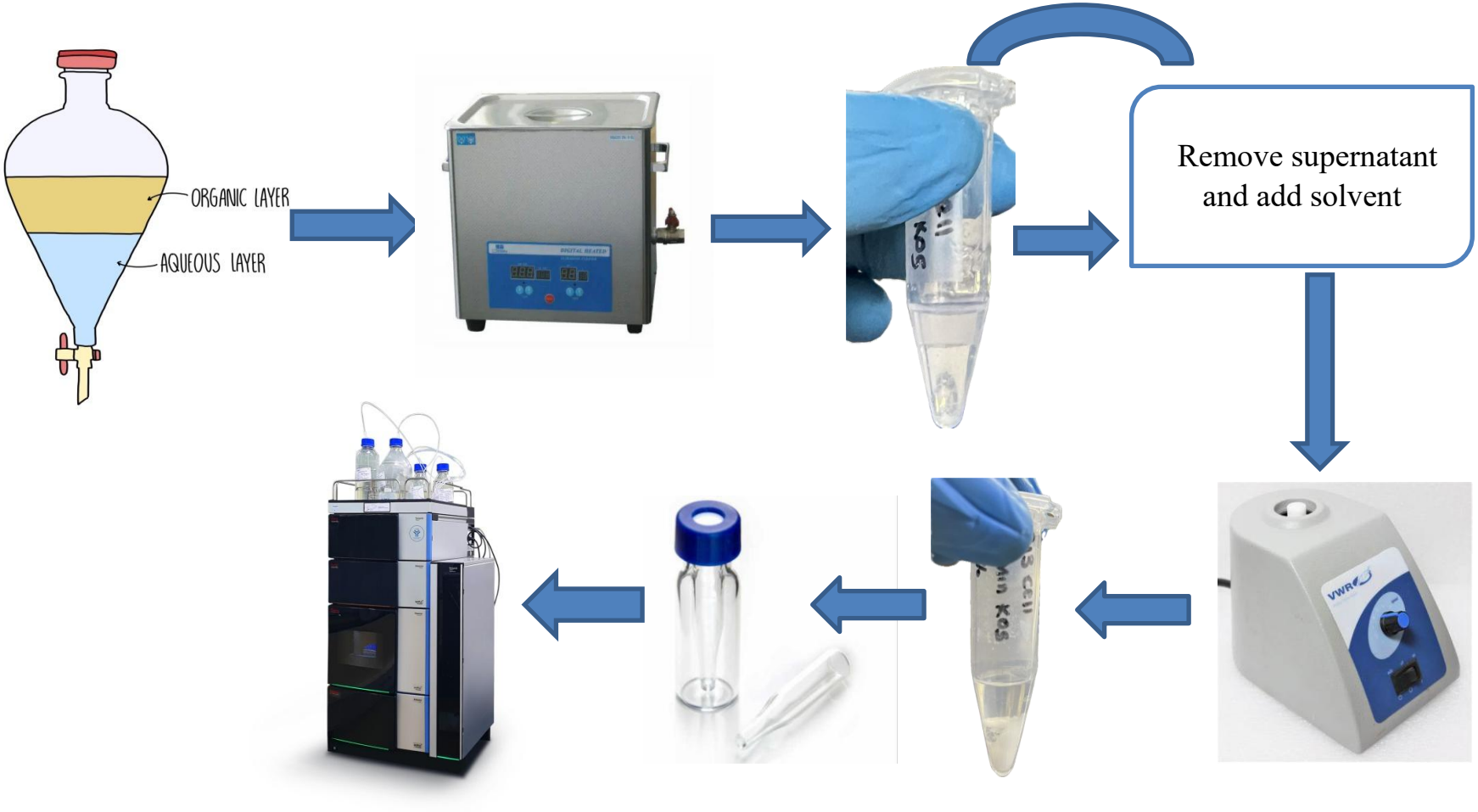


Figure 2.3: A schematic of the aqueous two-phase extraction

© University of Venda

Table 2.5: Summary of sulfonamide extraction using different sorbents

Sorbent	Sulfonamide	Reference
PEG-phosphate system	Sulfamethoxazole	Stefanova et al. (2020)
PEG-citrate system	Tetracycline	Zhang et al. (2020)
Magnetic nanoparticles in ATPE	Sulfadiazine	Singla and Sit (2023)

2.8. Optimization

Optimization is a process of enhancing the efficiency of a specific product, method, or system to produce the optimal response for measurement (Bezerra et al., 2021). This method is critical across fields, including engineering, economics, artificial intelligence (AI), and operations research. Optimization improves decision-making, resource allocation, cost reduction, and strategy planning in both basic and complex systems. Different types of optimization approaches cater to various applications; for example, linear programming is appropriate for simple relationships, but nonlinear programming is required for more complex scenarios. The goal of optimization is to create optimal design in relation to a collection of prioritized criteria or constraints. These include qualities such as productivity, strength, dependability, lifespan, efficiency, and usage (Novaes et al., 2021).

Optimization is especially important in the energy sector, as it aids in the integration of renewable resources such as wind and solar into power grids and allows for consistent energy management despite weather fluctuation (Zhou and Zhang, 2021). In healthcare, optimization models have improved patient scheduling, resource allocation, and emergency response planning, as evidenced by its use during the COVID-19 pandemic to manage key supplies such as ventilators and hospital beds (Yang et al., 2022). Extraction of sulfonamides can be optimized using a variety of approaches, including univariate and multivariate optimization.

2.8.1. Univariate vs multivariate optimization

Univariate and multivariate optimizations are important tools in mathematical modeling and machine learning, allowing you to optimize functions with one or more variables, respectively. Univariate optimization optimizes only one variable, reducing the task to finding a maximum or minimum point along a single axis (Bärmann et al., 2023). This makes univariate methods

© University of Venda

computationally efficient and simple to apply, as they use techniques such as line search or derivative-based methods where possible. However, univariate optimization is restricted to simpler situations in which only one component influences the output (Islam, 2022).

Multivariate is a strong nonlinear steady-state flowsheet simulation technique that is commonly utilized in the chemical process industry to enhance plant performance by boosting plant capacity or lowering energy consumption (Cerqueira et al., 2021). Multivariate optimization, on the other hand, works with functions that involve several variables, making it perfect for more complex models where multiple factors influence the outcome. Gradient descent, conjugate gradient, and Newton's methods enable efficient navigation through high-dimensional spaces in fields such as machine learning, economics, and engineering (Diwekar, 2020). The complexity of multivariate optimization necessitates higher computational demands but advances in computing power and algorithmic efficiency have significantly expanded their applicability in recent years, allowing researchers and practitioners to effectively handle large-scale, multidimensional datasets (Goodfellow et al., 2020).

2.8.2. Importance of RSM and CCD

Response Surface Methodology (RSM) and Central Composite Design (CCD) are important statistical techniques used in experimental design to optimize processes and make better decisions. RSM is a typical mathematical and statistical tool for modelling and evaluating a process in which the response of interest is influenced by several variables (Tirado-Kulieva et al., 2021). RSM is used to model and analyze the interactions between numerous independent factors and one or more dependent variables, assisting in the identification of the ideal circumstances that produce the best results while minimizing mistakes and variability in experimental data (Rigdon et al., 2022). RSM is especially effective in industries like pharmaceuticals, manufacturing, and food processing, where accuracy is required for quality control and process development. RSM is very useful to optimize variables/factors more practically as compared to just the statistical significance test for a particular point (point estimate is the statistical jargon) (Vamsi, 2022).

CCD is the most used fractional factorial design used in the response surface model (Bhattacharya, 2021). It is an effective approach to investigate quadratic models, making it excellent for situations in which the connection between variables is not linear. Central composite design is important because it creates orthogonal blocks, letting model terms and block effects be estimated independently and minimizing the variation in the regression

© University of Venda

coefficients (Loy et al., 2022). Central composite design is made up of a factorial or fractional factorial design with additional "star" points for estimating quadratic effects. This architecture aids in obtaining a more accurate model of the process while minimizing the number of experimental runs compared to standard methods (Xia et al., 2021). In this study, both Response Surface Methodology (RSM) and Central Composite Design (CCD) were employed to optimize experimental parameters and model the interactions between variables, ultimately enhancing the reliability and efficiency of the extraction and adsorption processes.

2.9. Theory of characterization techniques

2.9.1. Fourier Transform Infrared Spectroscopy (FTIR)

FTIR is a potent analytical method for identifying functional groups and molecular interactions in materials by measuring the absorption of infrared radiation at various wavelengths (Siddique, 2024). The approach is based on the vibrational transitions of chemical bonds within molecules when exposed to IR radiation, which provide a spectrum distinct to specific functional groups (Smith, 2020). FTIR spectra gives qualitative and semi-quantitative data on chemical composition, the presence of organic or inorganic moieties, and proof of successful functionalization or chemical changes (Cichy et al., 2025). This approach is commonly used in materials research to study surface chemistry and molecular interactions.

2.9.2. Brunauer-Emmett-Teller (BET) surface area analysis

BET analysis quantifies the specific surface area of porous and non-porous materials by measuring the physical adsorption of gas molecules (usually nitrogen) onto the sample surface at liquid nitrogen temperature (77 K) (Bardestani et al., 2019). The BET theory extends the Langmuir adsorption model to multilayer adsorption, enabling determination of surface area, pore volume, and pore size distribution (Patience et al., 2019). Measurement provides insights into the porosity and surface characteristics of materials, which are essential parameters influencing adsorption capacity, catalytic activity, and other surface-dependent properties (Kaliaguine et al., 2019).

2.9.3. X-ray diffraction (XRD)

XRD is a nondestructive technique for determining the crystallographic structure, phase identification, and degree of crystalline (Ali et al., 2022). When monochromatic X-rays strike a crystalline sample, constructive interference occurs as per Bragg's equation ($n\lambda = 2d \sin\theta$), where λ is the X-ray wavelength, d is the interplanar spacing, and θ is the diffraction angle

© University of Venda

(Sequeira, 2022). The resulting diffraction pattern is unique to the material's crystalline phases. XRD is useful for detecting changes in crystal structure following chemical treatments or synthesis procedures, indicating the production of new phases or structural modifications (Khan et al., 2020).

2.9.4. Scanning electron microscopy (SEM)

SEM provides high-resolution imaging of material surfaces by scanning a focussed electron beam across the sample (Mohammed and Abdullah, 2018). The interaction of electrons with the sample surface produces secondary electrons, which are then detected to give detailed topographical images (Nohl et al., 2022). Surface morphology, particle size, shape, and texture can all be examined with SEM, allowing for visualization of the microstructure and morphology of synthetic materials.

© University of Venda

Chapter 3: Materials and methods

© University of Venda

3.1. Introduction

This chapter details the functionalization of cellulose using adipic and oxalic acids to enhance its adsorption efficiency for removing sulfonamides from wastewater and food samples. The functionalized cellulose was characterized using a range of analytical techniques. X-ray diffraction (XRD) was employed to evaluate changes in crystallinity, while fourier-transform infrared spectroscopy (FTIR) confirmed the introduction of functional groups. Brunauer-Emmett-Teller (BET) analysis determined surface area and porosity, and scanning electron microscopy (SEM) examined surface morphology. Batch adsorption experiments were conducted specifically for wastewater samples to evaluate the material's adsorption performance. Key parameters such as adsorption time, sorbent mass, and temperature were investigated. In contrast, aqueous two-phase extraction (ATPE) was employed for the optimization of biological samples, including milk and honey, by adjusting factors such as sorbent mass, sonication time, salt concentration, and salt type. This integrated approach enabled a comprehensive assessment of the material's adsorption and extraction efficiency across different sample matrices, providing valuable insights into its potential application for sulfonamide removal from both environmental and biological systems.

3.2. Chemicals and reagents

The reagents used in this study were of analytical or chromatographic grade. Oxalic acid, adipic acid, cellulose, sodium chloride, and sodium carbonate were purchased from Rochelle Chemicals (Johannesburg, South Africa). Sulfonamide standards, sulfabenzamide and sulfachloropyradazine, were obtained from Associated Chemical Enterprises (Johannesburg, South Africa) and Sigma-Aldrich (Johannesburg, South Africa), respectively, and were used as standards in the analysis for batch and ATPE adsorption. Ethanol, methanol, and deionized water of HPLC/PDA grade were sourced from Van waters and rogers (VWR) (Midrand, South Africa). Deionized water was further purified using a Milli-Q system (Guyancourt, France).

3.3. Equipment

The chromatographic measurements were conducted using a Shimadzu LC-2030C 3D Plus series HPLC system, designed to withstand a maximum pressure of 63 MPa. The system was equipped with a photodiode array (PDA) detector to ensure accurate and sensitive detection across a broad wavelength range. Samples were prepared through hydrothermal treatment, utilizing an autoclave and an oven manufactured by Scientific Engineering (Roodepoort, Johannesburg). To ensure uniformity and complete mixing of the samples, a Eins-Sci

© University of Venda

Laboratory vortex mixer (Steeledale, Johannesburg) was used, followed by sonication with a sonicator provided by Labotec (Midrand, Johannesburg). These steps were essential for achieving consistent sample preparation and enhancing the reproducibility of the analytical results.

3.4. Sample preparation

A simplified methodology for functionalization of cellulose is summarized in Fig. 3.1. In this process, 1 g (0.006 mol) of cellulose was combined with either 2 g (0.014 mol) of adipic acid or 1.2 g (0.014 mol) of oxalic acid. This step aimed to create a balanced chemical mixture of 1:2 moles of cellulose to the organic acid (oxalic/adipic acid). The resulting mixture was then ground to a fine powder using a mortar and pestle to achieve homogeneity, ensuring uniformity for subsequent steps. Thereafter, 50 mL of distilled water was added to the ground mixture. The mixture was transferred into an autoclave, exposing it to high-pressure and high-temperature treatment to facilitate chemical reactions. During the autoclaving procedure, the sample was heated in an oven while optimizing temperature (50, 80, and 100°C) and time (30 and 60 min). the mixture was then filtered to separate the solid residues from the liquid. The solid residue obtained was then left to dry at room temperature. The dried material was then subjected to characterization using advanced analytical techniques, including FTIR, to analyze functional groups, XRD to determine the crystallinity structure of the sorbent, SEM to study surface morphology, and BET analysis to determine surface area and porosity. These techniques provided a comprehensive understanding of the material's structural, chemical, and morphological properties to confirm its suitability for the intended application.

© University of Venda

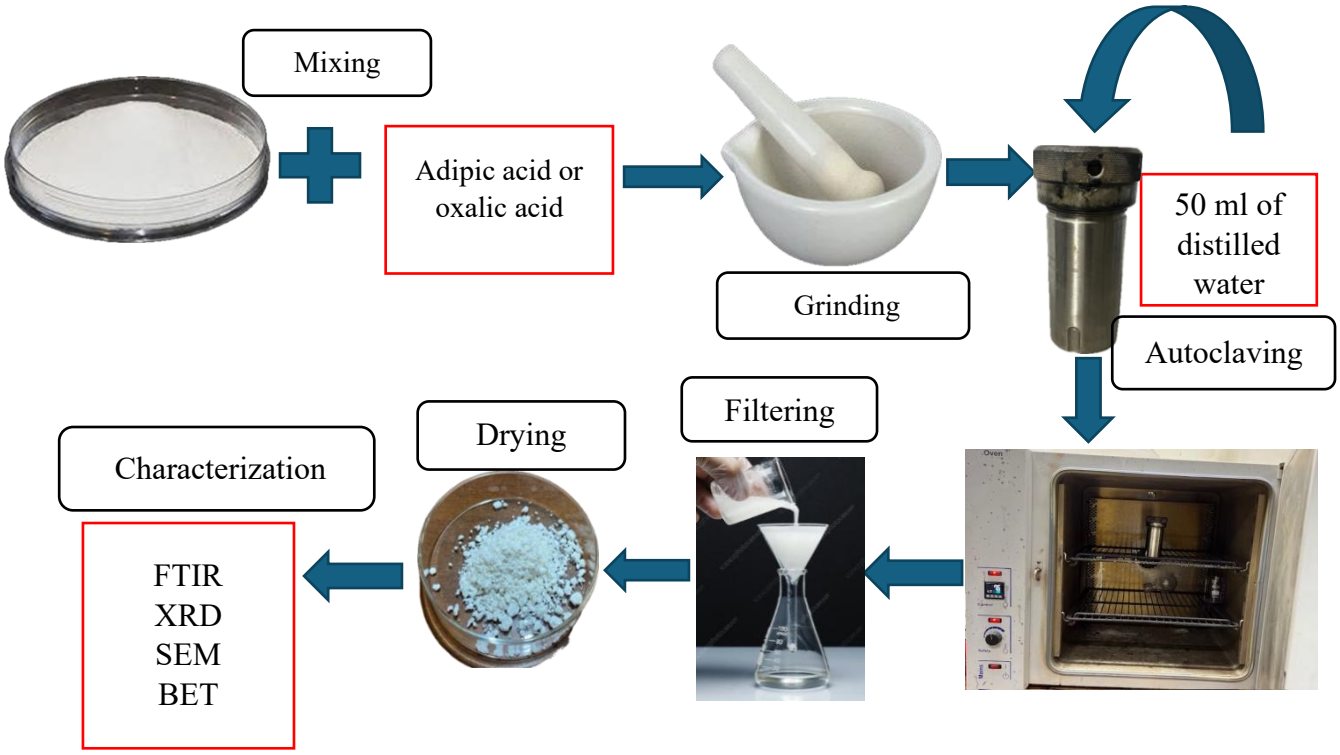


Figure 3.1: Simplified methodology for the functionalization of cellulose

3.4.1. Functional group analysis

FTIR analyses were performed using a PerkinElmer Spectrum 65 FTIR spectrometer equipped with an Attenuated Total Reflection (ATR) accessory. Approximately 2 mg of each sample, including cellulose, cellulose functionalized with adipic acid (cell@AA), and cellulose functionalized with oxalic acid (cell@OA) were analyzed on the FTIR. The spectra were recorded in the range of 500–4000 cm^{-1} at a resolution of 4 cm^{-1}, with 32 scans per minute averaged for each sample to improve the signal-to-noise ratio. Background spectra were collected prior to sample analysis using a clean ATR crystal to eliminate atmospheric interference. The spectrometer was calibrated using a standard polystyrene film to ensure accuracy. Absorption bands were analyzed to identify characteristic functional groups, and the results were compared to confirm the successful functionalization of cellulose.

3.4.2. Crystallinity analysis

PXRD analyses were carried out using a Bruker D8 Advance X-ray diffractometer equipped with a Cu-Kα radiation source (λ = 1.5406 Å). The samples, including cellulose and its functionalized derivatives, were finely ground and placed on a flat sample holder. Scans were conducted over a 2θ range of 5° to 80° at a step size of 0.02° and a scanning rate of 2° min^{-1}.

© University of Venda

Instrument calibration was performed using a standard silicon reference material to ensure accurate peak positions. Diffraction patterns were analyzed to identify crystalline phases and changes in the crystallinity index, particularly the impact of functionalization on cellulose structure.

3.4.3. Surface morphological studies

The surface morphology of the sorbent materials (cellulose and its functionalized derivatives) was studied using a JEOL JSM-7600F field emission SEM. The samples were coated with a thin layer of gold using a sputter coater to enhance conductivity and image quality. Micrographs were captured at an accelerating voltage of 15 kV with magnifications ranging from 340X to 1850X. The analysis focused on identifying morphological changes, such as roughness or porosity, introduced by functionalization with adipic and oxalic acids. The results provided insights into the surface characteristics and structural integrity of cellulose and its functionalized derivatives.

3.4.4. Surface area analysis

A Micromeritics ASAP 2020 surface area and porosity analyzer were used to examine the specific surface area, pore volume, and pore size distribution of cellulose and its functionalized forms. Before analysis, samples were degassed under vacuum at 120°C for 12 h to eliminate moisture and contaminants, assuring reliable adsorption results. Nitrogen gas adsorption-desorption isotherms were measured at 77 K with relative pressures ranging from 0.05 to 0.35. The specific surface area was calculated using the BET equation for the linear component of the isotherm, and the pore size distribution was assessed using the Barrett-Joyner-Halenda (BJH) method. The study sought to discover changes in surface area and porosity caused by functionalization with adipic and oxalic acid, to gain insight into the changed cellulose materials' textural qualities and possible reactivity.

3.4.5. Computational methods

Density Functional Theory (DFT) simulations were used to acquire molecular-level insight into the mechanisms of interaction between organic acid-functionalized cellulose and sulfonamide molecules. All computations were completed with the Gaussian 16 software suite. The B3LYP exchange-correlation functional was used in conjunction with the 6-31G(d,p) basis set to optimise the molecular geometries of the functionalised cellulose and sulfonamide. Frequency calculations were used to establish the optimised structures' stability as real minima on the

© University of Venda

potential energy surface. To back up the experimental extraction results and further understand the affinity between the extractant and target sulfonamides, frontier molecular orbital (FMO) analysis and interaction energy calculations were carried out.

3.5. Multivariate optimization

Central Composite Design (CCD), in conjunction with Response Surface Methodology (RSM), was used to optimize the experimental conditions for the efficient adsorption of sulfachloropyridazine and sulfabenzamide onto the functionalized cellulose. CCD was chosen because of its capacity to efficiently investigate response surfaces and assess the impacts of process factors. The experimental design and statistical analysis were carried out using Design-Expert® software (version 13, Stat-Ease Inc., Minneapolis, USA). A three-factor, five-level CCD was applied, involving three independent variables: adsorption time, sorbent mass, and temperature. The design consisted of 20 experimental runs, including 8 factorial points, 6 axial (star) points, and 6 center points to ensure the precision and reproducibility of the model. This design facilitated the development of a second-order polynomial equation that described the relationship between the input factors and the response variable adsorption efficiency allowing for accurate prediction of the optimal conditions for sulfonamide removal from wastewater. The design featured factorial, axial, and center points to provide accurate modeling and outcome prediction. The experimental data were examined using regression analysis to create a second-order polynomial model, and the model's significance was validated using Analysis of Variance (ANOVA). Response surface plots and contour maps were created to show how variables interact and anticipate optimal circumstances. The combined CCD-RSM technique allowed for a thorough understanding of process behavior, resulting in the development of parameters that enhance functionalization efficiency and improve surface features while preserving the structural integrity of the cellulose material.

3.6. Adsorption studies

3.6.1. Preparation and functionalization of cellulose

A standard solution of sulfonamides was prepared by dissolving 5 mg of sulfabenzamide and sulfachloropyridazine in 100 mL of methanol, yielding a concentration of 50mg L^{-1}. The solution was stirred thoroughly until the sulfonamide standards were completely dissolved. A Central Composite Design (CCD) was employed to optimize the extraction conditions, as presented in Table 3.1. The mass of the sorbent was one of the independent variables, and the values input into the software for this factor were 5.0 mg, 27.5 mg, and 50.0 mg, corresponding

© University of Venda

to the low, center, and high levels defined by the design. From the prepared stock solution, 800 µL was accurately pipetted and added according to the experimental runs generated by CCD. The mixtures were heated for controlled adsorption experiments under varying conditions. Heating durations of 30 min, 60 min, and 105 min were applied at temperatures of 25°C, 50°C, and 75°C, respectively as summarized in Table 3.1. The heating process was conducted on a regulated hotplate to ensure consistent temperature maintenance. after the elapsed times, the mixtures were filtered to remove the adsorbent materials, and the filtrates were collected in vials for further analysis. The concentration of sulfonamides in the filtrates was determined using HPLC) equipped with a PDA detector.

© University of Venda

Table 3.1: Experimental parameters for batch adsorption sorbent performance analysis

Run	Time (min)	Temperature (°C)	Mass of sorbent (mg) cell/cell@OA/cell@AA
1	180	75	5
2	105	50	50
3	105	50	27.5
4	180	50	27.5
5	30	75	50
6	105	75	27.5
7	30	75	5
8	105	50	5
9	180	75	50
10	105	25	27.5
11	105	50	27.5
12	30	25	50
13	30	50	2.5
14	30	25	5

© University of Venda

15	105	50	27.5
16	105	50	27.5
17	180	25	50
18	105	50	27.5
19	180	25	5
20	105	50	27.5

© University of Venda

3.6.2. Sample preparation for aqueous two-phase extraction

Aqueous two-phase extraction (ATPE) was specifically applied to biological samples, including milk and honey, to evaluate the extraction performance of functionalized cellulose sorbents under varying physicochemical conditions. To prepare the ATPE system, sodium chloride (NaCl), a chaotropic agent, and sodium carbonate (Na_2CO_3), a kosmotropic agent, were dissolved in distilled water at concentrations of 15%, 30%, and 35% (w/v) to induce phase separation. Table 3.2 outlines the experimental variables and conditions used to examine the effects of salt type and concentration on phase behavior and analyte partitioning. A sulfonamide standard mixture was prepared by dissolving 5 mg each of sulfabenzamide and sulfachloropyridazine in 100 mL of absolute ethanol. An 800 µL aliquot of this mixture was spiked into pre-treated milk and honey samples. Various masses of cellulose, cellulose@acetic acid (cell@AA), and cellulose@oxalic acid (cell@OA) (5 mg, 27.5 mg, and 50 mg) were added to the samples, followed by sonication at 25°C for 30, 60, and 90 min. After phase separation, the cellulose-containing phase was carefully collected and transferred into clean tubes. Desorption was facilitated by adding 100 µL of absolute ethanol and vortexing thoroughly. The final extracts were filtered and analyzed using HPLC-PDA. For aqueous samples such as wastewater, the same salt solutions were used not for phase separation but to induce a salting-out effect, which reduces the solubility of the target analytes and enhances their interaction with the cellulose-based sorbents. While this approach does not constitute a true aqueous two-phase extraction system, it contributes significantly to improving the recovery of sulfonamides from water matrices.

© University of Venda

Table 3.2: Experimental conditions and variables for the effects of salt type on sorbent performance for ATPE

A: Sonication time (min)	B: Mass of sorbent (mg)	C: Salt %	D: Salt type
60	27.5	30	Kosmotrope
90	50	15	Chaotrope
60	27.5	30	Chaotrope
30	5	15	Chaotrope
60	27.5	30	Chaotrope
90	27.5	30	Chaotrope
60	27.5	30	Chaotrope
60	27.5	30	Kosmotrope
60	27.5	30	Kosmotrope
90	50	45	Chaotrope
30	50	45	Chaotrope
90	27.5	30	Kosmotrope
30	50	15	Kosmotrope
90	50	15	Kosmotrope
90	5	45	Chaotrope

© University of Venda

60	27.5	45	Chaotrope
60	5	30	Chaotrope
60	27.5	30	Chaotrope
30	5	45	Kosmotrope
90	5	15	Chaotrope
60	27.5	30	Kosmotrope
90	5	15	Kosmotrope
60	27.5	45	Kosmotrope
60	27.5	30	Chaotrope
60	27.5	15	Chaotrope
60	27.5	15	Kosmotrope
60	50	30	Kosmotrope
30	50	15	Chaotrope
30	5	45	Chaotrope
60	27.5	30	Kosmotrope
30	5	15	Kosmotrope
30	27.5	30	Kosmotrope
30	27.5	30	Chaotrope

© University of Venda

60	5	30	Kosmotrope
90	5	45	Kosmotrope
60	50	30	Chaotrope
90	50	45	Kosmotrope
60	27.5	30	Kosmotrope
60	27.5	30	Chaotrope
30	50	45	Kosmotrope

© University of Venda

3.7. Site description and sampling

The wastewater treatment plant (WWTP) under study is situated in the Muledane area of Thohoyandou, within the Vhembe District, Limpopo Province, South Africa, at 30°28'28"E and 23°0'13"S (Fig. 3.2). The plant receives domestic sewage from residential areas, light industrial wastewater, effluents from academic institutions, trash from clinics and agricultural enterprises, and runoff from peri-urban areas and villages surrounding Thohoyandou, Shayandima, and Maniini. The treatment is based on biological filters. The plant was initially designed in 1981 with a capacity of 3 megaliters of wastewater per day but was later expanded to 6 megaliters per day due to population growth. However, the WWTP is currently overloaded, receiving around 13 megaliters of wastewater per day. The treated effluent is discharged into the Mvudi River, which provides water for domestic, recreational, and agricultural use, as well as water for the Nadoni Dam.

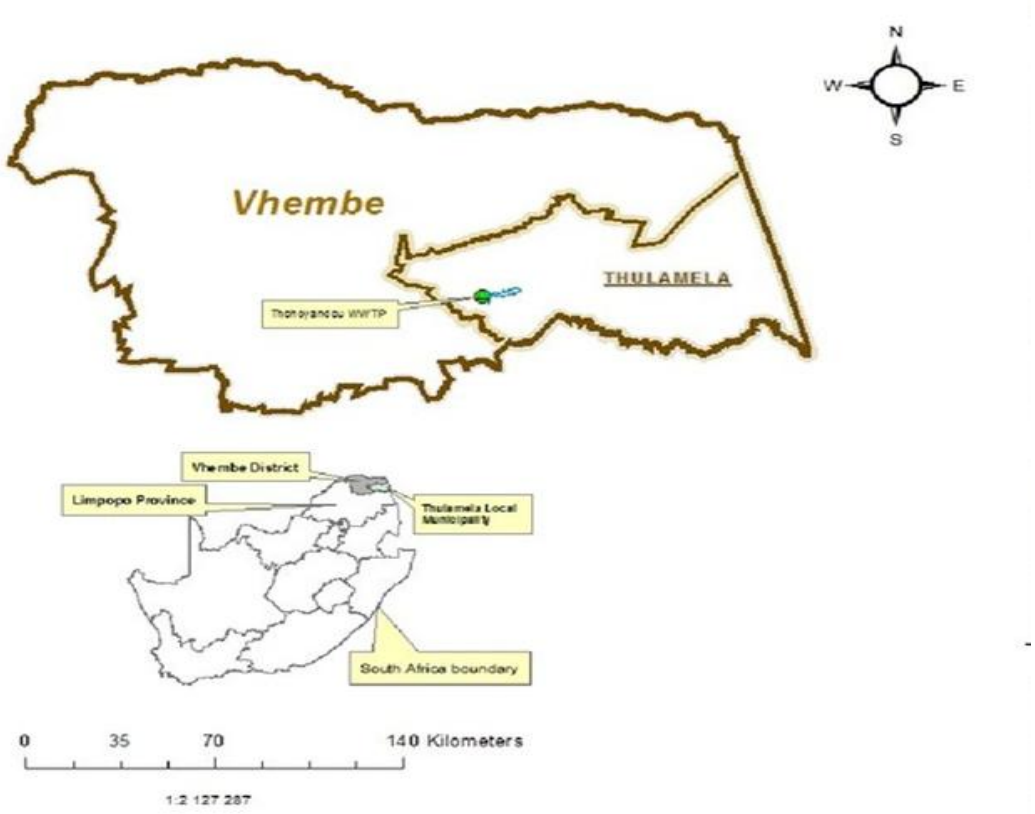


Figure 3.2: Map of the WWTP location in Muledane, Thohoyandou (Manungufala et al., 2011)

© University of Venda

3.7.1. Sample collection

Fig. 3.3 depicts the plant's basic unit operations. Wastewater samples were collected from three sites within the treatment facility, denoted as T1 (inlet) to T5 (outlet) as shown in Fig. 3.3. Wastewater samples were placed in polyethylene bottles that had been pre-washed with non-ionic detergent and rinsed with deionized water. Additionally, other matrices, such as milk and honey, were purchased from a retail outlet.

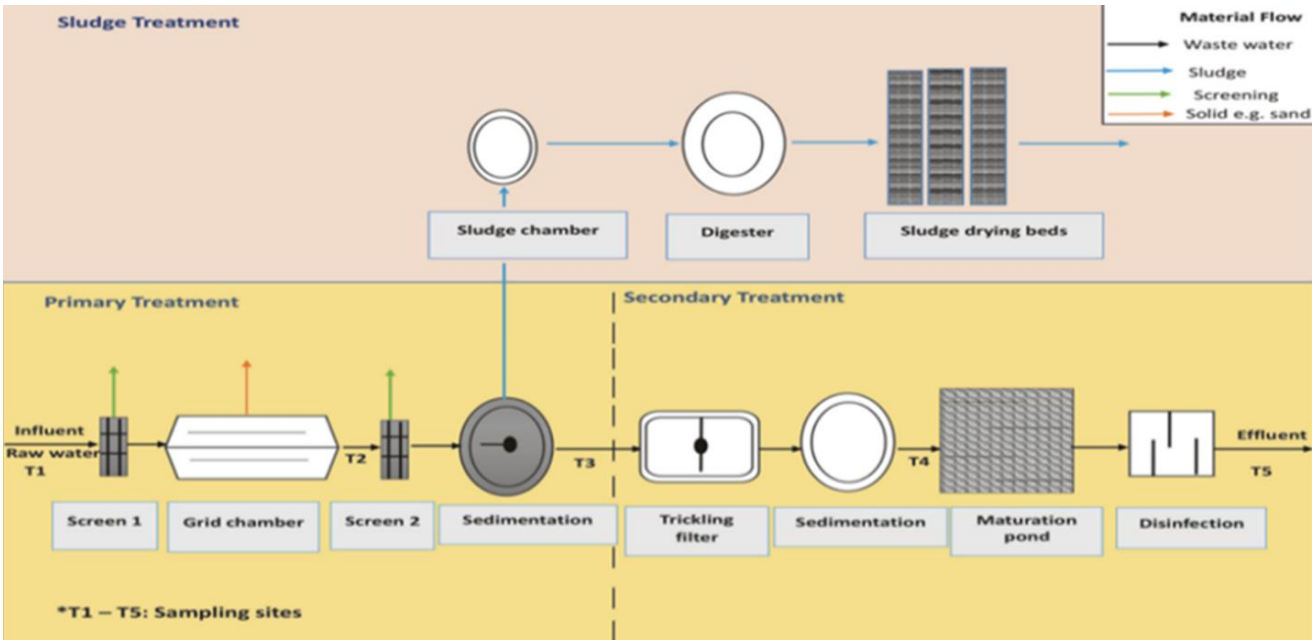


Figure 3.3: Basic processes in Thohoyandou WWTP (Manungufala et al., 2011)

3.7.2. Sample preparation and analysis

Wastewater, honey, and milk samples were prepared for application studies to assess extraction performance. Wastewater was collected from a local municipal treatment plant, filtered to remove suspended solids, and stored in a refrigerator at 4 °C until use. Honey was purchased from a retail outlet, diluted with deionised water in a 1:1 (v/v) ratio to reduce viscosity, and stored at 4 °C. Milk was also purchased from a retail outlet and stored under the same refrigerated conditions without any pretreatment. A volume of 800 µL of each sample was pipetted and used for the extraction.

© University of Venda

Chapter 4: Results and discussion

© University of Venda

4.1. Introduction

This chapter addresses the structural, thermal, and morphological properties of oxalic acid-functionalized cellulose, adipic acid-functionalized cellulose, and cellulose utilizing FTIR, PXRD, BET, and SEM. The functionalization method was optimized using batch trials and aqueous two-phase extraction (ATPE). In addition, a density functional theory (DFT) mechanism was carried out to determine the interaction processes and stability of the functionalized cellulose.

4.2. Characterization of cellulose and its functionalization

4.2.1. Functional group analysis

The Fourier-transform infrared (FTIR) spectra indicating the chemical and structural changes in cellulose, oxalic acid, and their combinations after 30 and 60 min of autoclave treatment is shown in Fig. 4.1. The pure cellulose spectrum (Fig. 4.1 a) shows distinct peaks, including a broad O-H stretching vibration around 3300 cm^{-1}, which represents the hydroxyl groups responsible for its hydrogen-bonded crystalline structure. The peaks around 2900 cm^{-1} corresponded to C-H stretching vibrations, whereas the fingerprint region (1000-1200 cm^{-1}) comprised C-O-C and C-H bending vibrations, highlighting the unique molecular structure of cellulose. The oxalic acid spectrum (Fig. 4.1 b) revealed different chemical characteristics. A prominent peak about 1700 cm^{-1} was identified, corresponding to C=O stretching in the carboxylic acid groups. Broad peaks at 1300-1400 cm^{-1} were attributed to C-O-H bending vibrations.

The combination of these spectra enabled the investigation of chemical interactions and structural changes when cellulose and oxalic acid were treated concurrently. When cellulose and oxalic acid were autoclaved for 30 min (Fig. 4.1 c), considerable spectrum changes were detected. The strength of the O-H stretching peak at 3300 cm^{-1} reduced, indicating the breakage of hydrogen bonds in cellulose due to interactions with oxalic acid. New peaks in the carbonyl region, about 1700 cm^{-1}, suggesting the formation of ester bonds or other carbonyl-containing compounds were observed. Furthermore, alterations in the fingerprint region indicated partial hydrolysis or chemical modification of the cellulose structure. The 60 min autoclave treatment (Fig. 4.1 d) produced considerably more significant spectrum alterations. The O–H stretching peak increased after autoclaving, suggesting enhanced hydroxyl availability or reformation of hydrogen bonds, which may indicate a reorganization or partial regeneration of surface hydroxyl groups during the

© University of Venda

functionalization process. Enhanced peaks in the 1700 cm^{-1} region indicated the formation of ester bonds, whereas large shifts in the fingerprint region indicated cellulose backbone hydrolysis and degradation (D'Acierno, 2021). These alterations imply that extended autoclave treatment resulted in maximum structural modification, making cellulose easier for chemicals to reach and react with.

The results indicate that the 60-minute autoclave treatment was optimal, as it facilitated the most significant interactions between oxalic acid and cellulose (Zambrano-Mite et al., 2023). Extended autoclaving enhances ester bond formation by increasing the structural openness of cellulose, thereby improving the accessibility of reactive groups. In the context of this study, the introduced carboxylic acid (–COOH) groups and remaining hydroxyl (–OH) groups on the functionalized cellulose are expected to interact with the amino ($–NH_2$) and sulfonyl ($–SO_2NH_2$) groups present in sulfonamide antibiotics through hydrogen bonding and electrostatic interactions. Longer autoclaving times promote ester bond formation by increasing cellulose structural openness, which allows for better interaction between reactive groups (Gupta et al., 2019). These interactions most likely included hydrolysis, esterification, and bond cleavage, which increased the material's (cell@OA-autoclaved for 60 min) suitability for adsorption study experiments. Modified cellulose produced under these conditions could be utilized to create bio-composites, biofuels, and sophisticated materials like membranes and hydrogels (Aziz et al., 2024).

© University of Venda

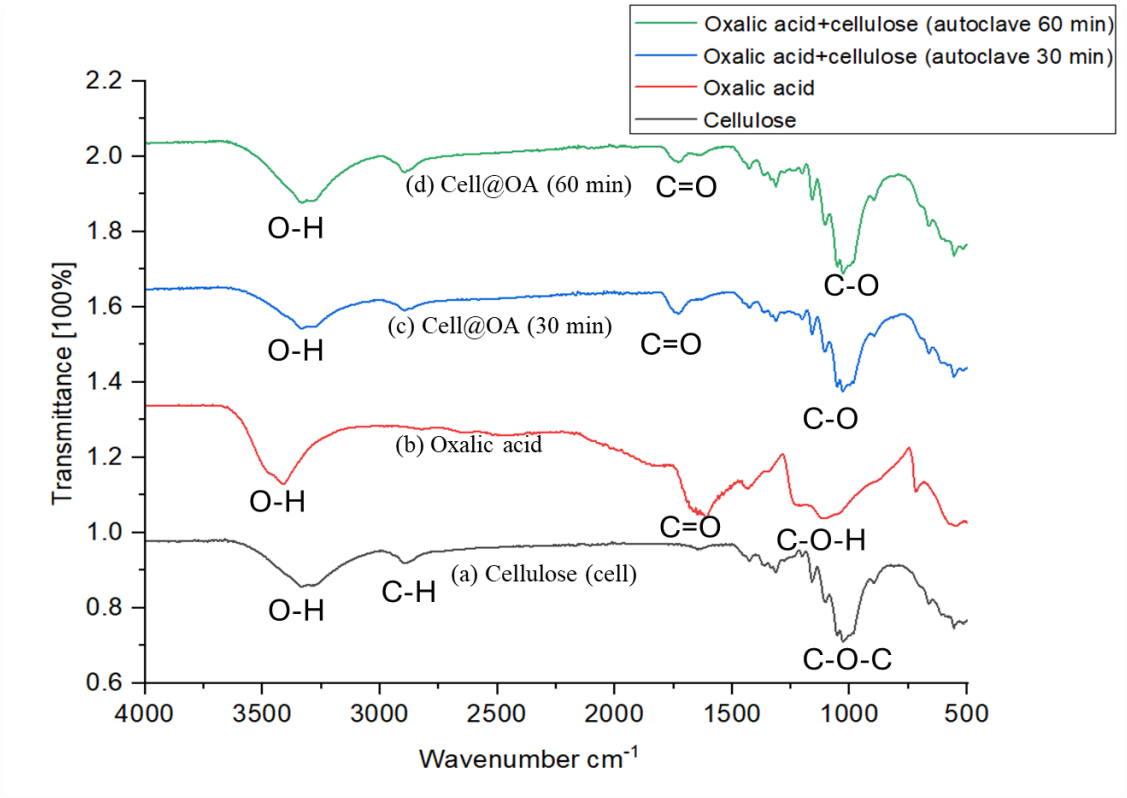


Figure 4.1: FTIR spectra of (a) cellulose, (b) oxalic acid, (c) cell@OA after 30 min autoclaving, and (d) cell@OA after 60 min autoclaving

Fig. 4.2 depicts the structural and chemical changes between cellulose and adipic acid under varied autoclave treatment durations using FTIR spectroscopy. Fig. 4.2 (a) showed pure cellulose with a broad peak at about 3300 cm^{-1} due to hydroxyl (-OH) stretching vibrations caused by intramolecular and intermolecular hydrogen bonding. The peak between 1000-1200 cm^{-1} corresponded to C-O stretching vibrations, which are characteristic of the glucose units comprising the cellulose backbone. The absence of substantial absorption near 1700 cm^{-1} confirmed the absence of carbonyl groups in the cellulose structure.

In Fig. 4.2 (b) of pure adipic acid, a sharp peak at 1700 cm^{-1}, indicating the C=O stretching vibration of the carboxylic group (-COOH) was observed, as well as a broad peak at 3000 cm^{-1}, indicating O-H stretching associated with the carboxylic acid group. Other peaks near 1200 cm^{-1} (C-O stretching) confirmed the adipic acid's molecular structure. Fig. 4.2 (c) and (d) depicted cellulose-adipic acid derivatives that had been autoclaved for 30 and 60 min, respectively. These

© University of Venda

spectra revealed considerable changes to both the hydroxyl (-OH) and carbonyl (C=O) functional groups, implying the formation of novel chemical interactions like hydrogen bonding, esterification, or condensation reactions (Costa et al., 2022). The hydroxyl peak at 3300 cm^{-1} broadened and decreased in intensity, showing esterification between cellulose's hydroxyl groups and adipic acid's carboxyl groups at 1700 cm^{-1} (Kamkar, 2024). The results showed that the best interaction occurred after 60 min of autoclave treatment, as demonstrated by Fig 4.2 (d). This spectrum exhibited the most substantial shifts in peak locations and intensities, indicating stronger interactions and chemical alterations. It was inferred that prolonged autoclave times increased chemical bonding, probably through extraction between cellulose and adipic acid (Khan et al., 2023).

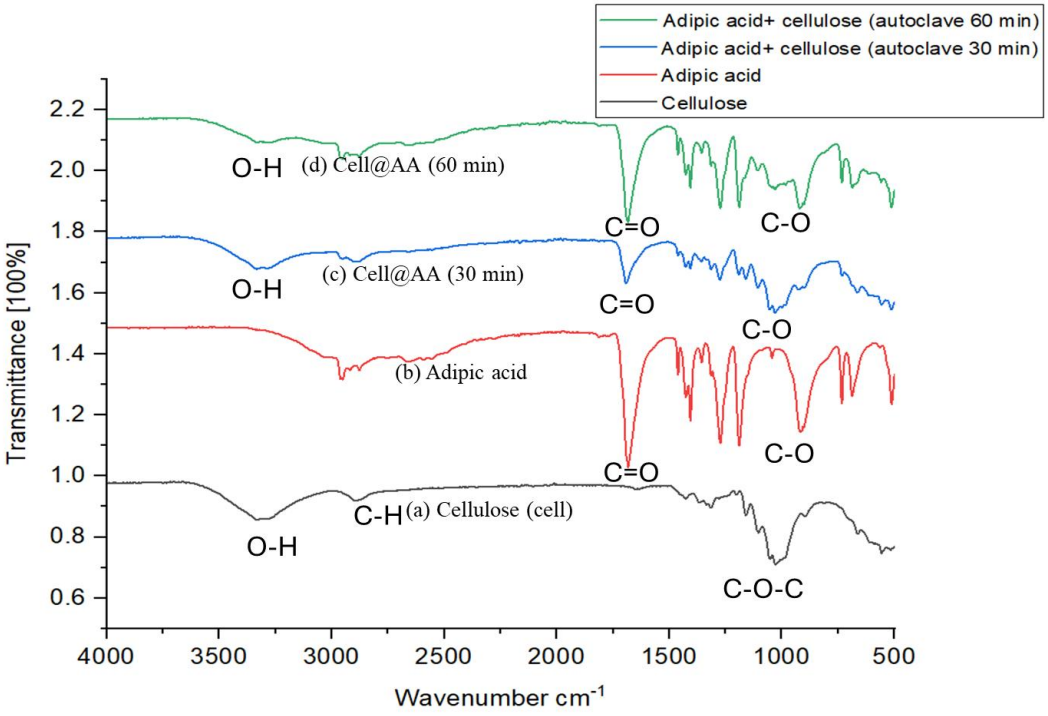


Figure 4.2: FTIR spectra of cellulose, adipic acid and cell@AA and their derivatives treated under autoclave conditions (min)

The 60 min autoclave time for both cell@OA and cell@AA was shown to be optimal. Extended autoclaving conditions allow a more complete reaction between cellulose and organic acids, which aids in the development of stronger ester linkages (Jiang et al., 2021). With enough reaction time,

© University of Venda

the esterification process improves, resulting in improved cellulose modification (Xu et al., 2022). This improved ester bond formation increases the material's stability and applicability for a variety of applications.

4.2.2 Crystallinity analysis

Powder X-ray diffraction (PXRD) is a fundamental technique for materials characterization (Riesel et al., 2024). It allows for the identification of phase composition, crystallinity, and lattice parameters, which are critical for understanding material properties (Ali et al., 2022). PXRD can also help analyze structural changes that occur during material processing, such as phase transitions or crystallization behaviors (Chiang et al., 2022). Fig. 4.3 depicts the crystallinity analysis of cellulose after 30 and 60 min of treatment with oxalic acid under autoclaving conditions. The PXRD pattern of pure cellulose (Fig. 4.3 a) showed broad peaks at $2\theta \approx 15°$ and 22°, indicating a semi crystalline structure with a combination of crystalline and amorphous regions. Cellulose includes many OH groups, which interact by creating intra- and intermolecular hydrogen bonds (Asif et al., 2022). The hydrogen bonding creates an organized arrangement of molecules (Ahmed et al., 2022). In contrast, the pattern for pure oxalic acid (Fig. 4.3 b) showed sharp and intense peaks, indicating that it is highly crystalline, and served as a reference for analyzing its interaction with cellulose.

© University of Venda

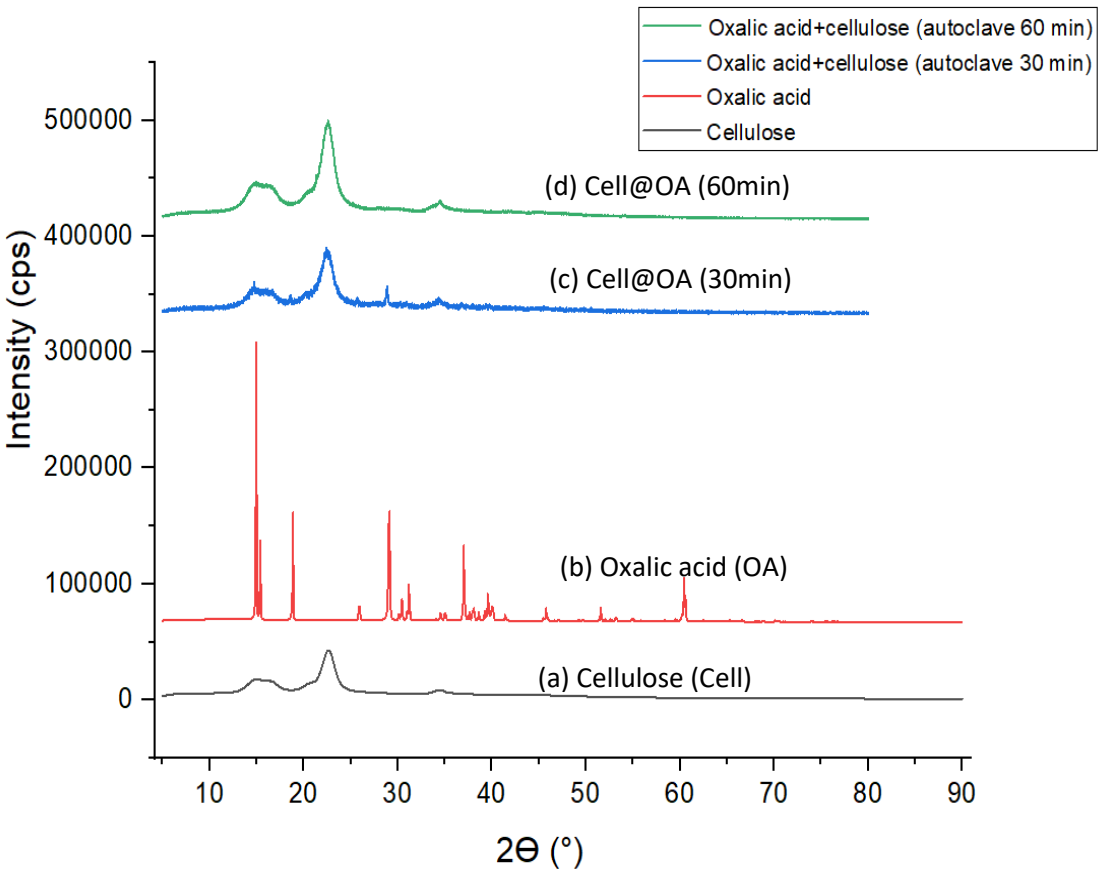


Figure 4.3: PXRD patterns of cellulose, oxalic acid and cell@OA treated samples under different autoclaving durations (min)

Autoclaving cellulose with oxalic acid for 30 min (Fig. 4.3 c) reduced peak intensity and broadened the PXRD pattern, especially at 2θ = 15° and 22°, compared to untreated cellulose. New peaks at 2θ ≈ 18°, 25° and 28° were found (Fig. 4.3 c), possibly indicating the development of oxalate-cellulose (cell@OA) composites or reaction by-products. These modifications revealed that the acid-catalyzed modification caused a partial breakdown of the cellulose crystalline structure (Heise et al., 2021). These peaks indicated structural changes inside the material, with the crystalline structure of cellulose being modified to newly ordered patterns (Delepierre et al., 2021). The treatment is thought to have affected the hydrogen bonding network within cellulose, allowing for the formation of new crystalline domains (Makarem et al., 2019). Furthermore, the appearance of these peaks suggested that a chemical reaction had occurred, resulting in new structural features separate from the initial cellulose and oxalic acid. Overall, the emergence of new peaks demonstrated that the autoclaving procedure caused significant structural and chemical changes in cellulose. The sample treated for 60 min (Fig. 4.3 d) exhibited more dramatic peak broadening and

© University of Venda

intensity fluctuations. Crystallinity decreased, resulting in less prominent peaks at 2θ ≈ 15° and 22°. Peak intensities at 2θ ≈ 18° and 24° increased, indicating deeper integration of oxalic acid into the cellulose matrix or the production of new crystalline phases. This result showed that longer autoclaving times resulted in more significant structural alteration of cellulose, making 60 min the optimal treatment time for maximum interaction between cellulose and oxalic acid.

Fig. 4.4 depicts the PXRD analysis of cellulose, adipic acid and cell@AA, which provided information about the crystalline and structural interactions between adipic acid and cellulose under various autoclaving conditions. Specifically, the study investigates the impacts of various autoclave durations (e.g., 30 and 60 min) and temperatures, demonstrating how these variables affect the cellulose esterification process and the subsequent material qualities. The PXRD patterns of pure cellulose (Fig. 4.4 a), pure adipic acid (Fig. 4.4 b), and their mixtures autoclaved for 30 min (Fig. 4.4 c) and 60 min (Fig. 4.4 d) compared to determined changes in crystallinity and structural composition**.** The PXRD pattern of pure cellulose (Fig. 4.4 a) exhibited a broad and weak diffraction feature, indicating its semi-crystalline structure. The absence of distinct peaks suggests a highly amorphous cellulose sample. Typically, cellulose has diffraction peaks at 2θ ≈ 15° and 22°. However, in this pattern, these peaks were not clearly discernible, implying that the cellulose sample utilized in the research was either primarily amorphous or weakly crystalline.

Pure adipic acid's PXRD pattern (Fig. 4.4 b) showed strong, powerful diffraction peaks, indicating that it is crystalline. These peaks correspond to adipic acid's orthorhombic crystalline structure, which is distinguished by a unique arrangement of molecules in three dimensions (Nisa et al., 2019). The high intensity and well-defined peaks indicate that the adipic acid sample was well organized, with no apparent amorphous components. The diffraction pattern of the mixture of adipic acid and cellulose (cell@AA) that was autoclaved for 30 min (Fig. 4.4 c) changed significantly when compared to the separate components. The prominent peaks of adipic acid remained visible, although some of them were slightly lowered in intensity and broadened, typically around 2θ values of 22° and 26°. This shows that the crystallinity of adipic acid was somewhat disrupted during autoclaving. In addition, the cellulose component showed a small shift in the broad peak characteristic of amorphous cellulose. These alterations in the diffraction pattern

© University of Venda

indicate that autoclaving facilitated some connection between adipic acid and cellulose, possibly via hydrogen bonding (Wu et al., 2023).

The PXRD pattern showed additional alterations for the mixture that was autoclaved for 60 min (Fig. 4.4 d). The sharp peaks linked with adipic acid were present in cell@AA, which included 2θ values of 12°, 22°, 26° and 32°, while the broadness of the peaks increased overall. This showed a more significant disruption of adipic acid's crystalline structure. Furthermore, the amorphous hump associated with cellulose seemed slightly more prominent, implying that the prolonged autoclaving increased interactions between adipic acid and cellulose. The overall pattern indicated the production of a less ordered or partially amorphous phase, which was most likely caused by autoclaving's temperature and pressure effects, as well as the possibility of chemical interactions between the two components.

These results are consistent with previous research on the effects of high temperature treatments on crystalline and semi-crystalline materials. Autoclaving has been proven in studies to modify the crystalline structure of tiny organic molecules and enhance molecular interaction between various composites (Zhao et al., 2021). Chen (2020) reported that co-crystallization processes involving organic acids and biopolymers resulted in PXRD pattern modifications comparable to those described here. Wang (2021) found that temperature treatments promoted amorphization and improved interactions in polymer-crystal system. The PXRD results indicate that autoclaving alters the crystalline structures of adipic acid and cellulose. PXRD study demonstrated that autoclaving at 60 min provided the best conditions for both cell@OA and cell@AA, resulting in increased crystallinity and better chemical interactions. This condition demonstrated the most significant increase in structural integrity.

Different phases of oxalic acid appear on cellulose at varying autoclave times due to time-dependent chemical reactions and diffusion. At 30 min, partial esterification and disruption of hydrogen bonds lead to new crystalline domains and moderate peak changes. By 60 min, deeper integration of oxalic acid formed stable oxalate-cellulose structures, causing significant peak broadening and intensity shifts. The fluctuations in PXRD intensities reflect changes in crystallinity and the formation of new ordered or amorphous phases. This demonstrated a structural transition from native cellulose to chemically modified composites over time.

© University of Venda

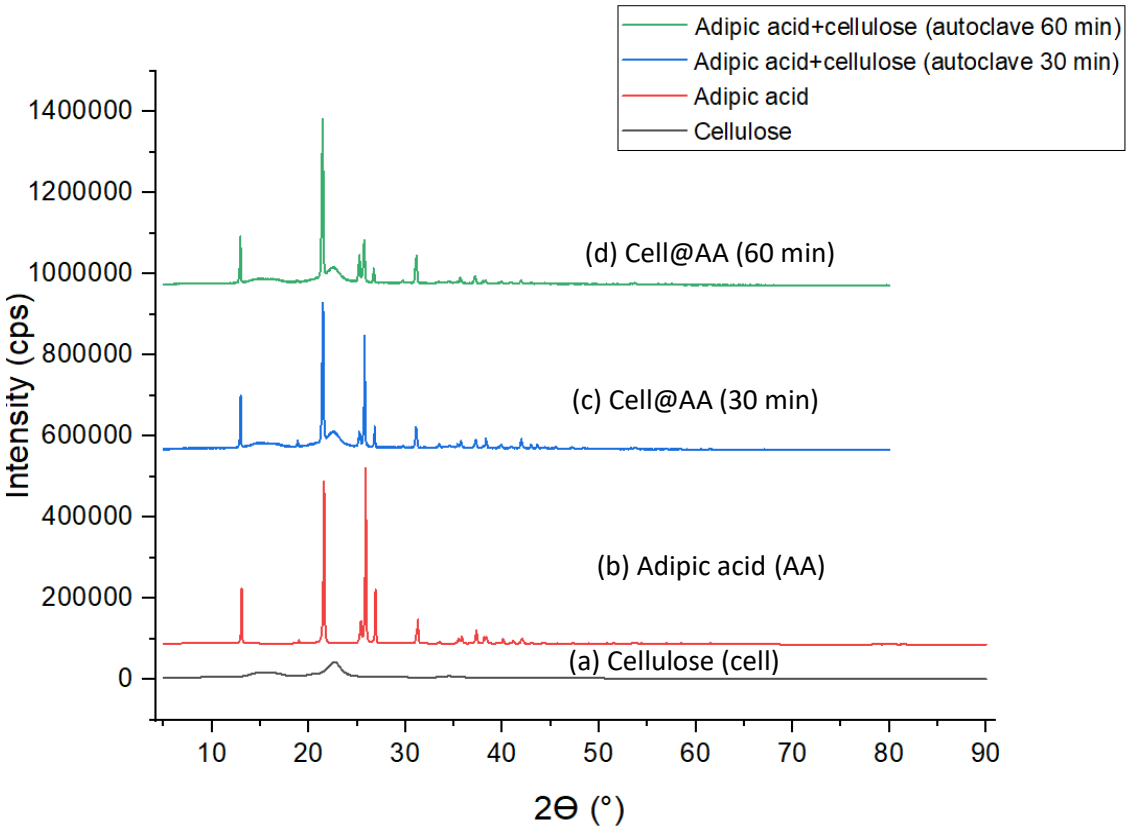


Figure 4.4: PXRD patterns of cellulose, adipic acid and cell@AA treated samples under different autoclaving durations (min)

4.2.3. Surface morphological analysis

The scanning electron microscope (SEM) is one of the most used instruments for examining and analyzing micro- and nanoparticle imaging and solid object characterization (Raval et al., 2019). Fig. 4.5 depicts the SEM analysis of microcrystalline cellulose (MCC), which provided information about its morphological characteristics under specific imaging conditions. The images were taken at a 15 kV accelerating voltage and revealed significant MCC structural features at different magnifications (from 350x to 1500x). Furthermore, the particle size distribution was predominantly within the micrometer range (50-100 µm), supporting its classification as microcrystalline. Fig. 4.5 (a) depicted the particles as densely packed aggregates with irregular shapes and rough, fibrous surfaces. This compact arrangement and surface irregularities were caused by the acid hydrolysis process used in MCC production, which breaks down cellulose fibers

© University of Venda

into smaller crystalline regions (Deng et al., 2024). Using a magnification of 1000x allowed for a closer look at MCC's surface roughness and voids, which are indicative of its high crystallinity

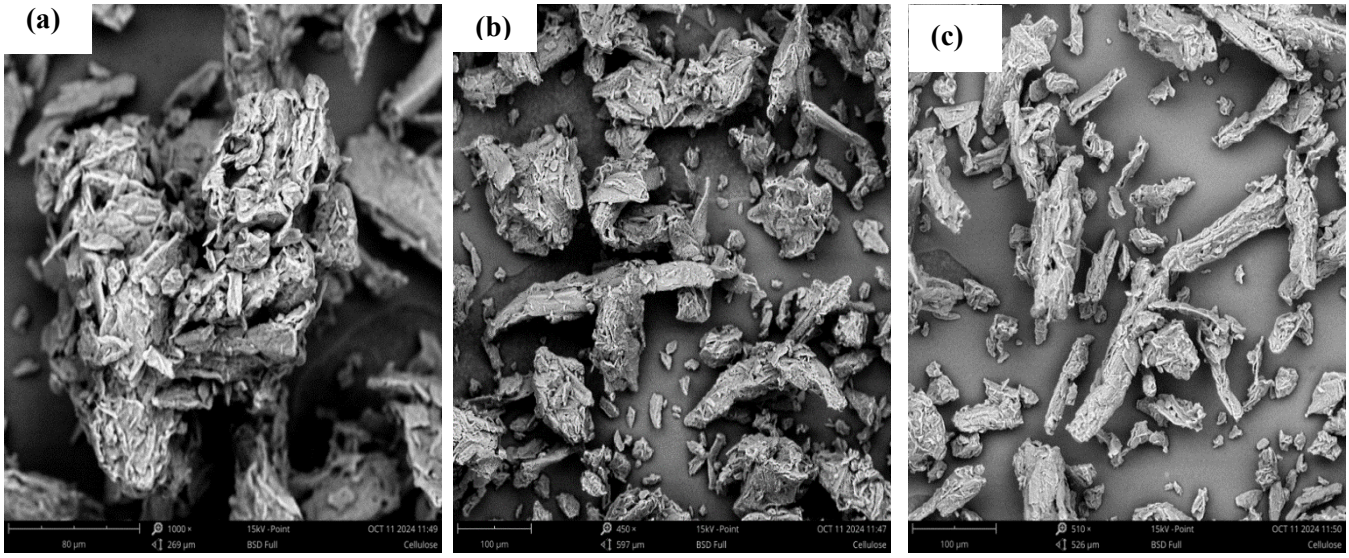


Figure 4.5: SEM micrographs of microcrystalline cellulose (MCC) at different magnifications (a) 1000x, (b) 450x, and (c) 510x at acceleration voltage of 15kV

Fig. 4.5 (b) shows a broader dispersion of MCC particles, including fragmented and irregularly shaped fragments. The imaging at 450x magnification revealed a diverse particle size distribution with sharp edges and variable diameters. This shape was most likely impacted by the milling and screening operations, which lowered particle size while preserving the structural integrity of cellulose (Fu et al., 2024). Milling and screening are important techniques for modifying particle size and form (Orisaleye et al., 2022). Milling reduces particle size by grinding or crushing, whereas screening separates particles by size to ensure uniform distribution (Jekayinfa et al., 2022). The various particle sizes seen in this figure showed increased compressibility and flowability, which are important features for adsorption (Li et al., 2022). Cellulose's porous structure and large surface area improve adsorption by providing more active sites for the attachment of molecules or ions (Etale et al., 2023). Fig. 4.5 (c) displayed a more dispersed arrangement of MCC particles, including elongated, fiber-like structures and smaller fragments. At 510x magnification, individual particles appeared less clustered than those in Fig. 4.5 (a), indicating a reduced degree of aggregation. The elongated forms and porous surface patterns

© University of Venda

suggested a higher surface area, which might enhance adsorption capacity and make MCC suited for use in composite materials.

Fig. 4.6 illustrates the SEM study of cell@OA after autoclaving for 30 and 60 min revealing different morphological changes that were influenced by the duration of the treatment. In both cases, the cellulose particles had an uneven, flaky, and plate-like appearance, indicating that oxalic acid had caused structural change to cellulose. The particles in the samples that had been autoclaved for 60 min (Fig. 4.6 a, b, c) appeared larger and more aggregated, with sharper and more defined edges (Krishna et al., 20204). These particles' surfaces were relatively smooth and compact, with few apparent pores, indicating densification and improved crosslinking because of extended heat exposure (Umadevi et al., 2024). The heat from autoclaving increased crosslinking between polymer chains, increasing the material's density and stability. This process resulted in smooth, compact surfaces with fewer pores (Hu et al., 2024). The SEM scale bar shows that the particle size in these samples ranged between 80 and 100 µm.

In contrast, samples autoclaved for 30 min (Fig. 4.6 d, e, f) had smaller, less aggregated, and more evenly distributed particles. The flaky and rough morphology was more noticeable, with prominent fractures and pores on the surfaces, indicating a less compact structure. Particle sizes ranged from 80 to 100 µm, indicating reduced agglomeration and improved dispersion. The shorter period seems to limit excessive crosslinking, keeping more of the intrinsic fibrous properties of cellulose (Acharya et al., 2021). Magnifications differed, with greater magnifications (80 µm scale) employed for surface features and lower magnifications (100 µm scale) for particle distribution**.** The SEM results showed that autoclaving time has a substantial impact on the shape of oxalic acid-functionalized cellulose. The images demonstrated changes in particle form, size, and surface roughness, emphasizing the trade-offs between functionalization and material preservation.

© University of Venda

University of Venda
Creating Future Leaders

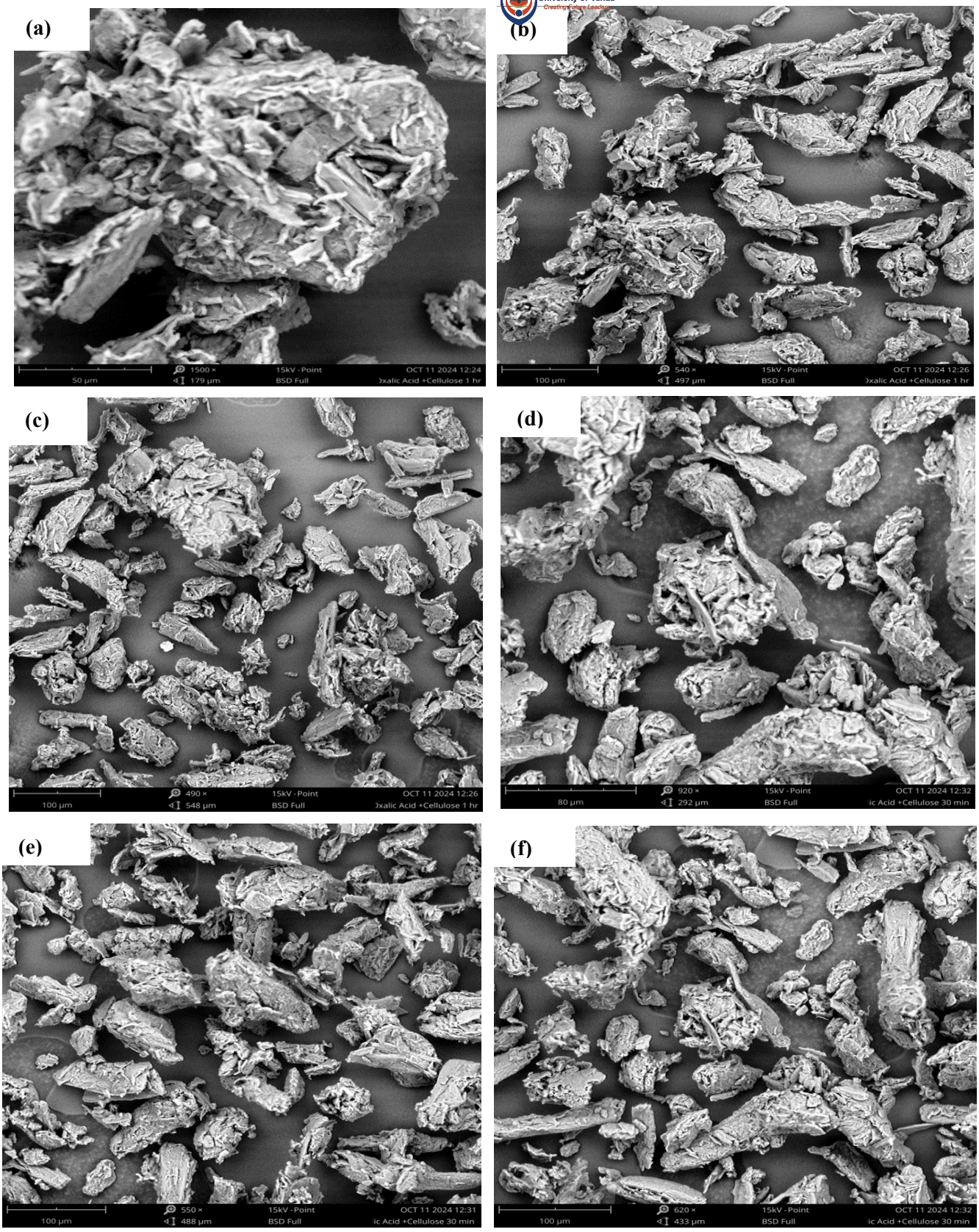


Figure 4.6: SEM micrographs of cell@OA after autoclaving for 60 min (a, b, c) and 30 min (d, e, f)

© University of Venda

Fig. 4.7 shows the SEM micrographs of cell@AA after 30 and 60 min of autoclaving, which revealed distinct morphological characteristics. The particles had irregular shapes, with fragmented and coarse structures. After 60 min (Fig. 4.7 a, b, c) of treatment, the cellulose particles appeared more compact, with sharp edges and prominent fragmentation, indicating effective functionalization (Aziz et al., 2022). In contrast, the 30 min (Fig. 4.7 d, e, f) treatment resulted in particles that appeared slightly smoother, indicating less extensive modification. The particle diameters varied from 80 µm to 100 µm based on the autoclaving process duration. The 60 min treatment time resulted in more uniform and defined structures, indicating a greater degree of functionalization than the 30 min treatment (Farid et al., 2022). The optimum processing time appeared to be 60 min between the two time periods. This duration enabled thorough functionalization and led to the formation of well-defined structures, as evidenced by the particles' distinct roughness and fragmentation. While the 30 min treatment functionalized the cellulose, it did not accomplish the same level of alteration as the lengthier time.

The observed difference in surface morphology trends between cell@OA and cell@AA may arise from the distinct chemical nature and reactivity of the organic acids used in each functionalization route. In the case of cell@AA, prolonged autoclaving (60 min) likely facilitated deeper penetration and stronger bonding of the acid groups, resulting in more pronounced fragmentation and sharper features which we associate with successful functionalization. For cell@OA, however, extended exposure (60 min) may have led to partial degradation or relaxation of surface features, producing smoother surfaces despite continued reaction time. The roughness of 30 min could thus reflect an earlier stage of aggressive surface modification before rearrangement or smoothing occurs at longer times. Despite this morphological difference, the choice of 60 min as optimum in both cases was based not only on SEM appearance but also on performance data (e.g., extraction efficiency, surface chemistry confirmation via FTIR and stability). Therefore, the selection of the 60 min treatment as optimal for both functionalized materials was grounded in overall performance metrics, not solely SEM roughness.

© University of Venda

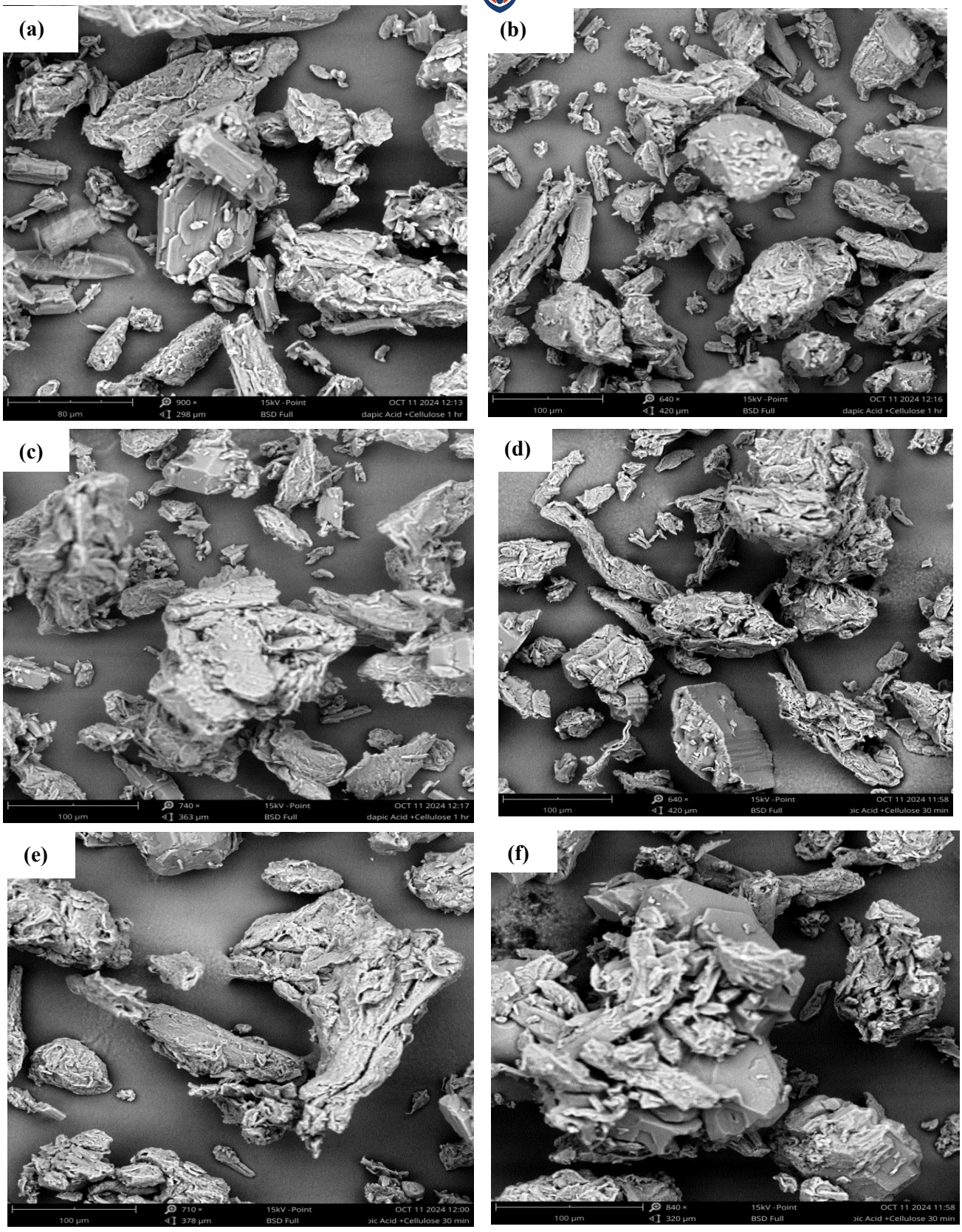


Figure 4.7: Surface morphology of cell@AA at different autoclaving times of 60 min (a, b, c) and 30 min (d, e, f)

© University of Venda

Based on SEM results, 60 min autoclave duration was found to be optimal for cell@OA and cell@AA. Longer autoclaving times allow for a more complete esterification process, which leads to stronger interactions between cellulose and organic acids. This longer reaction time improves the alteration of the cellulose surface, increasing structural integrity and material characteristics.

4.2.4. BET surface area analysis

The Brunauer-Emmett-Teller (BET) method is commonly used to precisely determine the surface area of porous materials (Irwansyah et al., 2024). Fig. 4.8 depicted the BET analysis of the cellulose sample, which revealed information about its surface area, pore volume, and pore size distribution, all of which were critical for assessing its adsorption capabilities. The surface area of the cellulose was 6.21 $m^2 g^{-1}$, indicating a limited number of active adsorption sites. The material's cumulative pore volume of 0.0137 cm^3/g indicates a modest porous structure. Fig. 4.8 (a) indicated a prominent pore width mode at 56.82 Å (5.68 nm), indicating that the material is mesoporous. The nitrogen adsorption-desorption isotherm in Fig. 4.8 (b) showed a classic Type IV hysteresis loop, which is characteristic of mesoporous materials and indicates capillary condensation in the pores (Baldovino-Medrano et al., 2023). Hysteresis also revealed pore connection and ink-bottle pore morphologies. The progressive increase in adsorption capacity with relative pressure indicated a moderate affinity for nitrogen, suggesting its viability for adsorption applications, while porosity modifications may have improved performance for extraction (Niño-Celis et al., 2023).

© University of Venda

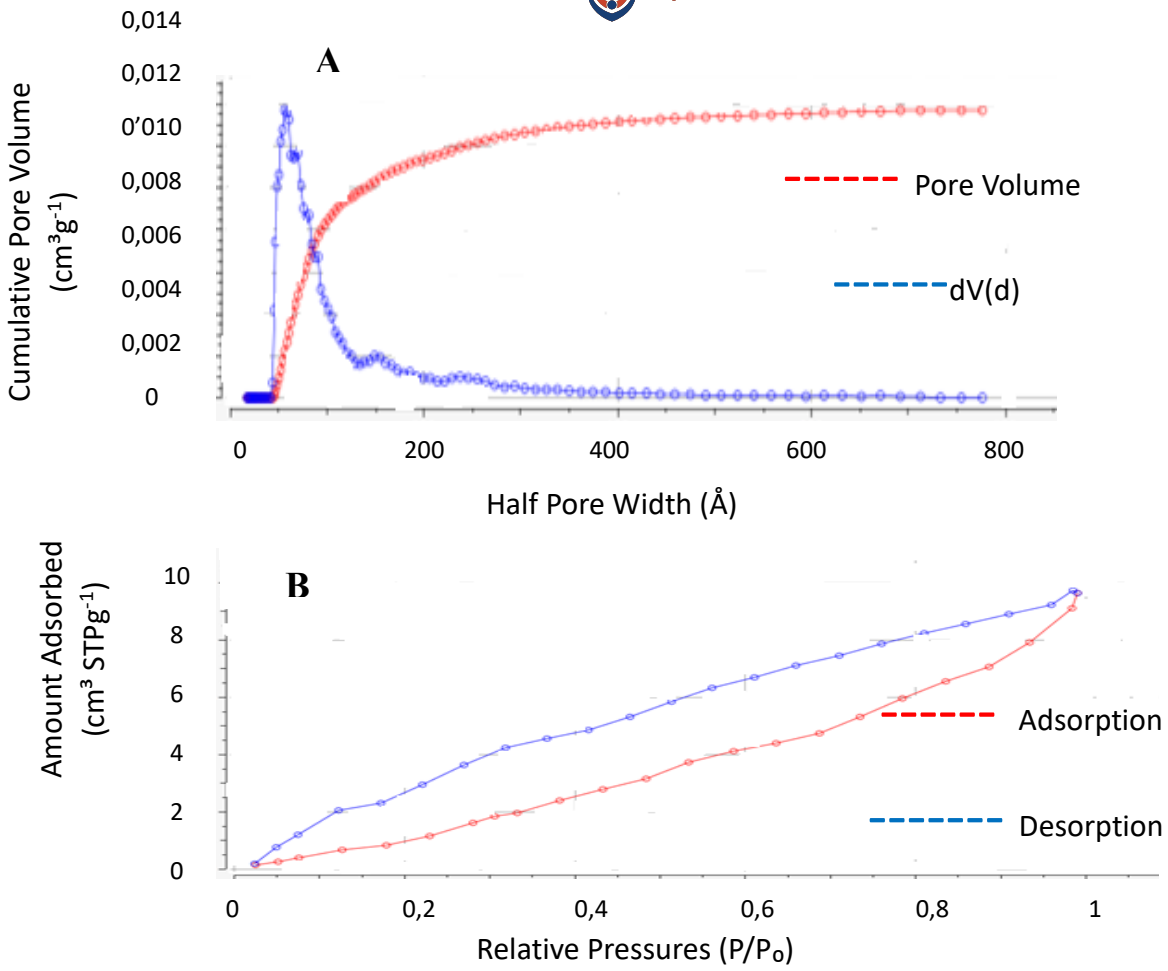


Figure 4.8: BET analysis of cellulose: (a) pore volume and pore size distribution (b) adsorption-desorption isotherm

The BET results for cell@OA show considerable mesoporosity and a well-structured pore system. In Fig. 4.9 (a), the red curve (cumulative pore volume) rapidly increases for lower pore widths (below ~100 Å) before plateauing. The surface area of cell@OA was 5.55 m^2g-1, and the material's cumulative pore volume was 0.0121 cm^3g-1. This pattern shows that micropores and small mesopores account for most of the pore volume. The differential pore volume distribution (blue curve) peaks at 58.8 Å, showing the material primarily comprises of mesopores, which are advantageous for adsorption applications. The plateau in cumulative pore volume at greater pore widths verifies the lack of considerable macroporosity, implying that the functionalization process retained the cellulose's structural integrity while increasing its adsorption capacity.

© University of Venda

Fig. 4.9 (a) shows the relationship between cumulative surface area (red curve) and differential surface area distribution (blue curve) as a function of half pore width. At pore widths below ~100 Å, the surface area rapidly increases before stabilizing, showing that micropores and small mesopores comprise most of the surface area. The differential surface area distribution curve shows a prominent peak at 58.8 Å, indicating that this pore size contributes significantly to the overall surface area. The rapid increase in cumulative surface area shows the presence of mesopores, which are important for adsorption efficiency (Kim et al., 2021). The blue curve (differential surface area) rapidly decreased after the peak, indicating that larger pores contribute less to total surface area. This pattern is consistent with mesoporous materials, which derive a large proportion of their total surface area from intermediate pore sizes rather than macropores.

In Fig. 4.9 (b), the nitrogen adsorption-desorption isotherm reveals information on the material's pore structure and adsorption behavior. The red curve of adsorption demonstrates a steady increase at low relative pressures (P/P_0), which is typical of monolayer adsorption in micropores. As the pressure rises, the adsorption rate increases, indicating multilayer adsorption and mesopore formation (Fu et al., 2021). The desorption curve (blue) is higher in trajectory than the adsorption curve, generating a hysteresis loop, which is a common sign of capillary condensation in mesopores. The presence of this loop indicates that the material comprises slit-shaped or inkbottle mesopores, with desorption delayed due to limited pore openings (Isaacs Giraldo et al., 2023). The steady rise in adsorption without a defined peak indicates a broad pore size distribution, which improves accessibility for a variety of compounds.

© University of Venda

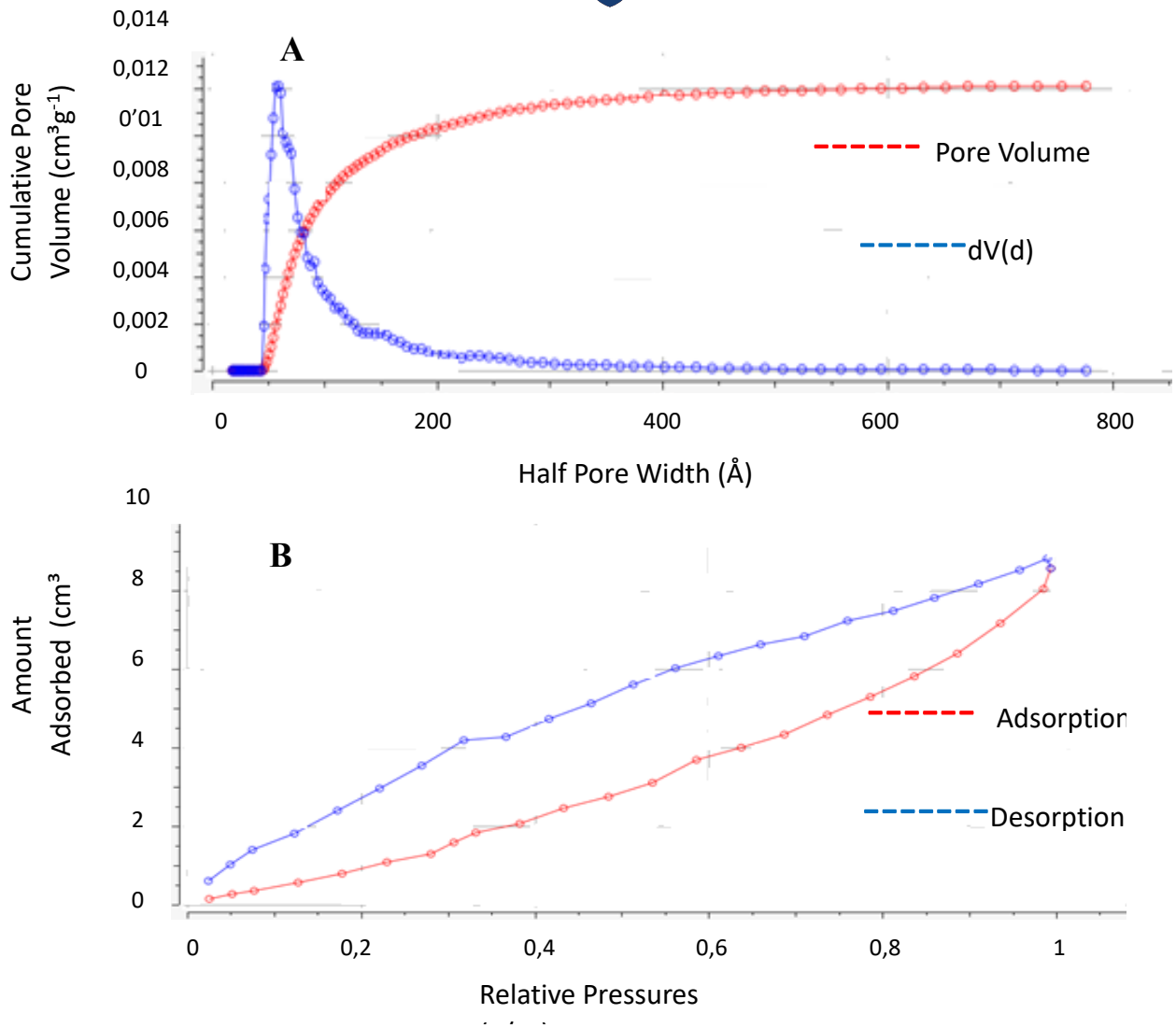


Figure 4.9: BET analysis of cell@OA: (a) pore volume and pore size distribution (b) adsorption-desorption isotherm

Fig. 4.10 (a) shows that adipic acid-functionalized cellulose is largely constituted of mesopores, with a dominating width of 58.8 Å and a total pore volume of 0.0125 cm^3/g. The cumulative pore volume (red curve) rapidly increases at decreasing pore widths and stabilizes beyond 200 Å, showing the restricted existence of macropores. The blue curve confirms the material's mesoporous character, with a peak at 58.8 Å. These characteristics make it useful for mesoporous applications including adsorption and catalysis. BET analysis of cell@AA confirms its mesoporous structure, with a low surface area of 5.8538 m^2/g and a notable pore width of 58.8 Å. Fig. 4.10 (b) depicts a Type IV adsorption-desorption isotherm, which is characteristic of mesoporous materials. The adsorption curve gradually rises at low relative pressures due to monolayer development before increasing dramatically in the mid-range as multilayer adsorption

© University of Venda

occurs. At greater relative pressures, capillary condensation within the mesopores causes a significant increase in adsorption (Numan et al., 2021). The occurrence of a hysteresis loop between adsorption and desorption adds to the material's mesoporous nature, implying that the pores are not fully cylindrical but have some degree of connection or irregularity (Baldovino-Medrano et al., 2023).

The reduction in surface area of cellulose after modification (cell@AA) was attributed to structural changes that occurred during the functionalization process. When cellulose was modified with organic acids, functional groups such as carboxyl, hydroxyl, or other polar moieties were introduced onto its surface. These groups partially blocked or filled the natural pores of the cellulose structure, making them less accessible during surface area analysis. Additionally, the modification process promoted cross-linking or hydrogen bonding between cellulose chains, which led to a more compact and less porous structure. This structural densification resulted in a reduced overall surface area available for gas adsorption. Furthermore, the grafted functional groups may have smoothed the surface of the cellulose, contributing to the decline in measurable surface roughness and porosity. Despite the decrease in physical surface area, the chemical functionality of the modified cellulose was enhanced, which likely improved its selectivity and efficiency in extracting sulfonamide residues from environmental or food samples.

© University of Venda

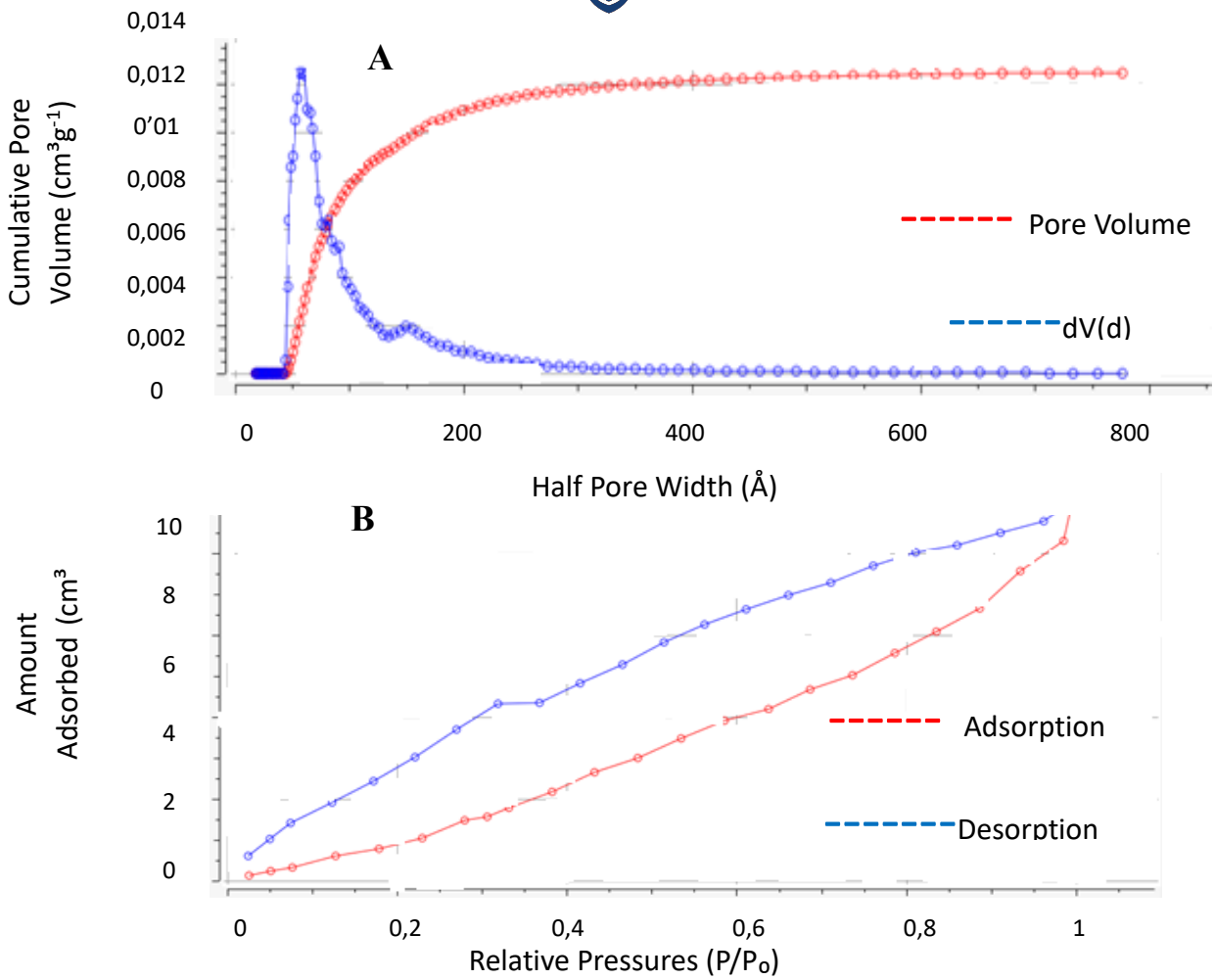


Figure 4.10: BET analysis of cell@AA: (a) pore volume and pore size distribution (b) adsorption-desorption isotherm

BET illustrates that cell@OA has a larger surface area than cell@AA due to variations in molecular structure and functional group interactions. Oxalic acid, as a smaller dicarboxylic acid, provides more functional sites per unit area, resulting in improved porosity. Furthermore, its high hydrogen bonding potential enables greater cellulose fiber dispersion, minimizing aggregation and ensuring a larger exposed surface. Adipic acid, with its longer carbon chain, tends to form a more compact structure, reducing total porosity. As a result, cell@OA has more active surface sites, which improves adsorption and catalysis.

© University of Venda

Table 4.1 presented below shows the surface area and pore volume characteristics of cellulose and two cellulose-based sorbents functionalized with organic acids, specifically oxalic acid (OA) and adipic acid (AA). The cellulose exhibited the highest surface area at 6.21 m^2g^{-1} and a pore volume of 0.0137 cm^3/g. Upon functionalization with oxalic acid (cell@OA), the surface area slightly decreased to 5.55 m^2g^{-1}, while the pore volume also reduced to 0.0121 cm^3/g. Similarly, cellulose functionalized with adipic acid (cell@AA) displayed a surface area of 5.85 m^2g^{-1} and a pore volume of 0.0125 cm^3g^{-1}. These observations suggested that the introduction of organic acid functional groups onto the cellulose structure slightly reduced both surface area and pore volume, likely due to partial pore blockage or structural rearrangements during the modification process. Despite this reduction, the values remained within a close range, indicating that the functionalization process preserved most of the original porous structure of the cellulose.

Table 4.1: Surface area and pore volume analysis of cellulose and functionalized cellulose sorbents

Sorbents	Surface area (m^2g^{-1})	Pore volume (cm^2g^{-1})
Cellulose	6.21	0.0137
Cell@OA	5.55	0.0121
Cell@AA	5.85	0.0125

© University of Venda

4.3. Density functional theory mechanism of adsorption

Density functional theory (DFT) is a well-known computational approach in chemistry that allows for the study of the electronic structure of molecules and materials using electron density rather than wave functions (Sholl and Steckel, 2022). The goal of DFT is to precisely predict molecular geometries, reaction energies, and other material properties, achieving a balance between computing efficiency and accuracy, making it indispensable in theoretical chemistry and materials research (Hu and Chen 2021). DFT has various advantages, including the capacity to handle huge systems at lower computing costs than classic wavefunction approaches (Bursch et al., 2022). It excels at predicting ground-state features and is frequently used in fields such as catalysis, nanotechnology, and semiconductor research (Mewes et al., 2022). Table 4.2 shows the interaction energies (ΔE_{inter}), enthalpies (ΔH), and Gibbs free energies (ΔG) for binding cellulose and organic acid-functionalized cellulose (containing adipic and oxalic acids) to various derivatives.

The Density Functional Theory (DFT) results provided valuable insight into the adsorption behavior of the two sulfonamide analytes sulfachloropyridazine (DR1) and sulfabenzamide (DR2) onto both unmodified and organic acid-functionalized cellulose. The interaction energies (ΔE_inter), enthalpies (ΔH), and Gibbs free energies (ΔG) were evaluated to understand the strength and stability of the adsorption interactions. It was found that cellulose-DR1d exhibited the lowest ΔE_inter (-15.191 kcal.mol^{-1}) among unmodified cellulose systems, indicating that sulfachloropyridazine interacted most stably in this configuration. This suggested that unmodified cellulose had a moderate affinity for sulfachloropyridazine and could effectively adsorb it under suitable conditions. However, the adsorption performance was significantly enhanced when cellulose was functionalized with organic acids. The (cellulose–adipic acid) DR2a complex showed the most negative ΔE_inter value (-23.220 kcal.mol^{-1}), followed by the (cellulose–oxalic acid) ·DR2a complex with ΔE_inter of -21.154 kcal.mol^{-1}. These results indicated that sulfabenzamide (DR2) had much stronger interactions with the functionalized cellulose surfaces compared to the unmodified one. The presence of carboxylic acid groups on adipic and oxalic acid likely facilitated stronger hydrogen bonding or electrostatic interactions with functional groups on sulfabenzamide, enhancing binding affinity and adsorption stability.

© University of Venda

Overall, the DFT data confirmed that the modification of cellulose using organic acids improved adsorption efficiency, particularly for sulfabenzamide. This demonstrated the potential of functionalized cellulose as a selective and sustainable adsorbent material in environmental and food sample cleanup applications. The analyte-specific interaction energies further implied that tailored functionalization strategies could be employed to selectively target different sulfonamide antibiotics, thereby improving extraction performance and aligning with green chemistry principles and the United Nations Sustainable Development Goals.

© University of Venda

Table 4.2: The relative energy (kcal/mol), enthalpies, and free energy for the interactions of cellulose, oxalic acid-functionalized (cell@OA) and adipic acid-functionalized cellulose (cell@AA) with DR1 and DR2 derivatives

Structure	ΔE_{inter}(kcal.mol^{-1})	ΔH	ΔG
Cellulose···DR1a	-8.699	-8.048	3.774
Cellulose···DR1b	-13.344	-12.854	-1.011
Cellulose···DR1c	-7.283	-7.185	5.452
Cellulose···DR1d	-15.191	-15.260	-0.446
Cellulose···DR1e	-8.377	-7.979	3.946
Cellulose···DR2a	-14.612	-14.340	-2.578
Cellulose···DR2b	-14626	-14.344	-2.403
Cellulose···DR2c	-8.444	-8.247	3.552
Cellulose···DR2d	-13.813	-14.089	0.621
Cellulose···DR2e	-6.618	-6.080	2.303
(Cellulose-AdipicAcid)···DR1a	-19.051	-19.419	-2.200
(Cellulose-AdipicAcid)···DR1b	-14.086	-13.590	-2.591
(Cellulose-AdipicAcid)···DR2a	-23.220	-23.870	-5.290
(Cellulose-AdipicAcid)···DR2b	-13.702	-13.324	-1.843
(Cellulose-OxalicAcid)···DR1a	-17.039	-17.009	-2.8665
(Cellulose-OxalicAcid)···DR1b	-14.447	-14.123	-2.2496
(Cellulose-OxalicAcid)···DR2a	-21.154	-21.448	-5.4681

© University of Venda

(Cellulose-OxalicAcid)···DR2b	-16.306	-15.973	-3.708

© University of Venda

Cellulose's DFT adsorption (Fig. 4.11) model identified DR1 as sulfachloropyridazine (SCP) based on structural characteristics. The chemical structure showed a six-membered pyridazine ring with two nitrogen atoms, which is a crucial differentiating property of SCP. The sulfonyl (-SO_2NH_2) functional group enhanced adsorption stability by facilitating strong hydrogen bonding interactions with cellulose's hydroxyl (-OH) groups as also explained by Mary et al. (2024). The chlorine (Cl) atom linked to the pyridazine ring provided more evidence that DR1 was SCP rather than sulfabenzamide (DR2). Hydrogen bonding, π-π stacking, and electrostatic interactions were the primary adsorption mechanisms. SCP's sulfonyl (-SO_2NH_2) and amide (-NH_2) groups formed hydrogen bonds with cellulose's hydroxyl (-OH) groups, leading to numerous connections (Bantho, 2022). Furthermore, π-π stacking between the pyridazine ring of SCP and the glucose rings of cellulose aided in stability. Electrostatic interactions between SCP's electronegative oxygen atoms and the hydroxyl (-OH) groups of cellulose also contributed to the adsorption process (Li et al., 2019).

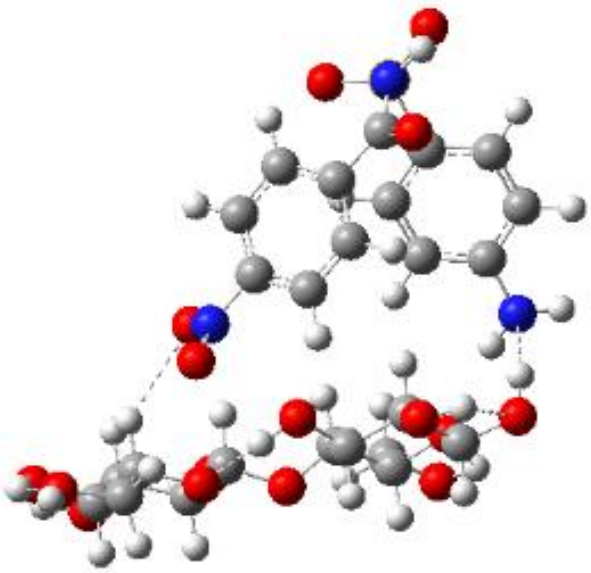


Figure 4.11: DFT optimization of sulfchloropyridazine adsorption on cellulose

The DFT analysis of oxalic-functionalized cellulose adsorption (Fig. 4.12) showed that oxalic acid groups created strong hydrogen bonds and electrostatic interactions with the cellulose surface, indicating successful functionalization. This interaction implies that the surface hydroxyl groups of cellulose were effectively modified, resulting in enhanced surface polarity, increased

© University of Venda

availability of active sites, and improved adsorption affinity toward sulfonamide molecules. Such surface modification is essential for improving the efficiency and selectivity of the adsorbent in wastewater treatment applications. The presence of oxygen-rich functional groups promoted stable adsorption via hydrogen bonding, dipole-dipole interactions, and potential charge transfer effects (Escudero-Curiel et al., 2024). The electronic structure computations revealed considerable adsorption energy, indicating a thermodynamically stable connection. Molecular orbital study revealed changes in electron density distribution, which influenced the system's electronic characteristics (Khan et al., 2019). Geometry optimization confirmed the creation of stable structures, with oxalic-functionalized groups orientated toward the cellulose surface to increase contact strength (Liyanage et al., 2021).

Sulfachloropyridazine (DR1) and sulfabenzamide (DR2) were tested for adsorption on oxalic-functionalized cellulose. While both compounds made contacts with the surface, sulfabenzamide had a more prominent role in adsorption due to its amide (-$CONH_2$) and sulfonamide (-SO_2-NH_2) groups. Adsorption energy estimates demonstrated a stable connection, and molecular orbital analysis revealed reduced HOMO-LUMO energy gaps, indicating charge transfer (Kanagathara et al., 2022). Electrostatic potential (ESP) mapping revealed a significant electron density around functional groups, confirming the strong adsorption process. This structural insight verifies the efficient adsorption of sulfabenzamide on oxalic-functionalized cellulose, emphasizing its potential for adsorption-based applications in different matrices such as environmental remediation and wastewater treatment.

© University of Venda

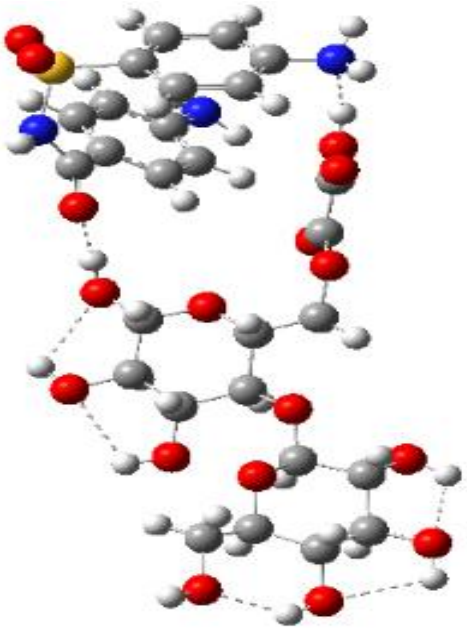


Figure 4.12: DFT Modeling of adsorption behavior on a functionalized matrix

DFT analysis of adipic acid-functionalized cellulose (Fig. 4.13) indicated that the carboxyl (-COOH) and hydroxyl (-OH) groups in adipic acid played an important role in adsorption via hydrogen bonding and electrostatic interactions with the cellulose surface. The larger aliphatic chain of adipic acid increased flexibility, allowing for numerous adsorption sites and molecular reorientation. Geometry optimization revealed a stable arrangement in which adipic acid's carboxyl groups interact efficiently with cellulose. The electronic structure computations revealed considerable adsorption energy, indicating a thermodynamically stable connection. The adsorption behavior of sulfachloropyridazine (DR1) and sulfabenzamide (DR2) was investigated on adipic acid-functionalized cellulose. While both compounds interacted with the surface, sulfabenzamide played a major impact in adsorption due to its amide ($-CONH_2$) and sulfonamide ($-SO_2-NH_2$) groups. These functional groups formed hydrogen bonds with the carboxyl and hydroxyl groups of adipic acid-functionalized cellulose and van der Waals interactions contributed to increased adsorption stability. The ESP mapping revealed localized electron density near functional groups, indicating selective adsorption sites. Molecular orbital analysis revealed a modest reduction in the HOMO-LUMO energy gap, indicating electronic rearrangement during adsorption. These findings revealed that adipic acid-functionalized cellulose provides a hydrophobic and structurally flexible

© University of Venda

adsorption substrate, making it appropriate for environmental applications, particularly in the removal of organic contaminants from aquatic environments.

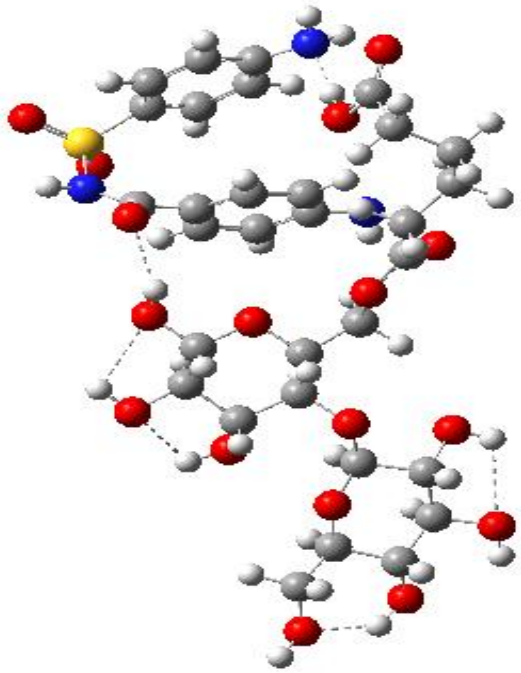


Figure 4.13: Optimized interaction geometry between adsorbent and target molecule

© University of Venda

4.4. Batch adsorption

Batch adsorption experiments were conducted to investigate the efficiency of organic acid-functionalized cellulose in removing sulfachloropyridazine and sulfabenzamide from aqueous solutions. This technique involved studying the effect of key operational parameters such as contact time, temperature, and sorbent mass under controlled conditions. The results obtained from these experiments are presented below. Tables 4.3, 4.4, and 4.5 provide the experimental settings utilized to determine the effects of time, temperature, and sorbent mass on the adsorption efficiency of sulfachloropyridazine and sulfabenzamide.

Tables 4.2 to 4.4 presented the extraction efficiencies of sulfachloropyridazine and sulfabenzamide under varying experimental conditions using unmodified cellulose (Table 4.2) and organic acid-functionalized cellulose (cell@OA; Tables 4.3 and 4.4). Overall, the use of cell@OA resulted in a marked improvement in extraction performance compared to unmodified cellulose. For instance, the highest extraction efficiency for sulfachloropyridazine using cellulose reached only 51%, whereas cell@OA achieved up to 64% (Tables 4.3 and 4.4, Runs 5, 6, 12, and 20). Similarly, sulfabenzamide extraction efficiency improved significantly with cell@OA, reaching a maximum of 75%, compared to 70% with cellulose. This indicated that functionalization substantially enhanced the sorption capacity of the material. Additionally, cell@OA performed more effectively across a broader range of conditions. Under shorter extraction times (30 min), cell@OA maintained relatively high extraction efficiencies (e.g., Runs 6 and 12 in Table 4.3), suggesting enhanced sorption kinetics. In contrast, cellulose required longer contact times and/or higher sorbent masses to reach comparable extraction levels, as observed in Table 4.2 (e.g., Runs 3 and 19).

Temperature also influenced extraction efficiency. For cell@OA, moderate temperatures (25–50 °C) generally resulted in better performance, while higher temperatures (75 °C) occasionally led to decreased extraction of sulfachloropyridazine, such as in Run 7 of Table 4.3, where only 19% was extracted. This suggested potential thermal degradation or reduced analyte-sorbent interactions at elevated temperatures. Both sorbents showed reduced efficiency at 75 °C when lower sorbent masses were used, highlighting possible thermal desorption or weakening of sorption affinity under such conditions.

© University of Venda

Table 4.3: Sulfachloropyridazine and sulfabenzamide extraction efficiency using cellulose as the sorbent under various conditions

Run	Time (min)	Temperature (°C)	Mass of sorbent (mg)	Sulfachloropyridazine % extraction	Sulfabenzamide % extraction
1	30	25	5	49	69
2	30	25	50	48	63
3	180	25	5	51	70
4	105	50	27.5	40	54
5	30	50	27.5	40	51
6	105	50	27.5	20	25
7	180	75	5	44	64
8	105	50	5	35	50
9	105	50	50	47	54
10	30	75	5	37	47
11	30	75	50	29	36

© University of Venda

12	105	50	27.5	40	60
13	105	50	27.5	29	54
14	105	75	27.5	43	61
15	105	50	27.5	26	39
16	105	50	27.5	30	40
17	180	50	27.5	24	36
18	180	75	50	49	50
19	180	25	50	51	69
20	105	25	27.5	38	37

© University of Venda

Table 4.4: Sulfachloropyridazine and sulfabenzamide extraction efficiency using cell@OA as the sorbent under various conditions

Run	Time (min)	Temperature (°C)	Mass of sorbent (mg)	Sulfachloropyridazine % extractiom	Sulfabenzamide % extraction
1	180	75	50	46	67
2	30	75	50	42	62
3	105	50	27.5	50	53
4	105	50	50	48	47
5	180	25	5	63	75
6	30	25	50	64	75
7	180	75	5	19	13
8	105	50	27.5	37	55
9	105	50	27.5	42	63
10	105	75	27.5	34	56
11	180	25	50	62	73

© University of Venda

12	30	25	5	64	75
13	30	50	27.5	46	64
14	105	50	27.5	40	61
15	180	50	27.5	53	71
16	105	50	5	8	7
17	105	50	27.5	34	56
18	30	75	5	47	67
19	105	50	27.5	31	36
20	105	25	27.5	64	75

© University of Venda

Table 4.5: Sulfachloropyridazine and sulfabenzamide extraction efficiency using cell@OA as the sorbent under various conditions

Run	Time (min)	Temperature (°C)	Mass of sorbent (mg)	Sulfachloropyridazine % extractiom	Sulfabenzamide % extraction
1	105	50	27.5	40	39
2	180	75	50	52	67
3	30	25	5	62	75
4	105	50	27.5	54	66
5	105	50	27.5	34	35
6	180	75	5	26	34
7	180	25	5	61	73
8	30	75	5	50	57
9	105	50	5	49	64
10	105	50	27.5	51	64
11	105	25	27.5	39	17

© University of Venda

12	105	50	27.5	24	17
13	105	50	27.5	37	35
14	105	75	27.5	43	60
15	30	50	27.5	59	71
16	105	50	50	58	71
17	180	50	27.5	40	39
18	30	75	50	54	65
19	30	25	50	62	73
20	180	25	50	60	73

© University of Venda

4.4.1. Response surface methodology for the extraction of sulfachloropyradazine and sulfabenzamide on cellulose

Fig. 4.14 illustrates response surface methodology (RSM) for sulfachloropyradazine extraction on cellulose, which were evaluated using three parameters: extraction time (A), temperature (B), and cellulose sorbent (C). The model equation highlighted each variable's independent and interacting influence on the extraction process. Positive coefficients indicated that increasing the relevant variable improved the extraction, whilst negative coefficients suggested a suppressive effect (More & Arya, 2021). The relationship between these parameters was represented by the quadratic model equation (1):

% extraction sulfachloropyridizine = +31.86 +1.60 x A +0.80 x B - 3.50 x C +1.75 x AB +2.75 x AC- 0.25 x BC 1.41 x A^2 +7.59 x B^2 +7.09 x C^2..... (1)

Where A represents the extraction time, B the temperature, and C the mass of the cellulose sorbent

The linear term (mass of cellulose sorbent) also showed that sorbent mass had a favourable impact on the process up to a certain point where the sorbent became saturated and could no longer absorb more effectively. The relationship between extraction time and temperature (Fig. 4.14a) shows that extraction efficiency does not always increase with increasing temperature. Initially, increasing the temperature reduces extraction efficiency, implying that sulfachloropyridazine or the cellulose matrix may be thermally degraded. However, at 55°C, an increase in temperature improves extraction efficiency. Furthermore, shorter extraction times at higher temperatures tend to diminish efficiency, exacerbating the effects of thermal deterioration. This observation is consistent with what was reported by Darmenbayeva et al. (2024) on maintaining cellulose sorbent integrity during adsorption.

The relationship between time and cellulose mass (Fig. 4.14 b), indicates that higher sorbent masses generally correlated with increased extraction efficiency, emphasizing the importance of having enough active sites for sulfachloropyradazine adsorption. However, when time was extended beyond 120-150 min, the marginal gains in extraction efficiency decreased, implying that equilibrium had been reached. This finding is consistent with previous studies that emphasize the importance of sorbent quantity in achieving effective contaminant removal (Wu & He, 2019).

© University of Venda

The response surface plot (Fig. 4.14 c) indicated that extraction efficiency was highest between 55°C and 65°C, with cellulose mass ranging from 32 to 41 mg. At low temperatures (25°C), adsorption was weak, resulting in limited efficiency. At extremely high temperatures (75°C), efficiency decreased, most likely due to thermal degradation or analyte desorption. These patterns were consistent with the literature highlighting the thermal sensitivity of cellulose-based sorbents during extraction processes (Rajasekharan et al., 2024). This model accounted for the components' linear, interaction, and quadratic impacts on extraction efficiency. The optimum conditions for the adsorption of sulfachloropyridazine on cellulose were determined to be a contact time of 180 min, a temperature of 25 °C, and a cellulose mass of 5 mg, achieving an extraction efficiency of 51%.

© University of Venda

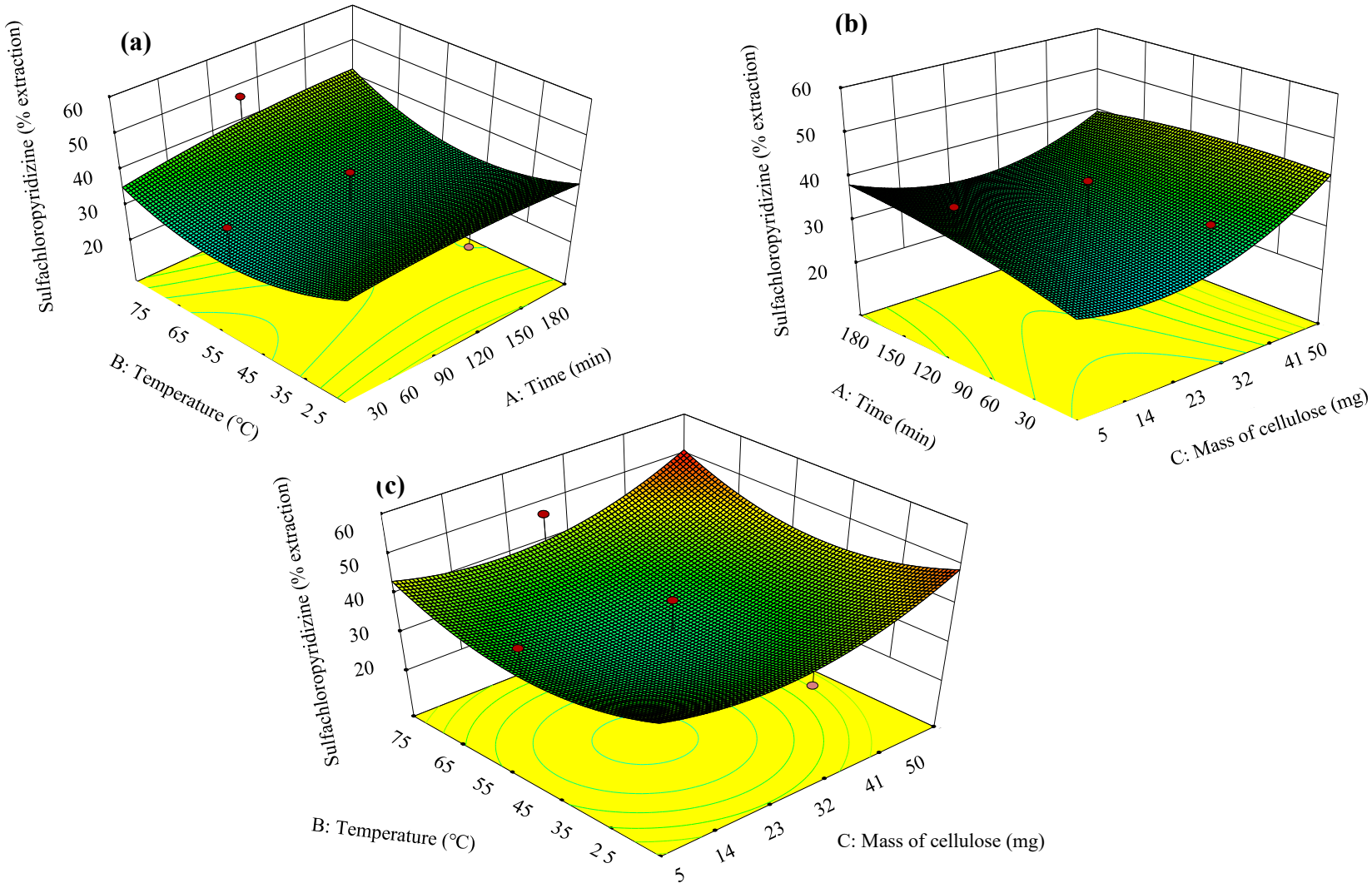


Figure 4.14: Response surface plots for the extraction efficiency of sulfabenzamide with cellulose: (a) the effect of time (A) and temperature (B), (b) the effect of time (A) and cellulose mass (C) and (c) the effect of temperature (B) and cellulose mass (C)

© University of Venda

The quadratic coefficients temperature (B^2) and sorbent mass (C^2) had the greatest impact, as shown in the equation and pareto chart (Fig. 4.15). The Pareto chart for sulfachloropyradazine extraction showed the P-values and F-values of each factor, indicating their relative significance of each factor in the extraction process. P-value is a probability value used to estimate the statistical significance of an observed result (Andrade, 2019). A low p-value (< 0.05) indicates that the result is unlikely attributable to chance, and hence the null hypothesis can be rejected (Di Leo & Sardanelli 2020). F-value is an ANOVA ratio that compares variation between group means to variance within groups (Mishra et al., 2019). The bars in Fig. 4.15 showed absolute P-values for each term in the model. In this analysis, none of the factors are statistically significant because their P-values are all greater than 0.05 (P > 0.05).

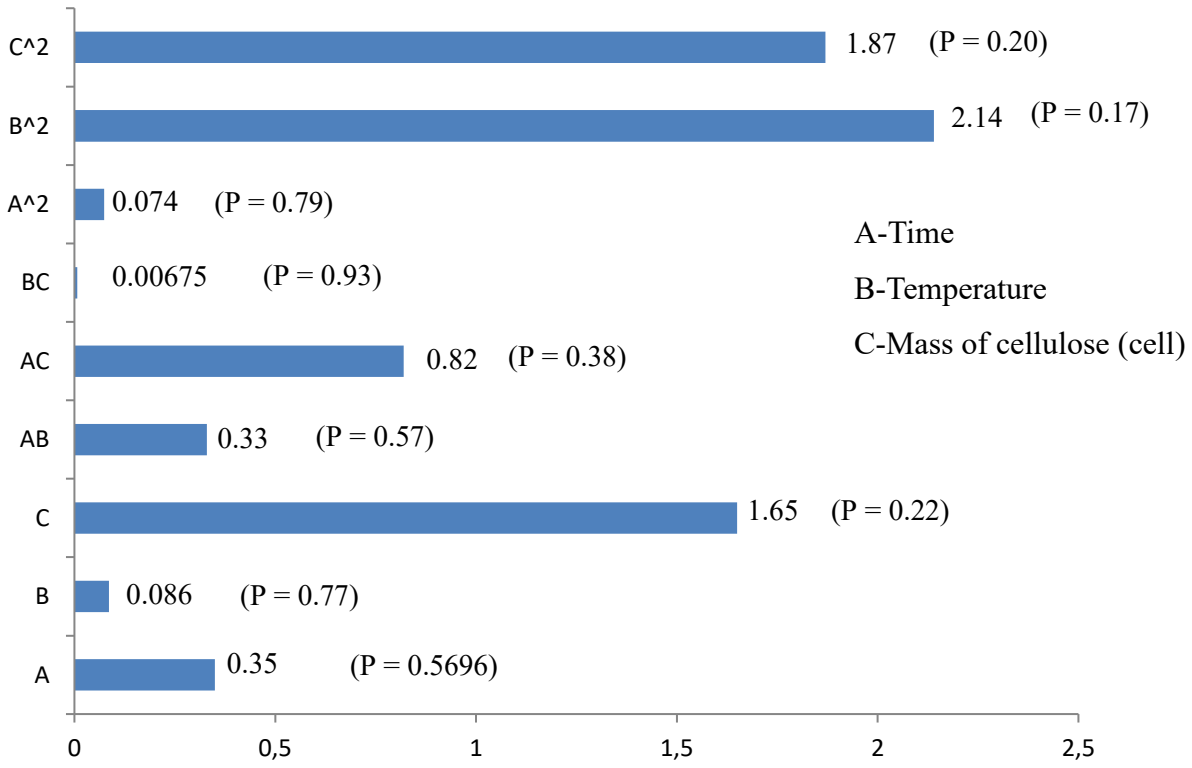


Figure 4.15: Pareto chart for sulfachloroyridazine extraction in cellulose

Fig. 4.16 depicts the RSM for determining the effects of time, temperature, and cellulose sorbent mass on sulfabenzamide extraction efficiency. All models had non-significant P-values and

© University of Venda

negative adjusted R^2 values, suggesting poor fitness and predictive performance. The model gave rise to the following equation:

%extraction sulfabenzamide = +91.86565-0.048316 x A - 0.84864 x B- 1.11618 x C +1.48148E-004 x AB+1.60000E-003 x AC- 4.00000E-003 x BC -2.42424E-005 x A^2+0.016521 x B^2 +8.58182E-003 x C^2……. (2)

Where A represents the extraction time, B the temperature, and C the mass of the cellulose sorbent.

The RSM (Fig. 4.16) analysis revealed distinct patterns in the influence of each parameter. The influence of extraction time. The RSM plot revealed that sulfabenzamide extraction from cellulose was primarily influenced by temperature and time (Fig. 4.16 a), affecting the adsorption process. Extraction efficiency increased with temperature, peaking at 55°C, most likely due to increased molecular interactions and active site availability on the cellulose surface. Time also had an important role, with adsorption improving up to 120 min before equilibrium was reached due to surface site saturation. Temperature showed a greater impact than time, highlighting its importance in fostering adsorbate-adsorbent interactions. Brzezińska et al. (2023) previously observed that high heating negatively influenced medicinal compound extraction due to thermal degradation. Fig 4.16 b illustrates the effect of time and cellulose mass on extraction efficiency. The effect of time revealed that as the time increased from 30 to 180 min, the % extraction increased marginally, particularly with larger cellulose mass. However, the increase was not linear, and a plateau was achieved, showing that going beyond 120 min did not considerably improve the extraction. Increasing the cellulose mass from 5 mg to roughly 50 mg resulted in greater extraction efficiency, with the sharpest increase occurring between 23 mg and 50 mg. Beyond this point, the impact started to stabilize.

Fig. 4.16 c shows a response surface plot demonstrating the effects of temperature (25-75°C) and cellulose mass (5-50 mg) on sulfabenzamide extraction efficiency. The plot showed a nonlinear trend in which extraction efficiency increased with increasing temperature and cellulose mass until it reached the optimum. The maximum extraction yield, around 55-60%, was obtained at a temperature of 65-75°C and a cellulose mass of 41-50 mg. Beyond these levels, the yield plateaued, most likely due to saturation of cellulose adsorption sites and probable thermal degradation at high temperatures. The contour plot at the base revealed that the best conditions for

© University of Venda

sulfabenzamide extraction occurred between 65 and 75°C, with cellulose mass ranging from 41 to 50 mg. The investigation revealed that controlling both temperature and cellulose mass was critical for maximizing sulfabenzamide extraction, while increasing both parameters did not significantly improve yield. The optimum conditions for the adsorption of sulfabenzamide on cellulose were achieved at a contact time of 180 min, a temperature of 25 °C, and a cellulose mass of 5 mg, resulting in a maximum extraction efficiency of 70%.

© University of Venda

University of Venda
Creating Future Leaders

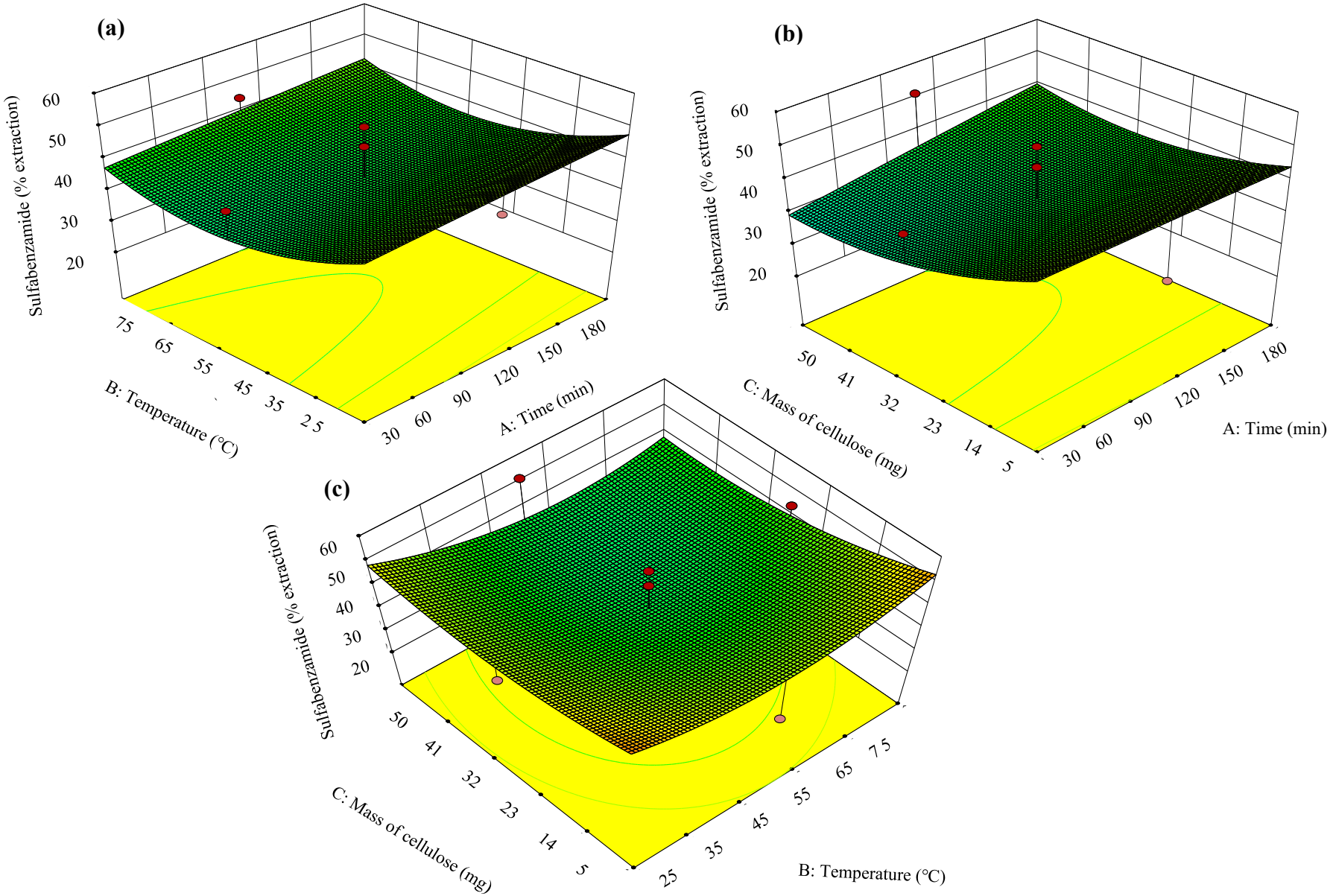


Figure 4.16: Response surface plots for the extraction efficiency of sulfabenzamide with cellulose: (a) the effect of time (A) and temperature (B), (b) the effect of time (A) and cellulose mass (C) and (c) the effect of temperature (B) and cellulose mass (C)

© University of Venda

Fig.4.17 shows a Pareto chart that depicts the influence of several variables on sulfabezamide extraction in cellulose. The horizontal bars show the amount of each factor's effect, while the accompanying P-values indicate statistical significance. The mass of cellulose (C) has the greatest effect (1.33, P > 0.27), followed by the quadratic term of temperature (B2) at 1.02 (P > 0.33). Other factors, such as time (A), temperature (B), and interactions (AB, AC, BC), have smaller effects, with P-values indicating lack statistical significance. This graph shows the relative importance of each parameter on the extraction process.

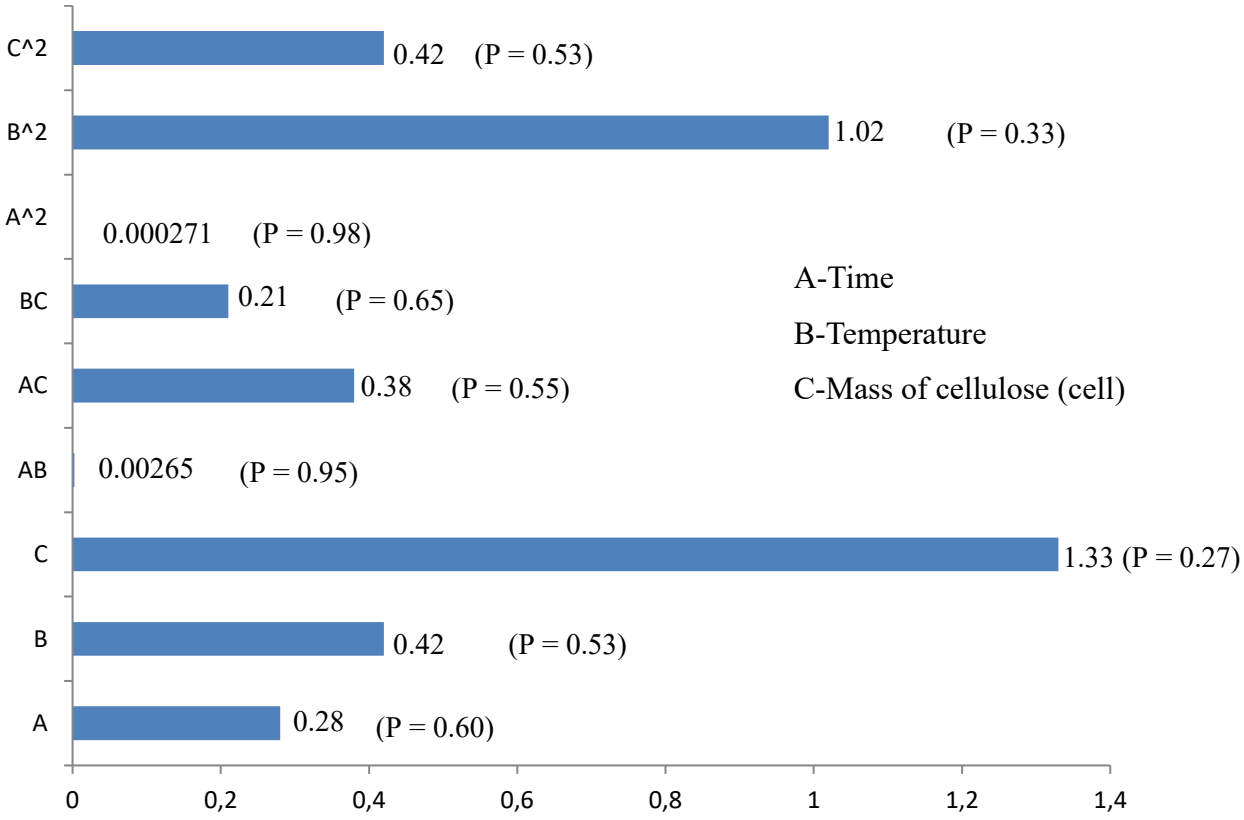


Figure 4.17: Pareto chart for sulfabezamide extraction in cellulose

4.4.2. Response surface methodology for the extraction of sulfachloropyridazine and sulfabenzamide using oxalic acid functionalized cellulose

RSM was used to assess the impact of three essential parameters: time (A), temperature (B), and oxalic acid functionalized cellulose mass (C), as illustrated in Fig. 4.18. The resulting response surfaces provided light on how these variables influenced extraction efficiency, showing their

© University of Venda

interdependence and nonlinear interactions. The following equation mathematically depicts the link between the parameters and the extraction efficiency:

% extraction sufachloropyridizine = +38.65 -2.00 x A +6.10 x B -12.90 x C +3.88 x AB -2.62 x AC+2.88 x BC+11.36 A^2 -10.14 x B^2 +10.86 x C^2 ..... (3)

Where A represents the extraction time, B the temperature, and C the mass of oxalic acid-functionalized cellulose.

Chaves et al. (2020) found that extending extraction times beyond the optimal range lowered yields in acid-mediated extraction systems. Oxalic acid functionalized cellulose was used as a sorbent in the extraction process. Its dual carboxylic functional groups promoted hydrogen bonding and chelation interactions with sulfachloropyridazine, increasing solubility and extraction efficiency (Chen et al., 2022). The presence of oxalic acid improved the analyte's efficiency for the sorbent material, which correlates with findings by Misiewicz et al. (2023), who explored its role in similar extraction methods.

The parameters' correlations were represented using response surface plots, as shown in Fig. 4.18. The time versus temperature plot (Fig. 4.18 a) showed that increasing temperature at shorter extraction times, improved extraction efficiency of sulfachloropyradizine. However, longer extraction times resulted in low extraction efficiency due to compound degradation. Similarly, the relationship between time and mass of cell@OA. (Fig. 4.18 b), revealed that the extraction % was lowest for the shortest extraction time (5 min) and the smallest mass of cell@OA (5mg). As the extraction time increased from 30 to 180 min and the mass increased from 5 to 50 mg, the extraction % increased. However, the plot had a concave curve, indicating a slower rate of improvement at higher values. The best extraction efficiency was recorded at the maximum extraction time (180 min) and the largest mass of cell@OA (50 mg), indicating that while both parameters favorably increased extraction, their combined effect achieved saturation. Fig. 4.18 c demonstrate that the extraction efficiency of sulfachloropyridazine increased with both temperature and cellulose@OA mass. At higher temperatures, notably around 75°C, molecular diffusion increased due to increased molecular motion, lowering solvent viscosity and improving mass transfer. A higher concentration of cellulose@OA, precisely 50 mg, supplied more adsorption sites, enabling for more Sulfachloropyridazine molecules to bind and be extracted

© University of Venda

successfully. Sulfachloropyridazine's solubility also increased at higher temperatures, allowing it to be released into the extraction medium more easily. In contrast, at lower temperatures around 25°C and a cellulose@OA mass of 5 mg, limited molecular mobility, fewer adsorption sites, and poorer solubility lead to the lowest extraction efficiency of about 30%. These findings align with Zhao et al. (2024), who found that increasing sorbent mass considerably increased extraction yields in acid-mediated systems by providing more active adsorption sites and improved overall efficiency. The optimum conditions for the adsorption of sulfachloropyridazine on oxalic acid-functionalized cellulose were established at a contact time of 30 min, a temperature of 25 °C, and a cellulose mass of 50 mg, yielding a maximum extraction efficiency of 64%. The Pareto chart (Fig. 4.19) supports the findings of RSM for the extraction efficiency of sulfachloropyridazine with cell@OA by demonstrating the relative importance of various factors influencing the extraction process.

© University of Venda

University of Venda
Creating Future Leaders

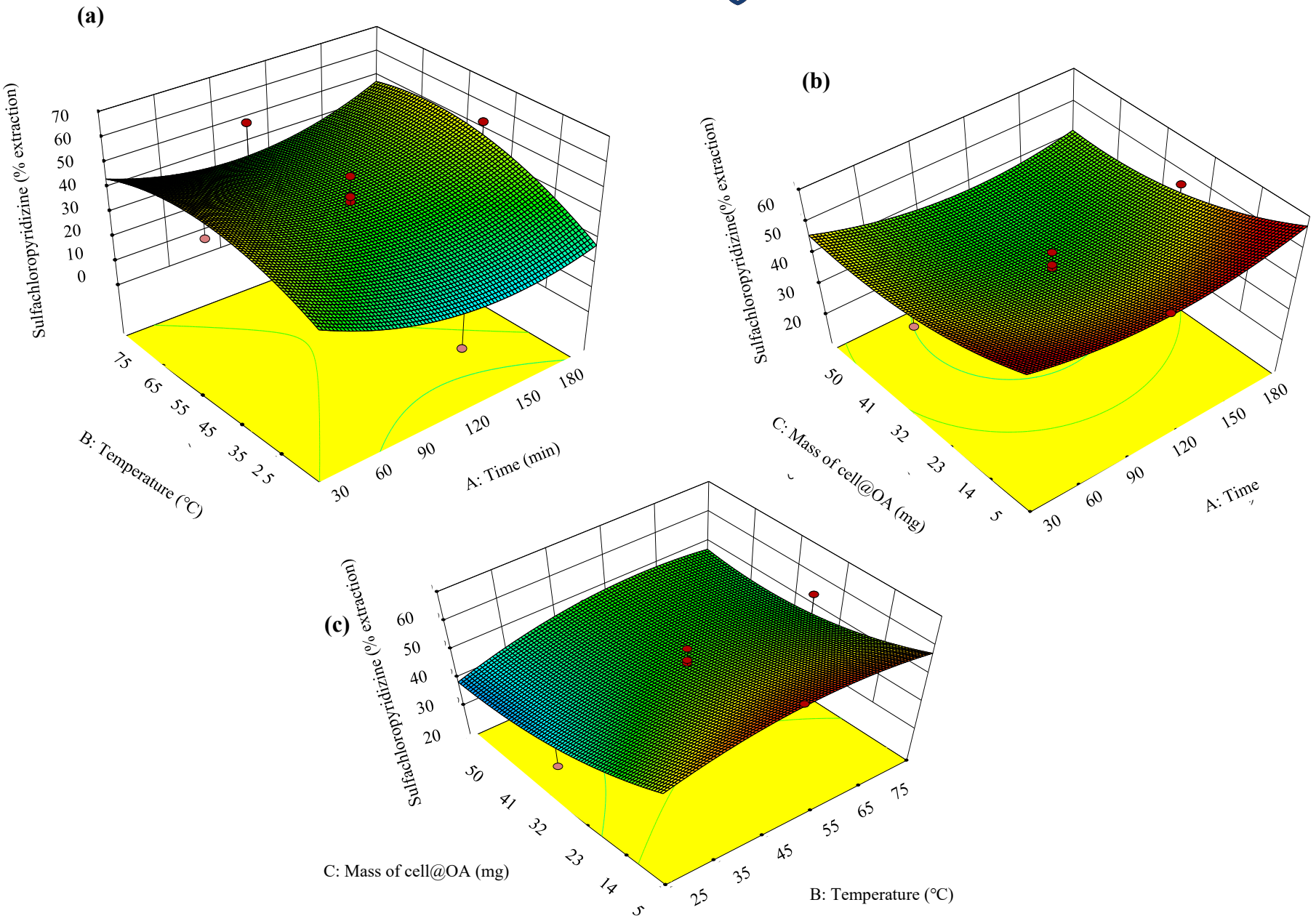


Figure 4.18: RSM plots for the extraction efficiency of sulfachloropyridazine with cell@OA: (a) the effect of time (A) and temperature (B), (b) the effect of time (A) and cell@OA mass (C) and (c) the effect of temperature (B) and cell@OA mass (C)

© University of Venda

The mass of cell@OA (C) had the greatest impact, followed by temperature (B), as illustrated in Fig. 4.19. The quadratic term (C^2) revealed a considerable non-linear effect, underscoring the critical significance of sorbent mass in optimizing the process. This suggested that increasing the sorbent mass beyond 50°C had a non-proportional effect on reaction efficiency, most likely due to saturation effects during the adsorption process. Furthermore, the interaction terms AB and BC demonstrated parameter synergy, indicating that temperature and time, as well as temperature and sorbent mass, controlled the extraction process collectively rather than independently. Although interaction terms AB and BC exhibited some level of synergy, Fig. 4.19 clearly shows that the most dominant effects were attributed to the individual parameter particularly sorbent mass (C) and temperature (B). This indicates that the extraction process was primarily influenced by individual variables rather than by their combined interactions. Factors with $p < 0.05$ were considered significant, but those with $P > 0.05$ were not. C was found to have a considerable impact on extraction efficiency, while other variables with $P > 0.05$ had no impact.

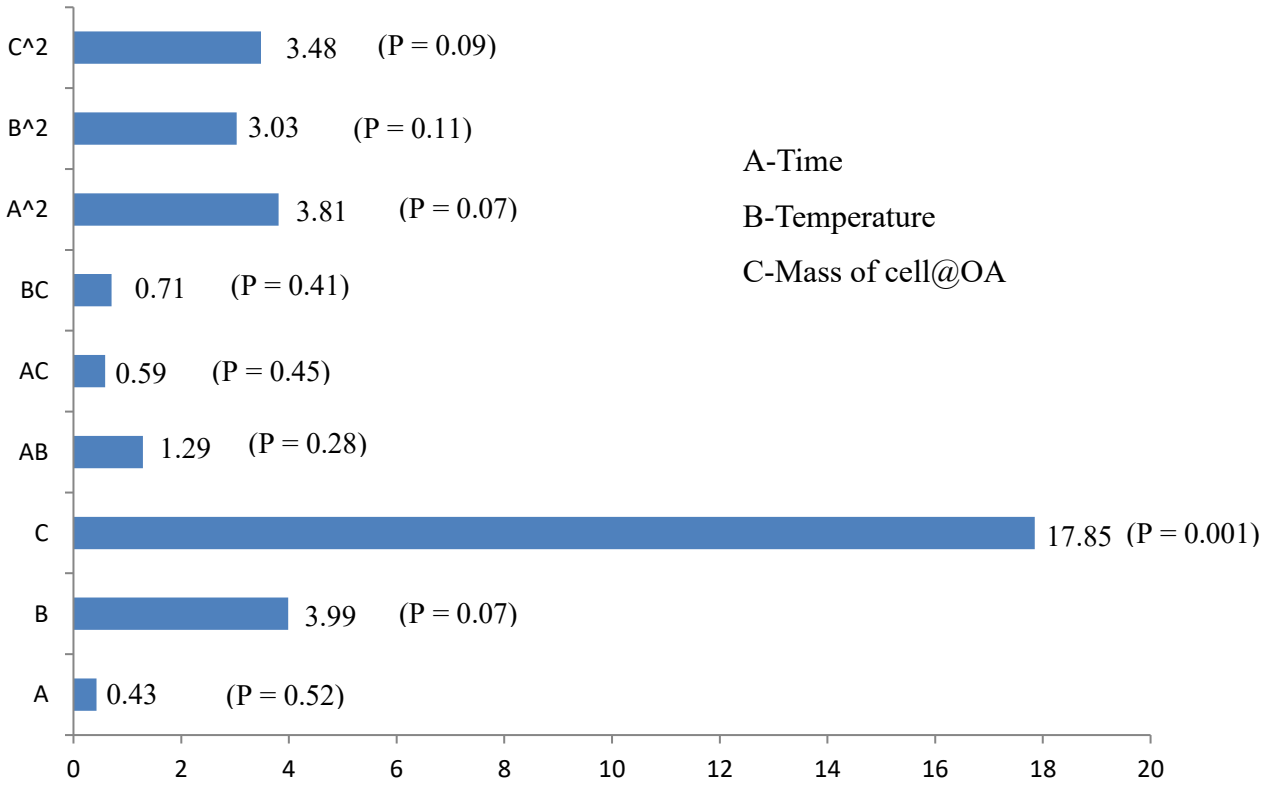


Figure 4.19: Pareto chart for sulfachloropyradazine extraction in cell@OA

© University of Venda

RSM was employed to evaluate the main, interaction, and quadratic effects of time (A), temperature (B), and mass of sorbent (C) on the extraction efficiency of sulfabenzamide, as illustrated in Fig. 4.20. The experimental data were fitted to a quadratic regression model, generated by the RSM software, as shown in Equation (4):

$$\% \text{ extraction sulfabenzamide} = +52.35 - 4.40 \times A + 8.70 \times B - 10.80 \times C + 7.13 \times AB - 5.87 \times AC + 6.38 \times BC + 17.64 \times A^2 - 22.8 \times B^2 + 15.64 \times C^2 \quad \ldots\ldots (4)$$

Where A represents the extraction time, B the temperature, and C the mass of oxalic acid-functionalized cellulose.

Temperature (B) and sorbent mass (C) had a significant impact on sulfabenzamide extraction, indicating a non-linear connection. The three-dimensional surface plots showed that temperature (B) and mass of sorbent (C) had a substantial impact on optimizing sulfabenzamide extraction. Furthermore, the relationship between temperature and sorbent mass (BC) made a significant contribution to the extraction process, as shown by the model. The RSM plot (time vs. temperature) (Fig 4.20 a) demonstrated that temperature (B) at low extraction times had a significant favorable effect on sulfabenzamide extraction. This trend suggested that higher temperatures improved sulfabenzamide adsorption, hence increasing extraction efficiency (Sanyal & Mathur, 2022). The Pareto chart (Fig. 4.21) confirmed that temperature (B) had the greatest impact ($P < 0.05$). The optimum conditions for the adsorption of sulfabenzamide on oxalic acid-functionalized cellulose were established at a contact time of 30 min, a temperature of 25 °C, and a cellulose mass of 50 mg, yielding a maximum extraction efficiency of 75%.

Fig. 4.20 b shows the influence of extraction time (30-180 min) and cell@OA acid mass (2.5-75 mg) on sulfabenazamide extraction %. The maximum extraction (~60%) was achieved at 30 min with 25 mg of cell@OA, whereas efficiency decreased with increasing mass and time. The contour map showed a saddle point at 90 min and 40 mg, indicating a local optimum. The experimental data points (red spheres) closely matched the model with minor variances. Fig. 4.20 c shows that sulfabenazamide extraction yield increases with oxalic-functionalized cellulose mass and temperature. The highest extraction yield was roughly 50% at the lowest mass (65 mg) and temperature (180°C), decreased masses (25-35 mg) and temperatures (30-60°C) resulted in decreased extraction efficiency (less than 20%). The response surface showed a nonlinear trend,

© University of Venda

with extraction efficiency stabilized at higher temperatures. The optimal extraction conditions appeared to be around 65 mg and 180°C.

© University of Venda

University of Venda
Creating Future Leaders

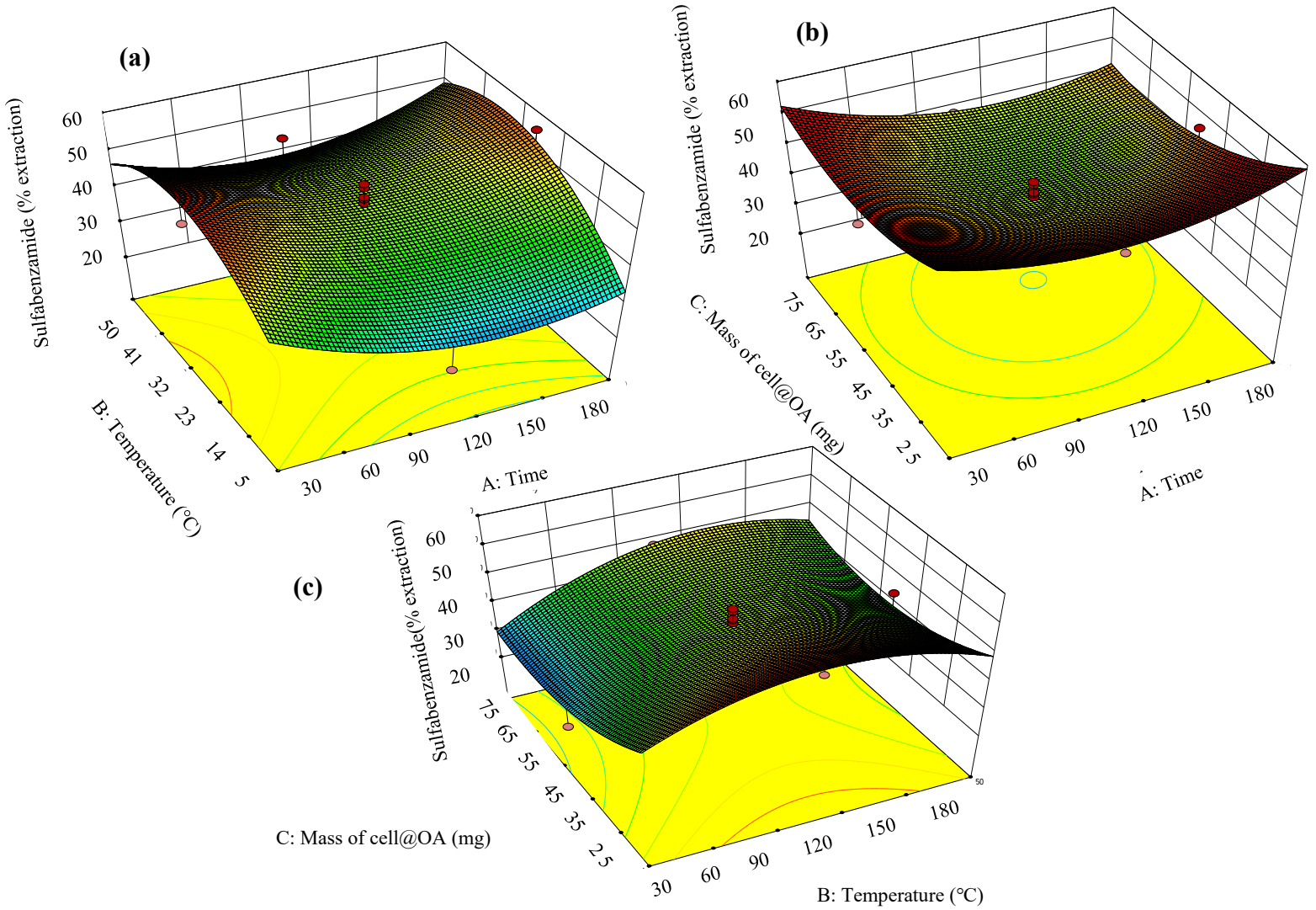


Figure 4.20: RSM plots for the extraction efficiency of sulfabenzamide with cell@OA: (a) the effect of time(A) and temperature (B), (b) the effect of time (A) and cell@OA mass (C) and (c) the effect of temperature (B) and cell@OA mass (C)

© University of Venda

The pareto chart (Fig. 4.21) was used to analyze the statistical significance of each element, with P-values indicating significance at $P < 0.05$ and insignificance at $P > 0.05$. Based on the analysis, sorbent mass (C) had the most significant effect on extraction yield ($P < 0.01$). Similarly, temperature (B) played an important role in improving sorption efficiency ($P < 0.04$). However, time (A) showed a little effect ($P > 0.27$), indicating that increasing extraction time beyond a certain point did not significantly improve sulfabenzamide recovery. The quadratic terms B^2 ($P < 0.01$), A^2 ($P < 0.03$), and C^2 ($P < 0.05$) were significant, showing non-linear impacts on the process. The interaction factors AB (time x temperature, $P > 0.12$), AC (time x sorbent mass, $P > 0.19$), and BC (temperature x sorbent mass, $P > 0.16$) were not statistically significant. In conclusion, response surface methodology (RSM) successfully identified the critical parameters influencing sulfabenzamide extraction in oxalic acid. Temperature (B) and sorbent mass (C) had the greatest influence on extraction efficiency, as evidenced by both the RSM plots and the Pareto chart. However, time (A) had a minimal influence on the process.

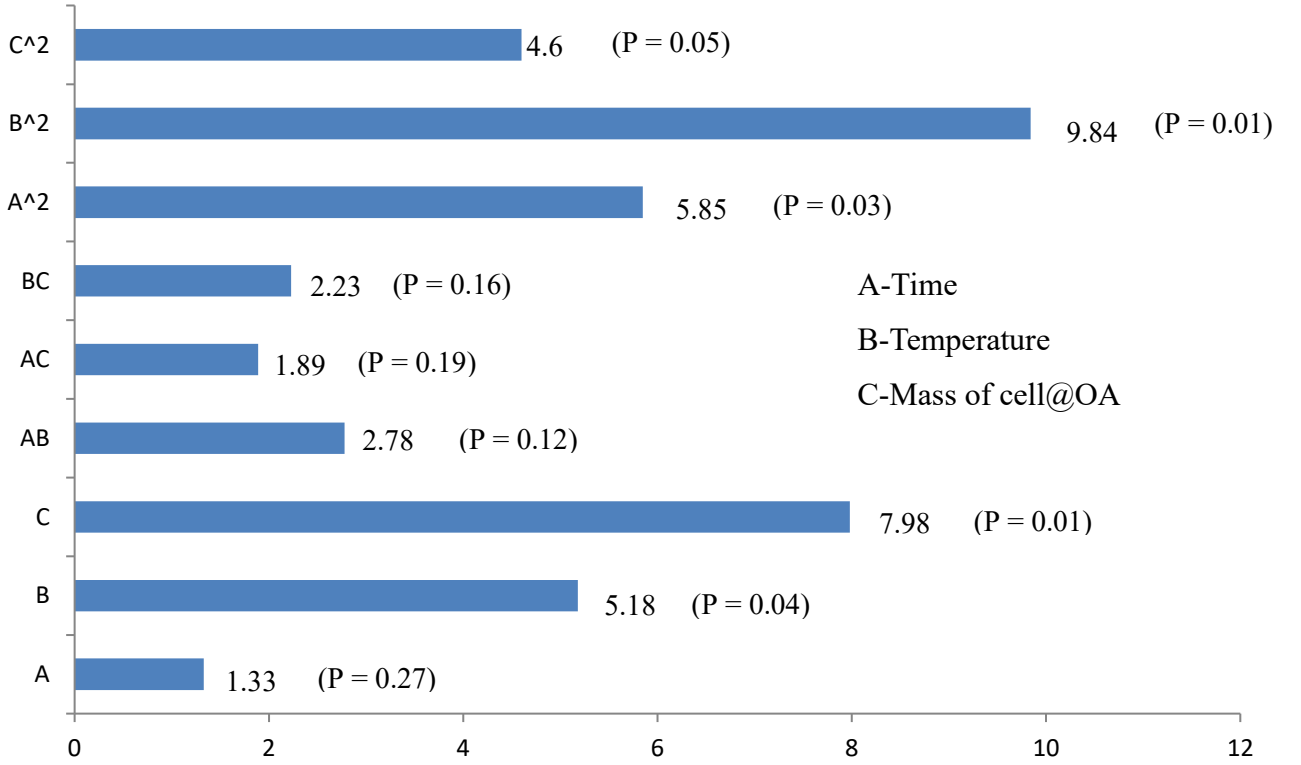


Figure 4.21: Pareto chart indicating parameter significance in sulfabenzamide extraction in cell@OA

© University of Venda

4.4.3. Response surface methodology for the extraction of sulfachloropyradazine and sulfabenzamide in adipic acid functionalized cellulose

RSM provided important insights into the extraction of sulfachloropyridazine with adipic acid functionalized cellulose as a sorbent. Three parameters influence extraction efficiency: time (A), temperature (B), and sorbent mass (C) as shown in Fig. 4.22. The following equation describes the relationship that governs sulfachloropyridazine extraction with cell@AA as a sorbent (5):

% extraction sulfachloropyridizine = +41.55 -4.80 x A +3.80 x B -5.90 x C+2.63 x AB -2.87 x AC +3.88 x BC +5.64 x A^2+9.64 x B^2 -2.86 x C^2 ……. (5)

Where A represents the extraction time, B the temperature, and C the mass of adipic acid-functionalized cellulose.

Equation (5) indicates the parameters' synergistic relationship. For example, the positive interaction between time and temperature (AB) indicated that a moderate period combined with higher temperatures increased extraction efficiency by balancing kinetic and thermodynamic components (Botelho Junior et al., 2022). On the other hand, the negative interaction between time and sorbent mass (AC) revealed that longer periods combined with extra sorbent mass reduced efficiency, most likely due to a combined effect of desorption and sorbent particle overpopulation (Rathi & Kumar, 2021). The interaction between temperature and sorbent mass (BC) was positive, indicating that higher temperatures mitigated the deleterious effects of excess sorbent mass by increasing analyte solubility and promoting sorbent-analyte interactions (Bagheri et al., 2022). Quadratic effects were also observed in the model. Temperature had a significant positive quadratic influence (B^2), indicating an ideal temperature range for maximum extraction efficiency. The first plot, which studied the effect of time and temperature (Fig. 4.22 a), revealed that as time increased particularly at higher temperatures, extraction efficiency improved. This suggested that longer reaction periods, paired with higher temperatures, resulted in more efficient extraction, most likely due to improved molecular interactions or solubility at high temperatures

Fig. 4.22 b how extraction time (A) and mass of cell@AA (C) affected the percentage of sulfachloropyridazine extraction. The extraction yield increased with longer extraction times, peaking at around 60%. However, increasing the mass of cell@AA above ~23 mg decreased extraction efficiency. The best conditions for maximal sulfachloropyridazine extraction were

© University of Venda

found at 150 min and 23 mg of cell@AA. The surface plot revealed a nonlinear connection, demonstrating the combined effect of both components. Similar results have been observed in research that optimize extraction techniques with RSM and functionalized cellulose materials. et Darmenbayeva et al. (2024) observed similar findings after optimizing extraction techniques using RSM and functionalized cellulose materials for pollutant removal from environmental water samples. The third plot, which investigated the effect of temperature and cell@AA mass (Fig. 4.22 c), revealed that for smaller masses, temperature had a greater influence on extraction efficiency, with higher temperatures boosting the process. However, as the mass of cell@AA increased, the effect of temperature decreased. This demonstrated that when there were enough active sites, temperature became less important for effective extraction. Beyond a certain threshold, increasing the mass and temperature did not appreciably improve extraction efficiency. The optimum conditions for the adsorption of sulfachloropyridazine on adipic acid-functionalized cellulose were determined to be a time of 30 min, a temperature of 25 °C, and a cellulose mass of 25 mg, resulting in a maximum extraction efficiency of 62%

© University of Venda

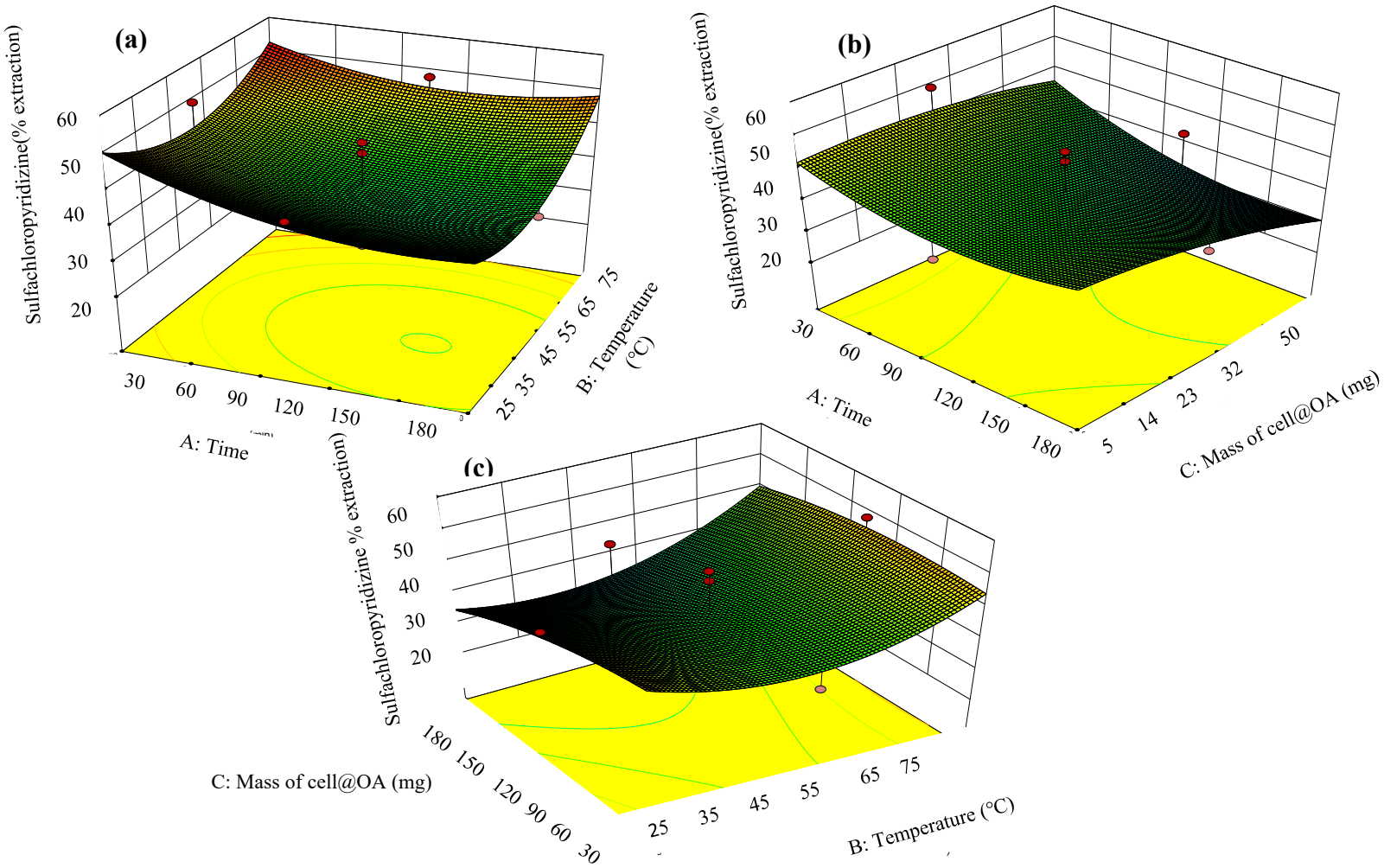


Figure 4.22: RSM plots for the extraction efficiency of sulfachloropyridazine with cell@AA: (a) the effect of time (A) and temperature (B), (b) the effect of time (A) and cell@OA mass (C), and (c) the effect of temperature (B) and cell@OA mass (C)

© University of Venda

The Pareto chart (Fig. 4.23) showed that none of the components were statistically significant, as all P-values were greater than 0.05 (P > 0.05). The mass of cell@AA (C) had the greatest effect (3.68, P > 0.08), followed by temperature (B) (1.53, P > 0.24), and time (A) (2.44, P > 0.14). The quadratic effect of temperature (B^2) was 2.7 (P > 0.13), showing a non-linear relationship but not statistically significant. Interaction terms, including BC (1.27, P > 0.28), AC (0.7, P > 0.42), and AB (0.58, P > 0.46), as well as the quadratic effect of mass (C^2 > 0.24, P > 0.63), exhibited minor effects and were not significant.

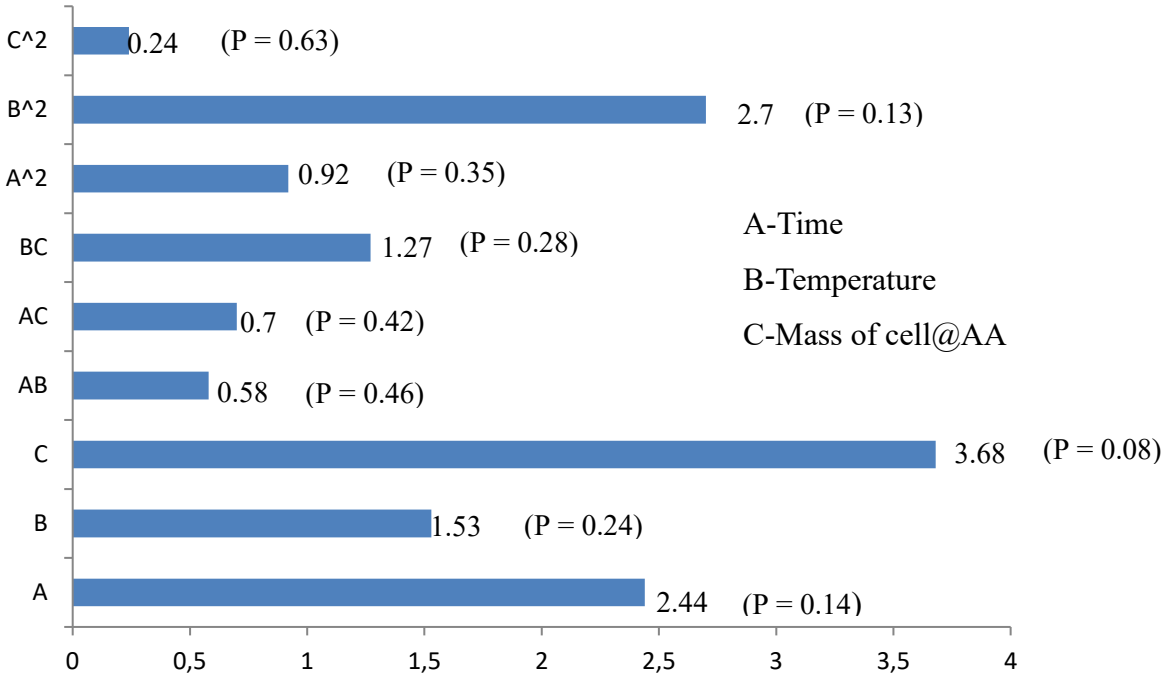


Figure 4.23: Pareto chart of sulfachloropyridazine extraction in cell@AA

As shown in Fig. 4.24, three factors were studied in a study that used response surface methodology (RSM) to optimize sulfabenzamide extraction using adipic acid-functionalized cellulose: extraction time (A), temperature (B), and sorbent mass (C). The derived quadratic model was:

% extracrion sulfabenzamide = +44.27 -5.50 x A+4.60 x B-2.80 x C+3.38 x AB-2.37 x AC +5.38 x BC+8.32 x A^2 +20.82 x B^2 -8.18 x C^2…… (6)

Where A represents the extraction time, B the temperature, and C the mass of adipic acid-functionalized cellulose.

© University of Venda

The analysis found that increasing temperature (B) improved extraction efficiency, most likely due to increased adsorption at higher temperatures (Gutema et al., 2022). However, the significant positive quadratic term for temperature (B^2) indicated that beyond an ideal range, further temperature rises could lead to lower efficiency, presumably due to analyte degradation. Prolonged extraction time (A) had a negative influence on efficiency which could be related to analyte degradation or adsorption over time. The sorbent mass (C) had a negative linear effect and a negative quadratic effect demonstrating that both insufficient and excessive amounts could lower efficiency, potentially due to inadequate adsorption sites. The interaction between extraction time and temperature (AB) indicated a moderate positive effect that as temperature increased and generally shorter extraction times, extraction of sulfabenzamide was optimized efficiently (Gopal et al., 2022). However, the relationship between extraction time and sorbent mass (AC) negatively influenced extraction, indicating that high sorbent, along with extended extraction time, led to ineffective recovery. Furthermore, the interaction between temperature and sorbent mass (BC) positively influenced extraction, emphasizing the necessity of optimizing these two parameters together.

Fig. 4.24 a shows that sulfabenzamide extraction efficiency increased with temperature and time, leading to increasing solubility and diffusion rates. The maximum extraction, around 60%, occurred at 75°C and 180 min, most likely because higher temperatures improved the interaction between sulfabenzamide and cell@OA, enhancing mass transfer. At 25°C for 30 min, extraction was less than 20%, most likely due to insufficient thermal energy and contact time for efficient adsorption. However, beyond 75°C, extraction efficiency plateaued or slightly decreased, perhaps due to deterioration or adsorption effects. Fig 4.24 b illustrates the influence of extraction time (30-180 min) and mass of adipic acid-functionalized cellulose (5-50 mg) on sulfabenzamide extraction efficiency. The extraction percentage ranged between about 0% and 60%. A progressive increase in mass resulted in a small improvement in extraction efficiency, whereas time had little effect beyond 90 min. The response surface was rather flat, indicating little interaction between the two parameters. The best conditions were seen around 50 mg of cellulose for 120-150 min, producing around 40-50% extraction efficiency.

Temperature (Fig. 4.24 c), on the other hand, reduced efficiency, most likely due to degradation, whereas high sorbent mass decreased efficiency, possibly due to an abundance of adsorption sites

© University of Venda

capturing standards. These findings are consistent with recent research in which RSM was used to optimize extraction procedures. For example, a study on the extraction of sulfonamide antibiotics emphasized the importance of temperature and extraction time as key determinants impacting effectiveness (Song et al., 2020). Similarly, another investigation into the removal of sulfamethoxazole from aqueous solutions using an ozone–electrocoagulation system identified pH and current density as significant parameters, emphasizing the importance of optimizing conditions for efficient extraction (Nghia et al., 2024).

© University of Venda

University of Venda
Creating Future Leaders

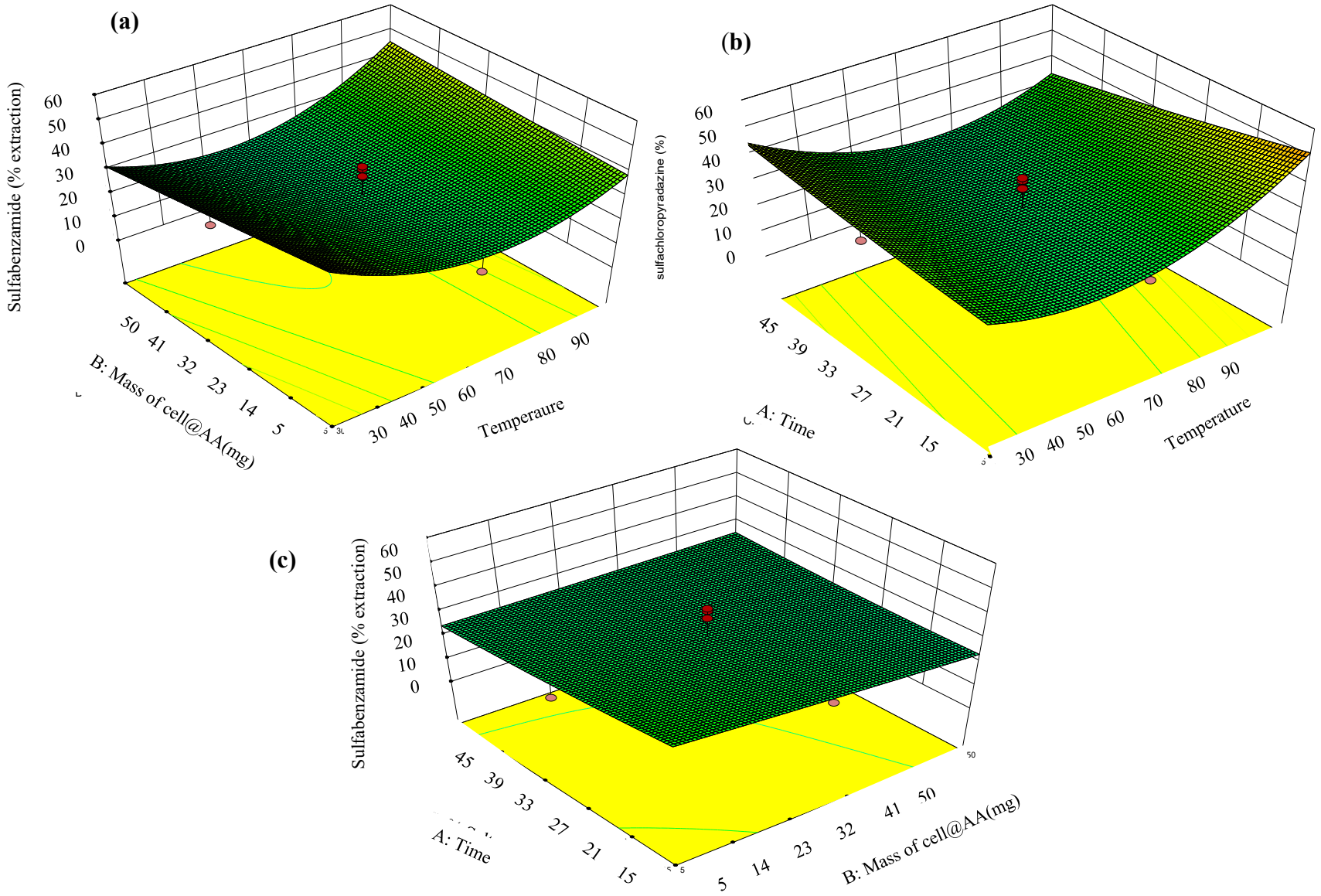


Figure 4.24: RSM plots for the extraction efficiency of sultabenzamide with cell@AA: the effect of time (A) and temperature (B), (b) the effect of time (A) and cell@AA mass (C), and (c) the effect of temperature (B) and cell@AA mass (C)

© University of Venda

The Pareto chart (Fig. 4.25), depicted the impact of several factors on a response variable, showing their relative importance. The x-axis depicted the magnitude of the impacts, and the y-axis listed the factors, including individual variables (A, B, C), interactions (AB, AC, BC), and squared terms (A2, B2, C2). The quadratic temperature term (B2) had the greatest impact, with an effect size of 3.25, according to the chart. Other variables, on the other hand, had significantly lesser effects. B^2 showed a moderate P-value of 0.10, whereas the other components had P-values more than 0.1, indicating that their effects were likely attributable to random variation rather than actual influence. In conclusion, time and temperature were the most important factors in optimizing sulfabenzamide extraction, with an ideal range required to achieve maximum efficiency. Extraction sorbent mass had a moderate influence, owing to interactions with other parameters.

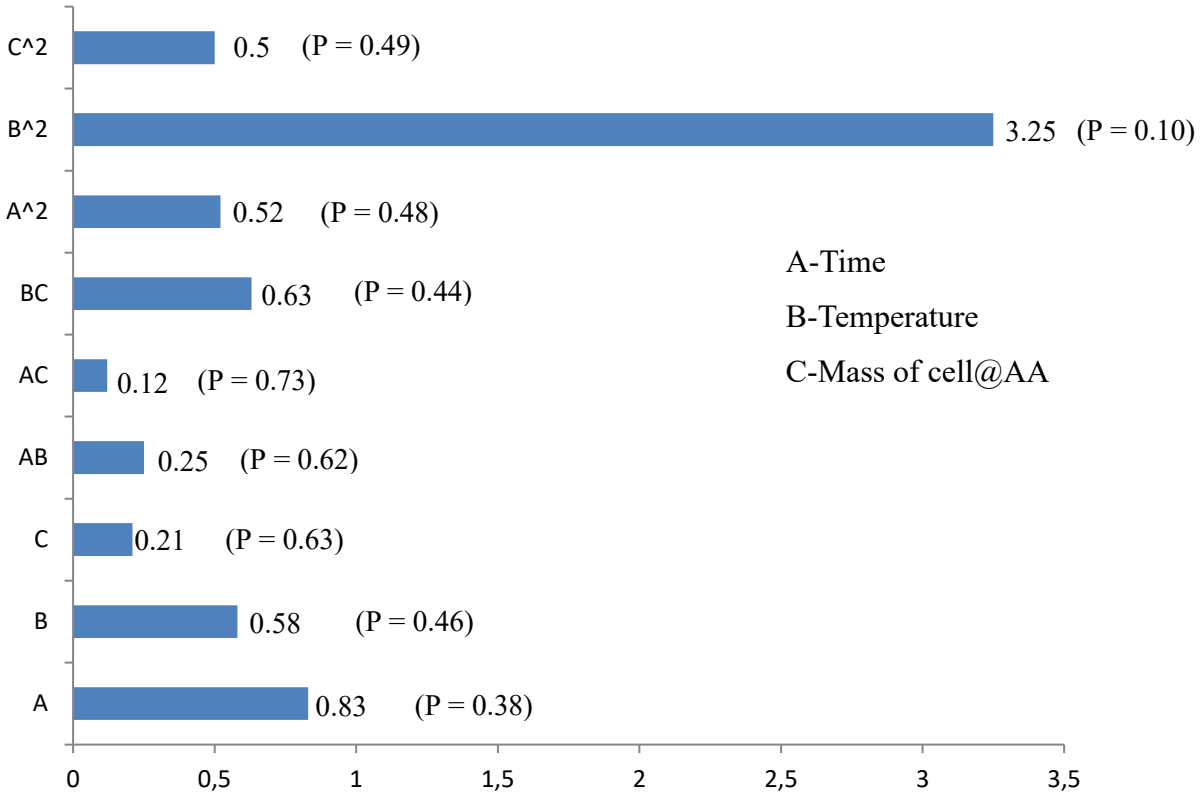


Figure 4.25: Pareto chart of sulfabenzamide extraction in cell@AA

© University of Venda

The optimum extraction of sulfabenzamide and sulfachloropyridazine from cellulose-based sorbents is significantly impacted by extraction time, temperature, and sorbent mass. The best extraction conditions for cellulose were 180 min, 25°C, and 5 mg of sorbent, yielding 70% extraction efficiency for sulfabenzamide and 51% for sulfachloropyridazine, but with lower desirability scores. This reduced effectiveness can be due to the cellulose's lack of functional groups, which would promote interaction with the analytes. However, when cellulose was functionalized with oxalic acid, the addition of carboxyl groups improved the extraction process. The best conditions for sulfabenzamide were 30 min, 25°C, and 50 mg of sorbent, producing 75% efficiency with a desirability of 1.000, whereas sulfachloropyridazine achieved 64% efficiency under the same conditions. Although cellulose sorbent provided reasonably good extraction efficiency (70% for sulfabenzamide with just 5 mg), it required a prolonged extraction time (180 min) and yielded lower desirability scores. Functionalization with oxalic acid, despite requiring a higher sorbent mass (50 mg), significantly reduced extraction time (to 30 min) and improved efficiency (75%) with a desirability of 1.000. These enhancements can be attributed to the presence of carboxyl groups that facilitate stronger interactions with the target sulfonamides. Therefore, functionalization represents a meaningful improvement in both speed and performance, especially important for real-world sample matrices where selectivity and robustness are crucial. Similarly, adipic acid-functionalized cellulose showed remarkable results, particularly for sulfabenzamide, at 30 min, 25°C, and 5 mg sorbent, with a 75% efficiency. The best conditions for sulfachloropyridazine were 30 min at 25°C and 25 mg sorbent, yielding 62% efficiency. The improved extraction efficiencies with functionalized cellulose are due to the added functional groups that create more active binding sites for the analytes.

© University of Venda

4.5 Application studies for batch adsorption

4.5.1. Extraction of sulfonamides from milk, honey, and wastewater using a cellulose-based sorbent

The chromatogram (Fig. 4.26) shows the HPLC analysis of three different sample matrices: wastewater (inlet), milk, and honey, all detected at 254 nm. The main objective was to find two sulfonamide antibiotics: sulfachloropyridazine (8.5 min retention time) and sulfabenzamide (9.2 min retention time). In the wastewater (inlet) sample, a peak at 7.5 min, which is sooner than the expected 8.5 min retention time for sulfachloropyridazine, is observed. This indicated a change in retention time, most likely due to matrix effects or instrumental alterations. At 9.2 min, no discernible peak was found, indicating that sulfabenzamide is either absent or below the detection limit in the wastewater. Peaks in milk (7.5 min) and honey (8.0 and 8.4 min) possibly correspond to sulfachloropyridazine or sulfabenzamide. The shifting of peaks in the chromatograms of wastewater, milk, and honey can be attributable to a variety of factors including matrix composition, mobile phase conditions, and methodological changes (Sabri, 2023). Matrix effects are important because differing sample compositions affect the interaction of analytes with the stationary phase.

The presence of various organic and inorganic chemicals in wastewater may cause early elution of sulfachloropyridazine, altering its retention time from 8.5 to 7.5 min. Similarly, in milk and honey, proteins, sugars, and other organic compounds can delay or accelerate elusion, influencing retention times (Van Ginkel et al., 2019). Another important element is pH fluctuations in the mobile phase, which can impact sulfonamide ionization and, thus, retention durations (Liem et al., 2019). Even minor variations from the ideal pH values can alter analyte-column interactions, leading to peak shifts (Stolker et al., 2019). Furthermore, column aging, co-elution or contamination might result in uneven retention durations and peak broadening, as a degraded stationary phase reduces separation efficiency (Sýkora et al., 2019). Furthermore, the presence of proteins, lipids, and carbohydrates in milk and honey makes sample-column interactions more complex, since they can bind to the stationary phase and impact sulfonamide retention (Chen et al., 2019). In wastewater, competing chemicals may interact with the column, altering the elution pattern of the target analytes (Morin-Crini et al., 2022).

© University of Venda

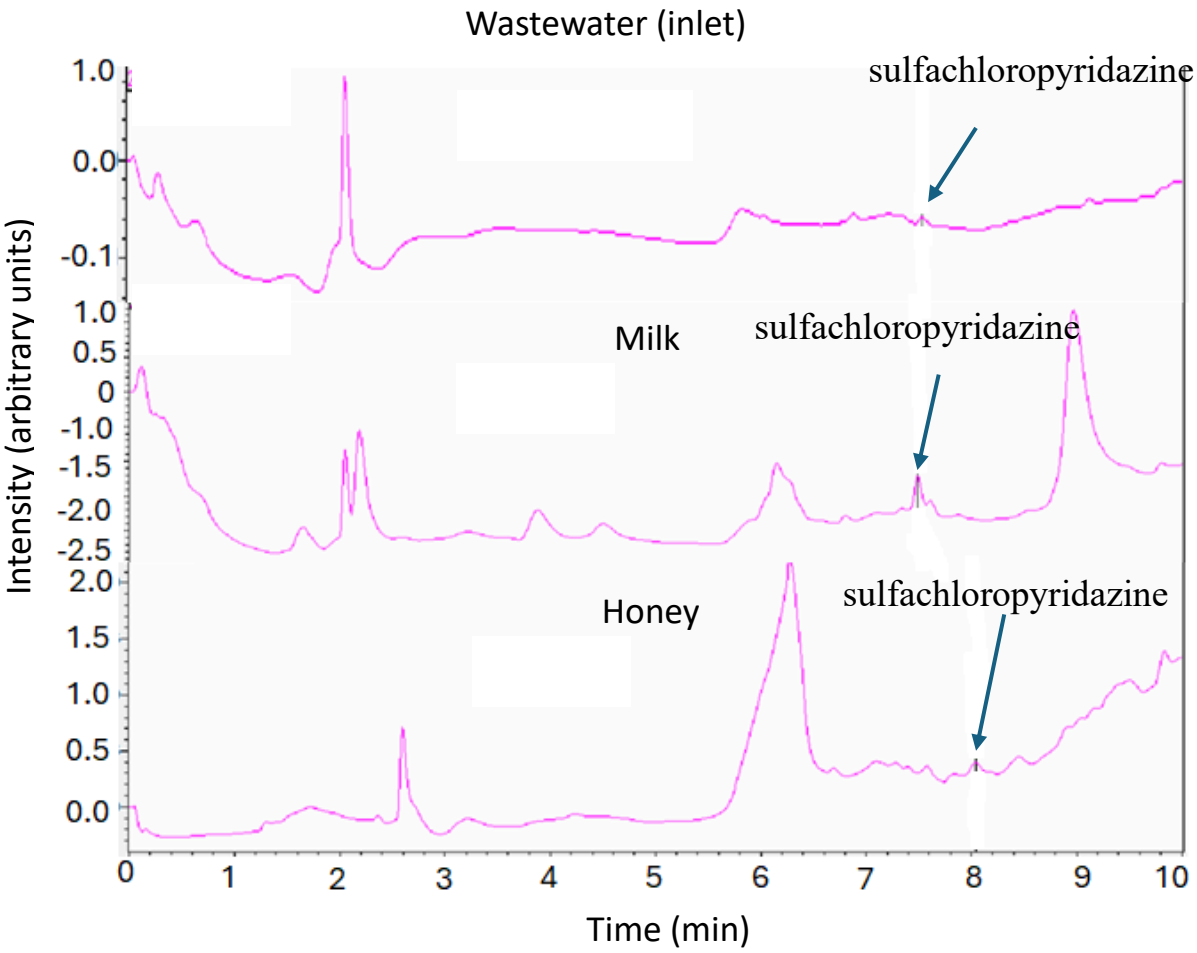


Figure 4.26: Chromatogram analysis of sulfachloropyridazine in different matrices

Table 4.6 shows the percentage extraction effectiveness of cellulose (Cell) as a sorbent for removing sulfonamides from various matrices (wastewater, honey, and milk). The studies were carried out under identical conditions: a time of 180 min, a temperature of 25°C, and a sorbent mass of 5 mg. The extraction efficiency for wastewater was 55% for sulfachloropyridazine only. The overall extraction efficiency in milk was 57% for sulfachloropyridazine, but sulfabenzamide was not detected. In the honey sample, both sulfonamides were not detected.

© University of Venda

Table 4.6: Extraction efficiency of the cellulose-based sorbent for sulfonamide removal from different matrices

Matrix	Time (min)	Temperature (°C)	Mass of sorbent (mg)	Sulfachloropyridazine % extraction	Sulfabenzamide % extraction
Wastewater (inlet)	180	25	5	55	-
Milk	180	25	5	57	-
Honey	180	25	5	-	-

The chromatographic analysis of sulfonamides in milk using a cellulose-based sorbent revealed a shift in the retention time of sulfachloropyridazine from 8.5 to 7.5 min, as shown in Fig. 4.27. The observed shift could most likely be due to changes in mobile phase composition, interactions with the sorbent, column aging, instrumental factors, or milk matrix effects. Furthermore, sulfabenzamide, which was expected to appear at 9.2 min, was not found, possibly due to poor extraction efficiency, insufficient UV absorbance at 254 nm, matrix suppression, co-elution with other chemicals, or degradation during sample preparation (von Eyken Bonafonte et al., 2019). Milk was shown to be the most successful for sulfachloropyridazine extraction, with more recovery and better chromatographic findings than the other matrices. Bitas et al. (2018) examined sample preparation techniques for sulfonamide extraction from food samples, such as milk and honey, followed by high-performance liquid chromatography (HPLC analysis). They emphasized the significance of improving extraction procedures to account for matrix-specific interactions, which can influence analyte recovery and detection.

© University of Venda

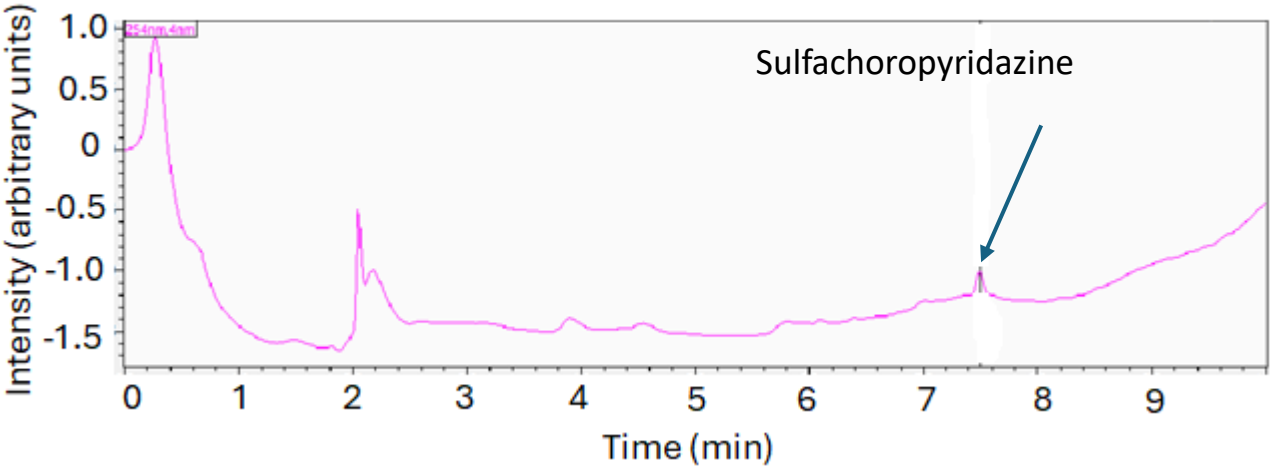


Figure 4.27: A chromatogram of sulfacholoropyridazine extracted from milk using a cellulose-based sorbent

4.5.2. Extraction of sulfonamides from milk, honey, and wastewater using a cell@OA sorbent

Table 4.7 shows the extraction efficiency of sulfachloropyridazine and sulfabenzamide from wastewater, honey, and milk with a cell@OA sorbent under optimum conditions (30 min, 25°C, and 50 mg sorbent mass). In milk, sulfachloropyridazine had the best extraction efficiency (86%), while sulfabenzamide had a substantially lower recovery rate (29%). Similarly, in wastewater, sulfachloropyridazine had a somewhat lower extraction efficiency of 76%, whereas sulfabenzamide was only removed at 15% efficiency. Notably, no sulfachloropyridazine or sulfabenzamide were found in honey. The findings indicated that the cell@OA sorbent was more successful in extracting sulfonamides from milk and wastewater than honey

© University of Venda

Table 4.7: Extraction efficiency of cell@OA sorbent for sulfonamide removal from different

Matrixes	Time (min)	Temperature (°C)	Mass of sorbent (mg)	Sulfachloropyridazine % extraction	Sulfabenzamide % extraction
Wastewater (inlet)	30	25	50	76	15
Milk	30	25	50	86	29
Honey	30	25	50	-	-

The chromatographic analysis (Fig. 4.28) of sulfonamides in milk with cell@OA sorbent indicated that sulfachloropyridazine and sulfabenzamide eluted earlier than expected. The addition of carboxyl (-COOH) groups via oxalic acid functionalization greatly increased cellulose polarity (Jia & Liu 2019), allowing for improved interactions with sulfonamides. These interactions, which included hydrogen bonding (Mei et al., 2024), dipole-dipole forces (Zhuang et al., 2024) and electrostatic attraction (Wang et al., 2024), resulted in a substantial shift in sulfonamide retention times. Sulfachloropyridazine eluted at 7.8 mim and sulfabenzamide at 8.2 min, but their estimated time of retention were 8.5 min and 9.2 min, respectively. These changes were principally due to the modified cellulose's capacity to engage in a variety of non-covalent interactions with the sulfonamides, modifying the adsorption dynamics (Liu et al., 2024).

The matrix effects of milk, a complex media containing proteins, lipids, and lactose, exacerbated the chromatographic analysis. Milk proteins, particularly casein, and lipids competed with sulfonamides for accessible binding sites on the sorbent, potentially lowering the quantity of analyte adsorbed and accelerating elution (Villa et al., 2020). Furthermore, protein-sulfonamide interactions in the milk solution may have generated complexes, reducing the free sulfonamide concentration available for binding to cellulose (Galus et al., 2020). While cell@OA demonstrated higher adsorption effectiveness for sulfachloropyridazine than other sorbents, the matrix impact of milk posed additional hurdles. To optimize the approach for accurate sulfonamide quantification, further experimental conditions, such as altering pH, ionic strength, and sorbent concentration, will be required to reduce matrix interference and stabilize retention times. Overall, this study demonstrated the promise of oxalic acid-functionalized cellulose as a selective and effective

© University of Venda

material for sulfonamide extraction from complex food matrices, with space for improvement in performance.

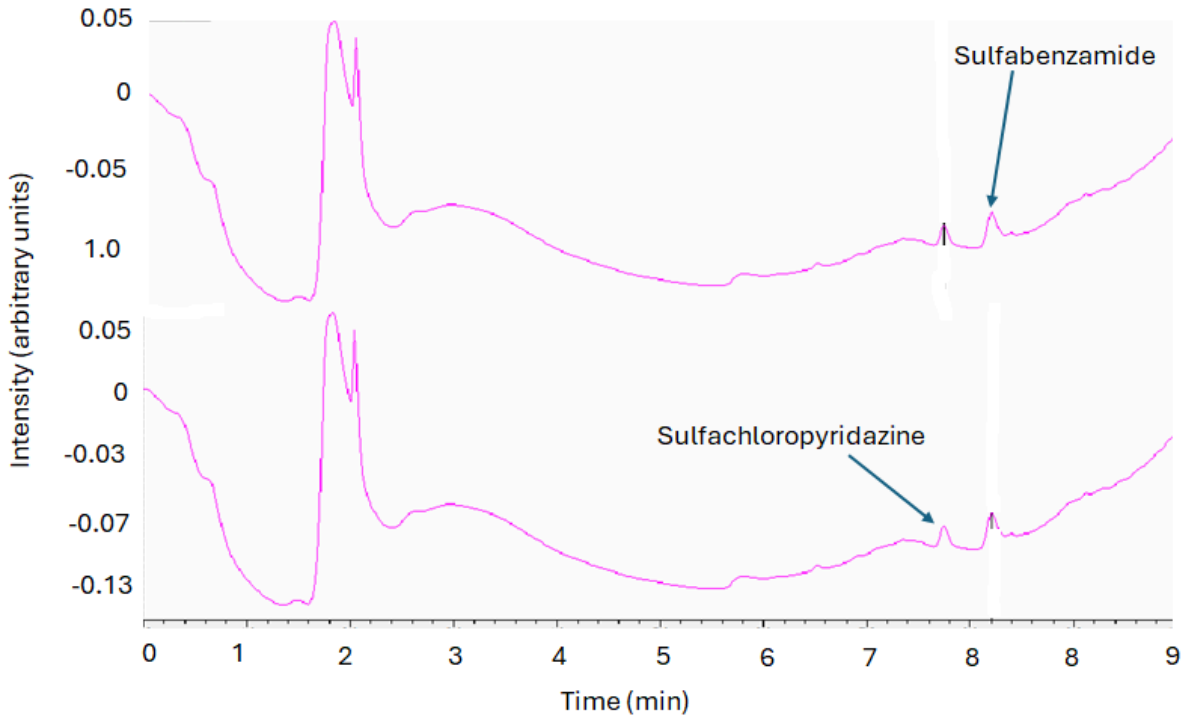


Figure 4.28: A chromatogram of sulfachloropyradizine and sulfabenzamide extracted from milk using a cell@OA sorbent

4.5.3. Extraction of sulfonamides from milk, honey, and wastewater using a cell@AA sorbent

Table 4.8 shows the percentage extraction of sulfachloropyridazine and sulfabenzamide with adipic acid-functionalized cellulose (cell@AA) as a sorbent under regulated conditions. The extractions were performed at 25°C for 30 min with a sorbent mass of 5 mg. Sulfachloropyridazine had 45% extraction efficiency in wastewater, but no sulfabenzamide was identified. In milk, sulfachloropyridazine extraction efficiency improved dramatically to 68%, while sulfabenzamide extraction was extracted at 31%. However, sulfachloropyridazine nor sulfabenzamide were found in honey.

© University of Venda

Table 4.8: Extraction efficiency of cell@AA sorbent for sulfonamide removal from different matrices

Matrixes	Time (min)	Temperature (°C)	Mass of sorbent (mg)	Sulfachloropyridazine % extraction	Sulfabenzamide % extraction
Wastewater (inlet)	30	25	5	45	-
Milk	30	25	5	68	31
Honey	30	25	5	-	-

The chromatogram (Fig. 4.29) shows the extraction efficiency of cell@AA as a sorbent for extracting sulfonamides from milk. The study was predicted to yield two different peaks: sulfachloropyridazine at 8.5 min and sulfabenzamide at 9.2 min. However, the results of the experiment indicated a change, with sulfachloropyridazine emerging at 7.8 min and sulfabenzamide at 8.2 min. This shift in retention time could be due to a variety of variables. One major explanation is the interaction of the cell@AA with the sulfonamides during the extraction process (Watson, 2023). Adipic acid, when grafted onto cellulose, introduces carboxylic groups capable of dipole-dipole interactions with the amine and sulfonyl groups of sulfonamides. Furthermore, the matrix impact of milk, which contains proteins, lipids, and sugars, could have contributed to minor differences in analyte retention, as the sulfonamides may have had different affinities during extraction compared to honey or wastewater solutions.

The chromatogram showed a larger % extraction of sulfachloropyridazine from milk than from honey and wastewater, implying that the functionalized cellulose sorbent was more effective in the dairy matrix. This could be because the adipic acid moieties have improved selectivity for sulfachloropyridazine, possibly by creating stronger hydrogen bonds or engaging in hydrophobic interactions (Isaeva et al., 2021). Furthermore, the shift in peak retention times could be due to modest fluctuations in column temperature (Haddad et al., 2020), mobile phase composition (Taraji et al., 2020), or flow rate (Szücs et al., 2020), all of which can impact chromatographic behavior. In conclusion, the cell@AA interacted with the analytes through a variety of routes,

© University of Venda

affecting their chromatographic retention times. The successful extraction from milk shows that this sorbent has potential applications for sulfonamide residue detection in complex food matrices, which aligns with the goals of sustainable water and food safety standards.

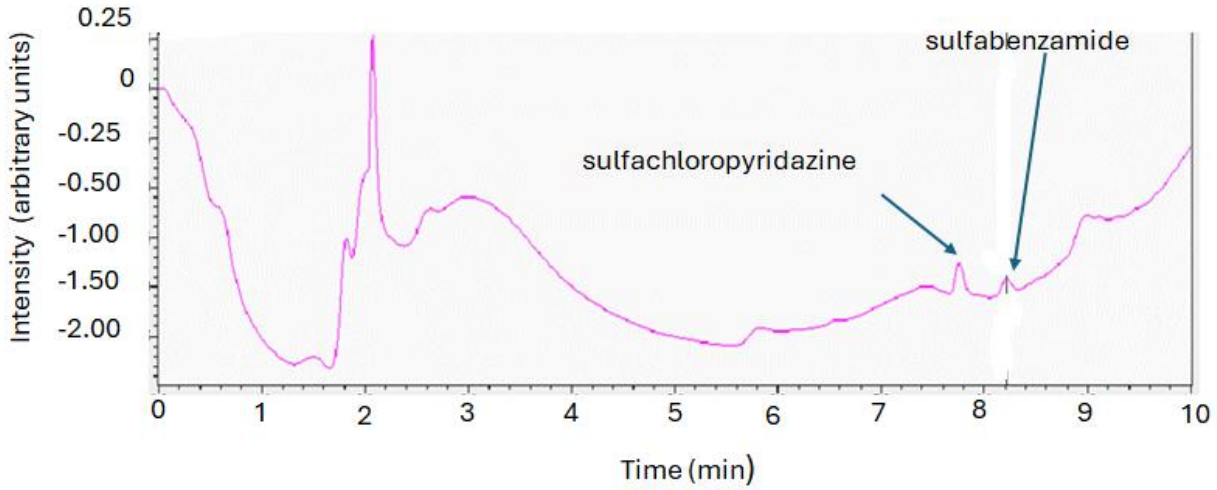


Figure 4.29: A chromatogram of sulfachloropyridazine and sulfabenzamide extracted from milk using a cell@AA sorbent

The three experimental sets were tested under optimal extraction conditions. The cellulose-based sorbent, utilized at 5 mg with a 180 min extraction at 25°C, revealed 55% extraction of sulfachloropyridazine in wastewater and 57% in milk. Sulfabenzamide was undetectable in both matrices. In comparison, the cell@OA sorbent was applied at 50 mg for 30 min at 25°C, providing significantly superior outcomes, i.e., 76% extraction for sulfachloropyridazine and 15% for sulfabenzamide in wastewater, 86% and 29% in milk, respectively. Both analytes were not detected in honey. Using the cell@AA sorbent at 5 mg for 30 min at 25°C yielded moderate results, with 45% extraction of sulfachloropyridazine in wastewater and 68% in milk, as well as 31% recovery of sulfabenzamide. The sorbent's functionalization, mass, and extraction times are all important elements in determining extraction efficiency.

The findings show that the functionalization of the sorbent, the mass used, and the extraction time are all important factors in determining extraction efficiency. Notably, the increased chemical functionality and mass of cell@OA considerably improved analyte adsorption, making it the best

© University of Venda

performer overall, particularly for sulfachloropyridazine. Furthermore, changes in matrix composition played an impact, with milk often providing higher recovery rates than wastewater, but honey consistently exhibited no measurable extraction for either analyte. These findings highlight the importance of both the sorbent's chemical properties and operational factors in obtaining maximum extraction efficiency for sulfonamide removal.

© University of Venda

4.6. Aqueous two-phase extraction adsorption

Aqueous two-phase extraction (ATPE) is a separation technique that exploits the ability of ternary water-based mixtures to exist in a two-phase state (Voshkin et al**.,** 2021). The technique was particularly useful for separating biomolecules such as proteins (Chen et al., 2023) and nucleic acids (Liang et al., 2023) because of its benign and biocompatible environment. It was widely employed in the biotechnology and pharmaceutical industries due to its ability to separate and purify delicate biological components (Chandler, 2021). The aqueous environment preserved the stability and activity of biomolecules, making it preferable to conventional organic solvent-based extraction procedures. ATPE's advantages include gentle settings that conserved biomolecules' native structure and function (Ferreira-Faria E et al., 2020). It is also regarded as a cost-effective strategy due to its simplicity (Aires-Barros et al., 2020), speed (Azevedo et al., 2020), and low cost (Ferreira-Faria et al., 2020). Furthermore, ATPE can easily be scaled for industrial purposes without requiring significant changes. The method proved extremely useful for extracting and purifying a variety of biological components, including cells, nucleic acids, proteins, antibodies, and tiny compounds (Aires-Barros et al., 2020). Its versatility to varied systems enabled specific applications in a variety of scientific and industrial domains. In this study, ATPE was utilized to optimize extraction sulfabenzamide and sulfachloropyradizine.

Table 4.9, 4.10 and 4.11 shows the experimental settings utilized in a study to determine the effects of sonication time, sorbent mass, salt concentration, and salt type. The sonication time ranged from 30 to 90 min, while the mass of the sorbent, which comprised of cell, cell@OA, and cell@AA, ranged from 5 to 50 mg. The salt concentrations studied were 15%, 30%, and 45% of the kosmotrope (Na_2CO_3) and chaotrope (NaCl).

© University of Venda

Table 4.9: Extraction efficiency of sulfachloropyridazine and sulfabenzamide using cellulose as sorbent under varying conditions

Ultrasonication time (min)	Mass of sorbent (mg)	% salt	Salt type	Sulfachloropyridazine % extraction	Sulfabenzamide % extraxtion
60	27.5	45	Kosmotrope	36	54
30	27.5	30	Chaotrope	11	13
60	27.5	30	Kosmotrope	25	27
60	27.5	30	Chaotrope	29	27
60	50	30	Kosmotrope	40	37
90	5	45	Chaotrope	70	74
90	50	15	Kosmotrope	45	42
90	50	15	Chaotrope	68	67
60	27.5	30	Chaotrope	43	100
60	5	30	Chaotrope	26	25
60	27.5	30	Kosmotrope	20	24
90	5	15	Kosmotrope	43	41
60	27.5	30	Chaotrope	45	43

© University of Venda

90	27.5	15	Chaotrope	55	52
60	5	30	Kosmotrope	41	41
60	27.5	30	Chaotrope	40	41
30	5	15	Kosmotrope	17	17
90	5	45	Kosmotrope	43	51
60	27.5	15	Kosmotrope	58	6
60	27.5	30	Kosmotrope	64	65
30	50	45	Chaotrope	65	100
30	5	45	Kosmotrope	24	27
30	5	15	Chaotrope	23	24
60	27.5	30	Chaotrope	78	78
30	50	15	Chaotrope	39	48
90	50	45	Kosmotrope	65	62
30	5	45	Kosmotrope	17	18
60	27.5	30	Kosmotrope	50	48
30	50	45	Kosmotrope	49	47

© University of Venda

90	27.5	30	Kosmotrope	21	20
60	27.5	30	Chaotrope	50	48
60	27.5	30	Kosmotrope	20	27
90	50	50	Chaotrope	65	63
60	27.5	30	Kosmotrope	37	36
60	27.5	45	Chaotrope	50	49
90	5	15	Chaotrope	39	37
90	27.5	30	Chaotrope	29	27
90	50	30	Chaotrope	12	100

© University of Venda

Table 4.10: Extraction efficiency of sulfachloropyridazine and sulfabenzamide using cell@OA as sorbent under varying condition

Ultrasonication time (min)	Mass of sorbent (mg)	% salt	Salt type	Sulfachloropyridazine % extraction	Sulfabenzamide % extraxtion
30	5	45	Kosmotrope	52	49
60	27.5	30	Chaotrope	25	19
60	27.5	30	Kosmotrope	37	45
60	27.5	15	Chaotrope	39	35
60	27.5	45	Kosmotrope	21	16
90	27.5	30	Kosmotrope	40	36
90	50	45	Kosmotrope	40	44
60	27.5	30	Kosmotrope	23	19
90	5	45	Kosmotrope	30	34
60	27.5	30	Chaotrope	52	47
60	27.5	30	Chaotrope	23	20
30	5	15	Kosmotrope	45	46
90	5	15	Kosmotrope	52	54

© University of Venda

60	27.5	30	Koamotrope	33	25
90	50	15	Kosmotrope	52	54
30	50	15	Kosmotrope		
60	27.5	30	Kosmotrope	36	27
60	25.7	15	Kosmotrope	26	23
60	5	30	Chaotrope	26	19
30	27.5	30	Kosmotrope	35	34
60	5	30	Kosmotrope	22	17
30	50	15	Chaotrope	5	1
30	27.5	30	Chaotrope	29	25
60	50	30	Chaotrope	44	51
30	5	45	Chaotrope	27	23
60	27.5	45	Chaotrope	60	50
60	27.5	30	Chaotrope	41	32
90	5	15	Chaotrope	29	35
90	50	45	Chaotrope	21	17

© University of Venda

90	5	45	Chaotrope	36	32
90	27.5	30	Chaotrope	17	12
60	27.5	30	Kosmotrope	3	3
30	50	45	Kosmotrope	41	100
30	5	15	Chaotrope	17	12
30	50	45	Chaotrope		
60	27.5	30	Chaotrope	3	3
60	27.5	30	Kosmotrope	33	32
60	27.5	30	Chaotrope	43	35

© University of Venda

Table 4.11: Extraction efficiency of sulfachloropyridazine and sulfabenzamide using cell@AA as sorbent under varying condition

Ultrasonication time (min)	Mass of sorbent (mg)	% salt	Salt type	Sulfachloropyridazine % extraction	Sulfabenzamide % extraxtion
30	5	45	Kosmotrope	31	86
60	27.5	30	Chaotrope	29	29
60	27.5	30	Kosmotrope	32	34
60	27.5	15	Chaotrope	27	34
60	27.5	45	Kosmotrope	26	25
90	27.5	30	Kosmotrope	20	18
90	50	45	Kosmotrope	37	34
60	27.5	30	Kosmotrope	45	59
90	5	45	Kosmotrope	33	29
60	27.5	30	Chaotrope	27	26
60	37.5	30	Chaotrope	39	44
30	5	15	Chaotrope		

© University of Venda

90	5	15	Chaotrope	25	22
90	90	15	Chaotrope	55	52
60	27.5	15	Kosmotrope	44	40
90	50	15	Chaotrope	38	31
30	50	15	Kosmotrope	14	13
60	27.5	30	Kosmotrope	56	55
60	27.5	15	Kosmotrope	17	16
60	5	30	Chaotrope	25	23
30	27.5	30	Kosmotrope	21	22
60	5	30	Kosmotrope	67	0
60	50	30	Chaotrope	91	38
30	27.5	30	Chaotrope	24	24
30	30	15	Chaotrope	39	48
90	90	45	Kosmotrope	65	62
30	30	45	Kosmotrope	17	18

© University of Venda

60	60	30	Kosmotrope	50	48
30	30	45	Kosmotrope	49	47
90	90	30	Kosmotrope	21	20
60	60	30	Chaotrope	50	48
60	60	30	Kosmotrope	20	27
90	90	50	Chaotrope	65	63
60	60	30	Kosmotrope	37	36
60	60	45	Chaotrope	50	49
90	90	15	Chaotrope	39	37
90	90	30	Chaotrope	29	27
90	90	30	Chaotrope	12	50

© University of Venda

Fig. 4.30 shows an HPLC chromatogram of sulfachlopyridazine after extraction with cellulose in the presence of NaCl as a chaotrope. The retention time for sulfalchlopyridazine was 7.8 min showing good retention and interaction with the cellulose phase. The presence of hydroxyl functional groups on cellulose likely improved interactions with sulfachlopyridazine via hydrogen bonding and van der Waals forces, hence increasing adsorption and selectivity (Zhu et al., 2022). The chromatographic profile demonstrates that cellulose provides a robust and reproducible extraction platform that allows for exact measurement and analysis of sulfalchlopyridazine.

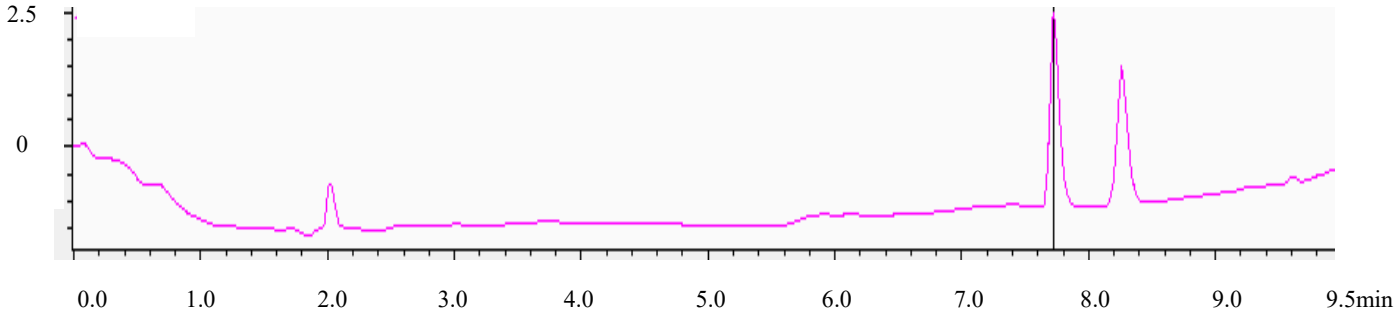


Figure 4.30: Optimal HPLC chromatogram of sulfachlopyridazine after extraction with cellulose in the presence of NaCl as a chaotrope

Fig. 4.31 shows the chromatographic analysis of sulfabenzamide extraction with cellulose sorbent and NaCl as a chaotrope demonstrates efficient retention at 8.2 min, with small peaks indicating a solvent peak. The hydroxyl groups in cellulose allow for selective interactions through hydrogen bonds and van der Waals forces. NaCl improves partitioning in the aqueous two-phase system, which ensures high extraction efficiency and reproducibility.

© University of Venda

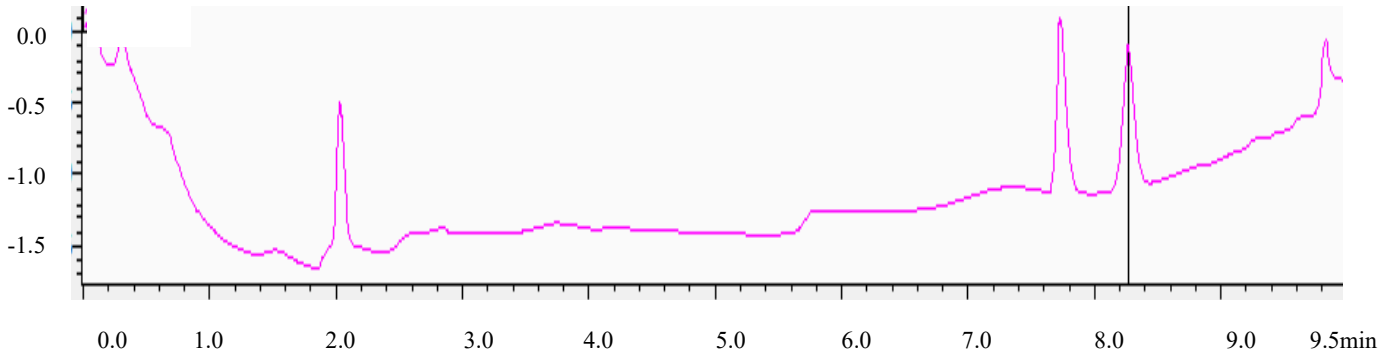


Figure 4.31: Optimal HPLC chromatogram of sulfabenzamide after extraction with cellulose in the presence of NaCl as a chaotrope

The chromatogram in Fig. 4.32 depicts the extraction and retention of sulfachloropyridazine on cell@OA under NaCl-induced chaotropic conditions. NaCl, as a chaotropic chemical, disturbs water's organized hydrogen bonding network, lowering hydration surrounding both the functionalized cellulose and the analyte. This disruption strengthens hydrophobic contacts while weakening water-mediated hydrogen bonds, altering the electrostatic and dipole-dipole interactions between sulfachloropyridazine and the modified cellulose (Selkälä, 2021). Oxalic acid functionalization adds carboxyl (-COOH) groups to the cellulose surface, enhancing its polarity and creating active sites for hydrogen bonding and electrostatic interactions. These carboxyl groups interact with the sulfonamide (-SO_2NH-) and pyridine nitrogen of sulfachloropyridazine via hydrogen bonds and acid-base interactions, allowing for selective adsorption and retention (Mangla et al., 2022).

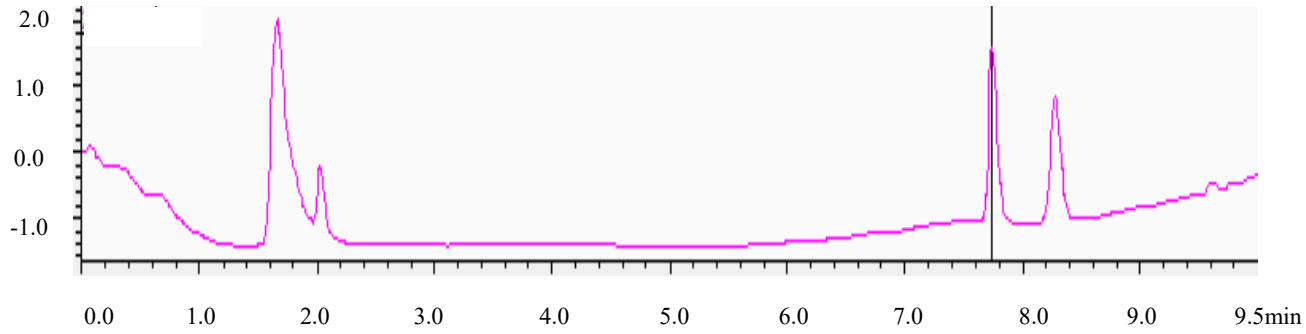


Figure 4.32: Chromatogram of sulfachloropyridazine after extraction with cell@OA in the presence of NaCl as a chaotrope

© University of Venda

The chromatogram in Fig. 4.33 shows the extraction and retention of sulfabenzamide on cell@OA under kosmotropic (Na_2CO_3) conditions. Na_2CO_3 improved water structure by enhancing hydrogen bonding networks and creating stronger connections between functionalized cellulose and the analyte. Sulfabenzamide retention was improved by enhanced hydrogen bonding and electrostatic interactions between its sulfonamide ($-SO_2NH_2$) and amide ($-CONH_2$) groups with the carboxyl (-COOH) functional groups on cellulose. The chromatographic profile displays numerous peaks, including a major one at roughly 8.2 min, suggesting a high retention effect caused by the kosmotropic Na_2CO_3.

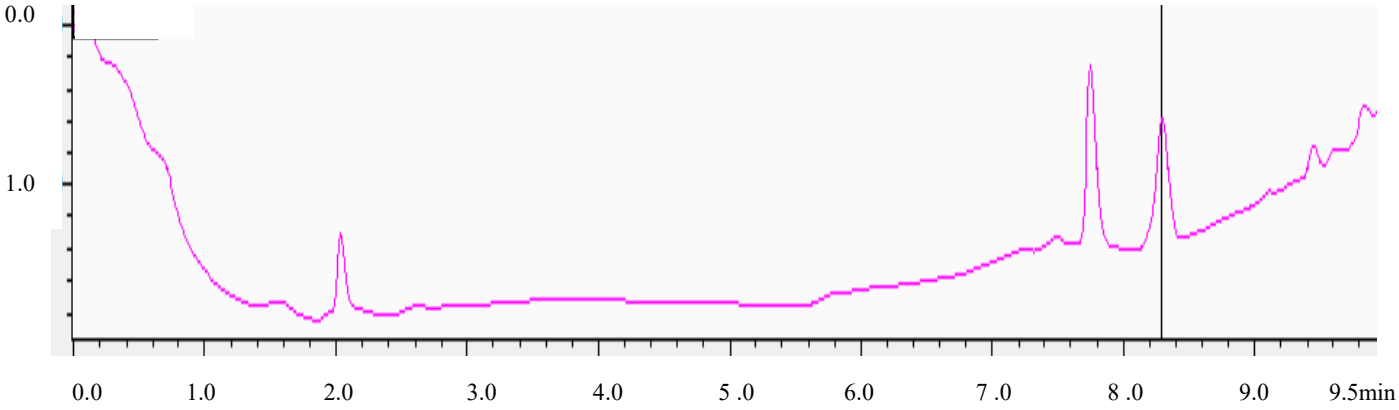


Figure 4.33: Chromatogram of sulfabenzamide after extraction with cell@OA in the presence of Na_2CO_3 as a kosmotrope

The chromatogram in Fig 4.34 depicts the profile of sulfachloropyridazine on adipic-functionalized cellulose in the presence of NaCl (chaotrope). A peak at 2 min shows a partial solvent peak whereas the high peak at 7.8 min indicates a considerable interaction between sulfachloropyridazine and functionalized cellulose via hydrogen bonding and ionic interactions. The chaotropic effect of NaCl disturbs hydration layers, increasing selective interactions.

© University of Venda

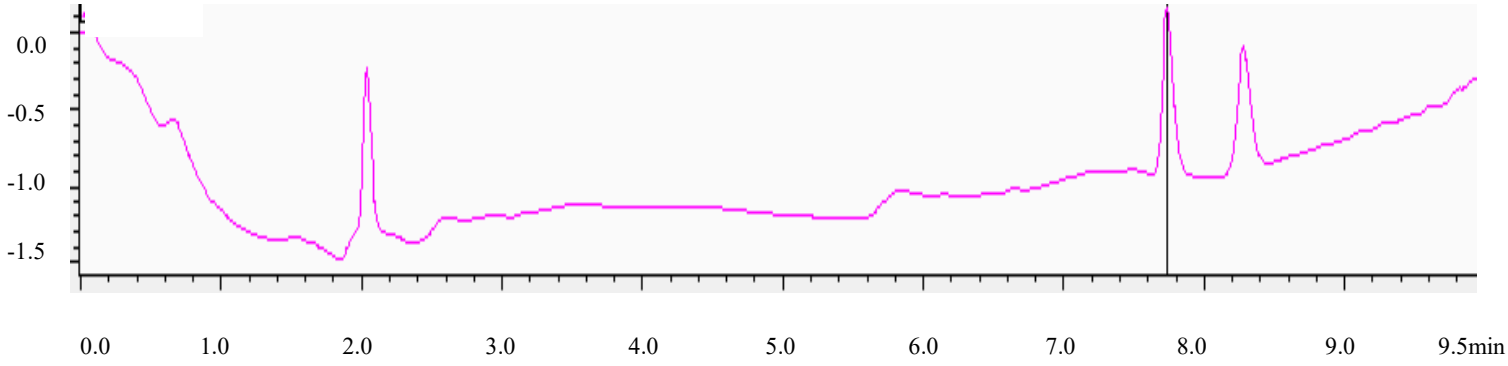


Figure 4.34: Chromatogram of sulfachloropyridazine after extraction with cell@AA in the presence of NaCl as a chaotrope

Fig. 4.35 illustrates the chromatographic retention of sulfabenzamide utilizing adipic acid-functionalized cellulose and Na_2CO_3 as a kosmotrope. The retention time of 8.2 min indicates a substantial interaction between sulfabenzamide and the modified sorbent due to increased hydrogen bonding and electrostatic forces. Na_2CO_3, a kosmotrope, organizes water molecules and stabilizes the contact between analyte and sorbent, resulting in longer retention (Yang et al., 2021). Unlike NaCl (chaotrope), which destroys hydration layers and allows elution, Na_2CO_3 enhances polarity effects, enhancing adsorption.

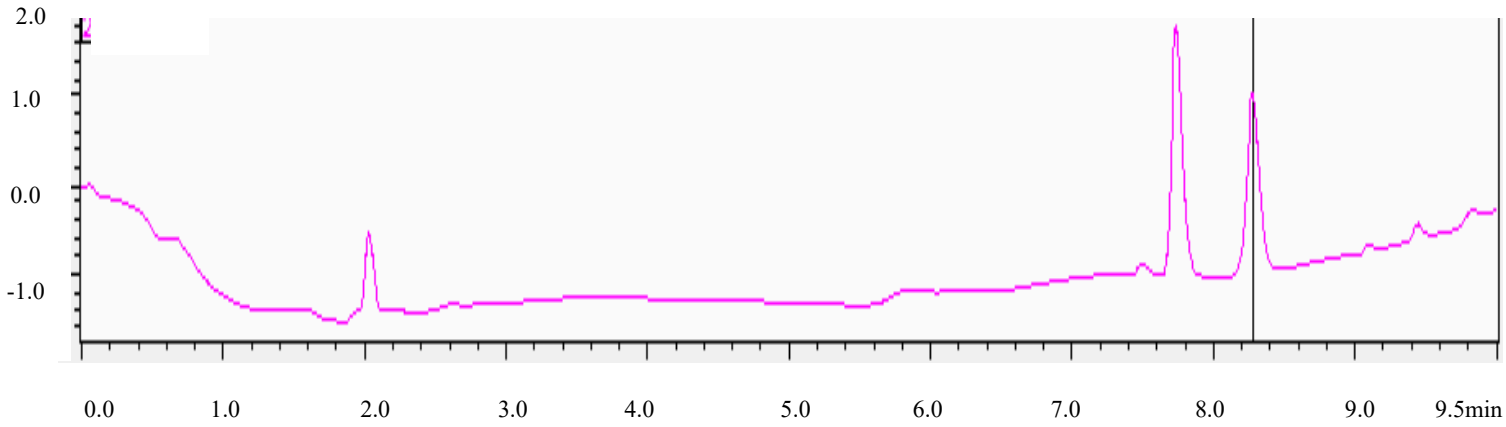


Figure 4.35: Chromatogram of sulfabenzamide after extraction with cell@AA in the presence of Na_2CO_3 as a kosmotrope

© University of Venda

4.6.1. Response surface methodology for the extraction of sulfachloropyradazine and sulfabenzamide from cellulose using aqueous two-phase extraction

The RSM results showed that three parameters influenced the extraction of sulfachloropyradazine: ultrasonication time (A), sorbent mass (B), and salt concentration (C). Fig. 4.36 (a), (b), and (c) showed the extraction efficiency using Na_2CO_3 (kosmotrope), while Fig. 4. 37 (d), (e) and (f) show the findings obtained using NaCl (chaotrope). The color-coded RSM plot depicted high and poor extraction regions, with specific parameter combinations showing higher efficiency. The following quadratic equation describes the extraction efficiency of sulfachloropyradazine**:**

% extraction sulfachloropyradazine = +37.49 +8.97 x A+7.56 x B +2.54 x C +2.31 x AB+1.14 x AC +0.86 x BC -11.51 x A^2 -1.34 x B^2 +18.66 x C^2 …… (7)

Where A is the ultrasonication time, B is the mass of the cellulose-based sorbent, and C is the salt concentration.

The kosmotropic salt (Na_2CO_3) (Fig. 4.36) improved extraction efficiency by promoting phase separation and enhancing the adsorption of sulfachloropyradazine onto cellulose (Tang et al., 2021). In contrast, NaCl (Fig. 4.37) as a chaotrope, disturbed the hydrogen bonding structure of water, limiting phase separation and hence diminishing extraction efficiency (Yang et al., 2021). The findings indicated that kosmotropes played an important role in enhancing extraction yields by stabilizing the two-phase system, whereas chaotropes reduced phase separation, resulting in decreased efficiency. The response surface plots for Na_2CO_3 (Fig. 4.36 a, b, and c) showed that increasing ultrasonication time and mass of sorbent improved extraction efficiency up to a certain point, after which additional increases resulted in a decrease. This pattern indicated that excessive ultrasonication could destabilize the extraction mechanism, resulting in lower adsorption. Similarly, salt concentration had a crucial role in strengthening extraction efficiency. Moderate concentrations of Na_2CO_3 improved extraction, but excessive levels generated saturation effects and reduced efficiency. The quadratic equation below represents the extraction efficiency for Na_2CO_3.

% extraction sulfachloropyradazine = +34.02642 +1.84877 x A+0.80338 x B-5.14625 x C -6.50700E-003 x AB +2.53828E-003 x AC+2.54155E-003 x BC-0.012789 x A^2-2.65019E-003 x B^2+0.082926x C^2…… (8)

© University of Venda

NaCl (Fig.4.37 d, e, and f) had a lower extraction efficiency than Na_2CO_3. The influence of ultrasonication time was less substantial than in the kosmotropic system. NaCl's chaotropic nature impeded efficient phase separation, resulting in reduced sulfachloropyradazine adsorption onto the sorbent. The extraction efficiency of NaCl was described by the following quadratic equation:

% extraction sulfachloropyradazine = +21.47095 +2.02411 x A+0.78882 x B-4.91108 x C-6.50700E-003 x AB+2.53828E-003 x AC+2.54155E-003 x mass of sorbent x % $salt^2$ -0.012789 x A^2-2.65019E-003 x B^2+0.082926 x C^2……. (9)

These patterns revealed that kosmotropic salts improved extraction by increasing phase separation, but chaotropic salts had the opposite effect.

© University of Venda

University of Venda
Creating Future Leaders

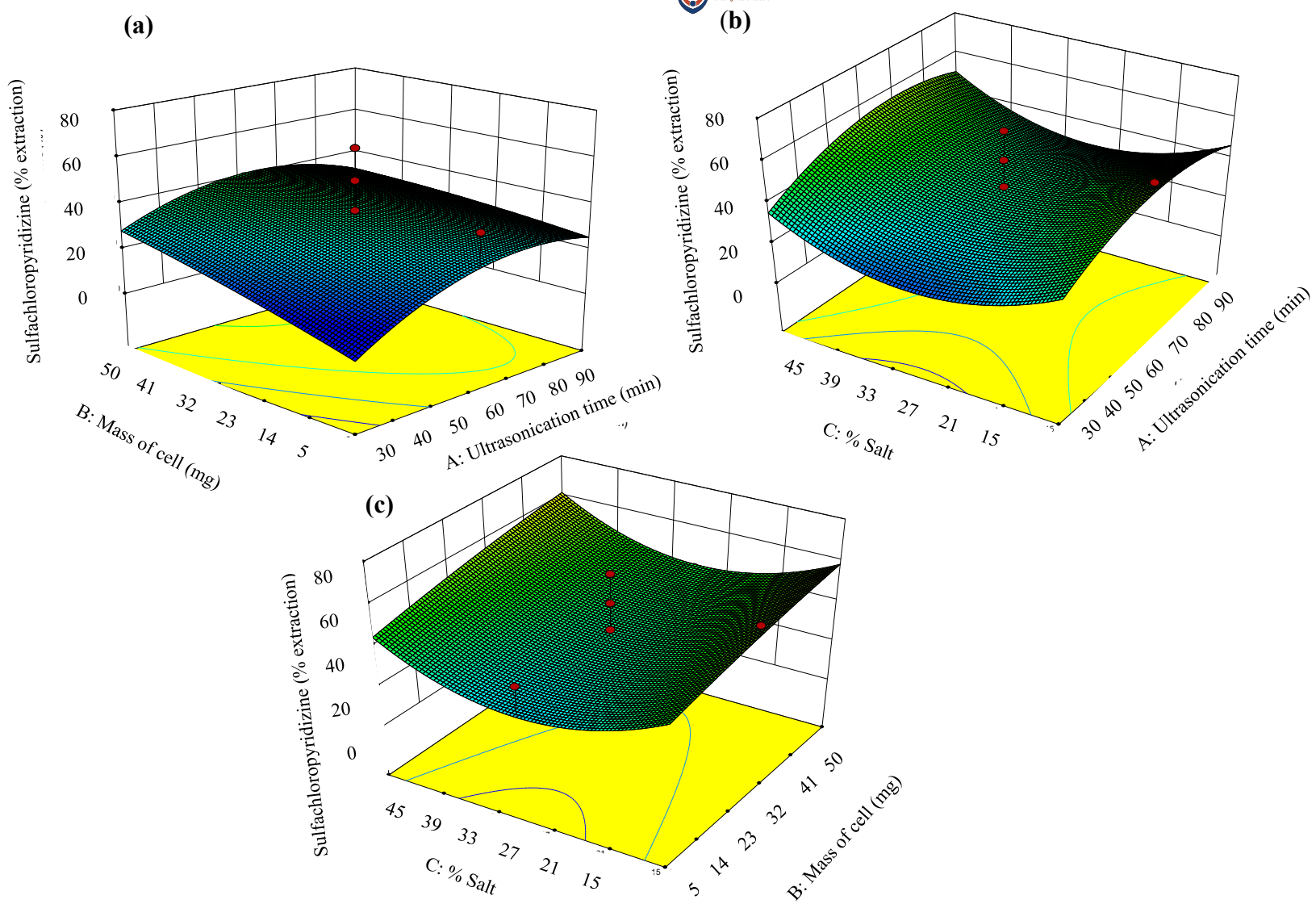


Figure 4.36: Response surface plots for kosmotrope extraction efficiency of sulfachloropyradazine using cellulose, with (a) effect of ultrasonication time and mass of sorbent, (b) effect of ultrasonication time and % salt and (c) effect of mass of sorbent and % salt

© University of Venda

University of Venda
Creating Future Leaders

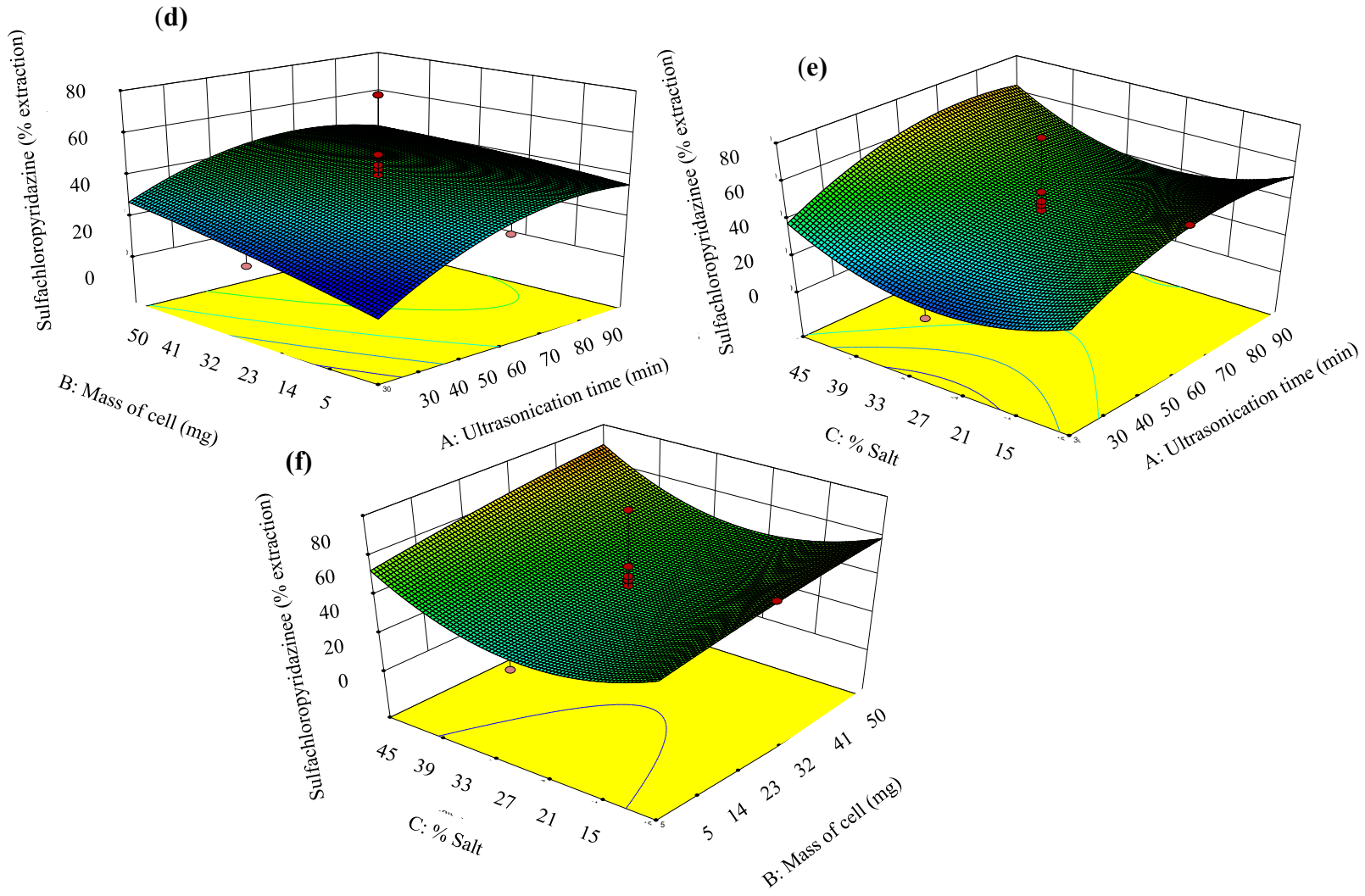


Figure 4.37: Response surface plots for chaotrope extraction efficiency of sulfachloropyradazine using cellulose, with (d) effect of ultrasonication time and mass of sorbent, (e) effect of ultrasonication time and %salt, and (f) effect of mass of sorbent and %salt

© University of Venda

The Pareto chart (Fig.4.38) further confirmed the RSM findings by providing insight into the significance of each parameter. Ultrasonication time (A) had the greatest influence on extraction efficiency, with a value of 4.78, highlighting its critical role in the process. The mass of sorbent (B) also showed a substantial effect, with a value of 3.79. In contrast, the quadratic term of % salt (C) had a minimal impact, with a much lower value of 0.43. The quadratic term of % salt (C^2) also had a significant influence (6.68). The statistical significance (P-values) indicated that characteristics with $p < 0.05$ were regarded significant, including ultrasonication time, and C^2. Interaction effects with $p > 0.05$ were less significant. These findings were consistent with recent research on aqueous two-phase antibiotic extraction utilizing kosmotropic and chaotropic salts (Yankov, 2020; Assis et al., 2021). The Pareto graphic confirmed the RSM findings by clearly demonstrating the significance of the quadratic salt term in influencing extraction efficiency.

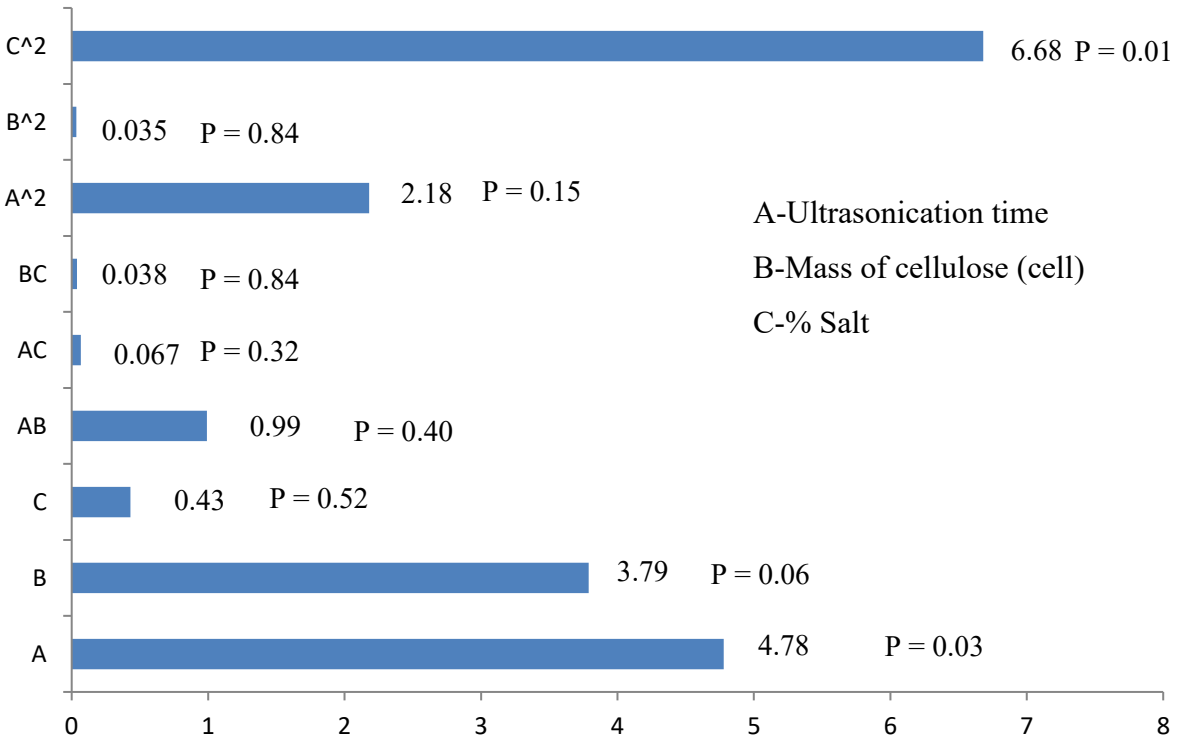


Figure 4.38: Pareto chart of extraction for sulfachloropyradazine using cellulose

The Response Surface Methodology (RSM) and pareto chart were used to assess the extraction efficiency of sulfabenazamide using cellulose as shown in Fig. 4.39 and Fig. 4.40. The pareto chart showed that the mass of cellulose had the greatest influence on extraction efficiency (6.18),

© University of Venda

followed by the % salt (4.3) and ultrasonication time (2.89). Quadratic impacts were noteworthy, with A^2 (4.12) and B^2 (3.34) having significant influence. Interaction terms like AB (1.34) showed a moderate influence, while AC (0.062) and BC (0.29) contributed very little. The RSM plots depicted the interactions of variables and their impacts on extraction performance. The quadratic model equation was generated as follows:

% extraction of sulfabenzamide = +42.22 +8.31 x A +11.50 x B +9.60 x C-6.07 x AB -1.31 x AC+2.81 x BC -18.85 x A^2 +15.70 x B^2 +5.20 x C^2…… (10)

Where A is the ultrasonication time, B is the mass of the cellulose-based sorbent, and C is the salt concentration.

© University of Venda

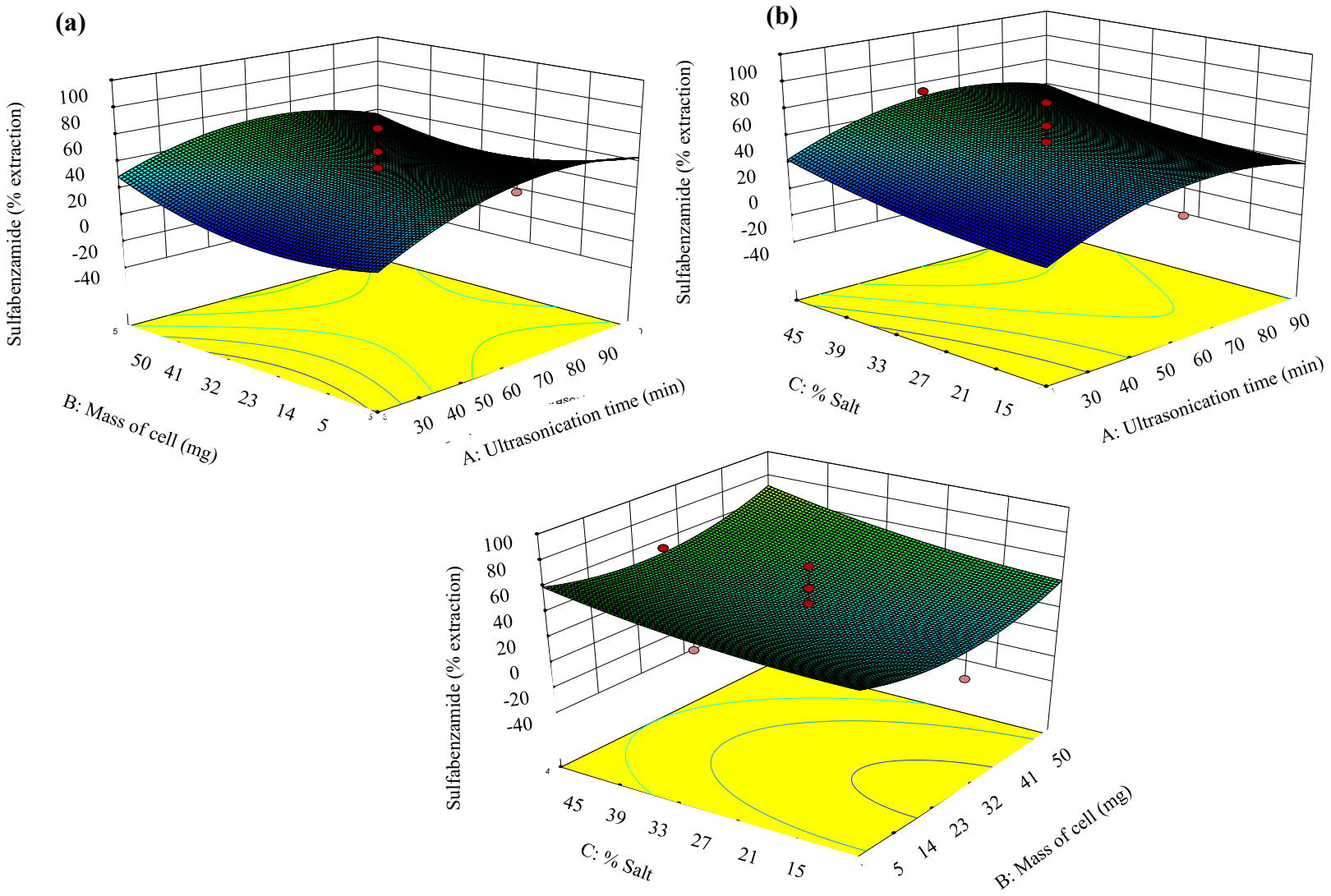


Figure 4.39: Response surface plots for kosmotrope extraction efficiency of sulfabenzamide using cellulose, with (a) effect of ultrasonication time and mass of sorbent, (b) effect of ultrasonication time and % salt and (c) effect of mass of sorbent and % salt

© University of Venda

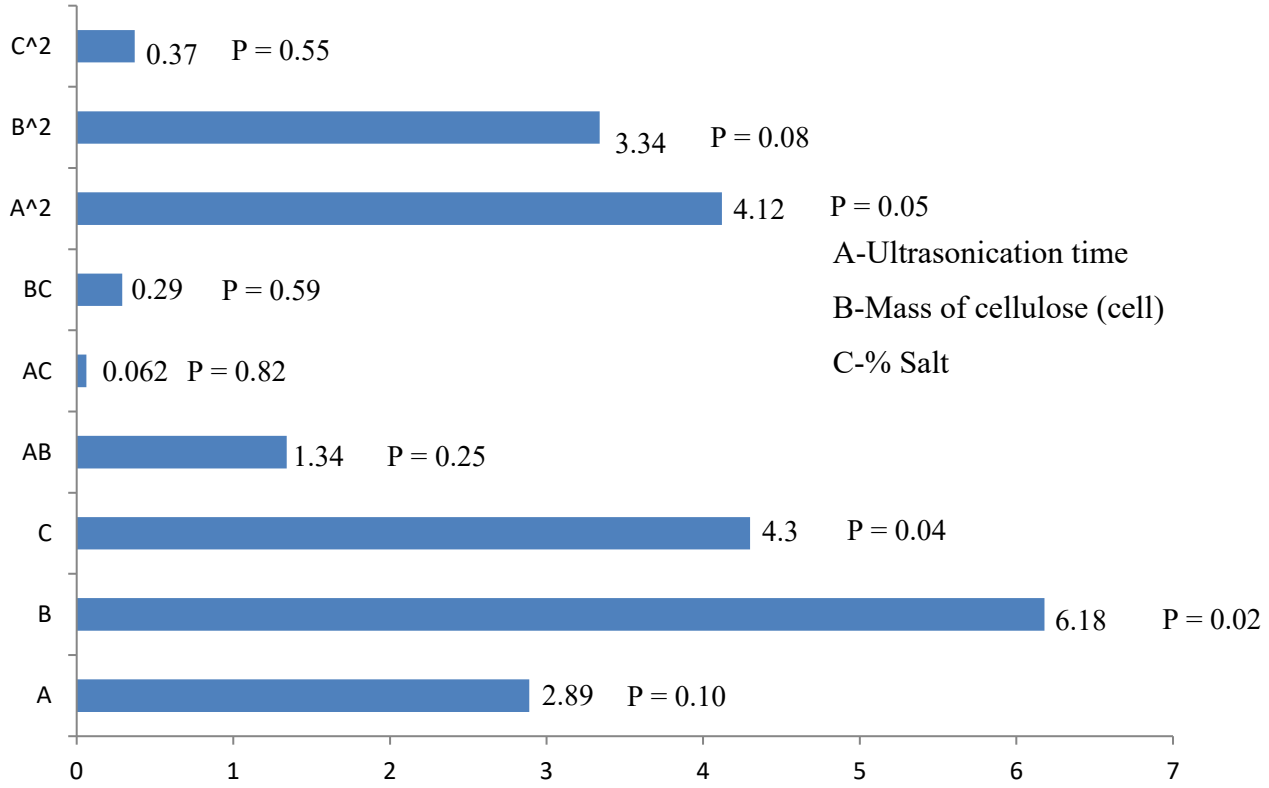


Figure 4.40: Pareto chart of extraction for sulfabenzamide using cellulose

4.6.2. RSM for the extraction of sulfachloropyradazine and sulfabenzamide from oxalic acid functionalized cellulose using aqueous two-phase extraction

The RSM findings for the extraction of sulfachloropyradazine utilizing aqueous two-phase extraction adsorption were examined using three parameters: ultrasonication time, sorbent mass, and %salt. The RSM plots were color-coded to show locations with low and high extraction efficiency. Fig. 4.41 (a), (b), and (c) show the kosmotrope-assisted extraction using Na_2CO_3, while Fig. 4.42 (d), (e), and (f) show the chaotrope-assisted extraction with NaCl. The extraction efficiency equation for the kosmotropic system was determined to be:

% extraction sulfachloropyradazine = +80.17857 -1.64720 x A-0.78873 x B+0.44968 x C+7.72487E-003 x AB-0.016032 x BC+7.30159E-003 x BC+0.016429x A^2+3.17460E-004 x B^2+3.49206E-003 x % C^2……..(11)

© University of Venda

The chaotropic system's extraction efficiency equation was:

% extraction sulfachloropyradazine = -26.51918 +2.63422 x A+0.45553 x B-2.12415 x C-0.013519 x AB-9.59742E-003 x AC+0.024815 x BC-0.017649 x A^2-7.67221E-003 B^2+0.047182x C^2…… 12)

The general extraction efficiency equation that included all parameters was:

% extraction sulfachloropyradazine = +29.97 -1.31 x A-1.37 x B +5.34 x C +4.38 x AB -5.77 x AC +5.42 x BC -0.55 x A^2 -1.86 x B^2 +5.70 x C^2…..... (13)

Where A is the ultrasonication time, B is the mass of the cellulose@OA, and C is the salt concentration.

The RSM results (Fig. 4.41). showed that ultrasonication time had variable effects on extraction efficiency based on the type of salt utilized. In the kosmotrope system, increasing the ultrasonication period initially improved extraction but then decreased it, implying that too much time could damage the sorbent's capacity. In contrast, in the chaotropic system, extended ultrasonication periods often improved extraction performance, possibly due to increased molecular interactions and dispersion of the sulfachloropyradazine molecules. The mass of sorbent had a similar effect in both systems, with an increase in mass initially increasing extraction, but an excessive quantity resulted in a saturation point where further improvement was marginal. The percentage of salt played an important influence, with kosmotropes improving extraction at modest levels.

The Pareto chart offered additional statistical confirmation for the major elements impacting extraction as shown on Fig.4.43. The interaction between ultrasonication time and percentage of salt (AC) had the greatest influence, followed by % salt (C). The quadratic term for %salt (C^2) was significant, indicating a non-linear relationship between salt concentration and extraction efficiency. Contrary to initial expectations, the parameters C, AC, BC, and C^2 had P-values of 0.26, 0.22, 0.34, and 0.79, respectively all of which are greater than 0.05 indicating no statistically significant effect at the 95% confidence level. These factors facilitated the kosmotropic effect, which improved phase separation and maximized extraction efficiency. The chaotropic effect

© University of Venda

increased solubility and reduced molecular interactions interaction between cell@OA and sulfachloropyridizine, resulting in greater extraction yields.

© University of Venda

University of Venda
Creating Future Leaders

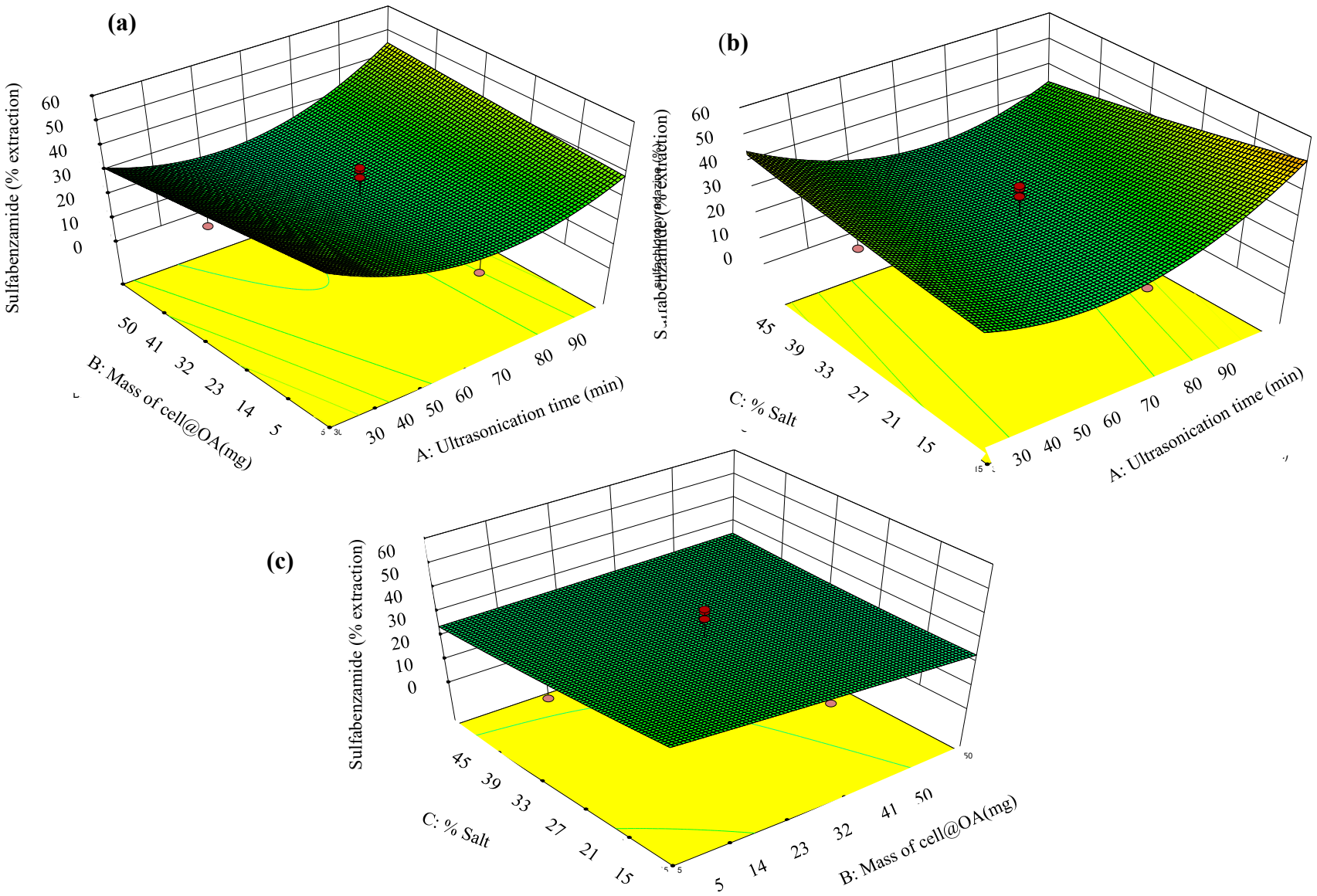


Figure 4.41: Response surface plots for kosmotrope extraction efficiency of sulfachloropyradazine using cell@OA, with (a) effect of ultrasonication time and mass of sorbent, (b) effect of ultrasonication time and % salt and (c) effect of mass of sorbent and % salt

© University of Venda

University of Venda
Creating Future Leaders

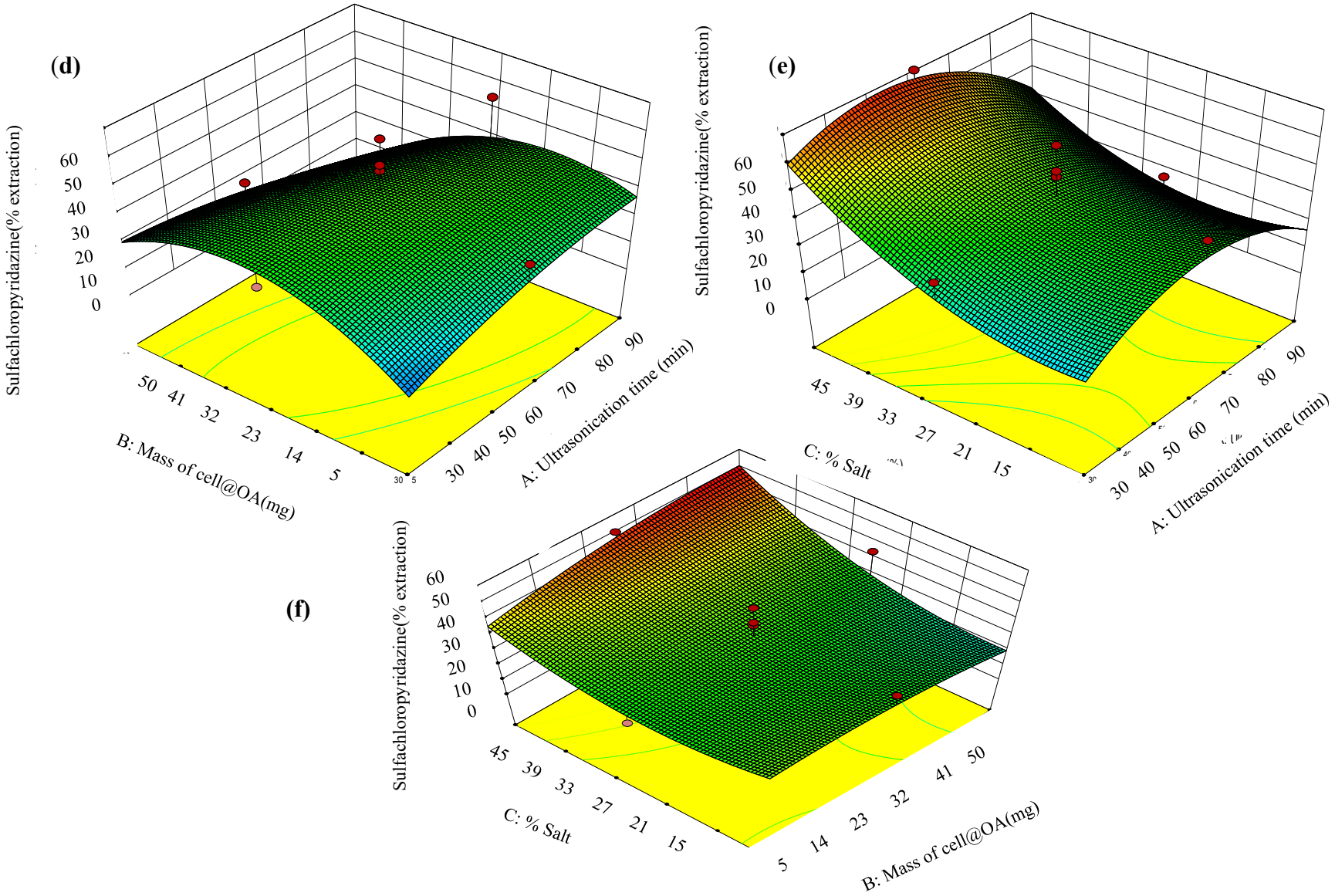


Figure 4.42: Response surface plots for chaotrope extraction efficiency of sulfachloropyradazine using cell@OA with (a) effect of ultrasonication time and mass of sorbent, (b) effect of ultrasonication time and % salt and (c) effect of mass of sorbent and % salt

© University of Venda

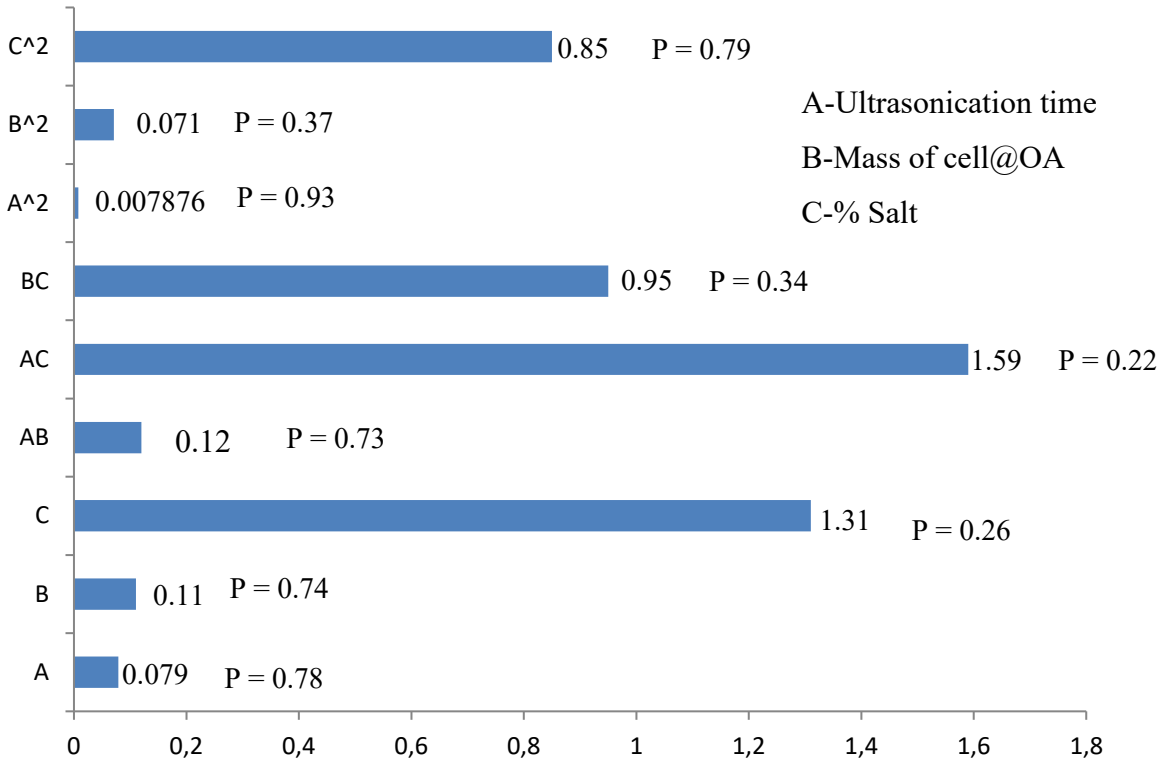


Figure 4.43: Pareto chart of extraction for sulfachloropyradazine using cell@OA

The RSM for the extraction of sulfabenzamide in cell@OA utilizing aqueous two-phase extraction with adsorption was impacted by three parameters: ultrasonication time (A), mass of sorbent (B), and % salt. The following quadratic equation describes the extraction efficiency of sulfabenzamide:

% extraction sulfabenzamide = +25.37 -5.71 x A +6.06 x B +4.94 x C -9.57 x AB -7.26 x AC

+6.80 x BC +1.71 x A^2+6.66 x B^2 + 5.96 x C^2…… (14)

Where A is the ultrasonication time, B is the mass of the cellulose-based sorbent, and C is the salt concentration.

The extraction efficiency of kosmotrope-assisted extraction was modelled using equation (2):

% extraction sulfabenzamide = +80.45635 -1.67550 x A-0.71349 B+0.23011 x C-0.012804 x AB-0.016349 x AC+0.012169 BC+0.018730 x A^2+0.030159 x B^2+6.03175E-003x C^2 …… (15)

© University of Venda

The extraction efficiency of chaotrope-assisted extraction was modelled using equation (16):

% extraction sulfabenzamide = -31.85403 +2.58734 x A+0.29665 B-1.92161 x C-0.015556 x AB-0.015910 x AC+0.028148 x BC-0.014936 A^2-3.83611E-003 x B^2+0.046924 x % C^2…… (16)

Fig. 4.46 depicts the pareto chart analysis, which was used to establish the statistical significance of the extracted parameters. The results showed that the mass of sorbent (B) and %salt (C) had a non-substantial effect on the extraction ($p > 0.05$). Furthermore, interactive impacts between the parameters were identified, particularly the AB (2.83) and AC (2.42) interactions, which positively impacted the extraction process. Furthermore, the addition of chaotropic salts, which have been shown to disrupt hydrogen bonding networks and promote molecular interactions in aqueous systems, had a significant impact on extraction efficiency when compared to kosmotropic salts (Cecchi, 2024). The color-coded RSM plots verified these findings. Fig. 4.44(a), (b), and (c) depict kosmotropic salt systems with regions of great extraction efficiency, as indicated by the bright colors. Fig. 4.45 (d), (e), and (f), which depict chaotropic salt systems, showed slightly lower extraction efficiency but nevertheless demonstrated the significant function of chaotropes in increasing sulfabenzamide partitioning into the sorbent phase.

The interaction of sulfabenzamide, kosmotropes, and chaotropes in the presence cell@OA was most likely regulated by hydrogen bonding and electrostatic forces. The effects of kosmotropic and chaotropic salts were interpreted using the Hofmeister series, which showed that kosmotropic salts strengthened water's hydrogen bonding network, allowing for greater sorbent interaction and sulfabenzamide adsorption (Jakubowska & Kozik, 2019). Chaotropic salts, on the other hand, disturbed water molecules' hydrogen bonding network, allowing sulfabenzamide to partition into the sorbent phase more easily. These findings were consistent with the Hofmeister series, which states that kosmotropic salts promote molecular ordering while chaotropic salts create molecular disorder (Cecchi, 2024) as previously described in the literature. The RSM analysis revealed the optimal extraction conditions for both kosmotrope-assisted and chaotrope-assisted extractions. The optimal extraction conditions were 60 min ultrasonication time, 50 mg of sorbent mass, 30% salt concentration. Under these conditions, a maximum extraction efficiency of 51% was achieved.

© University of Venda

University of Venda
Creating Future Leaders

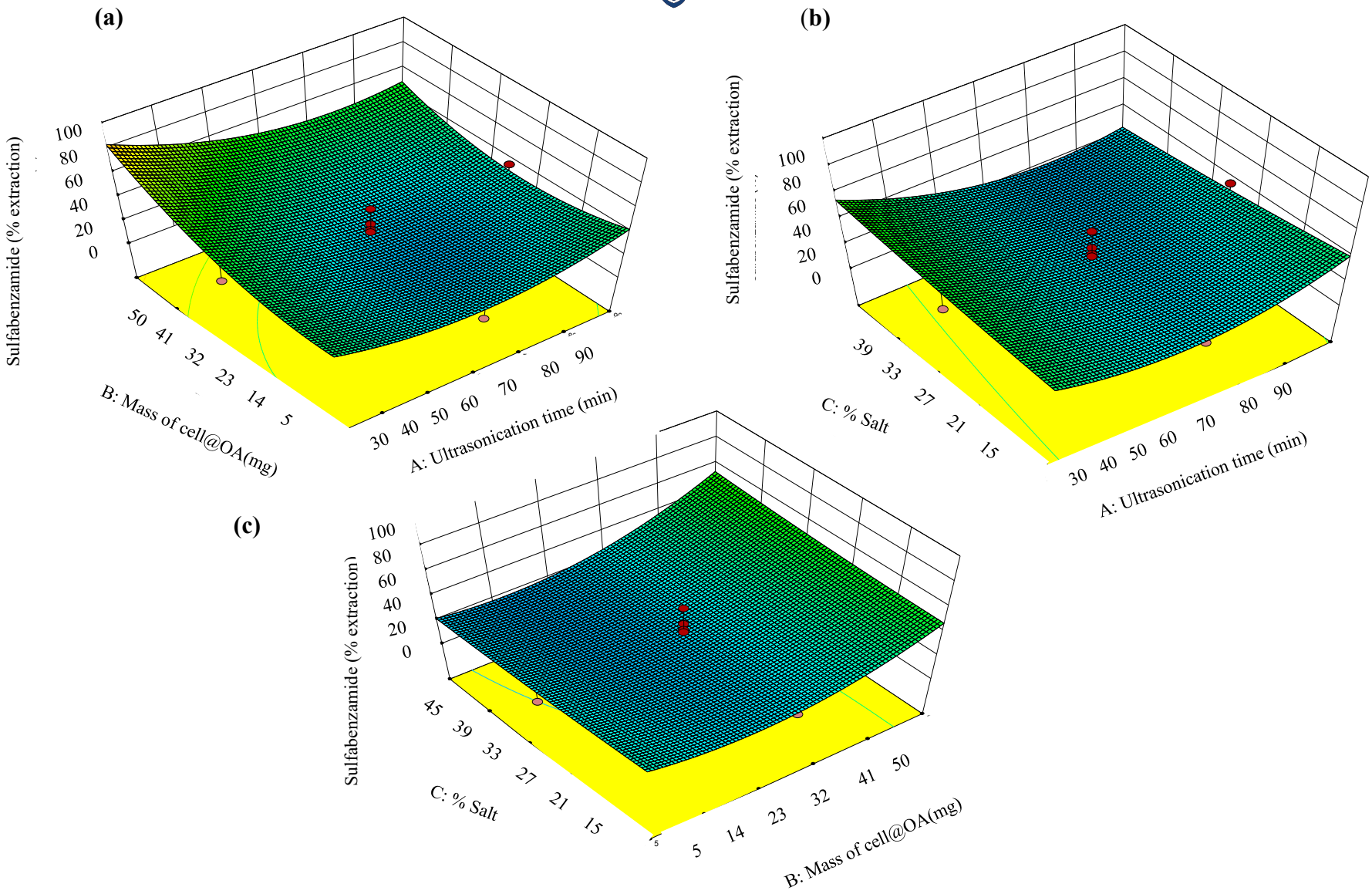


Figure 4.44: Response surface plots for kosmotrope extraction efficiency of sulfabenzamide using cell@OA, with (a) effect of ultrasonication time and mass of sorbent, (b) effect of ultrasonication time and % salt and (c) effect of mass of sorbent and % salt

© University of Venda

University of Venda
Creating Future Leaders

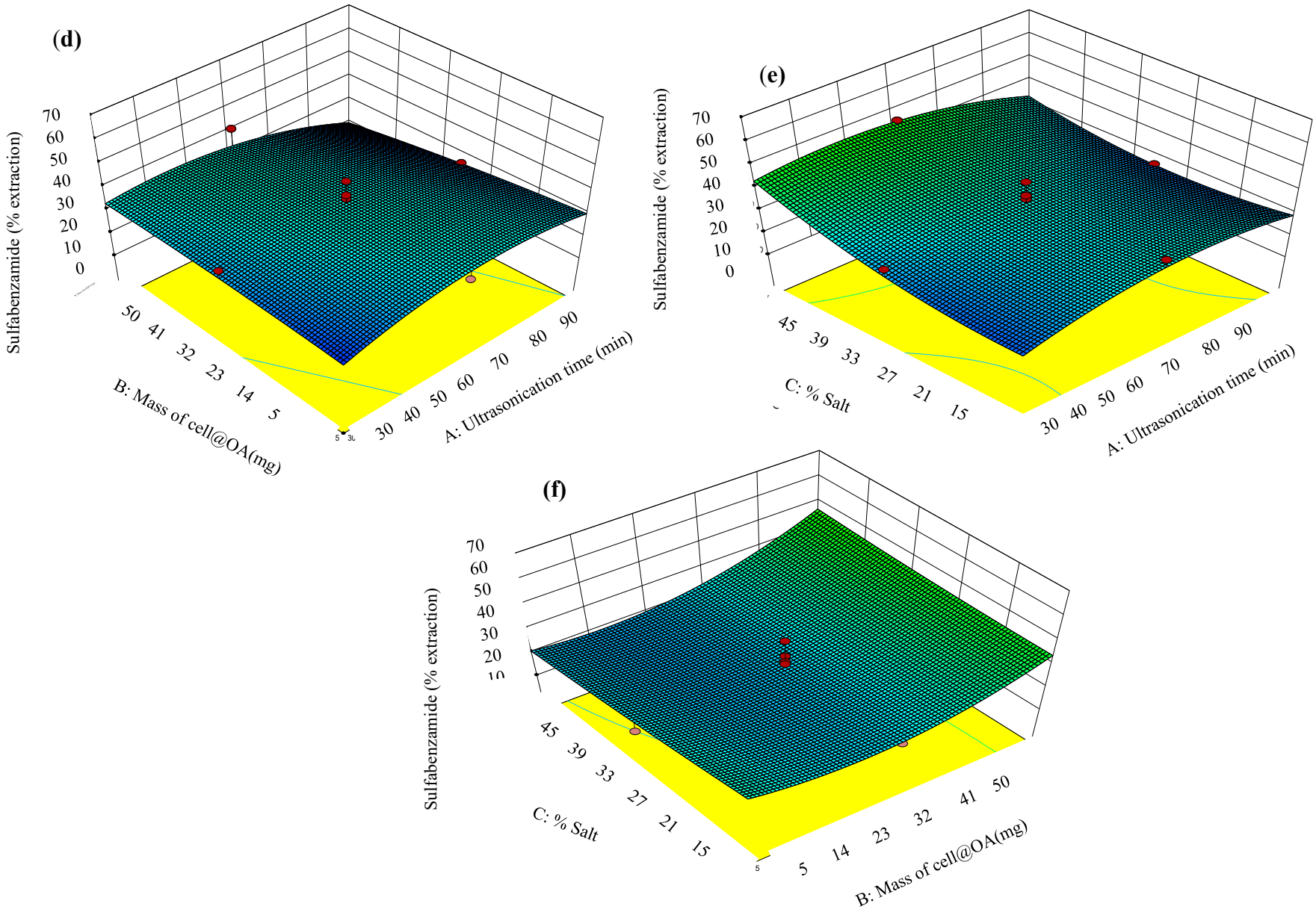


Figure 4.45: Response surface plots for chaotrope extraction efficiency of sulfabenzamide using cell@OA, with (a) effect of ultrasonication time and mass of sorbent, (b) effect of ultrasonication time and % salt and (c) effect of mass of sorbent and % salt

© University of Venda

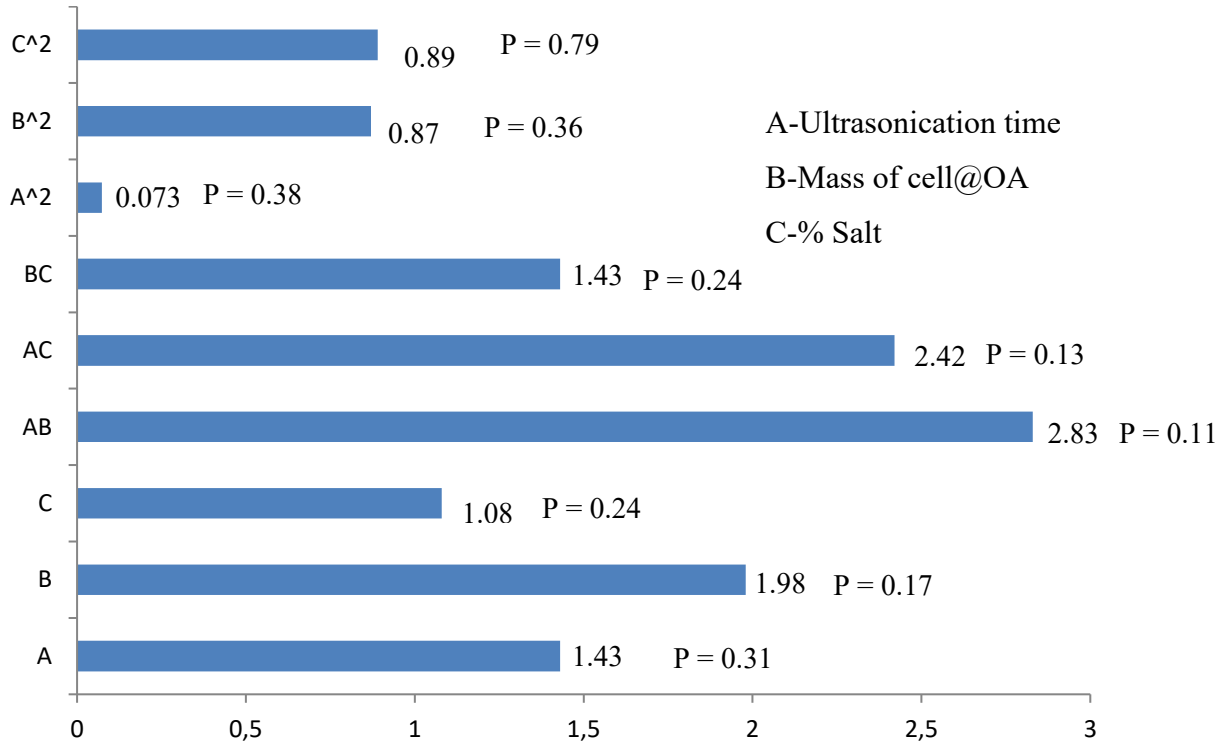


Figure 4.46: Pareto chart of extraction for sulfabenzamide using cell@OA

4.6.3. Response surface methodology for the extraction of sulfachloropyradazine and sulfabenzamide using cell@AA in aqueous two-phase extraction

Aqueous two-phase extraction has been extensively studied as a highly effective separation technique for medicinal substances such as sulfachloropyradazine. Kosmotropic (water-structuring) and chaotropic (water-disordering) salts had a considerable impact on the extraction process, influencing the drug's partitioning behavior (Cecch et al., 2024). Response surface methodology was used to investigate the effects of ultrasonication time, sorbent mass and salt concentration on extraction efficiency as shown in Fig. 4.47 and Fig. 4.48. The RSM results for kosmotrope showed how these parameters affected sulfachloropyradazine extraction efficiency. The response surface plots revealed that the mass of sorbent and % salt had a substantial effect on extraction efficiency. The relationship between these parameters was represented by the quadratic model equation:

© University of Venda

% extraction sulfachloropyradazine = -89.33173 +2.3116 x A-2.04156 x B+5.16328 x C+5.17314E-004 x AB-0.010258 x AC-1.08505E-003 x BC-0.016592 x A^2+0.039824 x B^2-0.065951 x % C^2……..... (17)

The surface plots showed that the best extraction efficiency was observed at moderate ultrasonication times and bigger sorbent mass with a little effect from amount of salt. Darker parts indicated decreased efficiency, whereas lighter portions suggested improved extraction. The RSM results for chaotrope showed a similar pattern, with sorbent mass and salt content having a substantial impact on sulfachloropyradazine extraction. The equation that governs the chaotrope system was:

Sulfachloropyradazine =-74.62198 +2.32238 x A-1.63450 x B+4.27089 x C+5.17314E-004 x AB-0.010258 x AC-1.08505E-003 x BC-0.016592 x A^2+0.039824 x B^2-0.065951 x % C^2…… (18)

The surface plots showed that increasing salt concentrations and sorbent mass resulted in higher extraction efficiency, although ultrasonication time had a relatively small effect on the process. The optimized settings led to better sulfachloropyradazine recovery. The pareto chart analysis demonstrated the significance of each parameter in the extraction process. The equation that determined the response was:

Sulfachloropyradazine = +40.54 + 0.97 × A + 7.89 × B + 1.72 × C + 0.35 × AB - 4.62 × AC - 0.37 × BC - 14.93 × A^2 + 20.1 × B^2 - 14.84 × C^2……. (19)

Where A is the ultrasonication time, B is the mass of the cell@AA, and C is the salt concentration.

The pareto chart (Fig. 4.49) shows that the mass of sorbent (B) has the most significant effect on extraction efficiency, followed by the percentage of salt (C^2) and ultrasonication time (A^2). The mass of the sorbent ($p < 0.05$) was a crucial role in the process, supporting the RSM findings. The interactions between ultrasonication time and salt concentration (AC), as well as sorbent mass and salt concentration (BC), were shown to be less significant ($p > 0.05$). The results showed that when the mass of sorbent increased extraction efficiency initially improved before plateauing. A higher sorbent mass increased the surface area available for adsorption, allowing for stronger interaction between sulfachloropyradazine and the sorbent material. However, with high sorbent mass, the

© University of Venda

extraction efficiency either stabilized or significantly deteriorated, most likely because of sorbent saturation or the drug's limited availability for adsorption. The amount of salt was a critical factor in influencing extraction efficiency.

The inclusion of kosmotropic salts improved extraction by decreasing the solubility of sulfachloropyradazine in the aqueous phase, allowing it to partition into the ethanol extraction phase. In contrast, chaotropic salts disturbed the water structure, enhancing the mobility of drug molecules and making them more available for adsorption (Yin et al., 2024). The interaction between sorbent mass and salt concentration revealed that at generally lower sorbent masses, salt concentration had a greater impact, whereas at higher sorbent masses, the influence of salt concentration was less prominent. The correlation between ultrasonication time and sorbent mass was also investigated. Ultrasonication time aided in the breakdown of particle agglomerates and improved mass transfer, resulting in increased extraction efficiency. However, prolonged ultrasonication resulted in a decrease in extraction efficiency, possibly due to desorption effects (Rao et al., 2021). The effect of ultrasonication was more significant in chaotropic systems, where the disrupted water structure allowed for better sulfachloropyradazine diffusion and enhanced interaction with the sorbent.

In conclusion, the results showed that kosmotropic salts had higher extraction efficiency than chaotropic salts because of their capacity to improve phase separation and enable adsorption. Kosmotropic systems were optimized by increasing salt concentration and sorbent mass, whereas chaotropic systems necessitated a finer balance of all three parameters. These findings were consistent with prior research that found improved extraction efficiency in kosmotrope-enhanced systems (Kumari et al., 2022). The study confirmed that adjusting salt type, concentration, and sorbent mass was critical to maximizing sulfachloropyradazine recovery in ATPE. The optimal extraction conditions were determined to be a 60 min ultrasonication time, 50 mg of sorbent mass, and a 30% salt concentration. Under these conditions, a maximum extraction efficiency of 91% was obtained.

© University of Venda

University of Venda
Creating Future Leaders

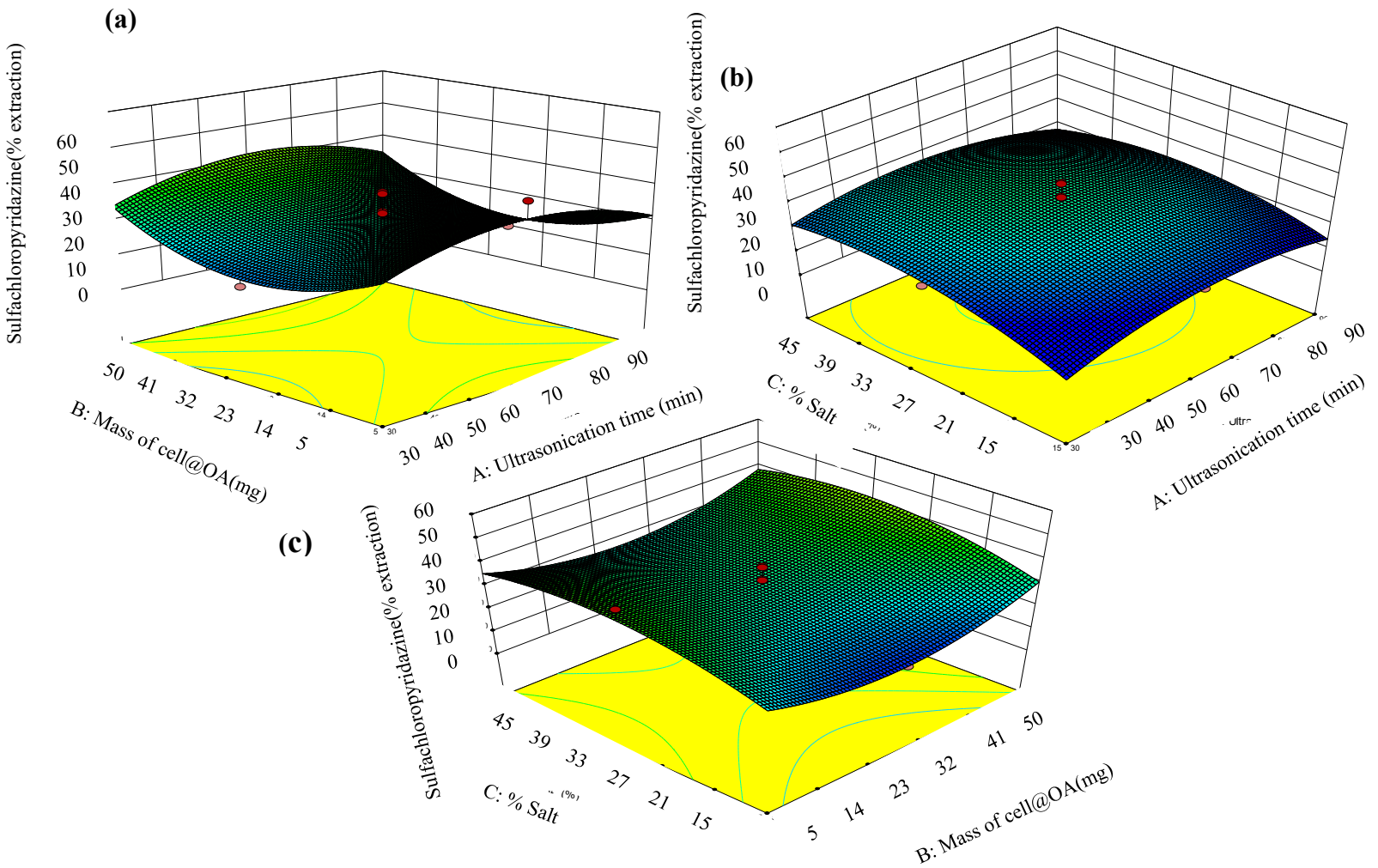


Figure 4.47: Response surface plots for kosmotrope extraction efficiency of sulfachloropyradazine using cell@AA, with (a) effect of ultrasonication time and mass of sorbent, (b) effect of ultrasonication time and salt concentration and (c) effect of mass of sorbent and salt concentration

© University of Venda

University of Venda
Creating Future Leaders

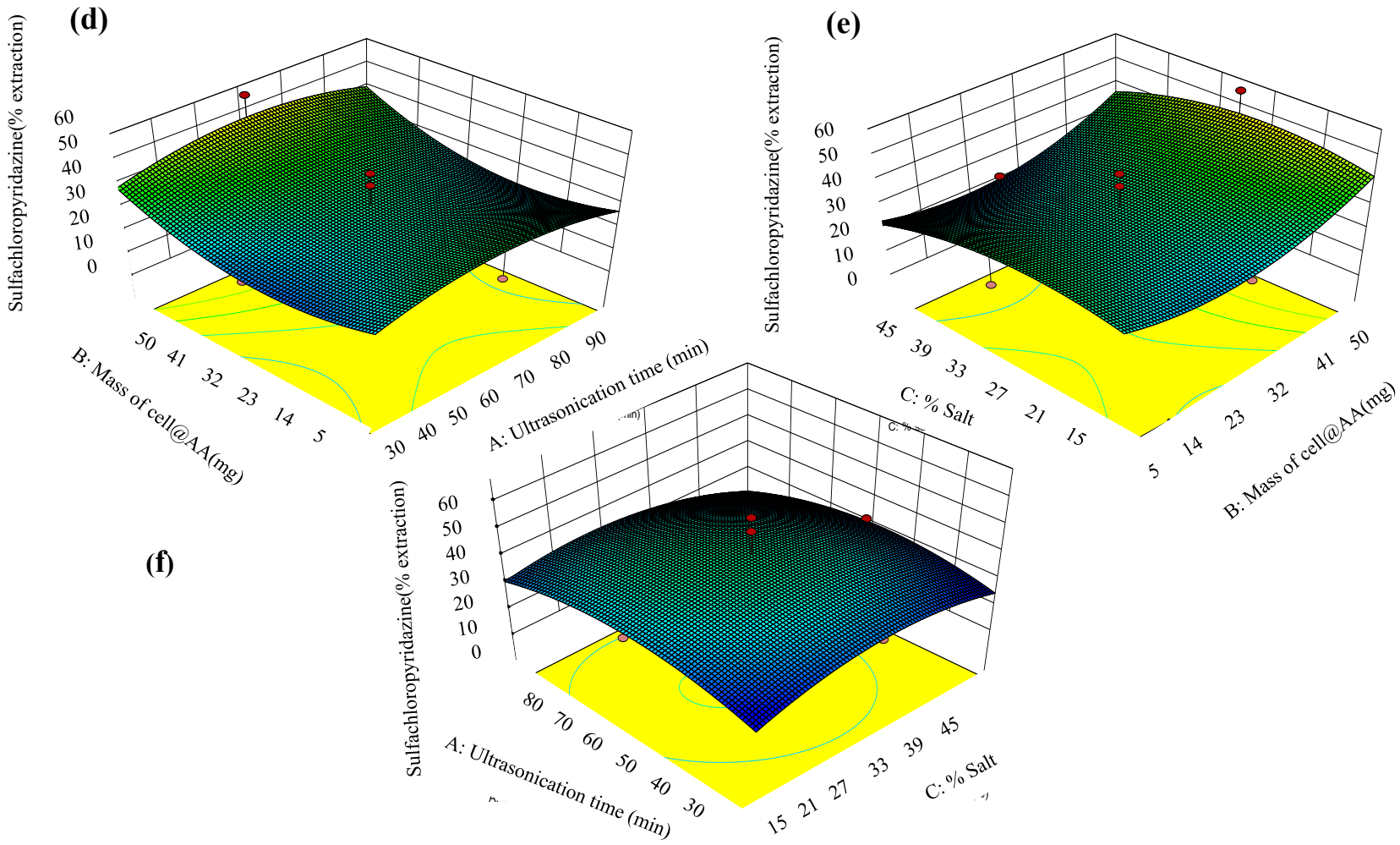


Figure 4.48: Response surface plots for chaotrope extraction efficiency of sulfachloropyradazine using cell@AA with (d) effect of ultrasonication time and mass of sorbent, (e) effect of ultrasonication time and salt concentration, and (f) effect of mass of sorbent and salt concentration

© University of Venda

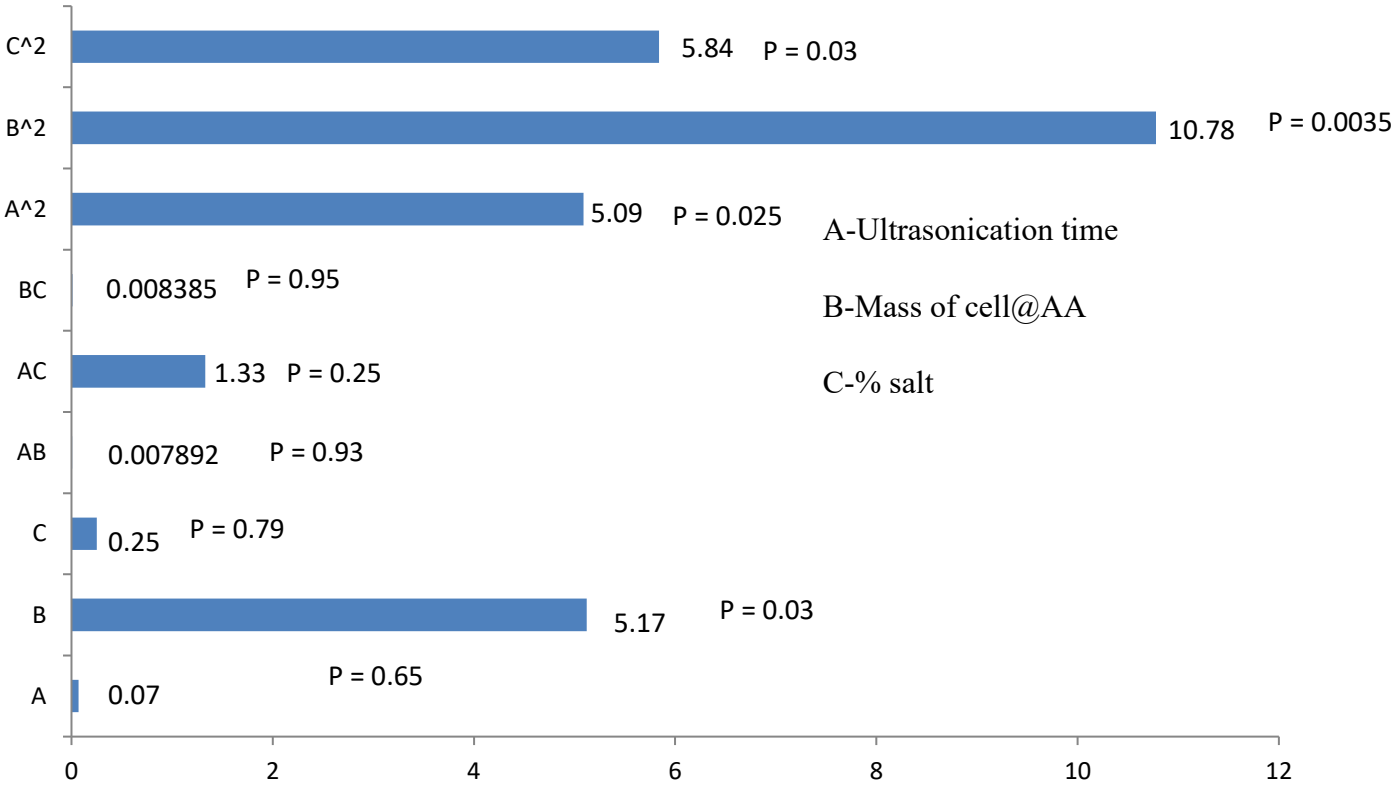


Figure 4.49: Pareto chart of extraction parameters for sulfachloropyradazine using cell@AA

The RSM results showed that ultrasonication time (A), sorbent mass (B), and salt concentration (C) all influenced sulfabenzamide extraction efficiency using adipic acid functionalized cellulose. The extracted percentage of sulfabenzamide was modeled using this equation:

% extraction sulfabenzamide = +38.10 -0.41 x A +10.74 x B +3.67 x C+4.92 x AB -11.43 x AC -5.68 x BC-5.53 x A^2 +8.25 x B^2 -7.25 x C^2 ……. (20)

Where A is the ultrasonication time, B is the mass of the cell@AA, and C is the salt concentration.

Fig. 4.50 (a), (b), and (c) depict the extraction efficiency using kosmotrope, as specified by equation (2),

% extraction sulfabenzamide = -75.33390 +1.08848 A-0.60234 x B+4.97219 x C+7.28635E-003 AB-0.025393 x AV-0.016820 x BC-6.14029E-003 xA^2+0.016304xB^2-0.032204x C^2…… (21)

© University of Venda

whereas Fig. 4.51 (d), (e), and (f) illustrate the extraction efficiency using chaotrope, as indicated by equation (21),

% extraction sulfabenzamide = -60.37040 +1.48038 x A-0.10148 x B+3.35332 x C+7.28635E-003 x ultrasonication time x mass of sorbent -0.025393 x ultrasonication time x % salt -0.016820 x mass of sorbent x % salt -6.14029E-003 x ultrasonication time^2 +0.016304 x mass of sorbent^2 x -0.032204 x %salt^2.....……..……..(22)

The pareto chart (Fig. 4.52) showed the statistical significance of each parameter. The mass of the sorbent (B) had the greatest impact on extraction, with a standardized effect of 5.83, followed by the interaction of ultrasonication time and salt concentration (AC), which had a value of 5.01. The quadratic terms of sorbent mass and salt concentration were also important, with values of 1.11 and 0.86, respectively. The ultrasonication time (A) had the least impact (0.00782), indicating that within the examined range, this parameter was less important than the other components. Statistical analysis revealed significant factors with p-values <0.05, indicating that sorbent mass and salt concentration were important in the extraction process. Parameters with p > 0.05, such as ultrasonication time, had a minor influence, as confirmed by the response surface data. These findings are consistent with studies on aqueous two-phase extraction, where kosmotropic and chaotropic effects are crucial in altering the solubility and adsorption properties (Casimiro et al., 2023).

Adipic acid was essential in functionalizing the cellulose, increasing the contact with sulfabenzamide via hydrogen bonding and electrostatic interactions. The inclusion of Na_2CO_3 (kosmotrope) resulted in salting-out effects, reducing solubility and enhancing adsorption on functionalized cellulose. In contrast, the process for NaCl (chaotrope) was based on the instability of hydration shells (Zeng et al., 2021), which improved sulfabenzamide mass transfer into the sorbent phase. Chaotrope-assisted extraction with NaCl outperformed kosmotrope-assisted extraction with Na_2CO_3. The ideal circumstances for chaotropic extraction comprised an ultrasonication time of 72 min, as opposed to 54 min for kosmotropic extraction. The optimal sorbent mass for both procedures was 50 mg, with a salt concentration of 22% for chaotropic extraction and 37% for kosmotropic extraction. Chaotropic extraction is more efficient because of its capacity to rupture the hydration shell around sulfabenzamide molecules, allowing for improved

© University of Venda

solubility and mass transfer to adipic acid-functionalized cellulose. Kosmotropes, on the other hand, promote phase separation by decreasing solubility, which improves adsorption but is less beneficial in terms of overall extraction efficiency. Based on the findings, chaotrope-assisted extraction was the superior method, providing increased efficiency and attractiveness for sulfabenzamide extraction. The optimal extraction conditions were a 30-minute ultrasonication time, 50 mg of sorbent mass, and 45% salt concentration. Under these conditions, a maximum extraction efficiency of 86%.

© University of Venda

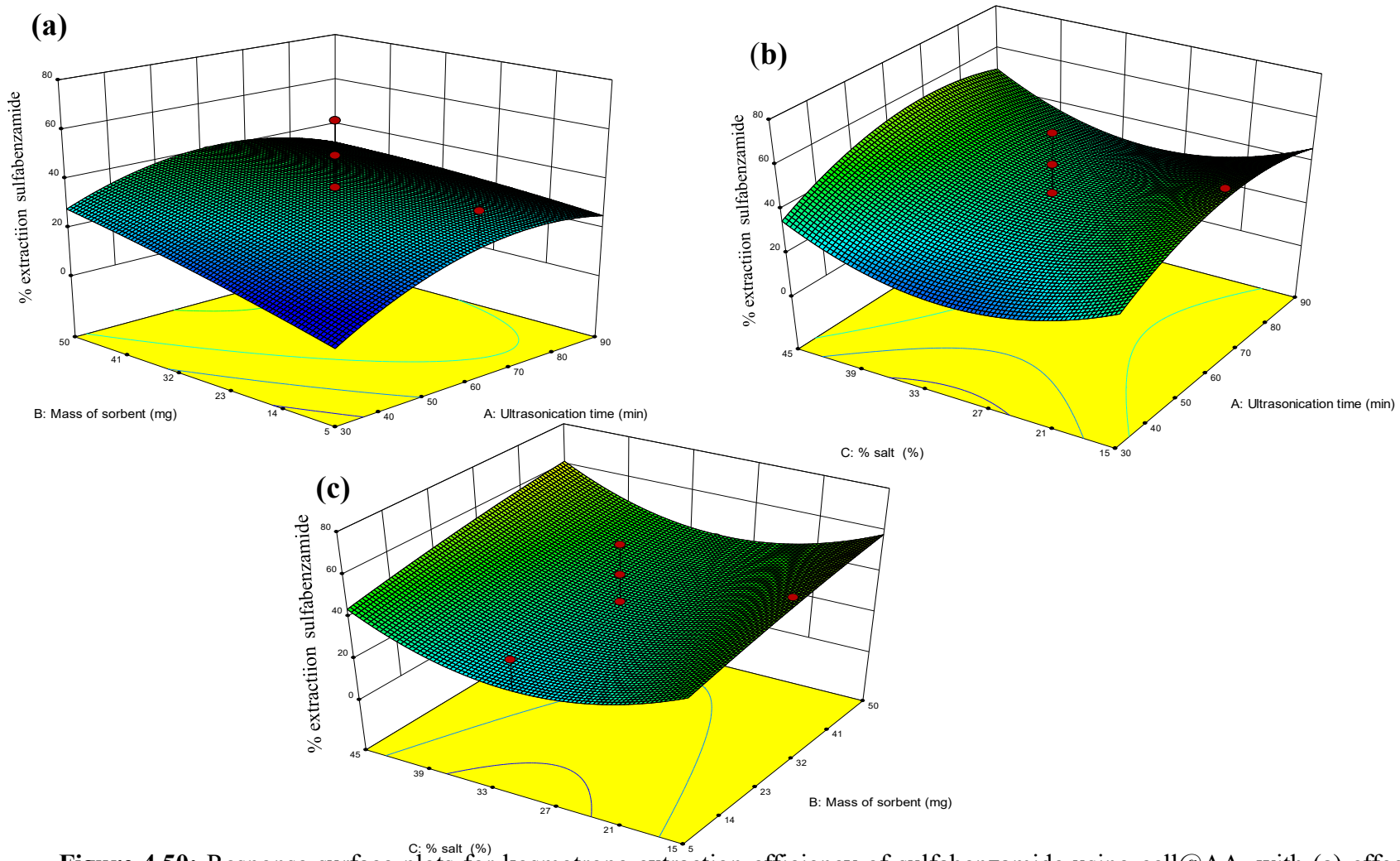


Figure 4.50: Response surface plots for kosmotrope extraction efficiency of sulfabenzamide using cell@AA, with (a) effect of ultrasonication time and mass of sorbent, (b) effect of ultrasonication time and salt concentration and (c) effect of mass of sorbent and salt concentration

© University of Venda

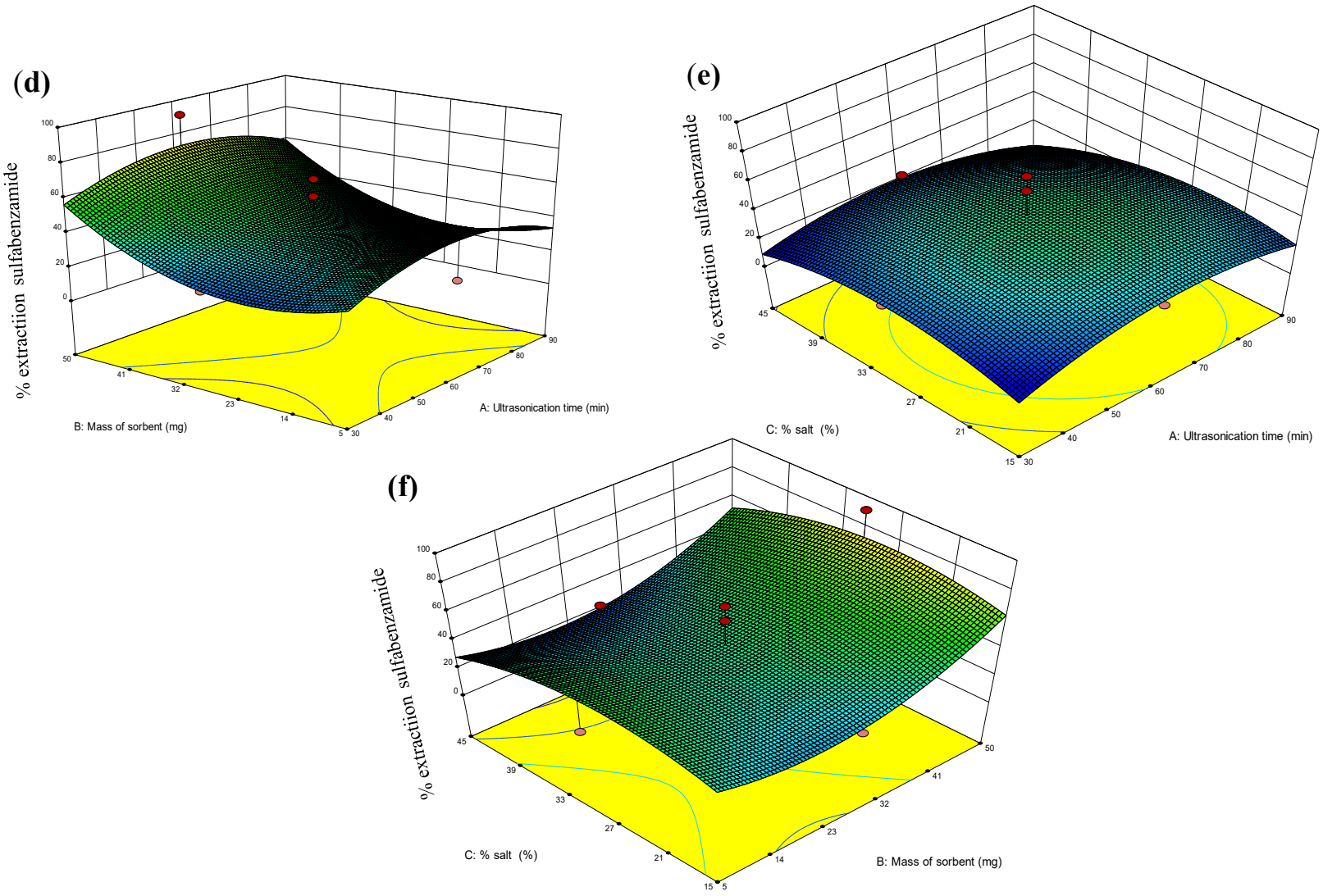


Figure 4.51: Response surface plots for chaotrope extraction efficiency of sulfabenzamide using cell@AA, with (d) effect of ultrasonication time and mass of sorbent, (e) effect of ultrasonication time and salt concentration, and (f) effect of mass of sorbent and salt concentration

© University of Venda

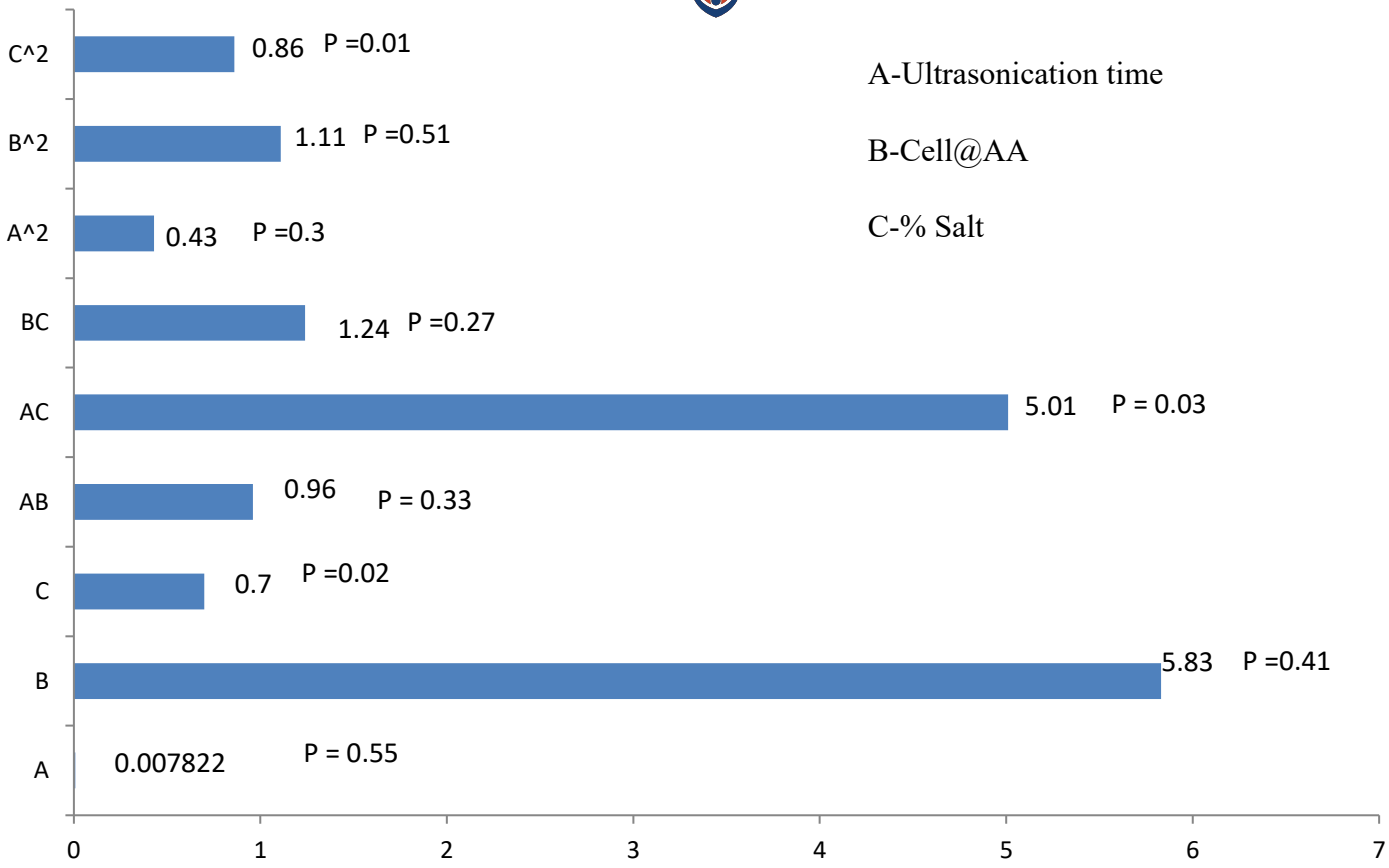


Figure 4.52: Pareto chart of extraction parameters for sulfabenzamide using cell@AA

Fig. 4.53 illustrates the proposed salting-out effect of sulfabenzamide and sulfachloropyridazine in the presence of NaCl and Na_2CO_3. For NaCl (a and b), the salt reduces the solubility of the sulfonamides by competing with them for water molecules, thereby decreasing their solvation and facilitating their precipitation. When Na_2CO_3 is used (c and d), the effect is more pronounced due to the presence of CO_3^{2-} ions, which have a stronger affinity for water, further reducing the hydration of sulfonamides and facilitating their aggregation. Additionally, electrostatic interactions between the negatively charged carbonate ions and the protonated sulfonamides enhance the precipitation process. Hydrophobic interactions also play a role, as the reduction in available water molecules forces the hydrophobic parts of the sulfonamides to aggregate, decreasing solubility. Ultimately, the combination of increased ionic strength, electrostatic interactions, and reduced hydration leads to the precipitation of the drug, which is significant in pharmaceutical purification and crystallization processes (Ovung and Bhattacharyya, 2021).

© University of Venda

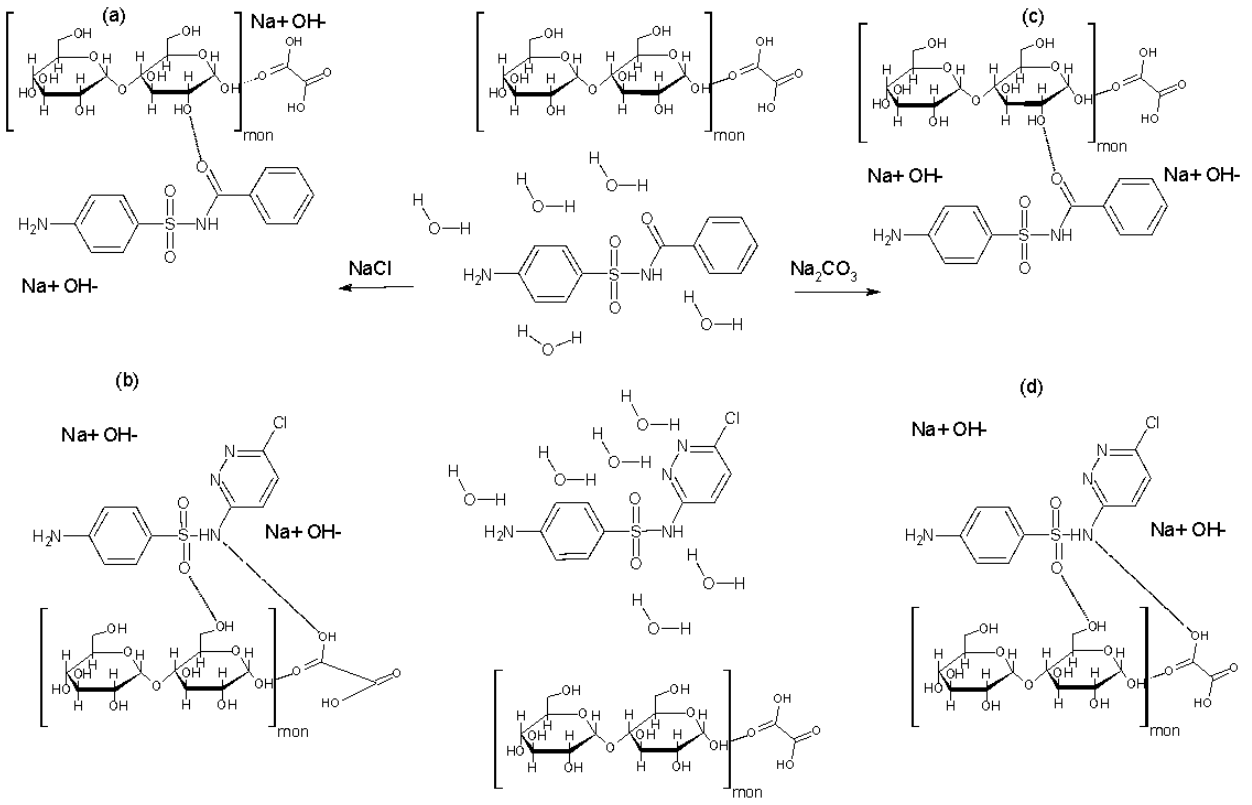


Figure 4.53: Proposed mechanism of salting-out of (a) sulfabenzamide and (b) sulfachloropyridazine in the presence of NaCl and salting out (c) sulfabezanamide and (d) sulfachloropyridazine in the presence of Na_2CO_3

4.7. Application studies of aqueous two-phase extraction

4.7.1. Sulfonamide extraction from wastewater, honey, and milk using a cellulose-based sorbent

Table 4.12 shows the extraction efficiency of a cellulose-based sorbent for sulfachloropyridazine in three distinct matrices, wastewater, milk, and honey. The parameters, such as ultrasonication time (60 min), sorbent mass (27.5 mg), and salt concentration (30% chaotrope), were optimized. The extraction efficiency varied, with milk exhibiting the highest percentage (75%), wastewater at 43%, and no measurable extraction in honey. This indicated that matrix composition has a substantial influence on the extraction process.

© University of Venda

The chromatogram (Fig. 4.54) shows that sulfachloropyridazine eluted at 7.6 min, which is earlier than its predicted retention time of 8.5 min. This earlier elution indicated weaker interactions between sulfachloropyridazine and the stationary phase (cellulose), leading to reduced retention during the chromatographic separation. Cellulose, being highly hydrophilic due to its abundance of surface hydroxyl (-OH) groups, can engage in hydrogen bonding with polar analytes like sulfachloropyridazine (Etale et al., 2023). However, these interactions may be relatively weak or insufficient for strong retention, particularly in reversed-phase systems where more hydrophobic interactions usually dominate. Furthermore, cellulose lacks the functional diversity required for tailored analyte retention, especially toward sulfonamide structures, contributing to the reduced interaction time and early elution (Onyianta et al., 2023).The presence of sodium chloride (NaCl), a chaotropic salt, likely influenced the analyte's behavior by disrupting the structured hydrogen-bonding network of water, thereby reducing solute-solvent interactions and promoting earlier migration through the chromatographic column (Cecchi, 2024). Additionally, NaCl may have increased the ionic strength of the mobile phase, affecting the solubility and mobility of sulfachloropyridazine, leading to faster elution. Despite the deviation in retention time, the extraction efficiency remained satisfactory. This suggests that even in the absence of strong retention mechanisms, cellulose facilitated the analyte's partitioning through mechanisms such as physical adsorption, weak hydrogen bonding, or dipole-dipole interactions.

Table 4.12: Extraction efficiency of cellulose-based sorbent for sulfachloropyridazine extraction from different matrices

Matrix	Ultrasonication time (min)	Mass of sorbent (mg)	% Salt	Salt type	Sulfachloropyridazine % extraction
Wastewater	60	27,5	30	Chaotrope	43
Milk	60	27,5	30	Chaotrope	75
Honey	60	27,5	30	Chaotrope	-

© University of Venda

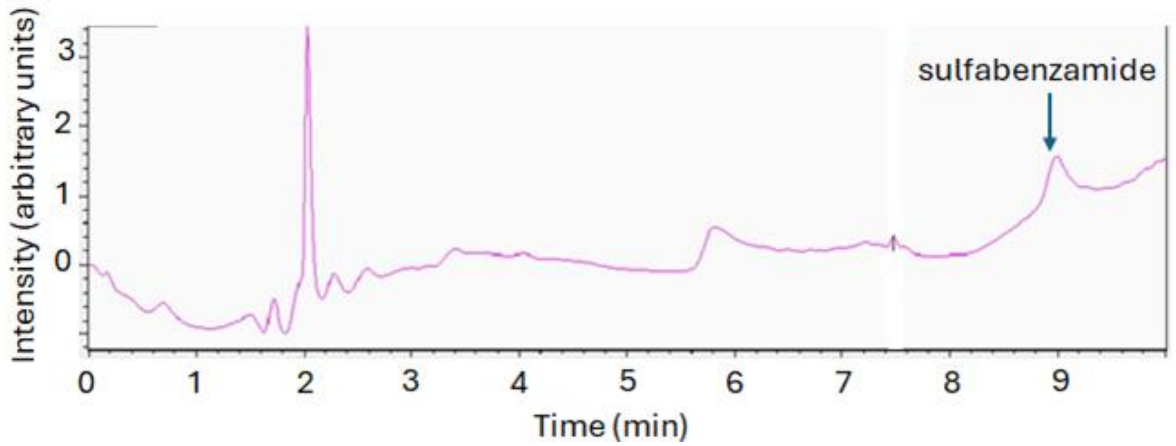


Figure 4.54: Chromatogram of sulfabenzamide extracted from milk using cellulose as the sorbent

Table 4.13 shows the extraction efficiency of sulfabenzamide from wastewater, milk, and honey utilizing cellulose as a sorbent under constant ultrasonication conditions. The extraction was carried out using 50 mg of sorbent and 30% chaotropic salt (NaCl). The findings show that sulfabenzamide had the lowest extraction efficiency from wastewater (15%), a moderate recovery from milk (24%), and was not found in honey. The variance in extraction efficiency among matrices suggests changes in matrix composition, possible interactions with cellulose, and the effect of chaotropic salt on sulfabenzamide solubility and partitioning.

Table 4.13: Extraction efficiency of cellulose-based sorbent for sulfabenzamide extraction from different matrices

Matrix	Ultrasonication time (min)	Mass of sorbent (mg)	% Salt	Salt type	Sulfabenzamide % extraction
Wastewater	60	50	30	Chaotrope	15
Milk	60	50	30	Chaotrope	24
Honey	60	50	30	Chaotrope	-

© University of Venda

The chromatogram (Fig. 4.55) indicates the successful extraction of sulfabenzamide from milk using unfunctionalized cellulose as a sorbent, with the expected retention time of 9.2 min, as precisely measured. The efficient recovery of sulfabenzamide in milk compared to honey suggests that cellulose effectively interacted with the sulfonamide through surface adsorption. This was likely facilitated by weak dipole interactions and hydrogen bonding between the hydroxyl groups of cellulose and the sulfonyl (-SO_2-) and amide (-$CONH_2$) groups of sulfabenzamide (Mosadegh et al., 2021). The presence of NaCl influenced solute-solvent interactions by disrupting the hydrogen-bonding network in the aqueous phase, consequently increasing sulfabenzamide desorption from the milk matrix and boosting its transfer onto the cellulose sorbent (Naseem et al., 2021). Furthermore, NaCl may have altered the ionic environment, lowered electrostatic repulsion and increased molecule affinity for the sorbent (Arif et al., 2021). The time required for retention was consistent with predictions, implying that no significant secondary interactions occurred to delay or accelerate the elution process, demonstrating that cellulose offered an efficient but non-selective adsorption medium for sulfabenzamide in milk.

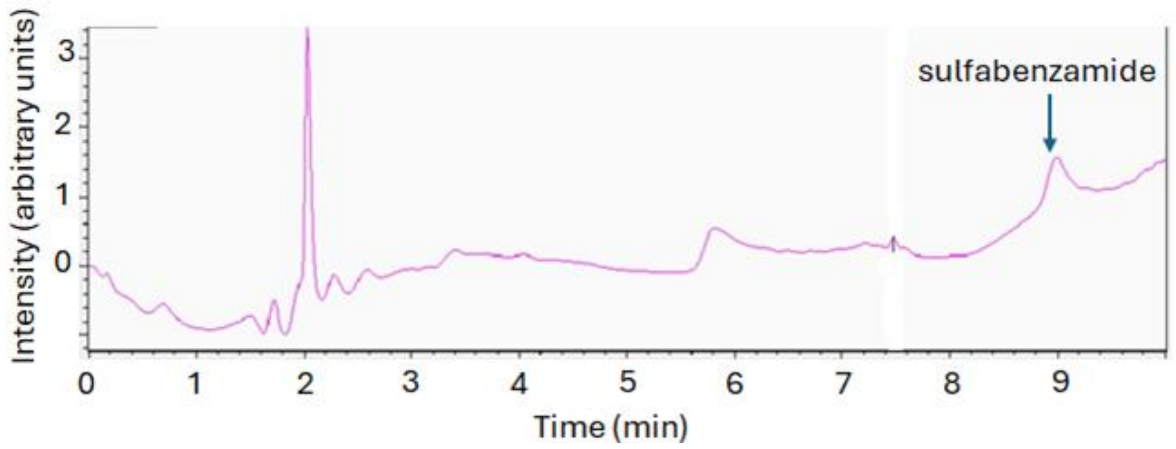


Figure 4.55: Chromatogram of sulfabenzamide extracted from milk using cellulose as the sorbent

4.7.2. Extraction of sulfonamides from wastewater, honey, and milk using a cell@OA-based sorbent

Table 4.14 shows the extraction efficiency of sulfachloropyridazine from various matrices (wastewater, milk, and honey) with cell@OA under identical conditions. Ultrasonication was carried out for 60 min using 27.5 mg of sorbent in the presence of 30% chaotropic salt. Sulfachloropyridazine was extracted from milk with a recovery of 21%; however, it was not

© University of Venda

detected in either wastewater or honey samples. The low recovery rate in milk indicates that the extraction was not efficient under these conditions. The change in extraction efficiency indicates that matrix composition altered the interaction of sulfachloropyridazine with the functionalized sorbent.

Table 4.14: Extraction efficiency of cell@OA-based sorbent for sulfachloropyridazine extraction from different matrices

Matrix	Ultrasonication time (min)	Mass of sorbent (mg)	% Salt	Salt type	Sulfachlopyridazine % extraction
Wastewater	60	27.5	30	Chaotrope	-
Milk	60	27.5	30	Chaotrope	21
Honey	60	27.5	30	Chaotrope	-

The chromatographic analysis (Fig. 4.56) of sulfachloropyridazine extracted using cell@OA sorbent from milk revealed a peak at 7.6 min, which differed from the expected retention time of 8.5 min. Several factors, including sorbent chemical changes (Liu et al., 2021), matrix effects (Sim et al., 2021), and ionic interactions (Lin et al., 2021), influenced the shift in retention time of sulfachloropyridazine from 8.5 to 7.6 min in the chromatogram of cell@OA sorbent for milk extraction. The addition of oxalic acid changed the sorbent's polarity and charge distribution, affecting its interaction with sulfachloropyridazine and shortening retention time. The milk matrix, with its proteins and lipids, most likely inhibited analyte movement, resulting in an earlier peak appearance (Goulding et al., 2020). Furthermore, the remarkable extraction efficiency in milk implied strong ion-exchange and chelation interactions between sulfachloropyridazine and cell@OA (Fox et al., 2020). The presence of NaCl as a chaotrope further disrupted hydrogen bonding and solvation, boosting hydrophobic contacts and changing electrostatic forces, ultimately influencing the analyte's retention behavior (Cecchi, 2024). These combined effects resulted in a faster elution of sulfachloropyridazine, optimizing extraction while moving the chromatographic peak.

© University of Venda

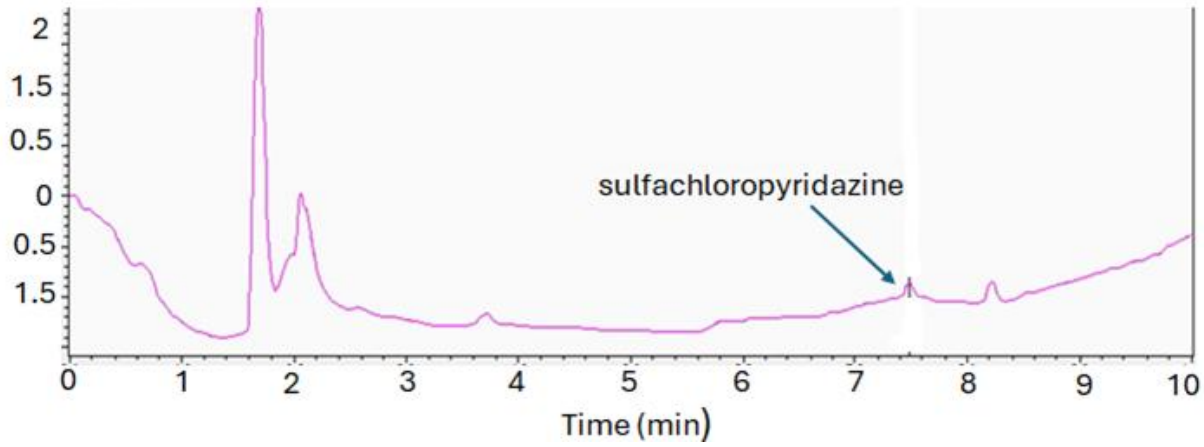


Figure 4.56: Chromatogram of sulfachloropyridazine extracted from milk using cell@OA as the sorbent

Table 4.15 presents the extraction performance of sulfabenzamide from wastewater, milk, and honey using oxalic acid-functionalized cellulose (cell@OA) under the same conditions. Ultrasonication was carried out for 30 min with 50 mg of sorbent in the presence of a 45% kosmotropic salt. Milk had the highest extraction efficiency (45%), followed by wastewater with 10% extraction and honey with no measurable extraction. The recovery differences indicated that matrix composition and kosmotropic salt effects altered sulfabenzamide's interaction with the sorbent.

© University of Venda

Table 4.15: Extraction efficiency of cell@OA-based sorbent for sulfabenzamide extraction from different matrices

Matrix	Ultrasonication time (min)	Mass of sorbent (mg)	% Salt	Salt type	Sulfabenzamide % extraction
Wastewater	30	50	45	Kosmotrope	10
Milk	30	50	45	Kosmotrope	45
Honey	30	50	45	Kosmotrope	-

The chromatogram (Fig. 4.57) of the cell@OA sorbent for extracting sulfabenzamide shows a retention time of 9.2 min. The functionalization introduced carboxyl groups, which altered the sorbent's binding characteristics and influenced how sulfabenzamide interacted with the stationary phase (Huang et al., 2024). Furthermore, the sample's composition affected the analyte's mobility, since dissolved organic molecules and ionic species changed its partitioning behavior (Zhang et al., 2024). The inclusion of Na_2CO_3 affected the extraction process by altering the solvation environment, reducing sulfabenzamide retention through kosmotropic effects and increasing its attraction for the sorbent. These parameters all contributed to the earlier elution of sulfabenzamide while optimizing its recovery in these conditions.

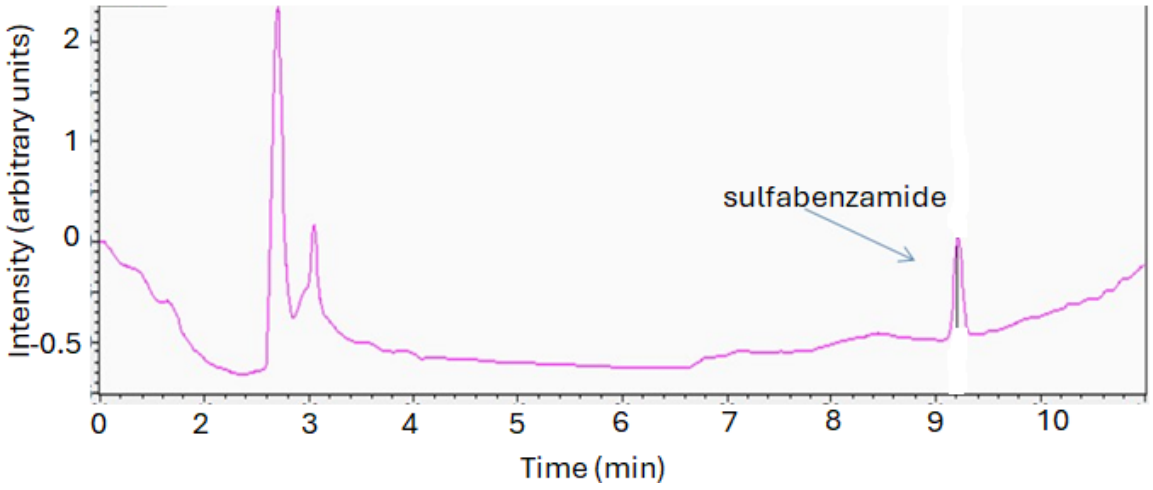


Figure 4.57: Chromatogram of sulfabenzamide extracted from milk using cell@OA as the sorbent

© University of Venda

4.7.3. Extraction of sulfonamide from wastewater, honey, and milk using a cell@AA-based sorbent

Table 4.16 shows the extraction efficiency of sulfachloropyridazine from wastewater, milk, and honey with adipic acid-functionalized cellulose (cell@AA) under optimized parameters, i.e., 60 min of ultrasonication, 50 mg of sorbent, and a 30% chaotropic salt. Milk had the highest extraction efficiency (82%), followed by wastewater (42%), and honey had the lowest (18%). The discrepancies in extraction rates are most likely attributable to matrix complexity, with milk presenting less interference than the more complex compositions of wastewater and honey.

Table 4.16: Extraction efficiency of cell@AA-based sorbent for sulfachloropyridazine extraction from different matrices

Matrix	Ultrasonication time (min)	Mass of sorbent (mg)	% Salt	Salt type	sulfachloropyridazine % extraction
Wastewater	60	50	30	Chaotrope	42
Milk	60	50	30	Chaotrope	82
Honey	60	50	30	Chaotrope	18

The chromatogram (Fig. 4.58) shows the extraction of sulfachloropyridazine from milk using adipic acid-functionalized cellulose, with the peak appearing at 6.8 min rather than the expected 8.5 min. This shift was most likely caused by the sorbent's changing surface chemistry, which changed the analyte's interaction strength and elution profile. Adipic acid introduced carboxyl groups, influencing polarity and binding behavior, but NaCl (BeMiller, 2025) disturbed solvation layers and altered ionic interactions, further influencing retention time. The sorbent had the highest extraction efficiency in milk when compared to honey and wastewater, which could be attributed to lower matrix complexity and fewer competitive interactions.

© University of Venda

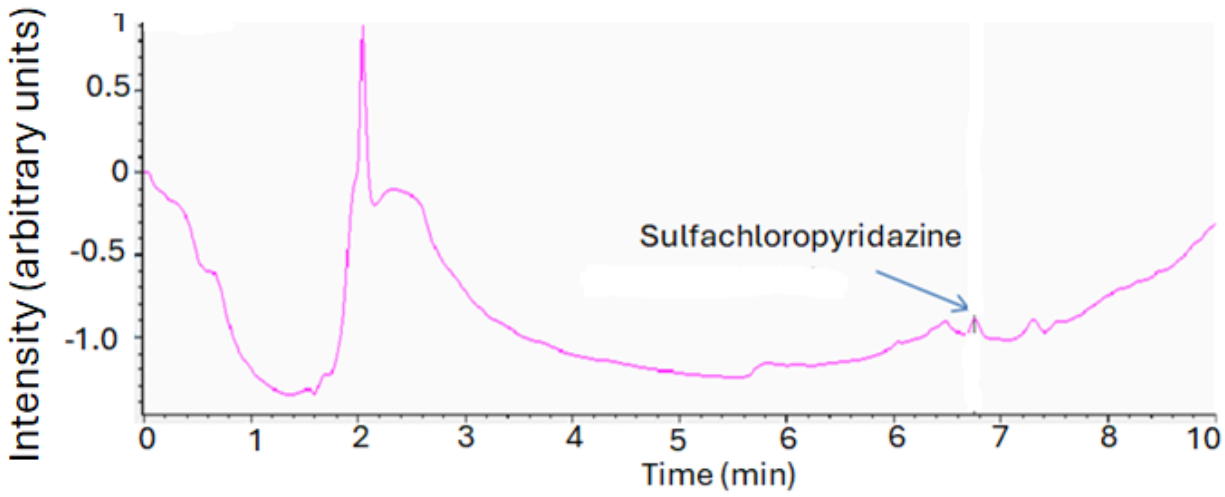


Figure 4.58: Chromatogram of sulfachloropyridazine extracted from milk using cell@AA as the sorbent

Table 4.17 illustrates the efficiency of extracting sulfabenzamide from wastewater, milk, and honey with adipic acid-functionalized cellulose (cell@AA) under consistent conditions, i.e. 60 min of ultrasonication, 50 mg of sorbent, and a 30% chaotropic salt. Milk had the highest extraction efficiency (43%) followed by wastewater (31%), while honey had the lowest efficiency (15%). The variable extraction rates are due to changes in matrix complexity and composition. Milk's comparatively simple matrix most likely promoted greater interaction between the analyte and the sorbent, whereas the organic load in wastewater and the high sugar content in honey may have interfered with the extraction process, resulting in lower efficiency.

© University of Venda

Table 4.17: Extraction efficiency of cell@AA-based sorbent for sulfabenzamide extraction from different matrices

Matrix	Ultrasonication time (min)	Mass of sorbent (mg)	% Salt	Salt type	Sulfabenzamide % extraction
Wastewater	30	5	45	Kosmotrope	31
Milk	30	5	45	Kosmotrope	43
Honey	30	5	45	Kosmotrope	15

The chromatogram (Fig. 4.59) shows sulfabenzamide extraction from milk employing a cell@AA sorbent, with a retention duration of 8.3 min rather than the expected 9.2 min. This alteration shows that the addition of carboxyl groups from adipic acid affected the surface polarity and binding properties of the analyte and the sorbent. The addition of sodium carbonate (Na_2CO_3), a kosmotropic chemical, facilitated this change by generating structured water layers and boosting ionic interactions, eventually shortening the analyte's retention time (Cechhi, 2024). Adipic acid functionalization of cellulose enhanced electrostatic and hydrogen bonding interactions, while Na_2CO_3 altered the solvent environment and affected the analyte's affinity for the stationary phase (Abid, 2024). Milk had the highest extraction efficiency as compared to honey and wastewater, most likely due to its simpler matrix and lesser interference, which allowed for greater interaction with the sorbent. In contrast, the high sugar content of honey and the complex organics in wastewater most likely interfered with the extraction process, affecting retention and efficiency.

The extraction efficiencies for sulfachloropyridazine showed that milk had the highest recovery under both kosmotropic (43%) and chaotropic (82%) conditions, followed by wastewater (31% and 42%), and honey (15% and 18%). These percentages reflect the relative amounts of antibiotic extracted from each matrix. No absolute concentrations were calculated, as the study focused on evaluating extraction efficiency rather than quantifying native or spiked levels.

© University of Venda

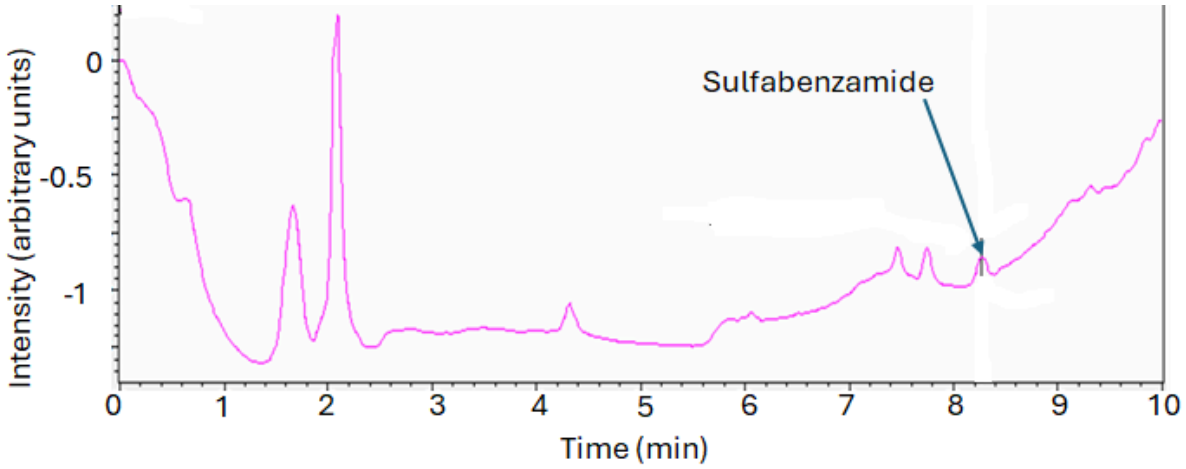


Figure 4.59: Chromatogram of sulfabenzamide extracted from milk using cell@AA as the sorbent

© University of Venda

Chapter 5: Conclusion, challenges and future work

© University of Venda

5.1. Conclusion

In conclusion, this study successfully established the potential of organic acid-functionalized cellulose as an efficient and sustainable sorbent for extracting sulfonamides from wastewater, honey, and milk by batch absorption and aqueous two-phase extraction (ATPE) methods. Functionalization with oxalic acid and adipic acid to the cellulose backbone increased its chemical reactivity, and affinity for sulfonamide analytes. These alterations were validated through comprehensive analysis with FTIR, PXRD, and SEM. The FTIR technique confirmed the successful integration of carboxyl groups, PXRD analysis revealed that incorporation of organic acids onto cellulose improved its crystallinity thereby increasing sorbent accessibility. Morphological analysis through SEM revealed a rougher, more porous surface, all of which contributed to improved adsorption capabilities.

In batch optimization studies, cell@OA was the most effective sorbent, extracting 75% of sulfabenzamide and 64% of sulfachloropyridazine under optimum conditions (30 min, 25°C and 50 mg sorbent). The presence of carboxyl groups promoted hydrogen bonding and electrostatic interactions with the sulfonamide functional groups, which accounted for the improved performance. When applied to real samples, cell@OA revealed high extraction efficiency in wastewater and milk but no quantifiable extraction in honey, most likely because of its high viscosity and complex matrix that impedes analyte diffusion.

In ATPE, cell@AA outperformed other sorbents, extracting sulfachloropyridazine and sulfabenzamide with extraction efficiencies of 91 and 83%, respectively. The relatively longer chain of adipic acid in cell@AA improved cellulose's hydrophilicity and improved its binding capacity, resulting in an increased extraction percentage. Generally, chaotropic salts enhanced the extraction of the less polar sulfachloropyridazine, whereas kosmotropic salts improved the extraction of sulfabenzamide. The type and concentration of salts were critical in phase separation and analyte partitioning, regulating solute interactions during the salting-out process.

Matrix composition during ATPE studies significantly influenced extraction outcomes when applied to real matrices. Milk generally had higher extraction percentages because of its protein and fat content, which improved analyte partitioning. Honey, on the other hand, was difficult to extract due to its high viscosity and sugar concentration. Wastewater, with its complex matrix of

© University of Venda

organic materials, salts, and possible pollutants, has varying impacts on extraction. High amounts of suspended particles and dissolved organic compounds may interfere with analyte recovery, although adequate treatment or pre-processing, such as filtration or diluting, can improve extraction results.

5.2. Challenges

- Cellulose generally has a relatively higher surface area compared to other adsorbents such as Cell@AA and Cell@OA.
- Analysis of spiked water samples is straightforward, however, qualitative and quantitative investigation of real environmental or food samples is a challenge because of matrix effects Moreover, real sample analysis has potential of producing coeluting peaks in HPLC UV-Vis.

5.3. Future work

- To investigate the toxicity of sulfonamides in relation to their environmental and health risks, providing a basis for the need for effective removal technologies in wastewater and food products
- Comparing performance to other adsorbents, such as activated carbon, zeolites, and commercial resins, to determine their efficacy in extracting sulfonamides from various matrices
- To study cellulose hyphenated with other biodegradable material (for example chitin) to improve its adsorption capacity
- To raise public awareness and education on the dangers of sulfonamide contamination, as well as the importance of proper removal strategies in preserving human health and ecosystems

© University of Venda

Chapter 6: References

© University of Venda

Acharya, S., Liyanage, S., Parajuli, P., Rumi, S. S., Shamshina, J. L., & Abidi, N. (2021). Utilization of cellulose to its full potential: a review on cellulose dissolution, regeneration, and applications. *Polymers*, *13*(24), 4344

Ahmed, N. J., Fouda, M. I., Fouda, D. I., & Foudah, A. I. (2020). The adverse effect reporting for the most commonly used antibiotics.

Ajala, O. A., Akinnawo, S. O., Bamisaye, A., Adedipe, D. T., Adesina, M. O., Okon-Akan, O. A., & Bello, O. S. (2023). Adsorptive removal of antibiotic pollutants from wastewater using biomass/biochar-based adsorbents. *RSC Advances*, *13*(7), 4678-4712.

Akıncı, İ. Y., & Albay, M. K. (2020). Etiological treatment of protozoer diarrhea in neonatal ruminants. *Veterinary Journal of Mehmet Akif Ersoy University*, *5*(1), 28-33.

Albertsson, P. Å., Johansson, G., & Tjerneld, F. (2020). Aqueous two-phase separations. *Separation Processes in Biotechnology*, 287-328.

Ali, A., Chiang, Y. W., & Santos, R. M. (2022). X-ray diffraction techniques for mineral characterization: A review for engineers of the fundamentals, applications, and research directions. *Minerals*, *12*(2), 205.

Ali, A., Chiang, Y. W., & Santos, R. M. (2022). X-ray diffraction techniques for mineral characterization: A review for engineers of the fundamentals, applications, and research directions. Minerals, 12(2), 205.

Andrade, C. (2019). The P value and statistical significance: misunderstandings, explanations, challenges, and alternatives. Indian journal of psychological medicine, 41(3), 210-215.

Arabkhani, P., Javadian, H., Asfaram, A., & Hosseini, S. N. (2021). A reusable mesoporous adsorbent for efficient treatment of hazardous triphenylmethane dye wastewater: RSM-CCD optimization and rapid microwave-assisted regeneration. *Scientific Reports*, *11*(1), 22751.

© University of Venda

Arshad, M. N., Faidallah, H. M., Asiri, A. M., Kosar, N., & Mahmood, T. (2020). Structural, spectroscopic and nonlinear optical properties of sulfonamide derivatives; experimental and theoretical study. *Journal of Molecular Structure*, *1202*, 127393.

Ashraf, D., Morsi, R., Usman, M., & Meetani, M. A. (2024). Recent Advances in the Chromatographic Analysis of Emerging Pollutants in Dairy Milk: A Review (2018–2023). *Molecules*, *29*(6), 1296.

Asif, M., Ahmed, D., Ahmad, N., Qamar, M. T., Alruwaili, N. K., & Bukhari, S. N. A. (2022). Extraction and characterization of microcrystalline cellulose from Lagenaria siceraria fruit pedicles. *Polymers*, *14*(9), 1867.

Aziz, T., Farid, A., Haq, F., Kiran, M., Ullah, A., Zhang, K., & Al Jaouni, S. K. (2022). A review on the modification of cellulose and its applications. *Polymers*, *14*(15), 3206.

Azzano, M. (2023). *Antibiotic Resistance and Alternative Therapeutic Proposals* (Master's thesis, Università di Parma. Dipartimento di Scienze Medico-Veterinarie).

Badawy, M. E., El-Nouby, M. A., Kimani, P. K., Lim, L. W., & Rabea, E. I. (2022). A review of the modern principles and applications of solid-phase extraction techniques in chromatographic analysis. Analytical Sciences, 38(12), 1457-1487.

Bagheri, A. R., Aramesh, N., Gong, Z., Cerda, V., & Lee, H. K. (2022). Two-dimensional materials as a platform in extraction methods: A review. *TrAC Trends in Analytical Chemistry*, *152*, 116606.

Baldovino-Medrano, V. G., Niño-Celis, V., & Isaacs Giraldo, R. (2023). Systematic analysis of the nitrogen adsorption–desorption isotherms recorded for a series of materials based on microporous–mesoporous amorphous aluminosilicates using classical methods. *Journal of Chemical & Engineering Data*, *68*(9), 2512-2528.

Bardestani, R., Patience, G. S., & Kaliaguine, S. (2019). Experimental methods in chemical engineering: specific surface area and pore size distribution measurements—BET, BJH, and DFT. The Canadian Journal of Chemical Engineering, 97(11), 2781-2791.

© University of Venda

Bärmann, A., Burlacu, R., Hager, L., & Kleinert, T. (2023). On piecewise linear approximations of bilinear terms: structural comparison of univariate and bivariate mixed-integer programming formulations. *Journal of Global Optimization*, 85(4), 789-819.

Barp, L., Višnjevec, A. M., & Moret, S. (2023). Pressurized Liquid Extraction: A powerful tool to implement extraction and purification of food contaminants. *Foods*, *12*(10), 2017.

Bhattacharya, S. (2021). Central composite design for response surface methodology and its application in pharmacy. In response surface methodology in engineering science. Intechopen.

Bilal, M., Mehmood, S., Rasheed, T., & Iqbal, H. M. (2020). Antibiotics traces in the aquatic environment: persistence and adverse environmental impact. *Current Opinion in Environmental Science & Health*, *13*, 68-74.

Bolla, G., Sarma, B., & Nangia, A. K. (2022). Crystal engineering of pharmaceutical cocrystals in the discovery and development of improved drugs. *Chemical reviews*, *122*(13), 11514-11603.

Bombaywala, S., Mandpe, A., Paliya, S., & Kumar, S. (2021). Antibiotic resistance in the environment: a critical insight on its occurrence, fate, and eco-toxicity. *Environmental Science and Pollution Research*, *28*, 24889-24916.

Botelho Junior, A. B., Pinheiro, E. F., Espinosa, D. C. R., Tenorio, J. A. S., & Baltazar, M. D. P. G. (2022). Adsorption of lanthanum and cerium on chelating ion exchange resins: kinetic and thermodynamic studies. *Separation Science and Technology*, *57*(1), 60-69.

Brzezińska, R., Górska, A., Wirkowska-Wojdyła, M., & Piasecka, I. (2023). Response surface methodology as a tool for optimization of extraction process of bioactive compounds from spent coffee grounds. *Applied Sciences*, *13*(13), 7634.

Capasso, C., & Supuran, C. T. (2019). Dihydropteroate synthase (sulfonamides) and dihydrofolate reductase inhibitors. *Bacterial resistance to antibiotics–From molecules to man*, 163-172.

© University of Venda

Capuozzo, M., Zovi, A., Langella, R., Ottaiano, A., Cascella, M., Scognamiglio, M., & Ferrara, F. (2024). Optimizing antibiotic use: Addressing resistance through effective strategies and health policies. *Antibiotics*, *13*(12), 1112.

Cerqueira, U. M. F. M., Bezerra, M. A., Ferreira, S. L. C., de Jesus Araújo, R., da Silva, B. N., & Novaes, C. G. (2021). Doehlert design in the optimization of procedures aiming food analysis–a review. *Food Chemistry*, *364*, 130429.

Chao, Y., & Shum, H. C. (2020). Emerging aqueous two-phase systems: from fundamentals of interfaces to biomedical applications. *Chemical Society Reviews*, *49*(1), 114-142.

Chaturvedi, P., Shukla, P., Giri, B. S., Chowdhary, P., Chandra, R., Gupta, P., & Pandey, A. (2021). Prevalence and hazardous impact of pharmaceutical and personal care products and antibiotics in environment: A review on emerging contaminants. *Environmental research*, *194*, 110664.

Chatzimitakos, T. G., Karali, K. K., & Stalikas, C. D. (2019). Magnetic graphene oxide as a convenient nanosorbent to streamline matrix solid-phase dispersion towards the extraction of pesticides from vegetables and their determination by GC–MS. *Microchemical Journal*, *151*, 104247.

Chaves, J. O., De Souza, M. C., Da Silva, L. C., Lachos-Perez, D., Torres-Mayanga, P. C., Machado, A. P. D. F., & Rostagno, M. A. (2020). Extraction of flavonoids from natural sources using modern techniques. *Frontiers in Chemistry*, *8*, 507887.

Chen, H. (2020). *Improve the manufacturability and dissolution performance of drugs through spherical crystallization* (Doctoral dissertation, University of Minnesota). Deng, Y., Zhu, T., Cheng, Y., Zhao, K., Meng, Z., Huang, J., & Lai, Y. (2024). Recent advances in functional cellulose-based materials: Classification, properties, and applications. *Advanced Fiber Materials*, *6*(5), 1343-1368.

Chen, J., Ying, G. G., & Deng, W. J. (2019). Antibiotic residues in food: extraction, analysis, and human health concerns. *Journal of Agricultural and Food Chemistry*, *67*(27), 7569-7586.

© University of Venda

Chen, Q., Zhou, M., Pan, Y., & Zhang, Y. (2023). Ligand-enhanced zero-valent iron for organic contaminants degradation: A mini review. *Processes*, *11*(2), 620.

Cheong, M. S., Seo, K. H., Chohra, H., Yoon, Y. E., Choe, H., Kantharaj, V., & Lee, Y. B. (2020). Influence of sulfonamide contamination derived from veterinary antibiotics on plant growth and development. *Antibiotics*, *9*(8), 456.

Chong, K. Y., Stefanova, R., Zhang, J., & Brooks, M. S. L. (2020). Aqueous two-phase extraction of bioactive compounds from haskap leaves (Lonicera caerulea): Comparison of salt/ethanol and sugar/propanol systems. *Separation and Purification Technology*, *252*, 117399.

Conde-Cid, M., Nóvoa-Muñoz, J. C., Núñez-Delgado, A., Fernández-Sanjurjo, M. J., Arias-Estévez, M., & Álvarez-Rodríguez, E. (2019). Experimental data and modeling for sulfachloropyridazine and sulfamethazine adsorption/desorption on agricultural acid soils. *Microporous and Mesoporous Materials*, *288*, 109601.

Costa, P., Pilli, R., Pinheiro, S., & Bakuzis, P. (2022). *The chemistry of carbonyl compounds and derivatives*. Royal Society of Chemistry.

Cui, H., Chang, H., Zheng, H., & Wan, Y. (2021). Determination and occurrence of sulfonamide transformation products in surface waters. *Science of the Total Environment*, *779*, 146562.

da Silva, J. J., da Silva, B. F., Stradiotto, N. R., Petrovic, M., Gago-Ferrero, P., & Gros, M. (2020). Pressurized Liquid Extraction (PLE) and QuEChERS evaluation for the analysis of antibiotics in agricultural soils. *MethodsX*, *7*, 101171.

D'Acierno, F. (2021). *Thermal behaviour of cellulose materials* (Doctoral dissertation, University of British Columbia).

Dai, J. J., Song, J. M., Li, X. G., Ma, J., Yuan, H. M., Duan, L. Q., & Wang, Q. D. (2023). Behavioral and ecotoxicology of sulfonamide metabolites in the aquatic environment. *Ying Yong Sheng tai xue bao= The Journal of Applied Ecology*, *34*(8), 2274-2284.

© University of Venda

Darmenbayeva, A., Rajasekharan, R., Massalimova, B., Bektenov, N., Taubayeva, R., Bazarbaeva, K., & Ungarbayeva, A. (2024). Cellulose-Based Sorbents: A Comprehensive Review of Current Advances in Water Remediation and Future Prospects. *Molecules*, *29*(24), 5969.

Das Mahapatra, A., Patra, C., Sepay, N., Sinha, C., & Chattopadhyay, D. (2024). Comparative study on Antibacterial efficacy of a series of chromone sulfonamide derivatives against drug-resistant and MDR-isolates. *Brazilian Journal of Microbiology*, *55*(1), 343-355.

Davis, J. (2024). Antimicrobial therapy in the neonatal foal. *Equine Neonatal Medicine*, 1328-1343.

Deng, Di Leo, G., & Sardanelli, F. (2020). Statistical significance: p value, 0.05 threshold, and applications to radiomics—reasons for a conservative approach. *European radiology experimental*, *4*, 1-8.

Diwekar, U. M. (2020). *Introduction to applied optimization* (Vol. 22). Springer nature.

Dluhošová, S., Bartáková, K., Vorlová, L., Navrátilová, P., Hanuš, O., & Samková, E. (2024). Dairy Chain Safety in the Context of Antibiotic Residues—Current Status of Confirmatory Liquid Chromatography Methods: A Review. *Antibiotics*, *13*(11), 1038.

Dmitrieva, E., Temerdashev, A., Azaryan, A., & Gashimova, E. (2020). Quantification of steroid hormones in human urine by DLLME and UHPLC-HRMS detection. *Journal of Chromatography B*, *1159*, 122390.

Du, J., Huang, W., Pan, Y., Xu, S., Li, H., Jin, M., & Liu, Q. (2024). Ecotoxicological Effects of Microplastics Combined With Antibiotics in the Aquatic Environment: Recent Developments and Prospects. *Environmental Toxicology and Chemistry*, *43*(9), 1950-1961.

Duan, W., Cui, H., Jia, X., & Huang, X. (2022). Occurrence and ecotoxicity of sulfonamides in the aquatic environment: A review. *Science of The Total Environment*, *820*, 153178.

© University of Venda

Durairaj, A., Maruthapandi, M., Saravanan, A., Luong, J. H., & Gedanken, A. (2022). Cellulose nanocrystals (CNC)-based functional materials for supercapacitor applications. *Nanomaterials, 12(11),* 1828.

El-Deen, A. K. (2024). An overview of recent advances and applications of matrix solid-phase dispersion. *Separation & Purification Reviews*, *53*(1), 100-117.

El-Gaby, M., A Ammar, Y., IH El-Qaliei, M., F Hussein, M., & A Faraghally, F. (2020). Sulfonamides: Synthesis and the recent applications in Medicinal Chemistry. *Egyptian Journal of Chemistry*, *63*(12), 5289-5327.

Eniola, J. O., Kumar, R., & Barakat, M. A. (2019). Adsorptive removal of antibiotics from water over natural and modified adsorbents. *Environmental Science and Pollution Research*, *26*(34), 34775-34788.

Etale, A., Onyianta, A. J., Turner, S. R., & Eichhorn, S. J. (2023). Cellulose: a review of water interactions, applications in composites, and water treatment. *Chemical reviews*, *123*(5), 2016-2048.

Felis, E., Kalka, J., Sochacki, A., Kowalska, K., Bajkacz, S., Harnisz, M., & Korzeniewska, E. (2020). Antimicrobial pharmaceuticals in the aquatic environment-occurrence and environmental implications. *European Journal of Pharmacology*, *866*, 172813.

Fu, C., Li, Y., Lin, Y., Zhang, W., Yang, J., Liu, Y., & Huang, L. (2024). Crucial role of fiber swelling in microfibrillated cellulose extraction via ball milling. *Industrial Crops and Products*, *218*, 118899.

Fu, S., Fang, Q., Li, A., Li, Z., Han, J., Dang, X., & Han, W. (2021). Accurate characterization of full pore size distribution of tight sandstones by low-temperature nitrogen gas adsorption and high-pressure mercury intrusion combination method. *Energy Science & Engineering*, *9*(1), 80-100.

Ganesh, V., Poorna Basuri, P., Sahini, K., & Nalini, C. N. (2023). Retention behaviour of analytes in reversed-phase high-performance liquid chromatography—A review. *Biomedical Chromatography*, *37*(7), e5482.

© University of Venda

Gao, S. W., Chen, L. H., Cui, Y. Y., & Yang, C. X. (2024). Sacrificial template synthesis of hollow sulfonate group functionalized microporous organic network for efficient solid phase extraction of sulfonamide antibiotics from milk and honey samples. *Journal of Chromatography A*, *1721*, 464844.

Goodfellow, I., Pouget-Abadie, J., Mirza, M., Xu, B., Warde-Farley, D., Ozair, S., & Bengio, Y. (2020). Generative adversarial networks. *Communications of the ACM*, *63*(11), 139-144.

Gupta, P. K., Raghunath, S. S., Prasanna, D. V., Venkat, P., Shree, V., Chithananthan, C., & Geetha, K. (2019). An Update on Overview of Cellulose, Its Structure and. *Cellulose*, 59.

Gutema, E. M., Gopal, M., & Lemu, H. G. (2022). Temperature optimization by using response surface methodology and desirability analysis of aluminium 6061. *Materials*, *15*(17), 5892.

Heise, K., Delepierre, G., King, A. W., Kostiainen, M. A., Zoppe, J., Weder, C., & Kontturi, E. (2021). Chemical modification of reducing end-groups in cellulose nanocrystals. *Angewandte Chemie International Edition*, *60*(1), 66-87.

Hu, R., Chen, Y., Zhang, C., Jiang, S., Hou, H., & Duan, G. (2024). Porous monoliths from polyimide: Synthesis, modifications and applications. *Progress in Materials Science*, 101284.

Huemer, M., Mairpady Shambat, S., Brugger, S. D., & Zinkernagel, A. S. (2020). Antibiotic resistance and persistence—Implications for human health and treatment perspectives. *EMBOReports*, 21(12), e51034.

Huo, Z., Zhao, S., Yi, J., Zhang, H., & Li, J. (2020). Biomass-based cellulose functionalized by phosphonic acid with high selectivity and capacity for capturing U (VI) in aqueous solution. *Applied Sciences*, *10*(16), 5455.

Hussein, H. K., Jabbar, B. A. A., Amin, S. S., Jawad, A. A., Abbas, R. K., & Jawad, S. A. (2023). Study of Drugs: Antibiotic and study mechanism and adverse effects. *Al-Nahrain Journal of Science*, *26*(1), 15-20.

Ibrahim, N. M., Fahim, S. H., Hassan, M., Farag, A. E., & Georgey, H. H. (2022). Design and synthesis of ciprofloxacin-sulfonamide hybrids to manipulate ciprofloxacin pharmacological

© University of Venda

qualities: Potency and side effects. *European Journal of Medicinal Chemistry*, *228*, 114021.

Ingrassia, E. B., Fiorentini, E. F., Dotto, G. L., & Escudero, L. B. (2024). When the use of derived wastes and effluents treatment is part of a responsible industrial production: a review. *Chemical Engineering and Processing-Process Intensification*, 109826.

Irwansyah, F. S., Amal, A. I., Diyanthi, E. W., Hadisantoso, E. P., Noviyanti, A. R., Eddy, D. R., & Risdiana, R. (2024). How to read and determine the specific surface area of inorganic materials using the Brunauer-Emmett-Teller (BET) method. *ASEAN Journal of Science and Engineering*, *4*(1), 61-70.

Islam, M. (2022). *Penalized Regression Splines-Based Tests for Comparing Two Time Series with Unequal Lengths* (Doctoral dissertation, University of New Hampshire).

Jandera, P., & Hájek, T. (2020). Mobile Phase Effects in Reversed-Phase and Hydrophilic Interaction Liquid Chromatography. In *Advances in Chromatography, Volume 57* (pp. 1-58). CRC Press.

Jhalora, V., & Bist, R. (2024). A Comprehensive Review of Molecular Mechanisms Leading to the Emergence of Multidrug Resistance in Bacteria. *Indian Journal of Microbiology*, 1-22.

Ji, Z., Wang, H., Canossa, S., Wuttke, S., & Yaghi, O. M. (2020). Pore chemistry of metal–organic frameworks. *Advanced Functional Materials*, *30*(41), 2000238.

Jiang, J., Zhu, Y., & Jiang, F. (2021). Sustainable isolation of nanocellulose from cellulose and lignocellulosic feedstocks: Recent progress and perspectives. *Carbohydrate polymers*, *267*, 118188.

Jo, W., Koh, E. S., & Chung, S. (2023). Therapeutic roles of thiazides and loop diuretics in blood pressure control and renal protection against chronic kidney disease. *Clinical Hypertension*, 29(1), 1-15.

Kamkar, M. (2024). *Examining Committee Membership* (Doctoral dissertation, University of Waterloo).

© University of Venda

Kergoat, L., Besse-Hoggan, P., Leremboure, M., Beguet, J., Devers, M., Martin-Laurent, F & Bonnineau, C. (2021). Environmental concentrations of sulfonamides can alter bacterial structure and induce diatom deformities in freshwater biofilm communities. *Frontiers in Microbiology*, *12*, 643719.

Khan, A., Raza, Z. A., Bhatti, H. N., & Sarwar, T. (2023). Synthesis of succinate-functionalized silver nanoparticles and their application in cellulose fabric coating. *Cellulose*, *30*(17), 11231-11247.

Khan, H., Yerramilli, A. S., D'Oliveira, A., Alford, T. L., Boffito, D. C., & Patience, G. S. (2020). Experimental methods in chemical engineering: X-ray diffraction spectroscopy—XRD. The Canadian journal of chemical engineering, 98(6), 1255-1266.

Khandale, N., Rajge, R. R., Singh, S. K., & Singh, G. (2023). Advances of hyphenated technique in impurity profiling of active pharmaceutical ingredients and pharmaceutical products. *Separation Science Plus*, *6*(9), 2300018.

Khatibi, S. A., Hamidi, S., & Siahi-Shadbad, M. R. (2021). Current trends in sample preparation by solid-phase extraction techniques for the determination of antibiotic residues in foodstuffs: a review. *Critical Reviews in Food Science and Nutrition*, 61(20), 3361-3382.

Kim, N. S., Numan, M., Nam, S. C., Park, S. E., & Jo, C. (2021). Dynamic adsorption/desorption of p-xylene on nanomorphic MFI zeolites: Effect of zeolite crystal thickness and mesopore architecture. *Journal of Hazardous Materials*, *403*, 123659.

Kovalakova, P., Cizmas, L., McDonald, T. J., Marsalek, B., Feng, M., & Sharma, V. K. (2020). Occurrence and toxicity of antibiotics in the aquatic environment: A review. *Chemosphere*, *251*, 126351.

Krishna, S. A., Umadevi, S., Dominic, C. M., Parameswaranpillai, J., Bhanu, A. A., George, J. S. & Vijayan, P. P. (2024). Biomass derived cellulose nanofiber loaded PVA-nanocurcumin coating for extending the shelf life of Mandarin oranges (Citrus reticulata). *Hybrid Advances*, *5*, 100162.

© University of Venda

Kumar, D., Aslam, A., Gautam, R., Gupta, A., Yadav, A., & Yadav, K. (2024). Livestock manure application causes the spread of antibiotic-resistant genes in agricultural lands. In *Antimicrobials in Agriculture* (pp. 55-69). CRC press.

Kumar, K., Srivastav, S., & Sharanagat, V. S. (2021). Ultrasound assisted extraction (UAE) of bioactive compounds from fruit and vegetable processing by-products: A review. *Ultrasonics Sonochemistry*, *70*, 105325.

Kushwaha, M., Agarwal, S., & Khan, S. (2023). Green Nanotechnology in Clean Water and Sanitation (SDG 6). *In Green Chemistry, its Role in Achieving Sustainable Development Goals, Volume1* (pp. 207-218). CRC Press.

Lajqi Berisha, N., Poceva Panovska, A., & Hajrulai-Musliu, Z. (2024). Antibiotic resistance and aquatic systems: importance in public health. *Water*, *16*(17), 2362.

Laws, M., Shaaban, A., & Rahman, K. M. (2019). Antibiotic resistance breakers: current approaches and future directions. FEMS *Microbiology Reviews*, 43(5), 490-516.

Leal, C. S., Mesquita, D. P., Amaral, A. L., Amaral, A. M., & Ferreira, E. C. (2020). Environmental impact and biological removal processes of pharmaceutically active compounds: The particular case of sulfonamides, anticonvulsants and steroid estrogens. *Critical Reviews in Environmental Science and Technology*, *50*(7), 698-742.

Lees, P., Pelligand, L., Giraud, E., & Toutain, P. L. (2021). A history of antimicrobial drugs in animals: Evolution and revolution. *Journal of Veterinary Pharmacology and Therapeutics*, *44*(2), 137-171.

Leong, Y. K., Yang, F. C., & Chang, J. S. (2021). Extraction of polysaccharides from edible mushrooms: Emerging technologies and recent advances. *Carbohydrate Polymers*, *251*, 117006.

Li, J., Wang, Z., Xiu, H., Zhao, X., Ma, F., Liu, L., & Ji, Y. (2022). Correlation between the powder characteristics and particle morphology of microcrystalline cellulose (MCC) and its tablet application performance. *Powder Technology*, *399*, 117194.

Li, S., Zhang, C., Tang, H. X., Gu, Y., Guo, A. J., Wang, K., & Lian, K. Q. (2023). Determination of 24 sulfonamide antibiotics in instant pastries by modified QuEChERS coupled with

© University of Venda

ultra performance liquid chromatography-tandem mass spectrometry. *Journal of Food and Drug Analysis*, *31*(1), 73.

Lim, A. H., Wong, S. T., Thian, S. Y., Tew, W. Y., Chiew, S. Y., Lee, X., & Hor, Y. Y. (2021). Antibiotic Prescribing Pattern in Primary Care Practice in Federal Territory Kuala Lumpur and Putrajaya, Malaysia. *International Journal of Advancement in Life Sciences Research*, 4(4), 15-24.

Liu, S., Li, Z., Yu, B., Wang, S., Shen, Y., & Cong, H. (2020). Recent advances on protein separation and purification methods. *Advances in Colloid and Interface Science*, *284*, 102254.

Liu, Z. Q., Zhang, Q., Liu, Y. L., Yu, X. Q., Chui, R. H., Zhang, L. L., & Ma, L. Y. (2024). Recent contributions of pyridazine as a privileged scaffold of anticancer agents in medicinal chemistry: An updated review. *Bioorganic & Medicinal Chemistry*, 117847.

Liyanage, S., Acharya, S., Parajuli, P., Shamshina, J. L., & Abidi, N. (2021). Production and surface modification of cellulose bioproducts. *Polymers*, *13*(19), 3433.

Loy, A. C. M., Samudrala, S. P., & Bhattacharya, S. (2022). Evaluation of porous honeycomb-shaped CuO/CeO2 catalyst in vapour phase glycerol reforming for sustainable hydrogen production. *Catalysts*, *12*(9), 941.

Ma, X., Wu, L., Wang, Y., Han, S., El-Dalatony, M. M., Feng, F., & Wang, Y. (2022). Diet and human reproductive system: Insight of omics approaches. *Food Science & Nutrition*, *10*(5), 1368-1384.

Makarem, M., Lee, C. M., Kafle, K., Huang, S., Chae, I., Yang, H., & Kim, S. H. (2019). Probing cellulose structures with vibrational spectroscopy. *Cellulose*, *26*, 35-79.

Mangla, D., Sharma, A., & Ikram, S. (2022). Critical review on adsorptive removal of antibiotics: Present situation, challenges and future perspective. *Journal of Hazardous Materials*, *425*, 127946.

Manungufala, T. E., Chimuka, L., Cukrowska, E., & Tutu, H. (2011). Evaluation of the performance of rural wastewater treatment plants using chemical measurements in combination

© University of Venda

with statistical techniques: a case study. *Toxicological & Environmental Chemistry*, *93*(6), 1123-1134.

Mehta, N., Kumar, P., Verma, A. K., Umaraw, P., Khatkar, S. K., Khatkar, A. B., & Sazili, A. Q. (2022). Ultrasound-Assisted Extraction and the Encapsulation of Bioactive Components for Food Applications. *Foods*, 11(19), 2973.

Mishra, P., Singh, U., Pandey, C. M., Mishra, P., & Pandey, G. (2019). Application of student's t-test, analysis of variance, and covariance. *Annals of cardiac anaesthesia*, *22*(4), 407-411.

Mishra, R. K., Mentha, S. S., Misra, Y., & Dwivedi, N. (2023). Emerging pollutants of severe environmental concern in water and wastewater: A comprehensive review on current developments and future research. *Water-Energy Nexus*, *6*, 74-95.

Misiewicz, B., Mencer, D., Terzaghi, W., & VanWert, A. L. (2023). Analytical methods for oxalate quantification: the ubiquitous organic anion. *Molecules*, *28*(7), 3206.

Mithuna, R., Tharanyalakshmi, R., Jain, I., Singhal, S., Sikarwar, D., Das, S., & Das, B. (2024). Emergence of antibiotic resistance due to the excessive use of antibiotics in medicines and feed additives: A global scenario with emphasis on the Indian perspective. *Emerging Contaminants*, 100389.

Mohammed, A., & Abdullah, A. (2018, November). Scanning electron microscopy (SEM): A review. In Proceedings of the 2018 international conference on hydraulics and pneumatics—HERVEX, Băile Govora, Romania (Vol. 2018, pp. 7-9).

Morariu, I. D., Avasilcai, L., Vieriu, M., Lupu, V. V., Ioniuc, I., Morariu, B. A., & Trandafir, L. (2024). A comprehensive narrative review on the hazards of bee honey adulteration and contamination. *Journal of Food Quality*, *2024*(1), 3512676.

More, P. R., & Arya, S. S. (2021). Intensification of bio-actives extraction from pomegranate peel using pulsed ultrasound: Effect of factors, correlation, optimization and antioxidant bioactivities. *Ultrasonics Sonochemistry*, *72*, 105423.

© University of Venda

Morin-Crini, N., Lichtfouse, E., Fourmentin, M., Ribeiro, A. R. L., Noutsopoulos, C., Mapelli, F., & Crini, G. (2022). Removal of emerging contaminants from wastewater using advanced treatments. A review. *Environmental Chemistry Letters*, *20*(2), 1333-1375.

Naboulsi, A., Haydari, I., Bouzid, T., Grich, A., Aziz, F., Regti, A., & Haddad, M. E. (2024). Fixed-bed adsorption of pesticide agricultural waste using cross-linked adsorptive hydrogel composite beads. *Environmental Science and Pollution Research*, *31*(22), 32320-32338.

Nghia, N. T., Tuyen, B. T. K., Quynh, N. T., Thuy, N. T. T., Nguyen, T. N., Nguyen, V. D., & Tran, T. K. N. (2023). Response Methodology Optimization and Artificial Neural Network Modeling for the Removal of Sulfamethoxazole Using an Ozone–Electrocoagulation Hybrid Process. *Molecules*, *28*(13), 5119.

Nguyen, H. A. (2020). Sustainable approaches in pharmaceutical discovery and development of sulfa drugs: A recommendation of green chromatography.

Noack, S., Chapman, H. D., & Selzer, P. M. (2019). Anticoccidial drugs of livestock and poultry industries. In coccidiosis in livestock, poultry, pompanion animals, and humans (pp. 66-77). Press

Nohl, J. F., Farr, N. T., Sun, Y., Hughes, G. M., Cussen, S. A., & Rodenburg, C. (2022). Low-voltage SEM of air-sensitive powders: From sample preparation to micro/nano analysis with secondary electron hyperspectral imaging. Micron, 156, 10323.

Ordonez, D., Podder, A., Valencia, A., Sadmani, A. A., Reinhart, D., & Chang, N. B. (2022). Continuous fixed-bed column adsorption of perfluorooctane sulfonic acid (PFOS) and perfluorooctanoic acid (PFOA) from canal water using zero-valent Iron-based filtration media. *Separation and Purification Technology*, *299*, 121800.

Orisaleye, J. I., Jekayinfa, S. O., Ogundare, A. A., Adefuye, O. A., & Bamido, E. (2022). Effect of screen size on particle size distribution and performance of a small-scale design for a combined chopping and milling machine. *Cleaner Engineering and Technology*, *7*, 100426.

© University of Venda

Ovung, A., & Bhattacharyya, J. (2021). Sulfonamide drugs: Structure, antibacterial property, toxicity, and biophysical interactions. *Biophysical Reviews*, *13*(2), 259-272.

Parashar, V., Chauhan, D., & Gupta, M. (2020). Influence of toxicity of antibiotics on aquatic environment: A serious concern. *Journal of Natural Remedies*, *21*(8 (1)), 362-380.

Pasieczna-Patkowska, S., Cichy, M., & Flieger, J. (2025). Application of Fourier Transform Infrared (FTIR) Spectroscopy in Characterization of Green Synthesized Nanoparticles. Molecules, 30(3), 684.

Patel, H. (2022). Comparison of batch and fixed bed column adsorption: a critical review. *International Journal of Environmental Science and Technology,* 19(10), 10409-10426.

Patel, K., Panchal, N., & Ingle, P. (2019). Review of extraction techniques. *International Journal of Advanced Research in Chemical Science,* 6(3), 6-21.

Perez-Vazquez, A., Carpena, M., Barciela, P., Cassani, L., Simal-Gandara, J., & Prieto, M. A. (2023). Pressurized liquid extraction for the recovery of bioactive compounds from seaweeds for food industry application: A review. *Antioxidants*, 12(3), 612.

Perveen, S. (2023). Evaluation of the potential risks of antibioticresistant bacteria and genes (ARBs & ARGs), and microplastics (MPs); and monitoring of their removal in water treatment processes.

Pezhhanfar, S., Farajzadeh, M. A., Hosseini-Yazdi, S. A., & Mogaddam, M. R. A. (2023). NiGA MOF-based dispersive micro solid phase extraction coupled to temperature-assisted evaporation using low boiling point solvents for the extraction and preconcentration of butylated hydroxytoluene and some phthalate and adipate esters. *RSC advances*, *13*(43), 30378-30390.

Picot-Allain, C., Mahomoodally, M. F., Ak, G., & Zengin, G. (2021). Conventional versus green extraction techniques—A comparative perspective. *Current Opinion in Food Science*, *40*, 144-156.

Qin, K., Chen, Y., Li, J., Xue, C., Wei, L., Song, X., & Zhao, Q. (2020). Removal trends of sulfonamides and their ARGs during soil aquifer treatment and subsequent chlorination: effect of

© University of Venda

aerobic and anaerobic biodegradation. *Environmental Science: Water Research & Technology*, *6*(9), 2331-2340.

Raj, R. S., & Krishnan, K. A. (2023). Batch adsorption studies incorporating response surface methodology for the elimination of acephate. *Environmental Sciences Proceedings*, 25(1), 98.

Rana, S., Kumar, A., Dhiman, P., Mola, G. T., Sharma, G., & Lai, C. W. (2023). Recent advances in photocatalytic removal of sulfonamides pollutants from wastewater by semiconductor heterojunctions: a review. *Materials Today Chemistry*, *30*, 101603.

Rathi, B. S., & Kumar, P. S. (2021). Application of adsorption process for effective removal of emerging contaminants from water and wastewater. *Environmental Pollution*, *280*, 116995.

Raval, N., Maheshwari, R., Kalyane, D., Youngren-Ortiz, S. R., Chougule, M. B., & Tekade, R. K. (2019). Importance of physicochemical characterization of nanoparticles in pharmaceutical product development. In *Basic Fundamentals of Drug Delivery* (pp. 369-400). Academic Press.

Riesel, E. A., Mackey, T., Nilforoshan, H., Xu, M., Badding, C. K., Altman, A. B., & Freedman, D. E. (2024). Crystal structure determination from powder diffraction patterns with generative machine learning. *Journal of the American Chemical Society*, *146*(44), 30340-30348.

Rigdon, S. E., Pan, R., Montgomery, D. C., & Freeman, L. (2022). *Design of experiments for reliability achievement* (Vol. 1). John Wiley & Sons.

Riya, J. F. I. (2021). *Sustainable Development Goals (SDGs) and antibiotic resistance: the need to search beyond* (Doctoral dissertation, Brac University).

Rohilla, S., & Sharma, D. (2023). Sulfonamides, quinolones, antiseptics, and disinfectants. In *Medicinal Chemistry of Chemotherapeutic Agents* (pp. 21-63). Academic Press.

Rykowska, I., Ziemblińska, J., & Nowak, I. (2018). Modern approaches in dispersive liquid-liquid microextraction (DLLME) based on ionic liquids: A review. *Journal of molecular liquids*, *259*, 319-339.

© University of Venda

Sadawarte, G., Jagatap, S., Patil, M., Jagrut, V., & Rajput, J. D. (2021). Synthesis of substituted pyridine based sulphonamides as an antidiabetic agent. *European Journal of Chemistry*, 12(3), 279-283.

Salve, S., Bahiram, Y., Jadhav, A., Rathod, R., & Tekade, R. K. (2023). Nanoplatform-integrated miniaturized solid-phase extraction techniques: A critical review. *Critical Reviews in Analytical Chemistry*, *53*(1), 46-68.

Sanyal, D., & Mathur, P. (2022). Advanced Adsorbent Mediated Extraction Techniques for the Separation of Antibiotics from Food, Biological, and Environmental Matrices. *Separation & Purification Reviews*, *51*(3), 373-407.

Sazali, N., Harun, Z., & Sazali, N. (2020). A review on batch and column adsorption of various adsorbent towards the removal of heavy metal. *Journal of Advanced Research in Fluid Mechanics and Thermal Sciences*, *67*(2), 66-88.

Scott, K. A., & Njardarson, J. T. (2019). Analysis of US FDA-approved drugs containing sulfur atoms. *Sulfur Chemistry*, 1-34.

Selkälä, T. (2021). Cellulose nanomaterials and their hybrid structures in the removal of aqueous micropollutants.

Sequeira, M. P. F. (2022). X-ray Diffraction: Principle and Applications.

Shao, Y., Wang, Y., Yuan, Y., & Xie, Y. (2021). A systematic review on antibiotics misuse in livestock and aquaculture and regulation implications in China. *Science of the Total Environment*, *798*, 149205.

Shen, F., Xiong, X., Fu, J., Yang, J., Qiu, M., Qi, X., & Tsang, D. C. (2020). Recent advances in mechanochemical production of chemicals and carbon materials from sustainable biomass resources. *Renewable and Sustainable Energy Reviews*, *130*, 109944.

Shi, K., Santiso, E. E., & Gubbins, K. E. (2021). Current advances in characterization of nano-porous materials: Pore size distribution and surface area. *Porous Materials: Theory and Its Application for Environmental Remediation*, 315-340.

© University of Venda

Singh, A., Pratap, S. G., & Raj, A. (2024). Occurrence and dissemination of antibiotic resistance in aquatic environment and its ecological implications: a review. *Environmental Science and Pollution Research*, *31*(35), 47505-47529.

Singh, P., & Sillanpää, M. (Eds.). (2022). *Degradation of Antibiotics and Antibiotic-resistant Bacteria from Various Sources*. Academic Press.

Singla, M., & Sit, N. (2023). Theoretical aspects and applications of aqueous two-phase systems. *ChemBioEng Reviews*, *10*(1), 65-80.

Smith, B. C. (2018). Infrared spectral interpretation: a systematic approach. CRC press.

Sun, Y., Zheng, L., Zheng, X., Xiao, D., Yang, Y., Zhang, Z., & Sheng, Z. (2022). Adsorption of sulfonamides in aqueous solution on reusable coconut-shell biochar modified by alkaline activation and magnetization. *Frontiers in Chemistry*, *9*, 814647.

Suseela, M. N. L., Viswanadh, M. K., Mehata, A. K., Priya, V., Setia, A., Malik, A. K., ... & Muthu, M. S. (2023). Advances in solid-phase extraction techniques: Role of nanosorbents for the enrichment of antibiotics for analytical quantification. Journal of Chromatography A, 1695, 463937.

Szarka, A., Búčiková, K., Kostić, I., & Hrouzková, S. (2020). Development of a multiresidue QuEChERS–DLLME—fast GC–MS method for determination of selected pesticides in yogurt samples. *Food Analytical Methods*, *13*, 1829-1841.

Taneja, N., & Sharma, M. (2019). Antimicrobial resistance in the environment: The Indian scenario. *Indian Journal of Medical Research*, *149*(2), 119-128.

Tang, J., Yang, M., & Yao, S. (2021). Pretreatment techniques for drug residues in the environment before their quantitation. *Current Analytical Chemistry*, 17(6), 768-801.

Tirado-Kulieva, V. A., Sánchez-Chero, M., Yarlequé, M. V., Aguilar, G. F. V., Carrión-Barco, G., & Santa Cruz, A. G. Y. (2021). An overview on the use of response surface methodology to model and optimize extraction processes in the food industry. *Current Research in Nutrition and Food Science Journal*, 9(3), 745-754.

© University of Venda

ul Nisa, Z., Tashi, L., Sen, C., Ashashi, N. A., Sahoo, S. C., & Sheikh, H. N. (2020). Synthesis of eight isostructural 2D lanthanide coordination polymers assembled by rigid furan-2, 5-dicarboxylic acid and flexible adipic acid as linkers and exploration of luminescent Eu/Tb polymers as efficient and sensitive sensors for nitroaromatic compounds. *New Journal of Chemistry*, *44*(19), 8125-8137.

Verma, T., Aggarwal, A., Singh, S., Sharma, S., & Sarma, S. J. (2022). Current challenges and advancements towards discovery and resistance of antibiotics. *Journal of Molecular Structure*, *1248*, 131380.

Wang, H. (2021). *Metal Salt Hydrolysis for Electrochemically Active Conducting Polymer Nanocomposites* (Doctoral dissertation, Washington University in St. Louis).

Wang, L. Y., Bu, F. Z., Yu, Y. M., Niu, Y. Y., Li, Y. T., Yan, C. W., & Wu, Z. Y. (2021). A novel crystalline molecular salt of sulfamethoxazole and amantadine hybridizing antiviral-antibacterial dual drugs with optimal in vitro/vivo pharmaceutical properties. *European Journal of Pharmaceutical Sciences*, *163*, 105883.

Wu, J. H., & He, C. Y. (2019). Advances in cellulose-based sorbents for extraction of pollutants in environmental samples. *Chromatographia*, *82*(8), 1151-1169.

Xia, J., Liu, S., Zhang, B., & Chen, Y. (2021). Central composite experiment design (CCD)-response surface method (RSM) to optimize the sintering process of Ti-6Al-4V alloy. *Metals*, *11*(2), 197.

Yang, Q., Gao, Y., Ke, J., Show, P. L., Ge, Y., Liu, Y., & Chen, J. (2021). Antibiotics: An overview on the environmental occurrence, toxicity, degradation, and removal methods. *Bioengineered*, 12(1), 7376-7416.

Yang, Y., Liu, L., Li, X., & Bao, R. (2024). Development of a simple UPLC-MS/MS method coupled with a modified QuEChERS for analyzing multiple antibiotics in vegetables and applied to pollution assessment. *Journal of Food Composition and Analysis*, *129*, 106135.

© University of Venda

Yao, T., Feng, C., & Yan, H. (2024). Current developments and applications of smart polymers based aqueous two-phase systems. *Microchemical Journal*, 111170.

Zambrano-Mite, L. F., Villasana, Y., Bejarano, M. L., Luciani, C., Niebieskikwiat, D., Álvarez, W., & Orejuela-Escobar, L. M. (2023). Optimization of microfibrillated cellulose isolation from cocoa pod husk via mild oxalic acid hydrolysis: A response surface methodology approach. *Heliyon*, *9*(6).Aziz, T., Li, W., Zhu, J., & Chen, B. (2024). Developing multifunctional cellulose derivatives for environmental and biomedical applications: Insights into modification processes and advanced material properties. *International Journal of Biological Macromolecules*, 134695.

Zgoła-Grześkowiak, A., Grześkowiak, T., Ligor, M., & Frankowski, R. (2024). Achievements and Challenges of Matrix Solid-Phase Dispersion Usage in the Extraction of Plants and Food Samples. *Processes*, *12*(6), 1146.

Zhang, J. H., Xie, S. M., & Yuan, L. M. (2022). Recent progress in the development of chiral stationary phases for high-performance liquid chromatography. *Journal of separation science*, *45*(1), 51-77.

Zhao, D., Yang, Y., & Chen, J. P. (2024). Performance of removing aqueous contaminant by zirconium based adsorbents: a critical review. *Frontiers in Chemical Engineering*, *6*, 1282076.

Zhao, Y., Zhang, X., & Hua, W. (2021). Review of preparation technologies of organic composite phase change materials in energy storage. *Journal of Molecular Liquids*, *336*, 115923.

Zhou, J., Yun, X., Wang, J., Li, Q., & Wang, Y. (2022). A review on the ecotoxicological effect of sulphonamides on aquatic organisms. *Toxicology Reports*, *9*, 534-540.

Zhou, Q., Yu, C., Meng, L., Ji, W., Liu, S., Pan, C., & Qu, B. (2024). Research progress of applications for nano-materials in improved QuEChERS method. *Critical Reviews in Food Science and Nutrition*, *64*(28), 10517-10536.

Zhou, Y., & Zhou, Z. X. (2021). Integrated inexact optimization for hybrid renewable energy systems. In *Renewable-Energy-Driven Future* (pp. 203-231). Academic Press.

© University of Venda

Zhu, B., Wang, K., Sun, W., Fu, Z., Ahmad, H., Fan, M., & Gao, H. (2022). Revealing the adsorption energy and interface characteristic of cellulose-graphene oxide composites by first-principles calculations. *Composites Science and Technology*, *218*, 109209.

© University of Venda

© University of Venda